CONF-710402
Vol. III

NEUTRON SOURCES AND APPLICATIONS

Proceedings of the American Nuclear Society
National Topical Meeting

April 19-21, 1971
Augusta, Georgia

SESSIONS III AND IV

Contributed Papers

DU PONT
REG. U.S. PAT. OFF.

ISSUED BY

Savannah River Laboratory

Aiken, South Carolina

Printed in the United States of America
Available from
National Technical Information Service
U. S. Department of Commerce
5285 Port Royal Road
Springfield, Virginia 22151
Price: Printed Copy $3.00; Microfiche $0.95

CONF-710402
Vol. III
General, Miscellaneous and
Progress Reports (TID-4500)

NEUTRON SOURCES AND APPLICATIONS

Proceedings of the American Nuclear Society
National Topical Meeting

April 19-21, 1971
Augusta, Georgia

Contributed Papers

SESSIONS III AND IV

April 1971

E. I. DU PONT DE NEMOURS & COMPANY
SAVANNAH RIVER LABORATORY
AIKEN, S. C. 29801

CONTRACT AT(07-2)-1 WITH THE
UNITED STATES ATOMIC ENERGY COMMISSION

FOREWORD

The speakers whose papers are published in Volume I were invited to discuss subjects in which they are acknowledged experts. To provide them with current information concerning the work of other scientists and to acknowledge the work of other persons, papers covering the many aspects of neutron sources and their applications were invited to be submitted on an international basis. Papers were accepted until March 1971. Submitted papers, which were summarized by invited speakers who acted as rapporteurs, are published here in Volumes II and III. The papers are reproduced from texts submitted by the authors and are unedited.

This system of combining summary talks and submitted papers was adopted because of the widely varying and interdisciplinary nature of the rapidly growing field of neutron source application. It is hoped that the publication of this material will provide a useful reference for all who are interested in neutron sources and their applications. By being available at the meeting, Volumes II and III may assist attendees and help to stimulate discussion. Volume I will contain the invited papers, the discussions at the meeting and the remaining contributed papers. Publication will follow shortly after the meeting.

CONTENTS

SESSION III: EXPLORATION AND PROTECTION OF NATURAL RESOURCES

SESSION IV: INDUSTRIAL USES OF NEUTRON SOURCES

Session III

EXPLORATION AND PROTECTION OF NATURAL RESOURCES

A BOREHOLE SONDE USING A ^{252}Cf SOURCE AND A Ge[Li] DETECTOR COOLED BY A MELTING CRYOGEN

Allan B. Tanner, Robert M. Moxham, and Frank E. Senftle

U. S. Geological Survey
Washington, D. C.

Joseph A. Baicker

Princeton Gamma-Tech, Inc.
Princeton, New Jersey

A sonde has been built for high-resolution measurement of natural or neutron-induced gamma rays in boreholes. The sonde is 7.3 cm in diameter and about 2.2 m in length and weighs about 16 kg. The lithium-compensated germanium semiconductor detector is stabilized at -188°C for as much as ten hours by a sealed cryostatic reservoir containing melting propane. During periods when the sonde is not in use the propane is kept frozen by a gravity-fed trickle of liquid nitrogen from a reservoir temporarily attached to the cryostat section. A ^{252}Cf source, shielded from the detector, may be placed in the bottom section of the sonde for analysis by measurement of neutron-activation or neutron-capture gamma rays. Stability of the sealed cryostat with changing hydrostatic pressure, absence of vibration, lack of need for power to the cryostat during operation, and freedom of orientation make the method desirable for borehole, undersea, space, and some laboratory applications.

INTRODUCTION

Analysis of natural or activation gamma rays in a borehole requires a radiation detector capable of good energy resolution. A NaI (Tℓ) scintillation detector, generally used for this purpose, has sufficient resolution to reveal many delayed gamma ray lines, but the resolution is less than desirable. This is particularly true if one wishes to record prompt, neutron-capture gamma-ray spectra. The high resolution needed to perform capture gamma-ray analysis can only be obtained with a semiconductor Ge(Li) detector. Ge(Li) detectors generally require operating temperatures below -180°C and use liquid nitrogen as the cryogen. The application of such a detector down a water-filled borehole or in an undersea environment presents a stringent constraint on the apparatus.

If the vapor from boiling nitrogen in a detector sonde exhausted itself by means of a check valve, there would be a buildup of pressure in the reservoir as the hydrostatic pressure increased with depth. As is shown in Figure 1, the boiling temperature of nitrogen would increase, causing an increase in the temperature of the cryostat. Instrumental drift, increased noise, and a loss of resolution could be expected. One could install a servomechanism to activate a pump to remove excess nitrogen from the reservoir and thus regulate the boiling temperature, but this seems to be an unduly complex solution to the problem. Several alternatives to liquid nitrogen, coolers using the thermoelectric (Peltier) effect, Joule-Thomson expansion, closed-cycle mechanical refrigerators, and sublimation of a solid cryogen, have been used successfully for infrared detectors (1,2,3).

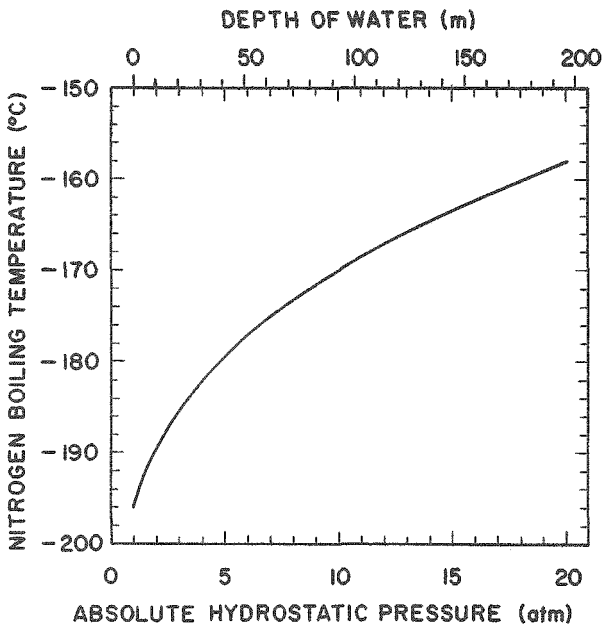

FIG. 1 BOILING TEMPERATURE OF NITROGEN AS A FUNCTION OF HYDROSTATIC PRESSURE

Publication authorized by the Director, U. S. Geological Survey.

Use of the thermoelectric effect (and possibly other means) has been anticipated for a borehole cryostat (4). For borehole or undersea applications we believe that the above techniques would have several disadvantages:

1. Unless some provision were made to use a liquid cryogen while the sonde was not in service, the thermoelectric or mechanical devices would have to be continuously powered.

2. There would be danger of permanent damage to the Ge(Li) detector if there were a loss of power lasting over an hour.

3. The mechanical coolers have high-speed moving parts and would tend to transmit vibration to the detector, which is quite microphonic.

A different alternative, which is considered in this paper, is the use of a solid cryogen with a melting point in the range of operating temperature desired. The melting point of a solid is not sensitive to hydrostatic pressure, as is the boiling point of a liquid. A judicious choice of solid cryogen permits design of a cryostat that is sealed, may be oriented in any position, requires no power during operation, generates no microphonic disturbance to the detector, and even provides radiation shielding.

THE CRYOGEN

SELECTION CRITERIA

The most desirable features of a solid cryogen for a semiconductor detector are (1) a melting point near the detector's optimum operating temperature, (2) a large latent heat of fusion, (3) high density of solid and liquid. For safety it is also desirable that the cryogen have a critical temperature above any ambient temperature that the sonde might accidentally warm up to and that the cryogen be nonflammable, nonexplosive, noncorrosive, and nontoxic. For operating convenience it is desirable that the difference between the freezing point of the cryogen and the temperature used to refreeze the cryogen (for instance, that of boiling nitrogen) be sufficient to refreeze during usual nonoperating times but not so great as to cause excessive delay between removal of the refreezing agent and stabilization of the cryostat at the melting temperature of the solid cryogen. For protection of the detector it may be desirable to choose a cryogen that has good shielding properties; for example, a Ge(Li) detector may receive significant protection from the fast neutrons of a ^{252}Cf source by an interposed cryostat containing a high density of hydrogen atoms. Characteristics such as supercooling, thermal conductivity, and phase density differences may also be significant.

OPERATING TEMPERATURE

Although Ge(Li) detectors are almost always operated with liquid-nitrogen cryostats (-195.8°C) and might perform better at even lower temperatures, respectable performance should be obtained at operating temperatures up to about -180°C. Table I lists various substances having low melting points, of which rather few melt in this range.

TABLE I

Melting and Boiling Points of Some Compounds*

	M.P. (°C)	B.P. (°C) at 1 atm.
Propane	-187.69§	- 44.5
Propene	-185.2	- 47.8
Carbon tetrafluoride	-184	-128
Ethane	-182.8	- 88.63
Methane	-182.48	-161.49
Chlorotrifluoromethane (R-13)†	-181	- 81.4‡
Ethene	-169.15	-104
Nitric oxide	-163.6	-151.8
Fluorine dioxide	-163.5	- 57
Trifluoromethane	-163	- 82.2
Trimethyl borine	-161.5	- 20
Chlorodifluoromethane (R-22)†	-160‡	- 40.75‡
Chloroethene	-160	- 13.9
2-methylbutane	-160	+ 27.9
1-fluoropropane	-159	- 2.5
Dichlorodifluoromethane (R-12)†	-158‡	- 27.79‡
Methylsilicane	-156.4	+ 31
Tetraethyllead	-136.80	+200 (decomposes)

*Unless otherwise noted, data from ref. (5).
†Commercial refrigerants known by trade names such as, "Freon", "Genetron", "Isotron", etc.
‡Data from ref. (6). §Data from ref. (7).

Detector crystals are sometimes found that exhibit low leakage at temperatures considerably higher, however, permitting a much wider choice of cryogens, of which the table can be only representative. For applications where holding time, high ambient temperatures, and radiation shielding are very important, selection of the detector crystal and use of one of the higher-melting-point cryogens appears to be indicated. An interesting

example is tetraethyllead, which has both the hydrogen atoms needed to shield fast neutrons and the high-mass lead needed to absorb the gamma rays produced by the neutron absorption.

PRINCIPAL CHOICES OF CRYOGEN

We have given most consideration to propane and to three commercial fluorocarbon refrigerants. Of the eligible hydrocarbons, propane has the highest boiling point and a comfortably high critical temperature (+96.81 °C). The fluorocarbon refrigerants have high densities and the inert characteristics desirable for a cryostat. Pertinent characteristics for these substances are given in Table II. Because density data were not

TABLE II

Characteristics of Several Cryogens

	Propane	R-13*	R-22*	R-12*
Melting Point (°C)	-187.69†	-181‡	-160§	-158§
Critical Temp. (°C)	96.81†	28.9§	96.0§	112.0§
Liquid Density at B.P. (g/cm^3)	0.61	1.49	1.38	1.44
Liquid Density near M.P. (g/cm^3)	0.71	1.73	1.63	1.73
Solid Density at M.P. (g/cm^3)	0.75	2.02	1.52	1.88
Heat of Fusion (cal/mol)	842.2†	980#	985.5¶	990¶
Heat of Fusion/Unit Volume (cal/cm^3)Δ	14.6	18.9	17.3	16.6

* See Table I for chemical identification.
‡ Data from ref. (5).
† Data from ref. (7).
§ Data from ref. (6).
# Estimated from values for R-22, R-12, and CHF_3 (970 cal/mol).
¶ Oral communication from R. C. Downing, E.I. duPont de Nemours & Co., Wilmington, Del.
Δ Heat of vaporization of nitrogen is 38.5 cal/cm^3.

available for the solid fluorocarbon refrigerants, new determinations were made and appear in the table. Where they could be compared with literature values, no discrepancies greater than four percent were found. It is noteworthy that the ice of R-22 (chlorodifluoromethane) floats on its melt liquid.

In order to use R-13 (chlorotrifluoromethane) in a sealed reservoir with safety, it would be necessary to provide pressure relief in the event of warmup. At the critical temperature (28.9°C) the pressure in a sealed reservoir would rise from 38 atmospheres to about 200 atmospheres. Incorporation of a pressure-relief element, such as a rupture disk, might require undesirable design compromises.

Use of R-22 or R-12 would permit long holding times because of the smaller differences between their melting points and ambient temperatures. Cryostats containing them could also be frozen quite rapidly by contact with liquid nitrogen; however, the time required for natural warmup to the melting point would be unacceptably long and would have to be accelerated. As noted above detector crystals for use at the melting points of R-22 and R-12 would have to be selected for extraordinarily low leakage.

Propane, which was chosen as the first solid cryogen to try, has a tendency to supercool, rather than to freeze, when held in clean glassware immersed in liquid nitrogen. We have not observed stable supercooling in the completed borehole cryostat. Of the various suitable cryogens, propane has the melting point nearest the temperature of liquid nitrogen; consequently it requires the longest time to refreeze but the shortest time to stabilize at operating temperature. The latter consideration is probably the more important.

THE BOREHOLE SONDE

The sonde is 7.3 cm (2-7/8 in.) in diameter and about 2 m (7 ft.) long, depending on the length of the shielding section placed between the neutron source holder and the cryostat section. From bottom to top, the sonde consists of six detachable sections [Figure 2]:

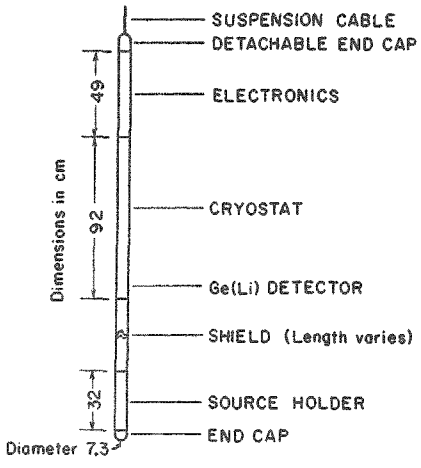

FIG. 2 SCHEMATIC DRAWING OF BOREHOLE SONDE

a rounded end piece, a holder for a ^{252}Cf source, a shield, a cryostat holding a coaxial Ge(Li) detector, an electronics unit, and an end piece into which the sonde cable is clamped. During storage and refreezing periods the cryostat section is detached from the others and held in a vertical position; a ten-liter liquid-nitrogen reservoir with a "chicken feeder" tube is mounted on the cryostat [Fig. 3]. The sonde weighs about 16 kg (35 pounds) plus the shield and source-holder filling material.

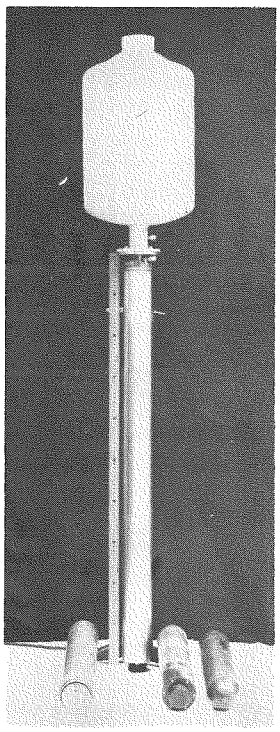

FIG. 3 DISASSEMBLED SONDE WITH LIQUID-NITROGEN RESERVOIR ATTACHED TO CRYOSTAT

SOURCE HOLDER AND SHIELD

To maximize moderation of the fast ^{252}Cf neutrons, the source holder and shield are made of densely compressed wood fiber ("Benelex"). The source holder is annular and accommodates the phenolic rods in which we usually mount the ^{252}Cf source capsules. The shield is also annular, to permit experimentation with different shielding materials. Shield sections of different lengths can be made at modest cost, because no electrical connections or watertight seals are needed.

CRYOSTAT AND DETECTOR

The choice of construction materials for the cryostat is an important one if capture gamma rays are to be measured. A relevant study of materials suitable for encapsulation of ^{252}Cf sources has been presented elsewhere (8). Because zirconium is one of the elements offering the least potential interference with capture gamma-ray analysis and has high resistance to corrosion, the body and casing of the cryostat are made of a zirconium alloy ("Zircaloy-2"). Zirconium's poor heat-transfer characteristics make it unsuitable for the cold finger, which is of copper.

Thermal insulation between the cryostat proper and the casing of the cryostat section is provided by conventional "superinsulation". A plot of cryostat temperature within the cold finger as a function of time after removal of the liquid-nitrogen reservoir is shown in Figure 4.

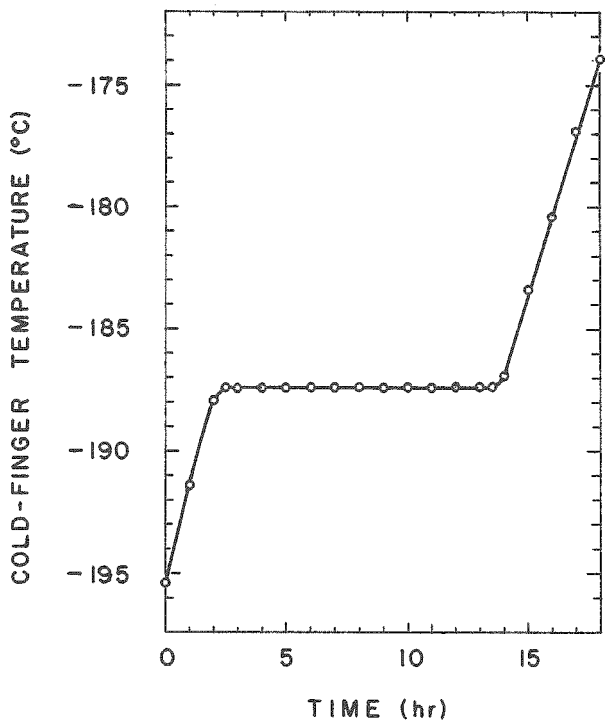

FIG. 4 CRYOSTAT TEMPERATURE vs. TIME AFTER REMOVAL OF LIQUID-NITROGEN RESERVOIR

The time during which the cold finger is stabilized at the propane melting point is somewhat greater than ten hours when the environment is at room temperature. (The Ge[Li] detector would be protected from decompensation for a much longer period.) Note that it takes several hours after removal of the liquid-nitrogen reservoir for the cryostat to absorb enough heat to reach the propane melting temperature. During this

period a gain shift corresponding to about 0.25 keV/°C has been observed.

Ports for evacuation of the cryostat and for access to the solid-cryogen reservoir, and an MHV-series connector to the detector are located within the top of the cryostat section. By attachment of an angle connector and a conventional preamplifier and bias supply the cryostat section may be used as a laboratory-style detector with the liquid-nitrogen reservoir in place. With the reservoir removed (or empty) the cryostat section may be used in any orientation and is free from microphonics associated with boiling nitrogen.

A coaxial, lithium-compensated germanium crystal of about 50 cm^3 volume is mounted near the bottom end of the cryostat section. When tested in a conventional cryostat, the detector achieved a resolution of 2.6-keV width at the half-maximum point on the 1.332-MeV gamma peak of ^{60}Co, a peak-to-Compton ratio of 24 to 1, and efficiency of 9.1 percent relative to a 3 x 3 NaI detector. As of this writing the electronics section is still in the prototype stage. Figure 5 is a spectrum in the range 0.4 - 2.3 MeV taken with the sonde and the prototype electronics. The spectrum consists of the fission-gamma-ray continuum of ^{252}Cf,

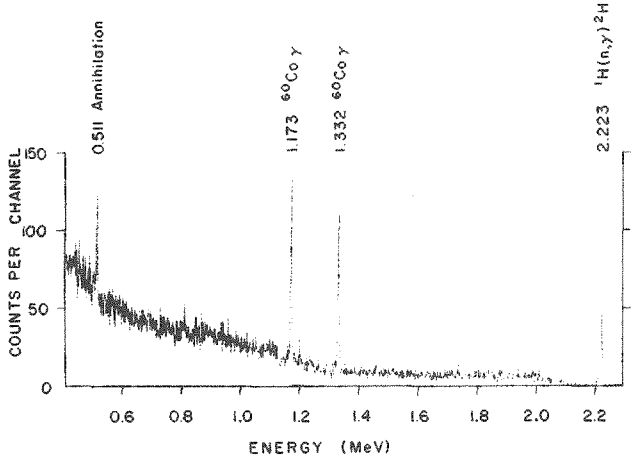

FIG. 5 MIXED SPECTRUM OF ^{60}Co AND MODERATED ^{252}Cf, 0.4 TO 2.3 MeV

attenuated by water and paraffin, the hydrogen capture-gamma peak at 2.223 MeV, the ^{60}Co peaks at 1.332 and 1.173 MeV, the 0.511-MeV annihilation peak, and various escape peaks.

ELECTRONICS

The electronics section consists of an adjustable high-voltage power-supply unit and a preamplifier-and-driver unit, each housed separately and incorporating its own voltage regulators. All power is furnished by positive and negative 24-volt lines in the shielded suspension cable. Signal pulses from a low-impedance driver are transmitted through a shielded coaxial element of the cable. Power-supply return is provided by an additional conductor.

CONCLUSIONS

At the time of writing, the sonde has been in a late prototype stage. Evaluation of its capabilities for neutron-activation and neutron-capture gamma-ray analysis has not yet been feasible. However, it is apparent that a basic high-resolution gamma-ray detector employing the design principles of the borehole sonde has useful qualifications for applications both inside and outside the field of borehole or well logging: in undersea work, the freedom from sensitivity to hydrostatic pressure; in space, the lack of need to vent the cryogen or to control a liquid in the absence of gravity; and in the laboratory, freedom to orient the detector as desired and freedom from bulky reservoirs during experiments.

In situations where liquid nitrogen is difficult to obtain but power is available during nonoperating periods, refreezing of the cryogen could be done by thermoelectric cooling or by small and efficient closed-cycle refrigerators now available (4,9). Such an arrangement would avoid the problems associated with power losses, high-power transmission down a cable carrying signals, and mechanical vibration, and would gain the temperature stability of the melting cryogen.

ACKNOWLEDGMENTS

We thank N. Stetson, Savannah River Operations Office, U. S. Atomic Energy Commission, for making available ^{252}Cf sources used in experiments with the borehole sonde. This work was supported in part by the National Aeronautics and Space Administration. Marvin Freifeld and Robert Perry, Princeton Gamma-Tech, Inc., were responsible respectively

for electronic design and for construction and testing of the sonde. P. W. Philbin, U. S. Geological Survey, assisted in the preliminary tests. Valued reference data were furnished by Eugene Domalski, National Bureau of Standards; R. C. Downing, E. I. duPont de Nemours & Company; and R. C. Wilhoit, Thermodynamics Research Center, Texas A & M University.

REFERENCES

1. M. B. Grier. "Lumped Parameter Behavior of the Single-stage Thermoelectric Microrefrigerator." Proc. Inst. Radio Engineers 47, 1515 (1959).

2. W. S. Gifford and H. E. Deabler. "A New Refrigeration Process and Its Application to Cooling of Infrared Detectors." Proc. Infrared Information Symposium 5 (7), 461 (1960).

3. A. I. Weinstein, A. S. Friedman, and U. E. Gross. "Cooling to Cryogenic Temperatures by Sublimation." Proc. Infrared Information Symposium 7 (2), 187 (1962).

4. J. T. Dewan. "Cryogenically Cooled Radioactivity Borehole Logging Technique." U. S. Patent No. 3,496,360 (1970).

5. R. C. Weast, ed. Handbook of Chemistry and Physics. 47th ed. The Chemical Rubber Co., Cleveland (1966).

6. E. I. duPont de Nemours and Co. Freon Product Information Bull. B-2 (1969).

7. American Petroleum Institute [Research Project 44]. Selected Values of Physical and Thermodynamic Properties of Hydrocarbons and Related Compounds. Carnegie Press, Pittsburgh (1953).

8. F. E. Senftle, A. G. Evans, D. Duffey, and P. F. Wiggins. "Construction Materials for Neutron Capture-Gamma-Ray Measurement Assembly Using Californium-252." Nuclear Technology 10, 204 (1971).

9. S. F. Malaker, J. DiLeo, J. B. Malaker, and C. B. Pawleski. "The Achievement of Superconducting Transitions with Miniature Closed-Cycle Cryogenic Refrigerators." Cryogenic Engineering News 3, 40 (1968).

UNDERSEA MINERAL ANALYSIS WITH CALIFORNIUM-252

John E. Noakes and Grover A. Smithwick
University of Georgia
Athens, Georgia

James L. Harding
Oceanonics, Inc.
Houston, Texas

Al Kirst, Jr.
Westinghouse Ocean Research Laboratory
San Diego, California

Present state-of-the-art methods employed in exploration of sea floor mineral deposits deal primarily with shipboard collection of samples and land-based laboratory analyses. Grab sampling and coring methods are the primary means for bottom sampling. Unfortunately these methods can result in the collection of distorted, unrepresentative samples of the sea floor. An undersea neutron activation analysis system has been developed which permits immediate elemental analysis from undisturbed sea floor mineral deposits. Californium-252 has been utilized as a neutron source for the activation analysis system. Elemental analyses of minerals in ore grade concentrations have been successfully demonstrated. Delivery of the activation analysis system to the sea floor has been accomplished by three different modes of operation: (1) an undersea submersible for deep water capabilities; (2) a sled for intermediate depths; and (3) scuba divers for shallow water operations. Minimum radiation hazards associated with the shipboard handling of ^{252}Cf have been demonstrated.

INTRODUCTION

In recent years, much has been written concerning the potential of mineral deposits on the sea floor. However, aside from beach deposits that have been worked for many years for mineral commodities and certain non-metallic deposits, such as shell, aragonite and phosphate, little progress has been noted in the exploration and correlatively less in the exploitation of actual marine mineral deposits. The problems associated with marine mining are formidable and many-faceted. Aside from various economic and legal aspects, principal among the limiting factors are the restrictions imposed by technological gaps in exploration practices.

Exploration methods presently employed are based primarily on shipboard collection of samples followed by land-based laboratory analyses. Hence, the project geologist must await the results of the latter in order to advance a given survey from a reconnaissance phase to a more detailed target pattern, or conversely, to have enough information to abandon the prospect. This practice usually necessitates repeated mobilization of expensive survey vessels and support equipment. Although some advances have been made involving shipboard analyses with atomic absorption spectrophotometry, such tests are not only time-consuming but are also destructive insofar as the sample is concerned. In many cases, it is imperative that a specific sample be saved for additional mineralogical tests.

A low-cost method for rapid, accurate and non-destructive analyses on shipboard would be an important incentive to the mineral industry for expansion of its marine exploration programs. It would be optimal if the same system could also measure mineral concentration values in situ, or on the sea floor, as this could find important applications in the location and choice of undersea sites for subsequent sampling. Furthermore, such in situ analysis would not disturb the surficial mantle of sediments, as is often the case in coring or dredging operations.

It was with these parameters in mind that the method of neutron activation analysis, as discussed in this paper, was selected for testing and evaluation. The choice of Californium-252 as the neutron source was made on the merits of its high neutron production and dependable operation above and within the marine environment. The in situ analysis of sea floor sediments where the actual analyses were performed on the ocean floor were the first research efforts associated with this study. The remainder of this paper will deal solely with

Research sponsored by the National Science Foundation Sea Grants, Westinghouse, Oceanonics, and the University of Georgia.

describing these initial activities and the results obtained from this work.

UNDERSEA NEUTRON ACTIVATION ANALYSIS

Neutron activation analysis is an analytical technique in which stable elements are made radioactive when they are bombarded with neutrons. The interactions occur within the nucleus of an element to produce radioisotopes of the element with the concurrent release of excess radiation energy. The newly-formed radioisotopes are unstable and radioactive. They exhibit this instability by a time-delayed decay emitting radiation energy equivalent to their raised excited state. Radiation measurements can be performed either on the prompt radiation released at the time of activation or on the decay of the radioisotope. Measurement of radiation energy and intensity permits identification of the element bombarded and an estimate of its concentration level.

The undersea neutron activation analysis procedure adopted for our studies was not radically different from the normally practiced technique except that it was done underwater. The transportation of the nuclear system to and about the sea floor was carried out with a variety of undersea vehicles. Sample activation on the sea floor was performed by positioning a Cf-252 neutron source on top of a sample for several minutes. Radiation measurements were accomplished after activating by positioning a radiation detector on the activated sample. Sea water proved to enhance the sample activation by thermalizing the higher energy Cf-252 neutrons. It also had the added advantage as a neutron shield for personnel in the water.

Radiation measurements on the activated samples proved to be one of the most difficult procedures. The decision was made early in the studies to measure the delayed radiation from radioisotope decay rather than prompt gamma radiation produced at the time of activation. This decision was based on the assumption that any advantages in measuring high energy prompt gamma radiation was offset by shielding problems associated with the close positioning of the neutron source and detector. The sequential activation and radiation measure of the activated samples did not require shielding other than the 6-7 feet of water between the neutron source and the detector. Also, the 30-40 second time delay in removing the neutron source and positioning the detector permitted most of the interfering short-lived isotopes to decay before measurements were made. A review of the possible elements that could be activated in 2-5 minutes with a flux of 10^7-10^8 thermal neutrons and be expected to have enough radioactivity for measurement were carefully scrutinized. Table I lists 25 elements which fall into this category. Of these, 14 were considered to be most promising.

Prior to undersea testing of the neutron activation analysis system the underwater sensitivity levels of the method for various elements of interest were investigated. This was accomplished by tank studies in the laboratory using sea water of 34 per cent salinity and activating synthetic ore grade samples. Simulated samples were made up of a clay-sand matrix with selected elements mixed at various concentration levels. The clay-sand mix was prepared with levels approaching the aluminum, silicon, oxygen ratio of commercial ores. Samples were packaged in one-gallon plastic jugs which facilitated underwater handling and in later studies, during transportation to the sea floor. The question of the lower level of element concentration that would be of initial interest was resolved by scrutinizing the element concentration of terresterial ores mined today (Table II). It was decided that the synthetic ores should contain element concentrations equivalent to the higher levels in terresterial ores, since marine mining is more costly and therefore would require higher element concentrations for ore grade levels. Accordingly, the elements marked with an asterisk in Table II were made up as synthetic ore samples in element concentration levels comparable to terresterial ores. Final selection of these elements was based partially on their nuclear properties for activation analysis and on the possible occurrence as ore bodies in the marine environment.

UNDERSEA VEHICLES

The primary purpose of the undersea vehicles employed in the undersea mineral exploration studies was not solely restricted to delivery of the analytical equipment to the floor of the ocean. Once on the sea floor, the vehicles were also used for diver transportation to and about areas of geologic interest, thereby permitting divers to observe geologic formations, select representative samples and analyze them in

place. Other advantages were the vehicles' potential for underwater sampling and assistance in surface shipboard sample collection.

Three different vehicles were used in the undersea activities. These vehicles were selected on a basis of their capacity to function at specific ocean bottom depths and perform desired underwater activities.

SCUBA DIVERS

A two-man scuba diving team was employed when bottom samples from 10-50 foot depth were being investigated. In the underwater operation one diver was equipped with the Cf-252 source housed in a water-tight, neutral bouyancy, steel container. This neutron source container was mounted to the end of a 7-foot steel handling tool, thereby reducing radiation hazards to the diver. The second diver carried the radiation detection system. This detection equipment was also encapsulated in a water-tight, neutral bouyancy container and carried at the end of a 7-foot steel handling tool. A small T.V. camera was mounted on the handling tool to facilitate observations of the undersea operations. The radiation detector equipment and T.V. camera were connected to the surface by umbilical line for electrical power and data retrieval. The analytical procedure involved diver positioning of the Cf-252 source on the sample to be analyzed. During periods of activation the T.V. camera was directed to view the operation so shipboard personnel could be alerted. After activation the neutron source was removed from the area and the nuclear detector positioned over the activated sample. T.V. monitoring of the operation allowed personnel aboard the surface ship to know precisely when to start data retrieval.

UNDERWATER SLED

An underwater sled was utilized where bottom depths ranged from 50-150 feet. Sled construction was of steel angle iron with dimensions 12 feet long and 4 feet wide. Two 4-inch wide steel runners were fabricated the full length of the bottom structure. A 4-foot upright, 4-inch diameter, steel pipe was erected in the center of the sled to support a T.V. camera and flood lights. The Cf-252 source was mounted in a bow position on the sled in a water-tight steel container. This container was attached to the sled on a 7-foot steel handling tool which was mounted on a swivel at the upright center post. The radiation detector was housed and attached in a similar manner aft of the center post. The swivel attachment allowed both the Cf-252 source and detector to be positioned in a 7-foot radius about the sled. An umbilical line was attached from the sled to the surface ship for electrical power and data retrieval. A tow line from the surface ship was attached forward of the bow of the sled to propel the sled about the sea floor. The underwater operations involved towing the sled with flood lights and T.V. viewing the sea floor. The sled's forward motion was stopped when the Cf-252 source was positioned over the sample to be activated. Radiation measurements were carried out by pulling the sled forward so the detector was positioned over the activated sample. A more efficient operation was achieved if a diver, equipped with a Scott mask and audio connection to the surface ship, rode the sled and directed the operation. In this mode of operation, the diver could easily position the Cf-252 source and radiation detector through a pivoting action of the two handling tools.

SUBMERSIBLE

The Westinghouse Electric Corporation's Deepstar 2000 submersible was the undersea vehicle used when bottom depths from 150 - >300 feet were to be explored. The submersible is 20 feet long, 10 feet at the beam, and weighs 9.5 tons in air. Its propulsion endurance is 1 knot for 12 hours with a maximum speed of 3 knots. Operation depth is down to 2260 feet. It is equipped with three viewports (2 observer and 1 photographic) and a manipulator device. The normal life support endurance for three men is 12 hours with a safety margin to 48 hours. In the use of the submersible the complete activation analysis system was housed aboard the vehicle, thereby eliminating umbilical connection to a surface ship. The Cf-252 source was housed in a water-tight steel container and was attached to the submersible on a boom 12 feet forward from the pressure hull and in full view of the observer ports. The radiation detector was also encapsulated in a water-tight steel container and attached in a forward position beneath the bow overhang and in full view of both observer viewports. (Photo 1) The analytical equipment (multichannel analyzer and printer) used to store and interpret the data was contained within the submersible (Photo 2). The undersea activation analysis

procedure was to maneuver the submersible on the ocean floor so that the neutron source was directly on top of the sample to be activated (Photo 3). Activation was carried out by holding the submersible in a motionless position. Radiation measurements were accomplished by moving the submersible forward 6 feet and positioning the detector on the activated sample. Data retrieval was carried out within the submersible.

ANALYTICAL RESULTS

The application of neutron activation analysis to marine mineral exploration first required establishing the operational parameters of the method for undersea work. At the initiation of this study no previous work had been published on this subject. It was therefore necessary to investigate the fundamental problems of undersea instrumentation delivery systems, procedural techniques for sample analysis, spectrum of elements that could be analyzed and their sensitivity levels of detection. In order to carry out these initial studies the 14 synthetic ore samples (described previously) were selected for the preliminary studies because of their known elemental content. The results reported here are for these man-made ore samples and are solely meant to serve as a guideline for later applied studies dealing with actual analyses of marine ore samples. The nuclear instrumentation used in these studies, the procedures for activation analysis and the analytical results obtained are described from actual undersea operation.

NUCLEAR EQUIPMENT

A 200μg Cf-252 source was used for the undersea sample activation. This quantity of Cf-252 proved both safe to handle aboard ship and high enough in neutron production for sample activation. The measured thermal neutron flux in sea water on the top layers of the synthetic ore samples was about 10^6 neutrons/cm^2/sec. A 3 inch x 3 inch sodium iodide thalium activated crystal detector was used for gamma ray measurements. Germanium lithium drifted detectors were evaluated for their high gamma ray resolution potential but presented problems with low temperature underwater operation. The high cross section of sodium iodide crystals for gamma ray detection and its less critical temperature operation were the deciding factors for its choice. Four different multichannel analyzers were used for data storage and pulse height analyses. They were a 100 channel Picker Nuclear Spectron 100, a 400 channel Texas Measurement Corporation, a 512 channel Nuclear Data and a 200 channel Packard 930. Instrument evaluation was based on reliable operation at sea, capabilities to handle desired data and data presentation. Of these instruments, the 400 TMC and the Packard 930 proved to be the better instruments, primarily because of their capability for battery-powered operation.

ANALYTICAL PROCEDURE

A study of the nuclear properties and ore abundances of the elements listed in Tables I and II showed that most elements of interest could be sufficiently activated in a 10-minute irradiation period to produce measurable radioactivity. Since in the actual undersea operation a wide spectrum of elements would be of interest, a 4-minute irraduation time was selected to permit investigation of most elements without undue delay in the undersea analysis. After activation a large amount of the sample's initial radioactivity was due to the short lived isotopes. A delay of 30 seconds prior to measurement of the induced radioactivity allowed most of the short lived isotopes to decay, which greatly decreased the background activity of the sample. The 30-second delay afforded the time for transfer of the neutron source and placement of the detector on the activated sample. Of the three vehicles used in the study, the scuba divers had no trouble meeting this transfer time; the submersible accomplished the task with practice, and the sled operation could meet it only with diver direction. Radioactive measurements of the activated ore samples were carried out for a 4-minute counting period. In some samples the radioactivity was high enough to register a 15-40% dead time in the analyzers.

ELEMENTS ANALYZED

The undersea analyses were carried out with two major goals in mind. First, to determine if undersea neutron activation analysis could detect element concentration levels comparable to terrestrial ores. The second goal was to establish the range of element detection that could be expected above or below ore grades at imposed undersea conditions and activation analyses parameters set for the analytical system. Since undersea work requires the conservative use of the

life support systems the most expedient method of element identification and estimate of element concentration was adopted. This was to establish element concentration levels at which photopeak energies for specific elements could be detected. In practice, if a photopeak was present in the analytical data it could be assumed the element content of the sample was at or above a predetermined concentration level. Conversely, if no photopeaks appeared then it could be assumed the element was not present or was at a low concentration of little commercial interest. It had originally been planned to use a computer-multichannel analyzer with an integrating light pen for rapid analysis, but lack of financial support for this instrumentation did not permit this approach. It was therefore decided to use a rather practical approach (described above) with equipment at hand to show the feasibility of the method. Photo 4 shows a multichannel analyzer, its scope and a television screen. On the multichannel scope can be seen a pictorial display of the accumulated data with a V-52 photopeak. The T.V. camera shows a underwater picture of the nuclear detector measuring the activated synthetic vanadium ore sample. Table III shows the undersea neutron activation results as element concentration levels that were detectable for the synthetic ore samples with the stated imposed activation analysis parameters. The lower detectable element concentration range in column 4 is estimated from the data collected in sample analyses.

HEALTH PHYSICS

Health physics parameters are a primary concern associated with the application of Cf-252 sources in undersea mineral exploration programs. An evaluation of these parameters is particularly important since excessive radiation doses to personnel routinely working with Cf-252 sources for shipboard operations would prohibit practical application of the system.

The Cf-252 source used in this program was approximately 200 micrograms, or 107 millicuries, which was encapsulated in a stainless steel primary capsule and an aluminum secondary capsule. The dimensions of the source are 1.5 inches in height by 0.75 inches cylinder diameter. The dose equivalent rates measured in air at 1.0 meter from the source with a Texas Nuclear, Model 9120, spherical neutron dosimeter and a Victoreen, Model 440, ionization chamber were 450 millirem per hour neutron and 35 millirem per hour gamma. Projected dose equivalent estimates were based on these measurements.

The most serious hazard from the Cf-252 source occurred when the source was out of the shipping container while being transferred to or from the undersea neutron source housing. A 55-gallon drum filled with water was employed for shielding and a quick-release bracket was used to position the housing in the drum during these loading and unloading procedures. The measured dose equivalent rates to personnel involved in these procedures were approximately 250 millirem per hour to the body and 500 millirem per hour to the hands. Less than 5 minutes were required to complete the transfer procedures for field operations. After the undersea neutron source housing was loaded with the source, it was stored in the shipping container and paraffin blocks were positioned around the container and on top of it for additional shielding.

Three different modes of operation were employed to position the Cf-252 source to achieve neutron activation of samples. When the Deepstar 2000 submersible was used a six-foot boom was appended to the bow of the submersible. After the submersible had been launched the loaded undersea neutron source housing was lowered over the side, with a handling line attached, to a diver who then swam to the submersible and mounted the source in a quick-release bracket at the end of the boom. Once mounted, the neutron source housing could be viewed by personnel inside the submersible. At the completion of a dive, the neutron source housing was retrieved by the diver and returned to the shielded container. The primary advantage of this procedure was to allow the sea to be used for shielding, thereby minimizing the radiation dose to deck personnel and personnel inside the submersible.

When the Cf-252 source was used on the undersea sled or hand-held in position by a scuba diver, a seven-foot handling tool was attached to the undersea neutron source housing. The housing remained in the shielding container while the tool was being attached with a quick-release clamp. This handling tool could then either be attached to the sled by a diver or used as a manipulating tool for hand-held operations, again allowing the sea to be used as shielding. During all operations divers were instructed to maintain a position that would allow currents to sweep activation products, primarily sodium and

chlorine, away from the diver in the direction of the Cf-252 source. No radioactivity was detected in water samples obtained by divers and dose equivalent estimates for divers during these operations were less than three millirem per hour. This estimate was based on measurements with an Eberline, Model PRM-5 neutron detector and a Victoreen, Model 440 ionization chamber when the Cf-252 source was submerged to a depth of 4 feet, the minimum working distance from the source.

Radiation doses for all personnel were monitored with a standard, commercial service film badge containing both beta-gamma and neutron track films. The highest dose reported was 50 millirem from gamma radiation and 30 millirem from neutron radiation. This dose was for an individual involved in the procedure to load and unload the Cf-252 source in the undersea housing and represents a level below the commonly used guide of 100 millirem per week.

In addition to film badges, personnel who worked in the immediate vicinity of the Cf-252 source were also monitored with tissue equivalent pocket chambers and health physics surveys were conducted to insure that radiation doses did not exceed safe working levels and to provide additional data for dose equivalent estimates. The highest estimated dose equivalent from this data was approximately 30 per cent higher than the measurements with the film badges.

SUMMARY

The undersea mineral exploration work reported in this paper has shown the feasibility of utilizing undersea vehicles and neutron activation analysis to evaluate undisturbed sea floor mineral deposits.

Three types of vehicles were used for undersea instrument transport and investigation of the sea floor. A scuba diver team proved to be an excellent method for investigating ocean bottom depths to 60 feet. The Westinghouse Deepstar 2000 submersible, with its self-contained power and life support system, was the superior vehicle for depths greater than 60 feet. The underwater sled was functional but demonstrated the need for self propulsion capabilities and diver direction. Great advantage was found in placement of personnel on the sea floor, either as divers or within a submersible, to select samples, maneuver instrumentation and assist in sample collection.

Sea floor neutron activation analyses were carried out on elements made up as synthetic ores. The results showed that samples could be analyzed for element concentration levels of commercial interest. It is anticipated that with state of the art instrumentation and application of analytical parameters specific to elements of interest, that some 14 elements could be feasibly detected.

The health physics study of the total marine exploration study showed that a Cf-252 source could be used in all phases of the marine work without undue radiation hazards to participating personnel.

TABLE I

ELEMENT NEUTRON ACTIVATION ANALYSIS

Element	Activation	Eγ (Mev)	Product T 1/2	σ (barns)	% Abundance	Approximate Branching Ratios	†† $S(1 - e^{-\lambda t})$
U	$^{238}U+n \rightarrow {}^{239}U+\gamma+\beta^-$	.074	23.5m	2.8	99.27	~.99	.16
Fe	$^{58}Fe+n \rightarrow {}^{59}Fe+\gamma+\beta^-$	1.1,1.29,0.19	45d	0.9	0.33	(.57,.43,.028)	Neglig.
*Mn	$^{55}Mn+n \rightarrow {}^{56}Mn+\gamma+\beta^-$	.85,0.8,2.1-3	2.58h	13.3	100.0	(>.5,~.3,~.2)	.02
Cr	$^{50}Cr+n \rightarrow {}^{51}Cr+\gamma$	.32	27d	16	4.4	.09	Neglig.
Ni	$^{64}Ni+n \rightarrow {}^{65}Ni+\gamma+\beta^-$	1.5,1.12,.37	2.56h	2	1.0	(~.29,~.14,)	~.02
*Mo	$^{100}Mo+n \rightarrow {}^{101}Mo+\beta^-$	.19,.96	15m	0.2	9.5	†	.21
*V	$^{51}V+n \rightarrow {}^{52}V+\gamma+\beta^-$	1.4	3.77m	4.5	99.75	1.0	.61
W	$^{182}W+n \rightarrow {}^{183}W+\gamma$	0.21,0.16	5.5 sec.	0.5	26.2	1.0	~ 1.0
*W	$^{184}W+n \rightarrow {}^{185m}W+\gamma$	0.13	1.7m	2.0	30.7	1.0	.87
*Co	$^{59}Co+n \rightarrow {}^{60m}Co+\gamma$	1.33	10.5m	18.0	100.0	~ 1.0	.28
*Cu	$^{65}Cu+n \rightarrow {}^{66}Cu+\gamma+\beta^-$	1.04	5.1m	2.2	31.0	.09	.50
*Pb	$^{206}Pb+n \rightarrow {}^{207m}Pb+\gamma$	1.07,0.57	.8 sec.	0.03	26.0	1.0,1.0	Saturation
Zn	$^{68}Zn+n \rightarrow {}^{69m}Zn+\gamma$	0.44	14 hr.	0.09	18.6	1.0	Neglig.
Zn	$^{70}Zn+n \rightarrow {}^{71}Zn+\gamma$	.4,.5,.6	3 hr.	0.09	0.63	1.0	Neglig.
*Sn	$^{124}Sn+n \rightarrow {}^{125}Sn+\beta^-+\gamma$	.33,1.4	9.5m	0.2	6.1	1.0,.02	.31
*Al	$^{27}Al+n \rightarrow {}^{28}Al+\gamma+\beta^-$	1.78	2.3m	0.23	100.0	1.0	.78
Au	$^{197}Au+n \rightarrow {}^{198}Au+\gamma+\beta^-$	.411,.68,1.09	2.7d	9.8	100.0	(.98,--)	Neglig.
*Ag	$^{107}Ag+n \rightarrow {}^{108}Ag+\gamma+\beta^++\beta^-$	.66,.43,.6(.511)	2.3m	3.0	51.4	(~.01 all)	.78
Be	$^{9}Be+n \rightarrow {}^{10}Be+\beta^-$	No γ	10^8 yr	0.01	100.0	X	Neglig.
*Hg	$^{204}Hg+n \rightarrow {}^{205m}Hg+\gamma+\beta^-$	0.2	5.2m	0.4	6.8	1.0	~ .5
*Ti	$^{50}Ti+n \rightarrow {}^{51}Ti+\gamma+\beta^-$	.32,.93,.61	5.8m	0.14	5.3	~.95, ~.05	~ .45
*Mg	$^{26}Mg+n \rightarrow {}^{27}Mg+\gamma+\beta^-$	.84,1.02,.18	9.5m	0.03	11.1	~.7, ~.3	.31
*S	$^{36}S+n \rightarrow {}^{37}S+\gamma+\beta^-$	3.1	5.0m	0.14	0.017	.9	.5
K	$^{41}K+n \rightarrow {}^{42}K+\gamma+\beta^-$	1.5,.32	12.5m	1.1	6.8	.18	Neglig.
P	$^{31}P+n \rightarrow {}^{32}P+\beta^-$	No γ	14.5d	0.20	100.0	X	Neglig.

† See later decay scheme

†† Assume $\phi = 8 \times 10^7$ n/cm^2/sec; 4" x 7" NaI(Tl); Yield = 0.1; Irradiation Time = 2-5 minutes.

* Promising

TABLE II

ORE GRADE OF CURRENTLY EXPLOITED TERRESTERIAL MINERALS

Element	Ore Grade (%)	Element Content (%)
U	0.1 - 0.2 $U_3 O_8$	0.175
Fe	20 - 70 Fe	20 - 70.0
* Mn	15 - 55 Mn	15 - 55.0
* Cr	15 - 68 $Cr_2 O_3$	46.0
Ni	0.9 Ni	0.9
* Mo	0.2 Mo	0.2
* V	1.0 - 2.0 $V_2 O_5$	1.1
* W	0.3 - 1.0 WO_3	0.8
* Co	0.2 - 1.5 Co	0.2 - 1.5
* Cu	0.4 Cu	0.5
* Pb	3.5 - 5.0 Pb	3.5 - 5.0
Zn	5.0 Zn	5.0
* Sn	0.5 Sn	0.5
* Al	50 $Al_2 O_3$	27.0
Au	~ 5 oz/ton Au	~ 0.0001
* Ag	~ 10 oz/ton Ag	~ 0.03
Be	10 - 12 BeO	4.3
* Hg	~ 5 lbs/ton Hg	.25
* Ti	20 - 60 TiO_2	36.0
* Mg	20 - 69 MgO	41.0
S	15 - 40 S	15 - 40.0
K	14 $K_2 O$	13.0
P	15 $P_2 O_5$	6.6

* Promising

Reference - *Mineral Resources* by Peter T. Fawn

TABLE III

UNDERSEA NEUTRON ACTIVATION ANALYSIS OF SYNTHETIC ORE SAMPLES WITH Cf-252

Element	Terresterial Ore Element Content (%)	Synthetic Ore Element Content (%) (Detected)	Synthetic Ore Element Content (%) (Estimated Lower Range)
Mn	15 - 55.0	10.0	0.1
V	1.1	1.0	0.5
Cu	0.5	10.0	2.0
Al	27.0	10.0	1.0
Sn	0.5	15.0	3.0
Ag	~ 0.03	5.0	0.3
Hg	0.25	20.0	10.0
Ti	36.0	20.0	4.0

Analytical Parameters:

Cf-252 thermal neutron flux ~ 1 x 10^6 n/cm^2/sec

4 minute irradiation, 30 second delay, 4 minute sample count

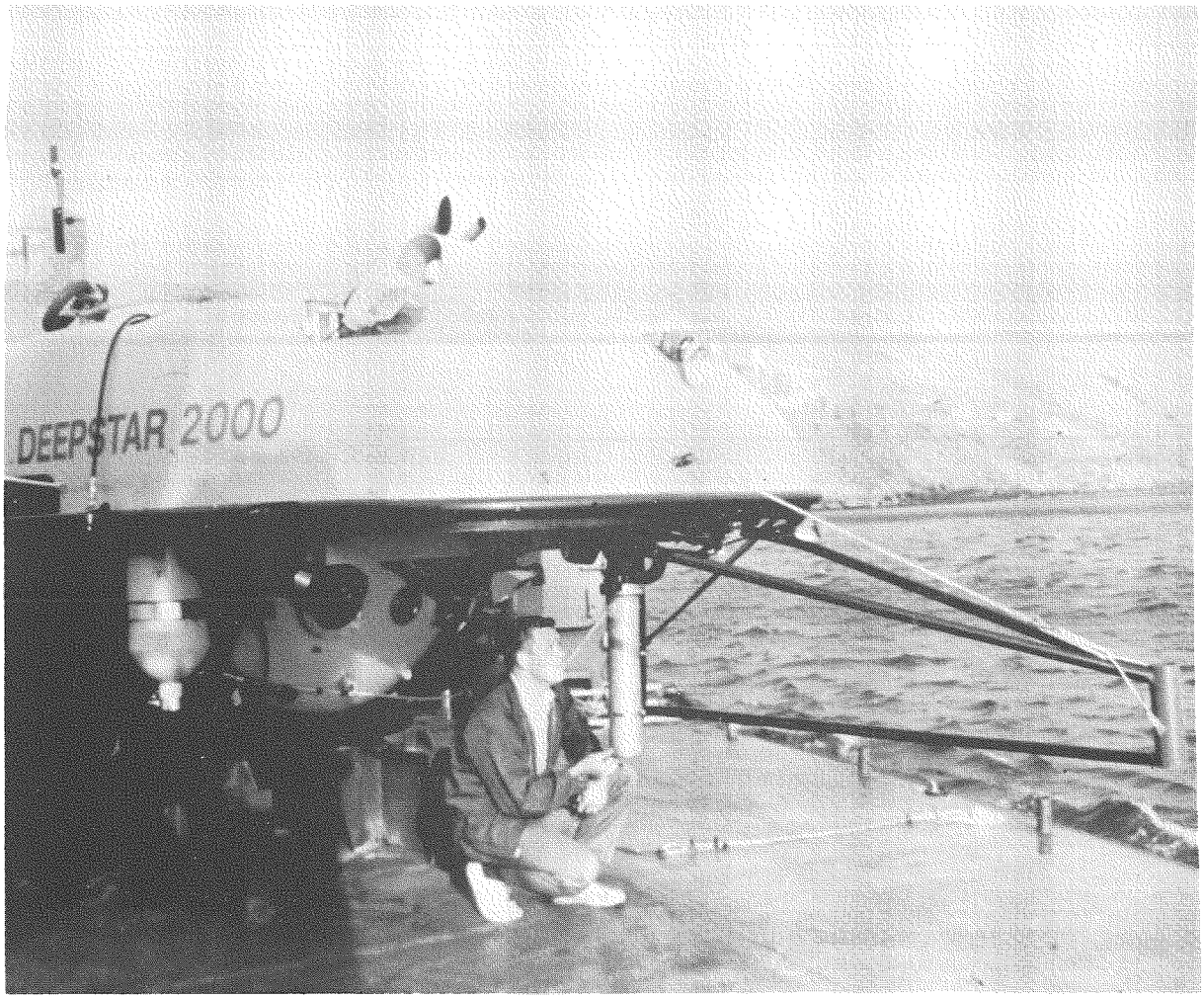

Photo 1

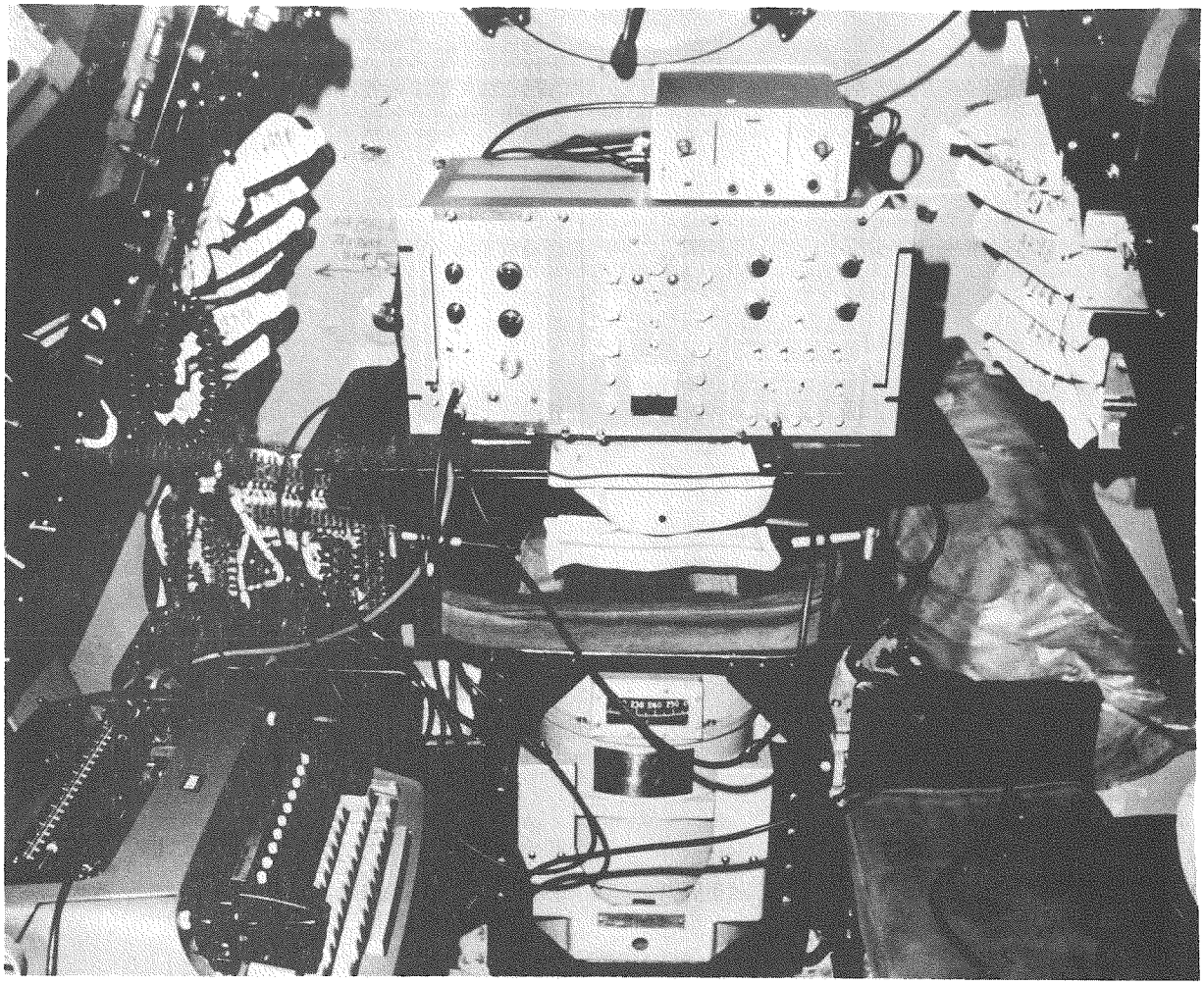

Photo 2

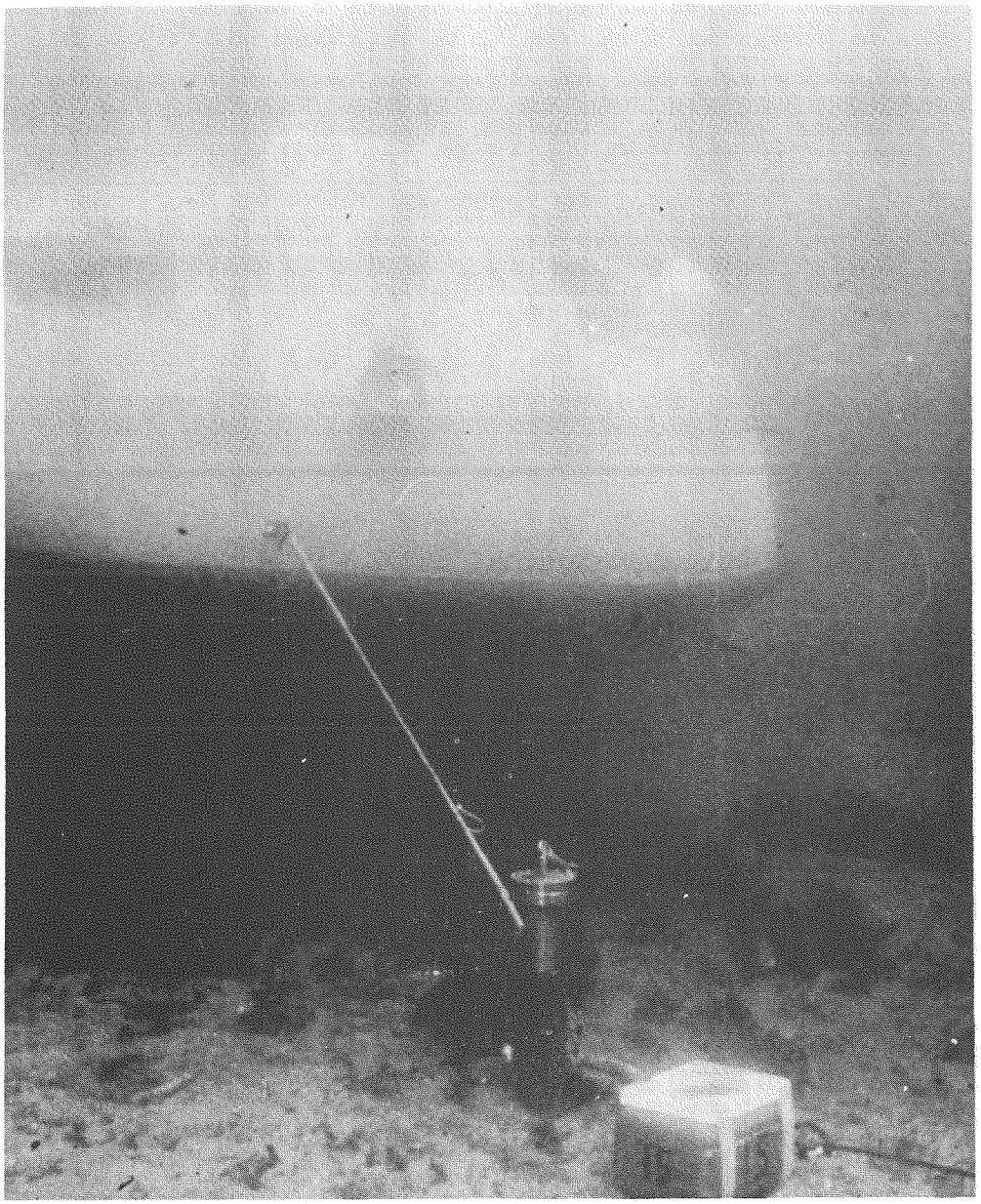

Photo 3

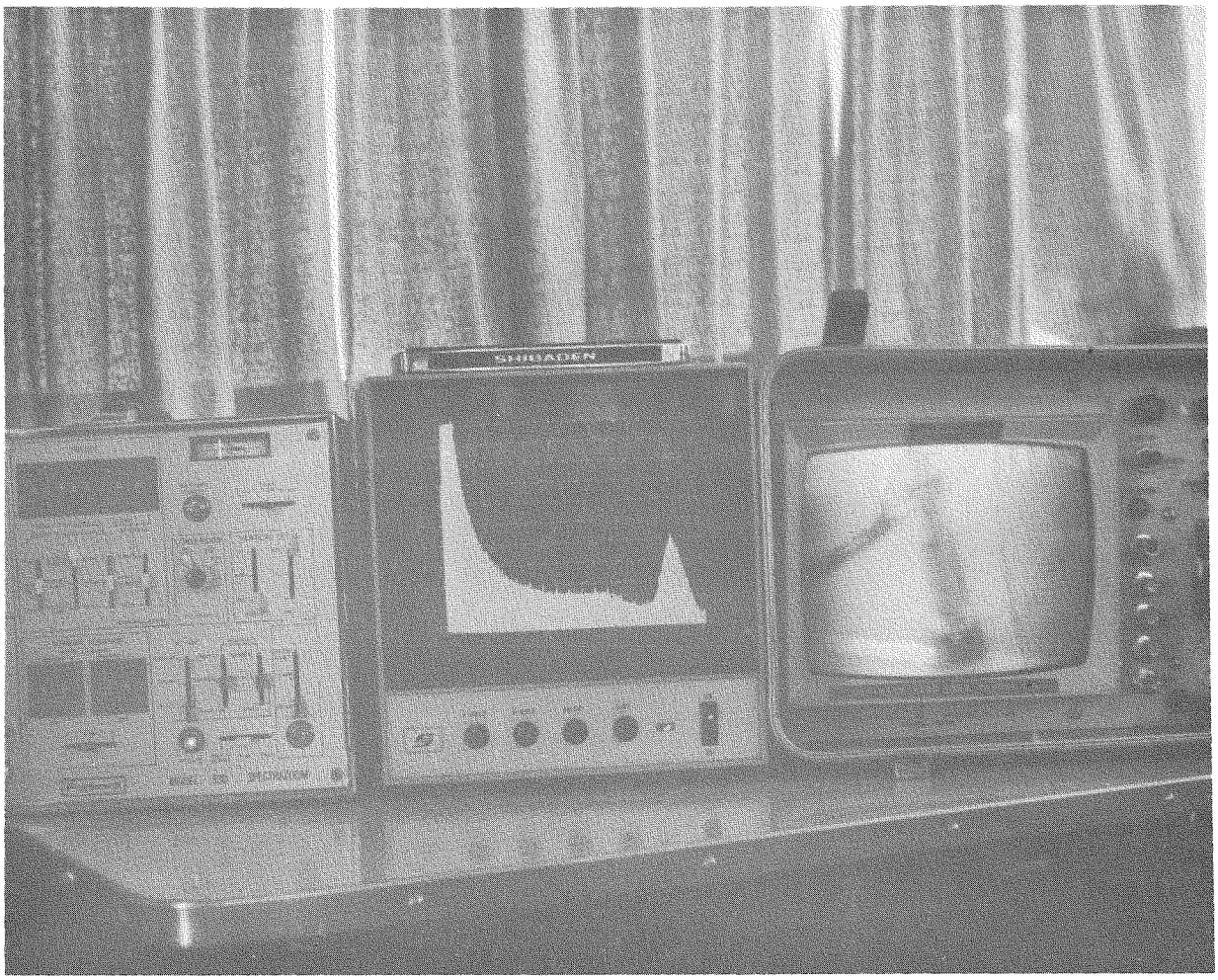

Photo 4

CALIFORNIUM-252 NEUTRON ACTIVATION FOR TERRESTRIAL, SEA FLOOR, AND POSSIBLE PLANETARY SURFACE ANALYSIS

R. W. Perkins, W. A. Haller, H. G. Rieck,

L. A. Rancitelli, and N. A. Wogman

Battelle-Northwest
Richland, Washington

The high neutron emission rates presently available from ^{252}Cf sources have dramatically improved the potential applications of both laboratory and *in situ* neutron activation analyses of minerals. In recent laboratory studies of 200 lb. ore samples, techniques have been developed which permit the very rapid analysis of more than 16 elements at concentrations which are generally well below those of commercial interest. These developments were based on studies conducted with 260 μg and 1.8 mg ^{252}Cf sources for neutron activation and a 50 cc Ge(Li) diode for the gamma-ray spectrometric analysis. In feasibility studies carried out in several feet of water in an ocean tidal zone, it was demonstrated that elements such as Au, Ag, and Mn could be measured in concentrations as low as a few ounces per ton. This report describes the technology which has been developed for either ground-based or shipboard laboratory mineral analysis, the technology and equipment which is being developed for *in situ* analysis of the floors of fresh and salt water basins, and the potential applications of this technology for planetary surface analysis.

INTRODUCTION

In situ elemental analysis is extremely desirable in a large number of applications. Mapping of the mineral composition of terrestrial areas and of the ocean floor could be greatly simplified by rapid in situ elemental analysis, while the surfaces of the planets could be analyzed remotely. In considering possible methods for multielement analysis, one normally considers x-ray, arc or mass spectrometry, and alpha scattering techniques. While these techniques are usually considered as laboratory tools, they can potentially be used for in situ analyses, and indeed, the alpha scattering techniques have received worldwide attention because of their successful implementation in analyzing major elements in the lunar surface. All of these procedures involve rather complex instrumentation and have not been seriously considered for hostile environments such as the ocean floor or for the surface analysis of planets with dense atmospheres.

Two major developments during the past few years have dramatically changed the potential of neutron activation analysis for both the quantitative measurements performed in mineral assay laboratories and for a variety of in situ mineral analyses. These include the production of useful quantities of the isotopic neutron source, ^{252}Cf, and the development of very efficient, high resolution Ge(Li) gamma-ray detectors for measuring the neutron activation products. The extremely compact nature of the ^{252}Cf source permits two different approaches to mineral analysis by neutron activation. When the neutrons are captured by the various elements in the mineral, "prompt gamma-rays" are emitted immediately, and their measurement can be employed to determine the elemental content of the sample. This method has been investigated for the measurement of manganese and gold[1] in simulated ocean floor conditions, and silver in simulated terrestrial deposits[2]. In addition, the capture of neutrons by most elements produces radionuclides of the element, and in their subsequent decay "delayed gamma-rays" are emitted which can be measured to determine the elemental content of the sample. The detection of prompt gamma-rays allows the measurement of certain elements such as iron and silicon, which cannot be determined by subsequent radionuclide analysis. However, the necessary physical proximity of the ^{252}Cf neutron source and detector for the prompt gamma-ray measurements makes a much less sensitive procedure for the nondestructive analysis of many of the elements in minerals. Recent studies in our laboratory have demonstrated that by induced radionuclide analyses the majority of elements of commercial interest can be measured in minerals at concentrations well below those of economic value[3]. These measurements also suggest that in situ analysis of terrestrial surfaces and the floors of fresh and salt water basins can be made with comparable sensitivities to those

which we have observed in the laboratory.

A major constraint in the use of ^{252}Cf sources for in situ analysis has been the relatively high radiation level associated with milligram-size ^{252}Cf sources which are required for this work. In recent developments at our laboratory, it has been demonstrated that neutron multiplication of 30 to 40 fold can be achieved in a small subcritical assembly[4]. This technology could allow a 30 to 40 fold smaller ^{252}Cf source to be used for the in situ analysis program. When an actual in situ neutron irradiation was to be made, the 30 to 40 fold multiplication could be obtained by mechanically inserting the source into the multiplier device. The major advantages of this technology in both economy of the ^{252}Cf source size and the radiation shield problems during shipment and non-use periods are obvious.

The present work has been concerned with determining the feasibility of seabed and terrestrial mineral analysis and with developing practical methods for implementing these types of measurements. These studies suggest the feasibility of this type of technology for application to planetary surface analysis on planets with both rare and very dense atmospheres.

TECHNOLOGY DESCRIPTION AND EXPERIMENTAL EVALUATION

Californium-252 provides essentially a point source of fission neutrons which require moderation for their most effective use in either laboratory or in situ activation analysis. The spontaneous fission decay mode of ^{252}Cf involves the emission of 2.34×10^9 $n.mg^{-1}.sec^{-1}$, thus the actual mass of the ^{252}Cf source is insignificant. In our initial laboratory feasibility studies[3], the ^{252}Cf source was contained in the center of a 4-inch thick slab of paraffin. A 200 liter drum located directly over this source served as a neutron moderator and contained a 3-inch diameter vertical access port through which mineral samples could be placed within about 2 inches of a 260 microgram ^{252}Cf source. The characteristic gamma-ray spectra for some 20 minerals, after 2-5 minute irradiation and counting periods, were obtained from this system. This information demonstrated the practicality of this technology for laboratory mineral analysis. To evaluate the potential of in situ neutron activation analysis of terrestrial and ocean floor regions, the experimental arrangement shown in Figure 1 was used. In this arrangement a 210 microgram ^{252}Cf source was located in the bottom of a 2 foot diameter by 4 foot high polyethylene tank. This container in turn was located in a 6 foot diameter water-filled polyethylene tank which served as a radiation shield. With this arrangement, bulk ore or simulated ore samples which represented an essentially infinite source could be irradiated. After a short irradiation, they could be rapidly removed and placed under a Ge(Li) diode detector for counting as shown in the illustration. The addition of seawater and fresh water around the ^{252}Cf source-moderator and the Ge(Li) diode detector permitted the simulation of the anticipated irradiation and counting geometries at the floor of ocean and fresh water basins. Without the water present, a terrestrial (earth's surface) analysis could be simulated. The radiation level at the surface of the 6 foot diameter shield was about 0.3 mr per hour. Measurements of the gamma-ray spectra of various types of ore and of simulated ore samples showed excellent photopeak resolution and indicated the feasibility of employing this type of technology for both terrestrial and ocean floor analysis.

An essential step in developing this technology for seabed mineral analysis was an actual in situ feasibility demonstration. This feasibility demonstration was conducted at the Battelle-Northwest Marine Research Laboratory at Sequim, Washington. For this study 200 pound samples of minerals, or simulated mineral samples containing known amounts of various elements, were placed in the tideland ocean floor during the low tide. These samples were contained in cut-off 55 gallon drums which were approximately 10 inches deep and 22 inches in diameter (see Figure 2). At high tide when the measurements were made, these samples were covered with 4-5 feet of seawater. The samples were irradiated with a 210 microgram ^{252}Cf source which was located about 2 inches from the bottom of a 6 inch diameter by 10 inch high paraffin moderator. This source was positioned directly over the center of the sample. Irradiation times of 120 seconds followed by a 30 to 40 second decay period and an in situ counting time of 200 seconds were employed. The gamma-ray spectrometric measurements were made with a 50 cm^3 Ge(Li) diode which was centered directly over the sample. Figure 3 shows the gamma-ray spectrum of a silver bearing dunite sample which was irradiated and counted under these conditions. The silver content of this sample was 0.05%,

while the manganese content was about 0.1%. The concentrations of Mn and Ag, as well as those of Mg, Al and V, were easily measurable from the photopeak areas. There was not a detectable photopeak from ^{24}Na and the photopeak from ^{38}Cl (37 min) was relatively small. This confirmed our laboratory observations that induced ^{24}Na and ^{38}Cl in the ocean floor should not significantly interfere with measurements of the mineral composition. As indicated in Figure 3, several elements can be observed and measured reasonably well from their photopeak areas after a short irradiation with the 210 microgram ^{252}Cf source; however, this source size is not sufficient for the measurement of all of the elements of interest. From consideration of the total acceptable counting rate, it appears that a 5 mg ^{252}Cf source would be about optimum for this type of application; however, radiation shielding and handling considerations dictate a source of 1 mg or less which should be adequate if a large, efficient Ge(Li) diode detector is used for analysis. If a neutron multiplier unit could be used, the needs for both the high flux during usage and the low flux during loading and shipping could be met.

A detailed study of the sensitivity with which the various elements in mineral samples can be measured with an approximate 2 mg ^{252}Cf irradiation source is being conducted in a laboratory mockup arrangement. The experimental arrangement used for this program is shown in Figure 4. As indicated, the ^{252}Cf source is located near the bottom of a 12 inch diameter by 12 inch high paraffin moderator. This moderator is centered at the bottom of a 6 foot diameter by 7 foot deep polyethylene tank which in turn is contained in a 15 foot diameter by 7 foot deep plastic swimming pool. With this shielding, no gamma or neutron flux could be observed at the edge of the pool or the surface of the water. However, a neutron dose rate of about 10 mr/hr was observed at the sample channel opening. The mineral samples to be analyzed were contained in 10 inch high by 22 inch diameter cylinders as previously described. With the sample channel and sample dolly arrangement shown in Figure 4, the samples could be placed directly under the source for neutron irradiations. The neutron flux at the surface of the sample and at various depths within it was determined by foil irradiation techniques. Figure 5 shows the thermal neutron flux at the surfaces of paraffin and seawater substrates in the irradiation position directly beneath the ^{252}Cf source. The thermal neutron flux is only reduced by about 25% at the surface of seawater relative to paraffin. The neutron fluxes at the surface of paraffin and fresh water substrates are almost identical. In Figure 6 the horizontal thermal flux profiles at the surface of a dry dunite sample, dunite saturated with fresh water, and a dunite sample saturated with seawater are shown. There is very little difference between the thermal flux at the surface of fresh and salt water saturated dunite, however, the neutron flux at the surface of the dry dunite is substantially less.

Saturation of the dunite with fresh water or seawater increases the density from 1.5 to about 1.8. However, water does serve as an excellent moderator and results in the substantially higher thermal neutron flux at the surface of these dunite samples. As shown in Figure 7, the maximum thermal neutron flux at the center of a seawater saturated dunite substrate is about 1.7×10^7 $n.cm^{-2}.sec^{-1}$ and this decreases somewhat faster with depth than with lateral distance from the source. In this substrate the average thermal neutron flux is about 2 fold less than this center value through the volume of a 20 cm diameter hemisphere and about 3 fold lower through a 35 cm hemisphere. In Figure 8 the thermal and epithermal neutron fluxes at the surface of a seawater saturated dunite substrate are presented. It is important to note that the epithermal flux even at the center of the sample is about 25 fold less than the thermal flux. In addition, the epithermal flux drops off much more rapidly than the thermal flux. Thus the neutron flux impinging on the sample is reasonably well moderated.

Major emphasis in this program has been toward determining the sensitivity with which some 30-40 trace elements can be measured in an ocean floor substrate and determining calibration constants which can be used for an actual seabed mineral analysis. Table I summarizes the sensitivities for the measurement of 16 elements based on the use of a 1.8 mg ^{252}Cf source in the irradiation facility shown in Figure 4, and the 50 cm^3 Ge(Li) diode detector system shown in Figure 1. These measured sensitivities were all determined for seawater saturated dunite containing known amounts of the elements of interest; however, several actual mineral samples have been measured and indicate sensitivities within the ranges shown in Table I. The sensitivities are based on a 2 minute irradiation followed by

a 30 to 60 second delay and a 2 minute counting period. Such irradiation and counting periods appear adequate for the in situ analysis of most elements. The sensitivities in Table I for the simulated in situ condition are similar to those which were observed earlier in our laboratory mineral assay facility[4]. As suggested from the neutron flux curves for fresh-water-saturated dunite, the sensitivity for elemental analysis at the floor of fresh water basins is only slightly better than for the ocean floor. The sensitivities for elemental measurements on terrestrial areas with a given neutron source size are somewhat less than on the ocean floor because of the lower thermal neutron flux near this substrate surface. However, the rather wide range in sensitivities presented in Table 1 certainly cover the sensitivities for all three types of substrates.

DISCUSSION

While there are numerous parameters affecting analysis of ocean and fresh-water basin floors and of terrestrial surfaces, they are adequately accounted for if the simulated samples very nearly resemble the actual study areas. There are compensating factors and even if one were to apply the detection efficiency factors obtained for sea floor analysis in the analysis of a dry terrestrial surface, the errors would be less than 50%. Where the actual density of the material is reasonably well known it appears that measurements to an accuracy of ± 10% will be possible. One problem which must be recognized, however, is that the observed sample sizes are somewhat different for each photon energy. For example, the sample size actually observed with ^{198}Au which emits a 0.41 MeV is much smaller than that from ^{26}Al which emits 1.779 MeV photons.

TERRESTRIAL MINERAL EXPLORATION

The very small physical sizes of both the ^{252}Cf source and the Ge(Li) diode detector make their combined use appear very attractive for in situ mineral exploration programs. From our laboratory studies in which massive (200-lb) ore samples were used, sensitivities comparable to those in Table 1 were obtained and these could be achieved for in situ terrestrial mineral analysis. For borehole measurements a "nuclear probe" consisting of a ^{252}Cf source separated by a specific distance from a Ge(Li) diode could be used in the simultaneous assay of several elements. The practicality of employing such a logging technique for multiple element analysis in wells or boreholes vs. collecting samples for laboratory analysis at the time of drilling would depend on the objectives of the programs.

SEABED MINERAL EXPLORATION

The continental shelf portions of the ocean floor are known to contain vast reserves of several minerals, yet relatively little exploration of these areas has been performed. The technology, described in this report, for rapid nondestructive mineral analysis in our earlier report[1] and in this work would be applicable to a shipboard laboratory and in situ analysis of the ocean floor respectively. Figure 9 shows a conceptual design of a nuclear probe which is being built for performing in situ mineral analysis of the ocean floor at depths of a few hundred feet. The operation will involve first the positioning of the probe on the ocean floor. A sequence will then be initiated which will rotate the ^{252}Cf source to the irradiation position, hold it there for a preset time of about 2 minutes, then reverse positions of the ^{252}Cf source and the Ge(Li) diode detector for a 2-minute count. With this procedure, a rather detailed mineral assay could be made in a 5-minute interval at each point of interest. The probe could be operated from a surface vessel using a TV monitor for probe positioning.

SUMMARY AND CONCLUSIONS

This study employing a ^{252}Cf neutron source for neutron activation, together with one of the best available Ge(Li) diode gamma-ray detectors, demonstrates the remarkably practical potential of this approach for in situ mineral exploration. Laboratory studies with a ^{252}Cf source indicated that most of the elements of commercial interest can be directly measured by a 2-minute irradiation and a 2-minute count. A 1-mg ^{252}Cf source would be adequate for such measurements and a rather detailed quantitative analysis of a substrate sample could be performed in 5 minutes by a trained technician.

The recent demonstration of the practicality of ^{252}Cf neutron flux multiplication[4] could permit the use of a 50 microgram source for this application and eliminate most of the shielding problems associated with its use.

In situ mineral exploration of the ocean floor, particularly on continental shelf

regions, appears feasible. Compared with any other potential method for in situ analysis, this approach appears extremely attractive. It could provide a rapid and practical approach to establishing the elemental content both of the ocean floors and of the floors of the large fresh water areas of the world.

In situ analysis of terrestrial surfaces and in boreholes or wells also appears feasible and may prove extremely useful. This approach could allow the rapid logging of boreholes for a wide spectrum of elements. It is obvious that a similar approach could be employed on a roving vehicle for unmanned planetary mineral analysis.

ACKNOWLEDGMENTS

The authors wish to express their appreciation to J. A. Cooper for assistance in design of the underwater detector system and for help in analysis of the gamma-ray spectrometric measurements and to D. R. Edwards, J. H. Reeves, and W. L. Butcher for assistance in the gamma-ray spectrometric measurements.

This paper is based on work performed under U. S. Atomic Energy Commission Contract No. AT(45-1)-1830.

REFERENCES

1. F. E. Senftle, Dick Duffey, and P. F. Wiggins. "Mineral Exploration of the Ocean Floor by In Situ Neutron Absorption Using a Californium-252 (^{252}Cf) Source." Marine Technol. Soc. J. 3, 5 pp. 9-16 (1969).

2. F. E. Senftle, P. W. Philbin, and P. Sarigianist. "Use of ^{252}Cf for Mineral Exploration: Comparison with Accelerators for In Situ Neutron Activation of Silver." Isotopes and Rad. Tech. 7, 4 pp. 411-418 (1970).

3. R. W. Perkins, L. A. Rancitelli, J. A. Cooper, and R. E. Brown. "Laboratory and Environmental Mineral Analysis Using A Californium-252 Neutron Source." Nucl. Appl. and Tech. 9, 861-874 (1970).

4. L. F. Hansen, N. A. Wogman, R. W. Perkins, and E. D. Clayton. "Subcritical Multiplication of ^{252}Cf Neutrons and Its Applications." To be published in the transactions of the 17th Annual American Nuclear Society to be held in Boston June 13-17, 1971.

SENSITIVITIES FOR THE MEASUREMENT OF TRACE ELEMENTS IN A SIMULATE OCEAN FLOOR MATRIX*

Element]	Isotope	Half Life	Detectable Concentrations
Indium	^{116m}In	54 min	1-10 ppm
Selenium	^{77m}Se	18 sec	10-100 ppm
Silver	^{108}Ag	2.4 min	10-100 ppm
Titanium	^{51}Ti	5.8 min	10-100 ppm
Vanadium	^{52}V	3.77 min	10-100 ppm
Gold	^{198}Au	64.8 hr	10-100 ppm
Manganese	^{56}Mn	2.5 hr	0.01- 0.1%
Aluminum	^{28}Al	2.3 min	0.1 - 1%
Arsenic	^{76}As	26.5 hr	0.1 - 1%
Cobalt	^{60m}Co	10.5 min	0.1 - 1%
Copper	^{66}Cu	5.1 min	0.1 - 1%
Molybdenum	^{101}Mo	14.6 min	0.1 - 1%
Antimony	^{122}Sb	2.8 day	1-10%
Cadmium	^{111m}Cd	49 min	1-10%
Magnesium	^{27}Mg	9.5 min	1-10%
Nickel	^{65}Ni	2.5 hr	1-10%

* Two minute irradiation
Two minute count

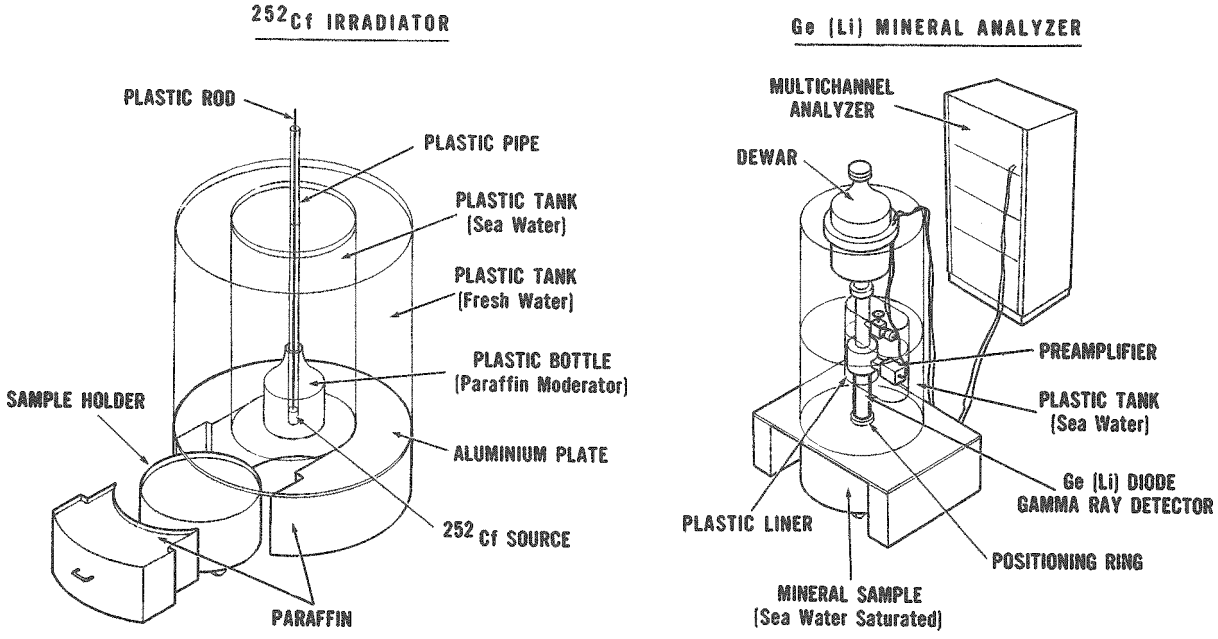

Figure 1 ^{252}Cf Neutron Irradiation Facility (Laboratory Prototype for in situ Seabed Mineral Analysis).

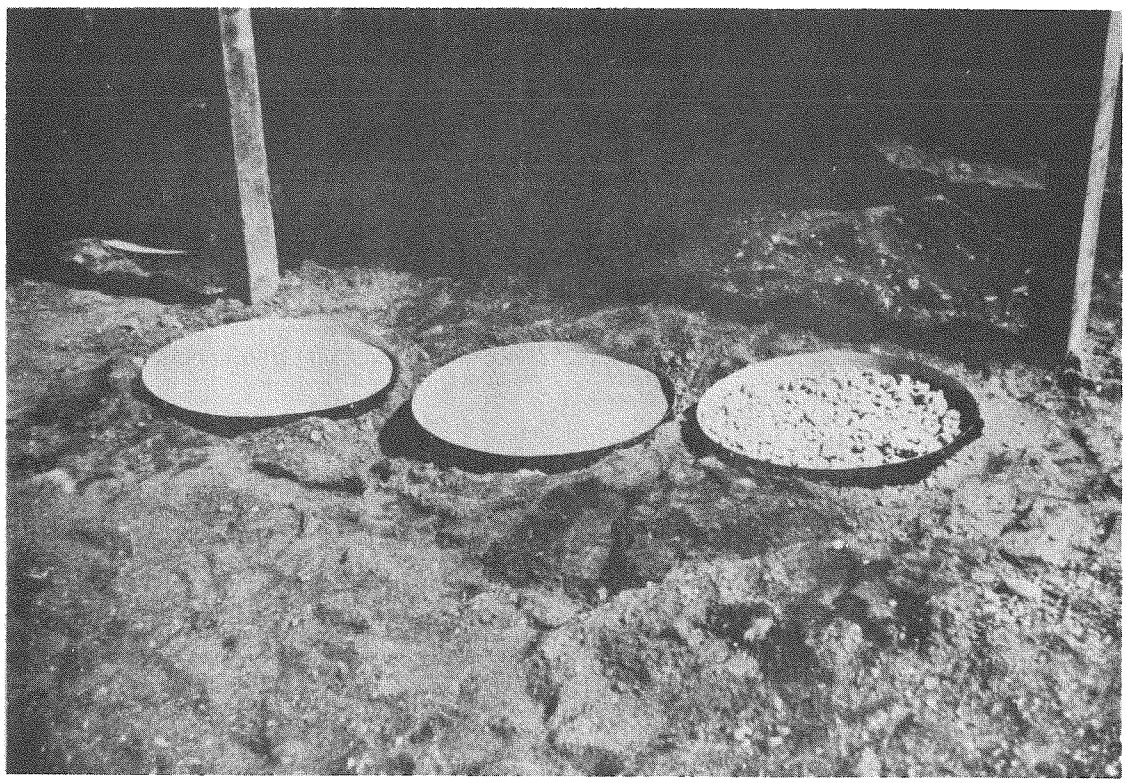

Figure 2 Mineral Samples Contained in Cut off 55-gallon Drums

Figure 3

GAMMA-RAY SPECTRUM OF SILVER BEARING DUNITE ON THE OCEAN FLOOR

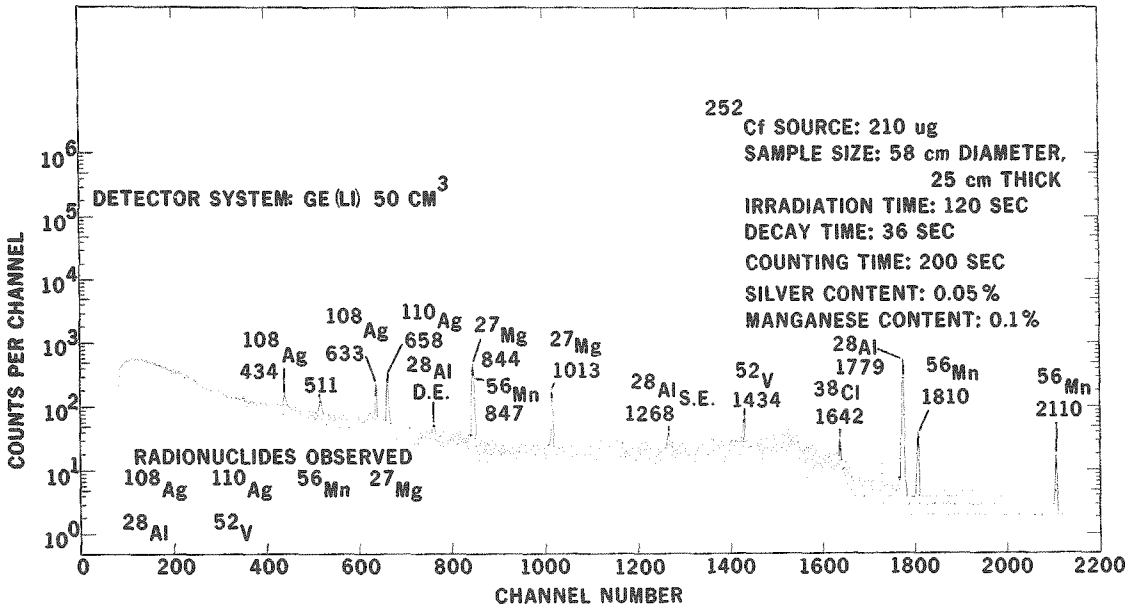

Figure 4

252CF IRRADIATION FACILITY

SIMULATION SYSTEM FOR SEA BED MINERAL ANALYSIS

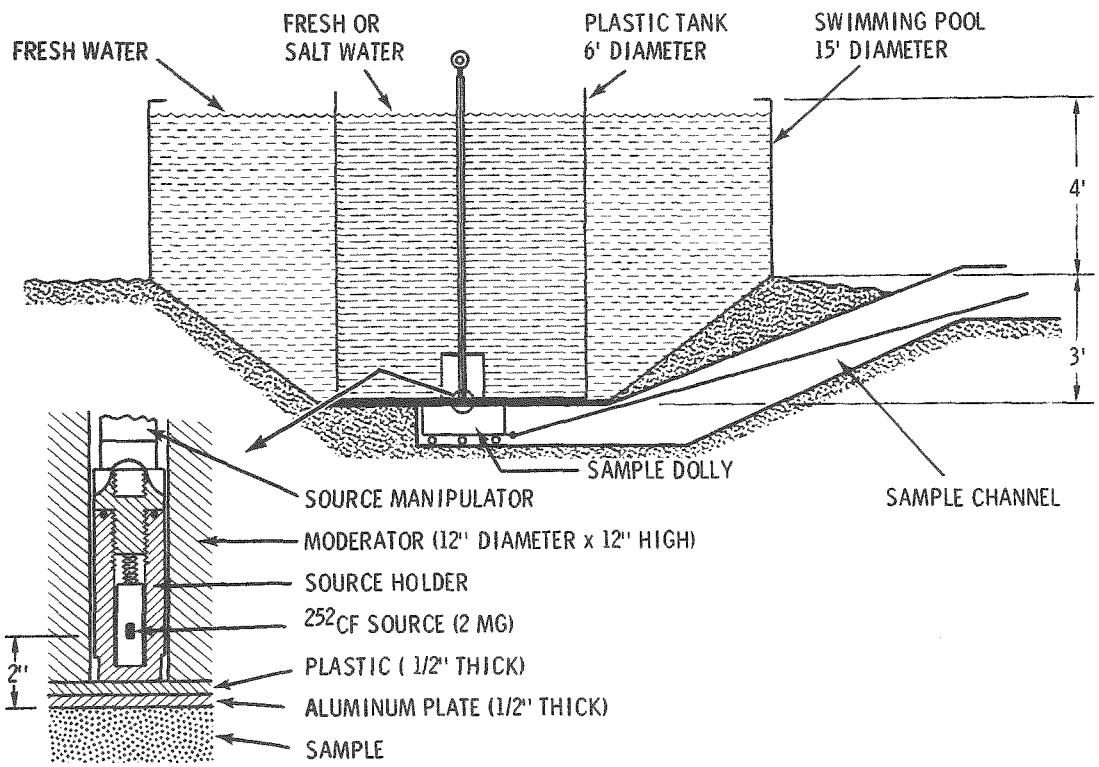

Figure 5

HORIZONTAL FLUX PROFILE AT THE SURFACE OF PARAFFIN AND SEA WATER SUBSTRATE BENEATH A ^{252}Cf SOURCE

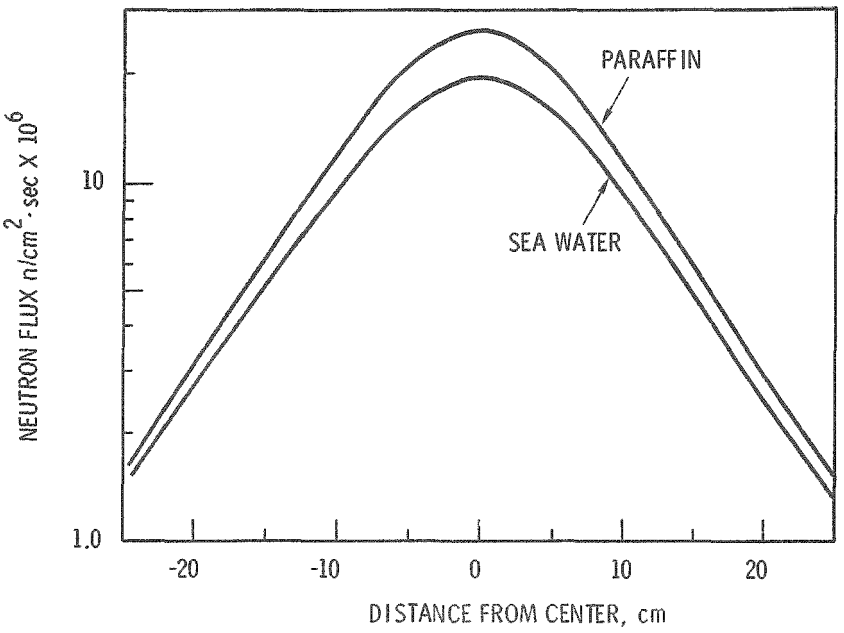

Figure 6

HORIZONTAL FLUX PROFILES AT THE SURFACE OF DUNITE SUBSTRATES BENEATH A ^{252}Cf SOURCE

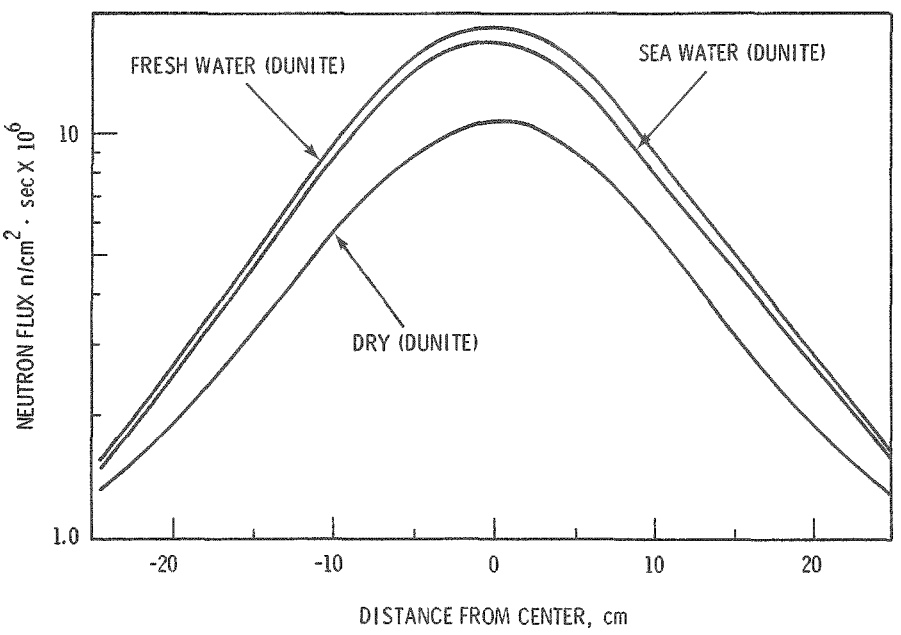

Figure 7

HORIZONTAL FLUX PROFILE AS A FUNCTION OF DEPTH
IN DUNITE SATURATED WITH SEA WATER

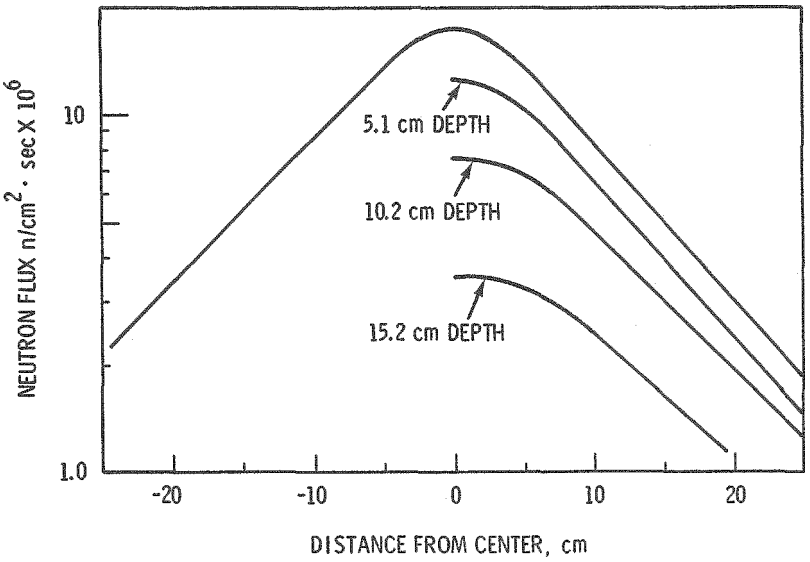

Figure 8

HORIZONTAL NEUTRON FLUX PROFILE AT THE SURFACE
OF SEA WATER SATURATED DUNITE

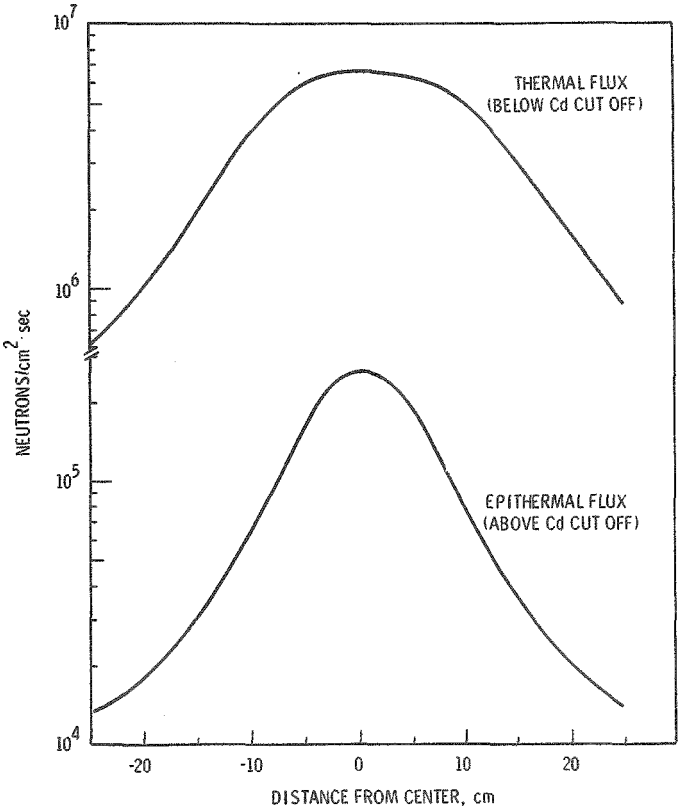

Figure 9

Seabed Mineral Exploration Probe Using a ^{252}Cf Neutron Source and a Ge(Li) Gamma-Ray Detector System

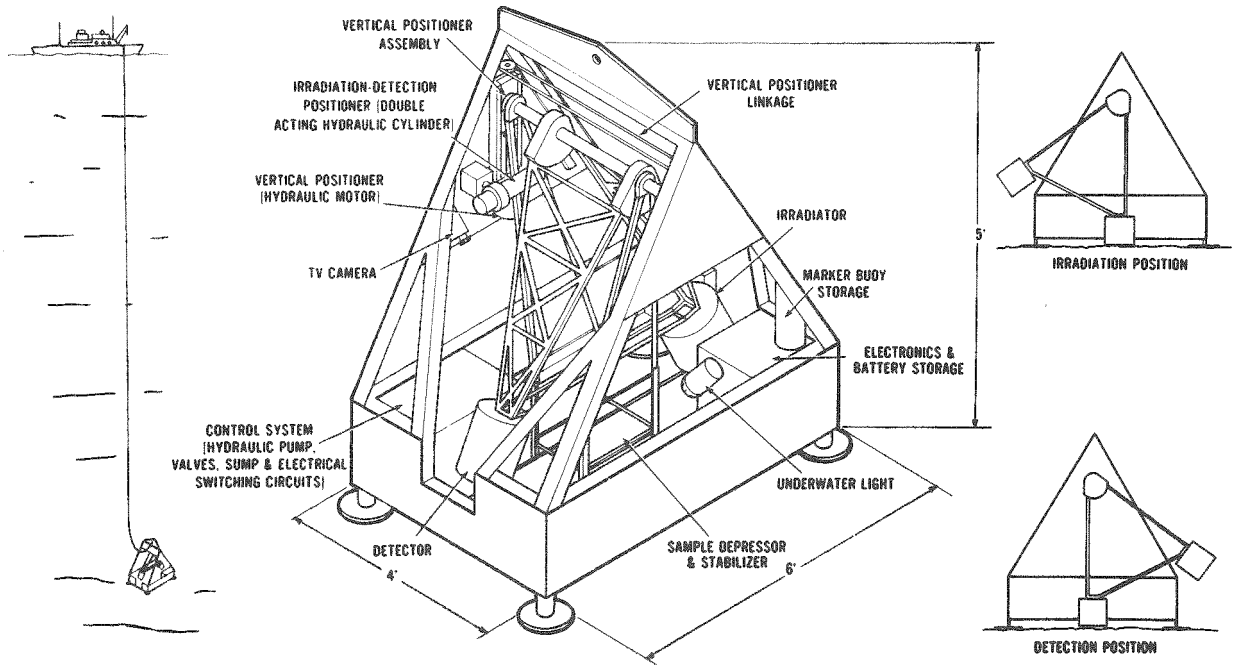

THE USE OF ^{252}Cf AS A NEUTRON SOURCE FOR WELL LOGGING

Hans J. Paap

Hugh D. Scott

Texaco Inc.
Bellaire Research Laboratories
Bellaire, Texas

A major goal of the well logging industry is the identification of potential oil producing horizons in the earth formations surrounding a borehole. Neutron logs are used to determine porosity, salinity, and the presence of gas. Improvements and new techniques possible with higher intensity ^{252}Cf neutron sources are discussed.

INTRODUCTION

Most oil and gas is produced from accumulations in the pore spaces of reservoir rocks. An important phase in exploration for oil and gas is the measurement of the properties of the earth formations surrounding a borehole to accurately identify the presence of potential producing horizons. This is known as well logging (Slide 1). The major parameters needed to evaluate a reservoir are the bed thickness, the rock porosity, the permeability and the hydrocarbon content. In situ measurements are made by lowering logging instruments into the borehole to measure the electrical, acoustical and nuclear properties of the formation. In Slide 1 a neutron log is being obtained by lowering an instrument into the borehole using a multiconductor cable. The instrument contains a neutron source and a detector to measure gamma rays produced by interaction of the neutrons with the rock formation.

Electric logs are used to differentiate between oil bearing and water bearing formations by measuring the resistivity of these formations. Acoustic logs are used to determine porosity, and nuclear logs can also be used to measure the formation density, porosity, and saltwater content. Combinations of acoustic and nuclear logs can be used to obtain better knowledge of lithology since they respond differently to rock type, and in favorable situations to distinguish between oil and gas.

True formation measurements are complicated by the fact that the borehole fluids used in drilling the well invade and contaminate the formations. After the borehole has been cased with steel pipe and cement, the problem of obtaining further logs to re-evaluate the well is essentially limited to nuclear methods since neutrons and gamma rays can penetrate steel and cement.

NEUTRON SOURCES

Neutron sources have been used for oil well logging since 1941. For several years Po-Be and Ra-Be neutron sources were used emitting about 10^7 neutrons/second. More recently Pu-Be sources have become the standard type of source due to the lower gamma ray output, but the neutron source strength has remained about the same. Systems using the d-t reaction in miniature accelerators have also been developed for pulsed neutron logging by the well logging industry.

A comparison of isotopic neutron sources available commercially for oil well logging is shown in Slide 2. Pu-Be has a very long half life, is

relatively cheap, but is limited in neutron yield by physical size. Am-Be sources can be made which emit 10^8 neutrons/second but the price is prohibitive for large scale commercial use. A source which will be marketed soon and which looks very attractive from neutron yield, half life, and price considerations, is Ac-Be. This source will probably be used in the future by the well logging industry. Po-Be sources can be made with a yield of 10^9 neutrons/second, but the short half life of 138 days makes this source uneconomical. The availability of Cf^{252} in the near future at the recently announced price of $10 per microgram (1 microgram of Cf^{252} emits 2.3×10^6 neutrons/second) will make this source the strongest and cheapest available with a reasonable half life. In Slide 2 the data for Cf^{252} do not include handling and encapsulation charges for individual sources since these are not yet available.

NEUTRON LOGGING

Neutron logs of a well are obtained by lowering into the borehole a source of fast neutrons together with a detector of neutrons or gamma rays spaced at a specific distance from the source. The neutrons are slowed down in the borehole and the surrounding formation by successive collisions losing most energy in collisions with hydrogen nuclei. When the neutrons have been slowed down to thermal velocities, they diffuse randomly until they are captured by nuclei of atoms such as hydrogen, silicon, and chlorine. As a result of these captures, high energy gamma rays are emitted, some of which enter the borehole and may be detected in the logging instrument. The energies of these gamma rays are characteristic of the element capturing the neutron and serve to identify the presence of these elements. As an alternative to detecting the capture gamma rays, the logging instrument can detect neutrons diffusing back into the borehole. Since the population of neutrons at a particular distance from the neutron source is sensitive to the hydrogen content of the formation, the neutron intensity can be related to the formation fluid content and thus the formation porosity.

Since the depth of investigation of conventional neutron logs is only a few inches, a large proportion of the measured response comes from the borehole mudcake and zone of invasion in open hole logging and from the casing column and cement in cased hole logging. It is generally believed that if the source to detector spacing is increased, the ratio of the formation to borehole signal can be improved. However, this cannot be accomplished without a considerable increase in neutron source strength.

The possible availability of Cf^{252} for industrial applications has encouraged us to investigate the potential of this isotope as a neutron source in well logging. Two sources containing 61 and 702μg Cf^{252} on loan from the AEC and emitting 1.4×10^8 and 1.6×10^9 neutrons per second, respectively, are being used for this work.

TRANSPORTATION AND HANDLING OF CF^{252} SOURCES

The use of these high intensity sources for oil well logging presented some new problems in handling and transportation. A photograph of the mobile radiation shield is shown in Slide 3. Both sources are stored independently in this shield and the radiation level at the edge of the truck bed is less than 2 millirems/hour as required by the State of Texas. The design of this shield is shown in Slide 4. The neutron moderating material is petrolatum to which boron has been added in the form of borax to absorb thermal neutrons. Lead around the source chamber absorbs most of the gamma rays emitted by the source. A cable is attached to the source holder, and a push rod is provided to remove the source holder from the shield.

The shield was designed so that the 700μg source could be remotely transferred from the shield to the logging sonde. (Slide 5). To load the 700μg source into the sonde

1) a special ramp holding the logging sonde is placed close to the port of the shield. The logging cable is attached to the top of the sonde.

2) the lucite plug is removed from the shield and the ramp is aligned with the port.

3) the source still attached to the winch cable is pushed from the shield into the bottom of the sonde with the 6' long push rod.

4) the sonde is automatically pulled by the logging cable until it is suspended above the wellhead.

5) the winch cable is detached from the source with a 30-foot long actuating rod and the sonde is lowered into the well.

This sequence is reversed to remove the sonde from the well and replace the source in the shield. The radiation dose to personnel during this operation is in the range of 0.5 to 1.0 millirem.

CF^{252} LOGGING RESEARCH

The investigation has been divided into five areas of interest as shown in Slide 6.

1) Activation logging
2) Dual spaced neutron logging for porosity
3) Chlorine logging
4) Neutron-gamma logging for gas
5) Neutron capture gamma ray spectra

1. Activation Logging

The technique of activation logging has been developed mostly in the USSR where logging speed is not an important commercial factor. A continuous activation log is made by moving the neutron source down the borehole to activate the formations followed by a detector to measure the delayed gamma rays emitted as radioactive nuclei decay (Slide 7). Tests have shown that neutrons can produce Al^{28} in shales by the reaction $Al^{27}(n,\gamma)Al^{28}$, and can also produce Al^{28} in sands by the fast neutron reaction $Si^{28}(n,p)Al^{28}$. Al^{28} decays with a half life of 2.3 mins and emits a gamma ray with an energy of 1.78 MeV. For Pu-Be neutrons which have an average energy of 4.5 MeV, many neutrons exceed the threshold energy of 3.85 MeV for the $Si^{28}(n,p)Al^{28}$ reaction. Cf^{252} neutrons have a lower average energy of 2.3 MeV so that fewer neutrons from this source exceed the silicon threshold. This results in less silicon interference with Cf^{252} as shown in the next slide (Slide 8). This shows the results of activating formations containing various amounts of quartz sand and alumina. From the magnitude of the intercept on the vertical axis, it can be seen that the interference from silicon if Cf^{252} is used is much less than if Pu-Be is used. For the range 10-20% Al_2O_3 this interference is 7-9 times smaller if Cf^{252} is used.

The second advantage of Cf^{252} over Pu-Be for aluminum activation logging is that Cf^{252} sources are not as limited in neutron output (Slide 9). The largest Pu-Be sources in use in well logging emit only 10^7 neutrons/second. With this source strength activation logs must be run at about 3 feet/minute to achieve acceptable detector count rates. This speed is obviously uneconomical for commercial logging. With a Cf^{252} source emitting 10^9 neutrons/second, detector count rates of 100-200 cps can be obtained and a logging speed of 20 ft/min can be used.

A typical activation log obtained with the 700μg Cf^{252} source is shown in Slide 10. This log shows three beds containing different amounts of aluminum or shale. The natural gamma ray log must be subtracted from the activation log for quantitative analysis.

2. Dual-Spaced Neutron Logging for Porosity

Several parameters which can affect neutron porosity logs are shown in Slide 11.

Borehole region:

1. Borehole size
2. Borehole fluid (mud, saltwater)
3. Mudcake on side of borehole
4. Sonde position in borehole
5. Borehole casing
6. Cement between casing and formation

Formation region:

7. Formation matrix (lime, sand, dolomite)
8. Salinity of formation fluid

9. Shaliness of formation
10. Formation temperature

Many of the neutron porosity logging instruments operated today by the commercial well logging service companies use a single epithermal neutron detector spaced at some specific distance from a 10^7 neutron/second Pu-Be or Am-Be neutron source[1]. Epithermal neutron detection is used to minimize the perturbing effects of strong thermal neutron absorbers in the formation and borehole. Slide 12 shows an improved type of porosity logging instrument using two detectors. This system was suggested by Allen et al[2] and requires detectors at large spacings from an intense source emitting more than 5×10^8 neutrons/second. This system is based on the fact that the borehole strongly attenuates the neutrons, whereas the formation is a relatively weak attenuator. Thus, to increase the sensitivity to the formation the detectors should be positioned as far as possible from the source. By using two detectors and taking the ratio of the counts in these, it should be possible to minimize the effects of variations in the borehole parameters. This technique uses two thermal neutron detectors to measure the neutron slowing down length L which is an epithermal neutron parameter. This can be used to determine the formation porosity if the formation matrix is known.

The availability of Cf^{252} sources emitting more than 10^9 neutrons/second now makes this technique possible. We have made porosity logs using two He^3 neutron detectors at spacings up to 72 and 102 cms from a 700μg Cf^{252} source. In Slide 13 are shown typical neutron distributions measured in freshwater limestone and dolomite formations. The increase in slope with porosity corresponds to the decrease in slowing down length L. The position of the dolomite curve illustrates the presence of the matrix effect.

The response of the dual neutron detector system in cased test formations is shown in Slide 14. Freshwater sandstones, limestones, and dolomite have been investigated. The limestones were also saturated with saltwater and borated water. Borehole sizes used were 6", $7\frac{1}{2}$", and 9". From this it can be seen that this log

(a) is only slightly affected by borehole size variations
(b) is only slightly affected by saltwater and boron in the formation, but
(c) is quite sensitive to the formation matrix composition.

Calibration lines are therefore necessary for sandstone, limestone and dolomite and if the porosity measurement is to be valid, the matrix composition must be derived independently from another type of log.

Further measurements indicated that this log is

(a) essentially insensitive to the presence of casing in the borehole
(b) is almost insensitive to variations in the borehole salinity, and
(c) is only slightly affected by the position of the logging instrument in the borehole.

In the next slide (15) the results obtained with a single epithermal neutron detector in the sonde are shown. It can be seen that this detector produces a response which is very sensitive to borehole size and the position of the instrument in the borehole. For comparison, the next slide (16) shows the much smaller effects of these parameters on the dual detector porosity log. Variation of borehole size from 6" to 9" produces a very small change in response. A typical dual thermal neutron detector porosity log is shown on the next slide (17). Log #1 was obtained with the shorter spaced detector at 60cm from the source and log #2 was for the longer spaced detector at 90cm. Assuming a limestone matrix, the ratio shows that the porosity varies from 20% to 0.5%.

In general, it can be concluded that the dual detector system is much less sensitive to variations in

borehole parameters. This should make the dual detector log particularly useful for cased wells where insensitivity to borehole casing and cement is required. A limitation of the log is that the formation matrix must be known.

3. Chlorine Logging

Results obtained with the Texaco chlorine logging system using the 61μg Cf^{252} source have been reported fully in the AEC Cf^{252} Progress Report No. 4, and, therefore, will not be covered in detail here.

Briefly, a chlorine log of a well delineates low-salinity zones which may contain oil. The chlorine log essentially depends upon the high thermal neutron capture cross section of chlorine which is present in the saltwater of the formation traversed by the borehole. By moving a sonde containing a neutron source and a NaI(Tl) gamma ray detector through the borehole, chlorine capture gamma rays can be measured in the borehole as a function of depth. Zones of low salinity, possibly bearing oil, can be delineated by comparing the chlorine log with a log measured simultaneously which is essentially independent of chlorine.

By using the 61μg Cf^{252} source for the Texaco experimental chlorine log in cased holes instead of a 10^7 neutron/second Pu-Be source, it has been possible to improve the signal-to-noise ratio by 65%. This can be used to increase the logging speed from 10 to 30 ft/min.

4. Neutron Gamma Logging for Gas

One method used to differentiate between oil and gas in a new well is to run two neutron porosity logs on the same day with different spacings and hence with different depths of investigation. In favorable cases these logs will indicate equal porosities where there is only water and oil but different porosities where there is gas, since the longer spaced detector is less influenced by the invaded zone than the shorter spaced detector. Since this technique is limited to source-detector spacings compatible with good detector count rates, an investigation is being made into extending this method to much larger spacings and larger depths of investigation using the stronger Cf^{252} sources.

This work is presently in progress. An illustration of the possibilities of the method is shown in the next Slide (18). The mud used for this well was heavily weighted with iron oxide. This had deeply invaded the formations and had a strong attenuating effect on the capture gamma rays so that the structure in the logs was heavily suppressed. The slide shows logs of a section which includes two known gas sands separated by a shale interval. The invasion of the mud in the shale interval was less than in the gas sands and consequently the logs track quite closely in the shale interval. However, in the gas sands the Cf^{252} log shows a much deeper response to the gas and clearly detects the gas beyond the zone of mud invasion.

At the same time it was possible to log at twice the speed with the 61μg Cf^{252} source and obtain the same statistical fluctuations as with the Pu-Be source.

5. Neutron Capture Gamma Ray Spectra (Slide 19)

Capture gamma ray spectra in borehole formations can be measured by stopping a logging instrument with a standard Pu-Be neutron source and NaI(Tl) gamma ray detector opposite a formation of interest. Analysis of this spectrum by a least squares technique[3] can be used to diagnose the cause of a particular anomaly in the logs run previously in the well. This slide shows the components from H, Ca, Si, Fe, and Cl which add to produce the observed spectrum. Point by point measurements are usually uneconomical unless the data are of extreme practical value and in open holes the technique is hazardous because of instability of the borehole. (Slide 20.) By analyzing spectra accumulated with the sonde moving very slowly up the well, it is possible to obtain logs for calcium, silicon, chlorine, and hydrogen. These help to define and quantitate

the limestone, sand/shale sequences in the well. The stronger Cf^{252} neutron sources are now being used to investigate what improvements can be made in logging speed with this system and how the spectra can be improved in quality.

The next Slide (21) shows spectra taken at two different source to detector spacings. From this slide it can be seen that the gamma rays from the iron casing become less relative to the calcium gamma rays from the formation as the spacing is increased. This improvement is shown on the next slide (22). From this slide it can be seen that the formation signal can be increased significantly relative to the borehole response by increasing the source to detector spacing. It is hoped that this improvement in formation to borehole signal which can be achieved with Cf^{252} sources can be used to advantage in a continuous logging system.

CONCLUSIONS

In summary, the results obtained so far using Cf^{252} for well logging are very encouraging. By using the stronger Cf^{252} neutron sources, it has been possible to use larger spacings between the neutron source and detectors in the logging instrument. This increases sensitivity to the formation parameters and reduces spurious borehole effects, thus improving log quality significantly. Additionally, the use of stronger Cf^{252} sources has increased logging speeds significantly. It appears that the techniques and improvements made possible by the availability of Cf^{252} neutron sources in the near future will be a valuable addition to the petroleum industry.

ACKNOWLEDGMENTS

We wish to thank Texaco Inc. for cooperation in making this work possible and gratefully acknowledge permission to present this paper.

The Cf^{252} used in this investigation was furnished to Texaco Inc. by the AEC, Savannah River Operations Office, under contract AT(38-1)-540.

This investigation would not have been possible without the cooperation of many of our colleagues at the Bellaire Research Laboratories.

This paper was originally presented at the Symposium on Applications of Radioisotopes, 63rd Annual Meeting of the AIChE, Chicago, November 29 - December 3, 1970, Chemical Engineering Progress Series No. 106, Volume 66, page No. 88, (1970).

REFERENCES

1. "The Sidewall Epithermal Neutron Porosity Log," J. Tittman, H. Sherman, W. A. Nagel and R. P. Alger, JOURNAL OF PETROLEUM TECHNOLOGY, 18, 1351 (1966).

2. "Dual-Spaced Neutron Logging for Porosity," L. S. Allen, C. W. Tittle, W. R. Mills and R. L. Caldwell, GEOPHYSICS, XXXII, 60 (1967).

3. "Analysis of Gamma Ray Energy Spectrum for Constituent Identification," J. H. Moran and Jay Tittman, U. S. Patent 3,521,064.

SLIDE 1

OIL WELL LOGGING
WITH NEUTRONS

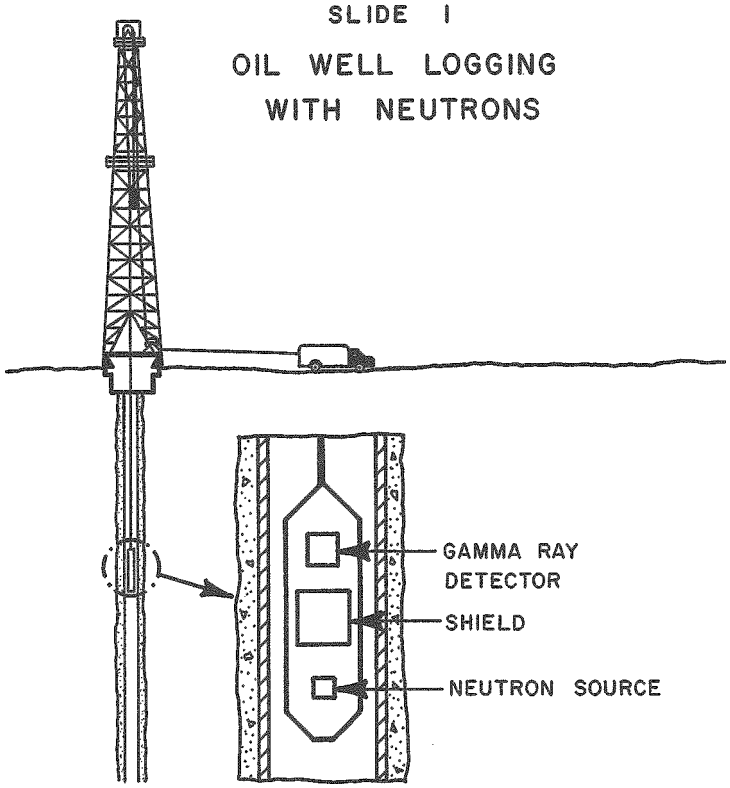

SLIDE 2

COMPARISON OF NEUTRON SOURCES
FOR WELL LOGGING

	HALF LIFE	*MEAN ENERGY (MeV)*	*YIELD NPS*	*APPROX. COST ($) 10^6 NPS*
^{239}Pu - Be	24,360 y	4.5	1.7×10^7	91
^{241}Am - Be	458 y	~4	10^7	250
			10^8	200
^{227}Ac - Be	22 y	~4	10^8	40
^{210}Po - Be	138 d	4.3	2.5×10^8	21
^{252}Cf	2.65 y	2.3	10^8	4.3
			10^9	4.3

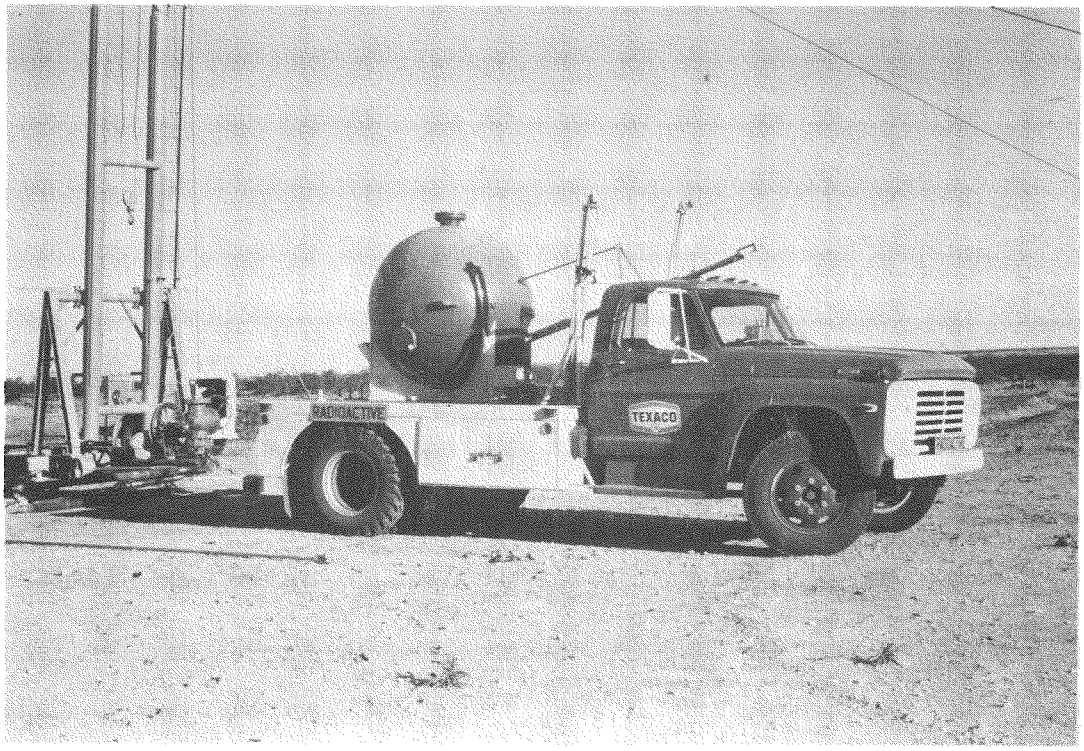

SLIDE 3

SLIDE 4

CROSS - SECTION OF ^{252}Cf SHIELD

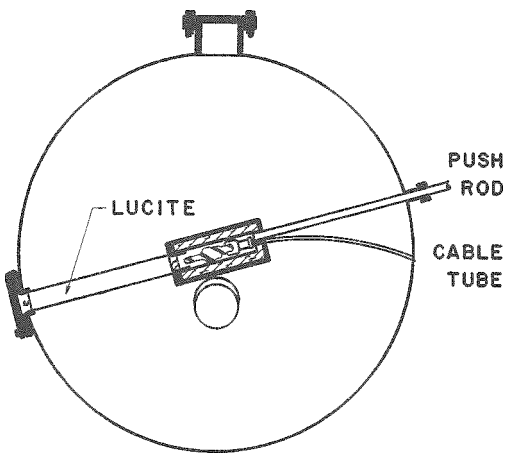

STEEL

TEXACO 1231 PETROLATUM & BORAX

LEAD SHIELD

700 μg ^{252}Cf SOURCE

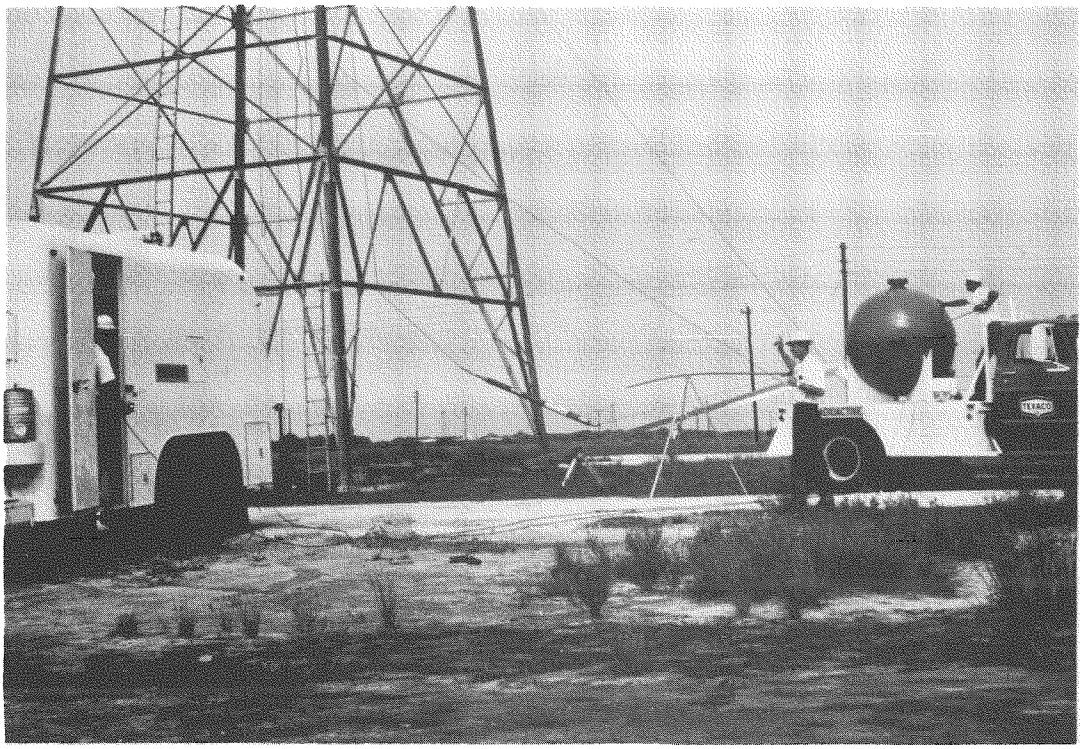

SLIDE 5

SLIDE 6

USE OF ^{252}Cf IN LOGGING

1. ACTIVATION LOGGING
2. DUAL-SPACED NEUTRON LOGGING FOR POROSITY
3. CHLORINE LOGGING
4. NEUTRON-GAMMA LOGGING FOR GAS
5. NEUTRON-CAPTURE GAMMA RAY SPECTRA

SLIDE 7

ACTIVATION LOGGING

FORMATION	REACTION	THRESHOLD ENERGY (MeV)
SHALE	$Al^{27}(n,\gamma)Al^{28}$	0
SAND	$Si^{28}(n,p)Al^{28}$	3.85

SOURCE	MEAN ENERGY (MeV)
PuBe	4.5
^{252}Cf	2.3

DECAY

$$Al^{28} \xrightarrow[2.3\ MIN]{\beta^-} Si^{28} + \gamma(1.78\ MeV)$$

SLIDE 9

ALUMINUM ACTIVATION LOGGING

NEUTRON SOURCE	LOGGING SPEED	DETECTOR COUNT RATE (1-2 MeV)
10^7 N/S Pu-Be	3 FT/MIN	5-10 CPS
10^9 N/S ^{252}Cf	20 FT/MIN	100-200 CPS

NEUTRON ACTIVATION OF Al_2O_3 / SiO_2 FORMATIONS

SLIDE 8

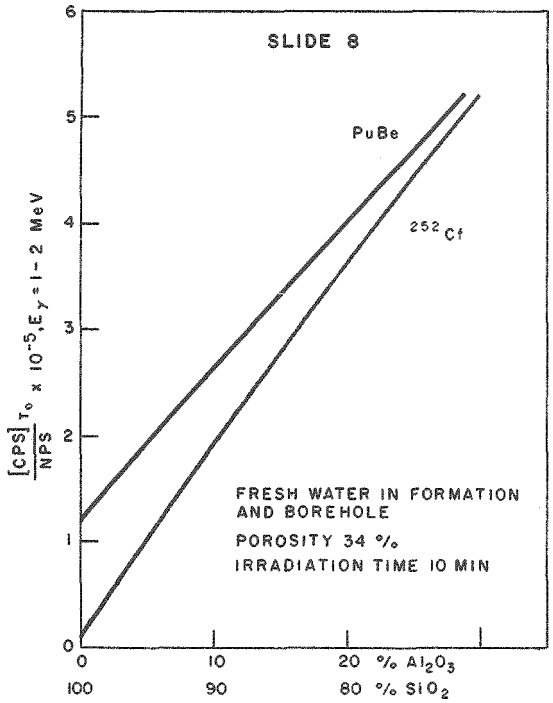

SLIDE 10

ACTIVATION LOG 700μg ^{252}Cf

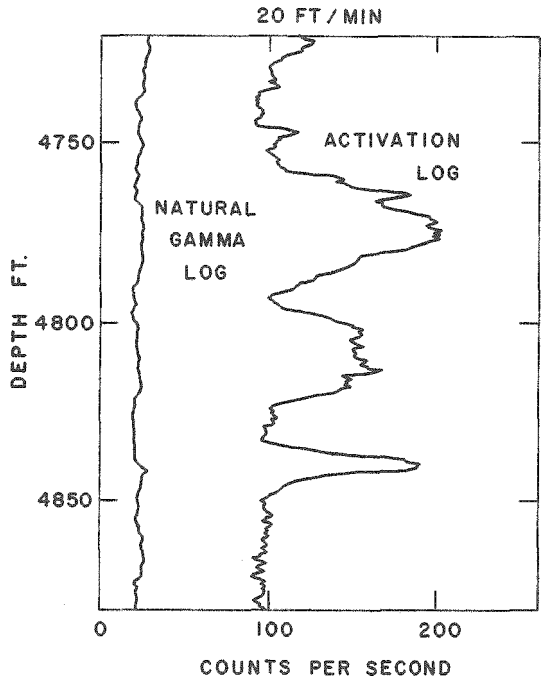

SLIDE 11

PARAMETERS AFFECTING NEUTRON POROSITY LOGS

BOREHOLE REGION

1. BOREHOLE SIZE
2. BOREHOLE FLUID *(MUD, SALTWATER)*
3. MUDCAKE ON SIDE OF BOREHOLE
4. SONDE POSITION IN BOREHOLE
5. BOREHOLE CASING
6. CEMENT BETWEEN CASING AND FORMATION

FORMATION REGION

7. FORMATION MATRIX *(LIME, SAND, DOLOMITE)*
8. SALINITY OF FORMATION FLUID
9. SHALINESS OF FORMATION
10. FORMATION TEMPERATURE

SLIDE 13

MEASURED NEUTRON DISTRIBUTION

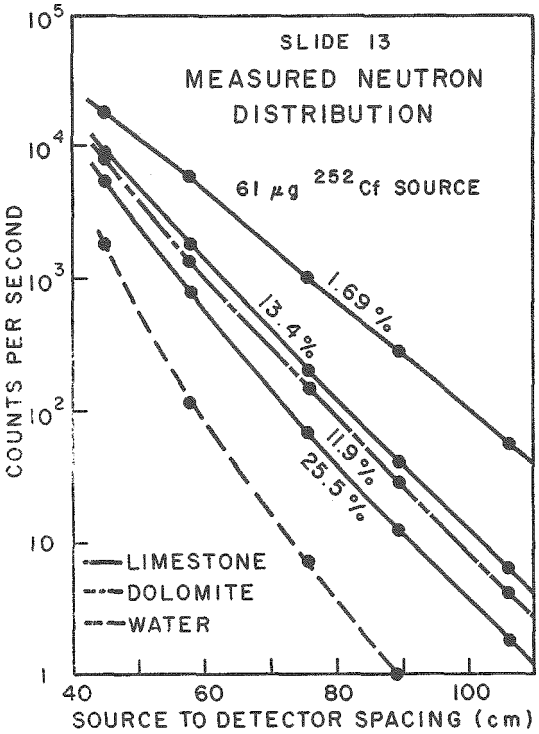

SLIDE 12

DUAL SPACED NEUTRON LOGGING FOR POROSITY

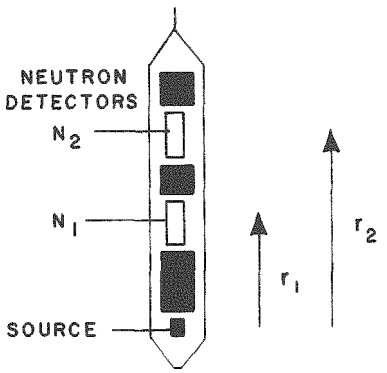

$$\text{RATIO}\ \frac{C(N_2)}{C(N_1)} = \frac{r_1}{r_2}\, e^{-\left(\frac{r_2 - r_1}{L}\right)}$$

$$L = f(\phi, m)$$

L = NEUTRON SLOWING DOWN LENGTH

ϕ = FORMATION POROSITY

m = FORMATION MATRIX

DUAL DETECTOR POROSITY LOG CASED FORMATIONS

SLIDE 14

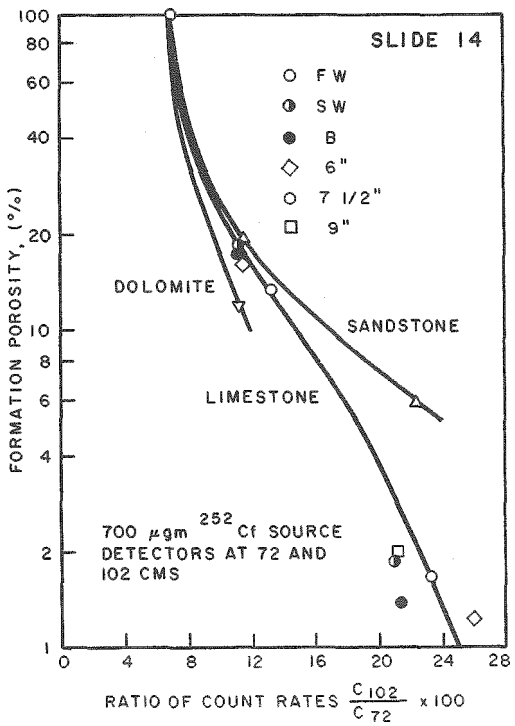

SLIDE 15

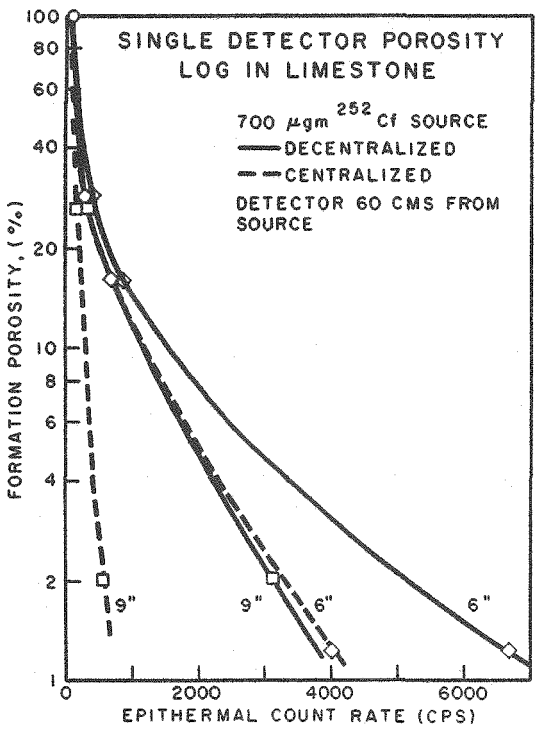

DUAL DETECTOR POROSITY LOG

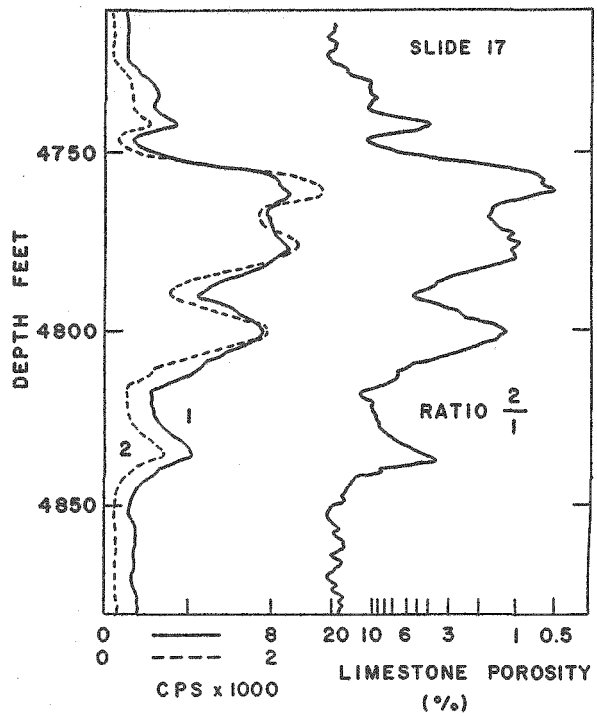

DUAL DETECTOR POROSITY LOG IN LIMESTONE

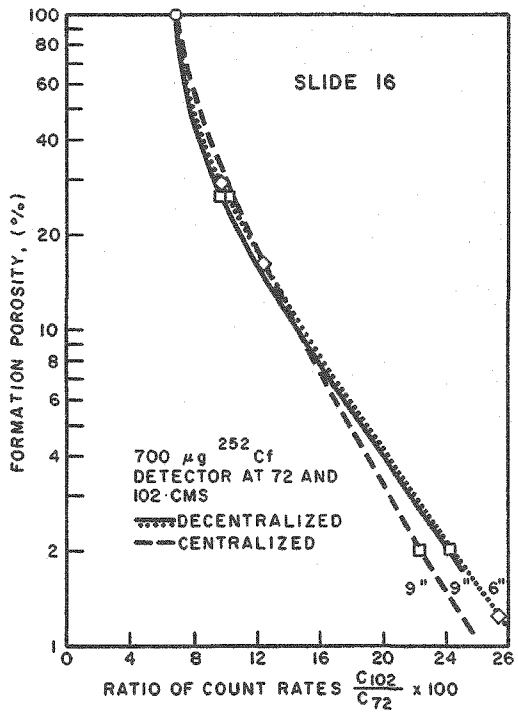

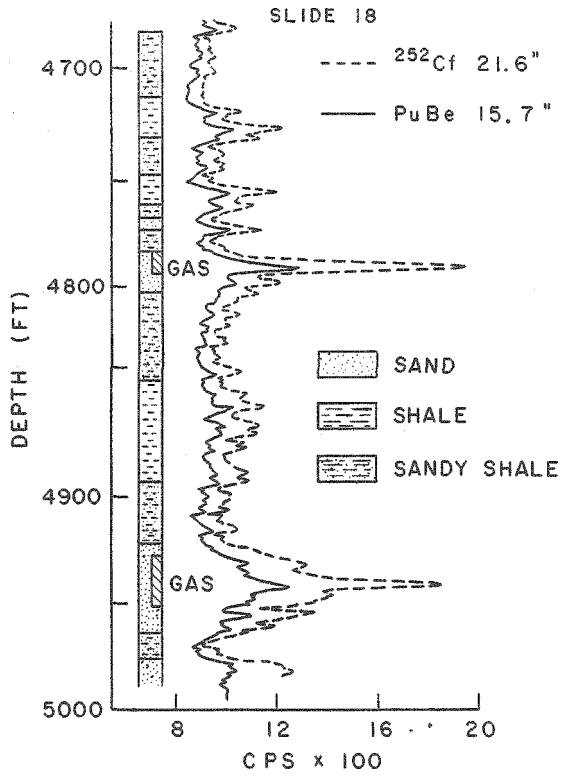

SLIDE 19

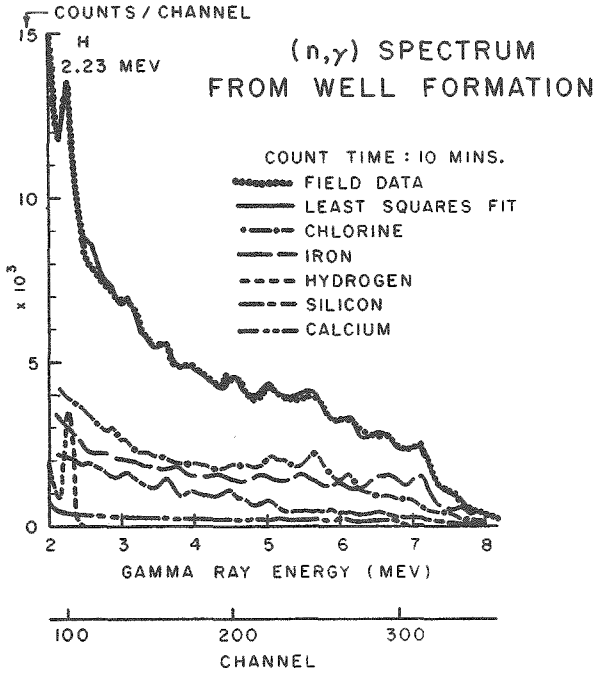

SLIDE 21

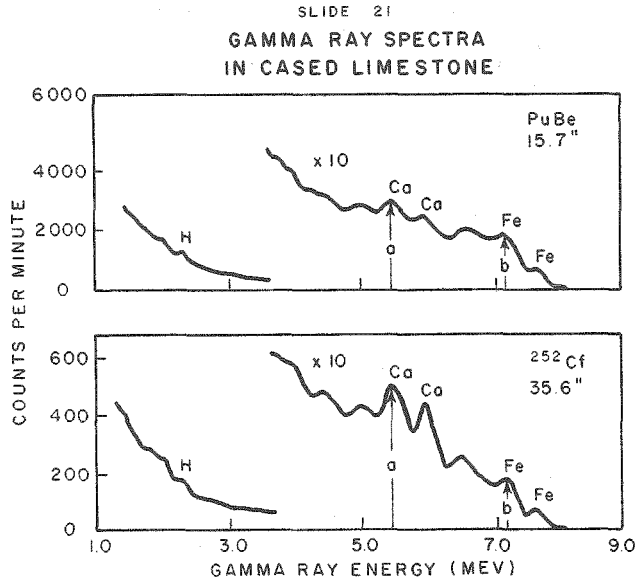

SLIDE 20

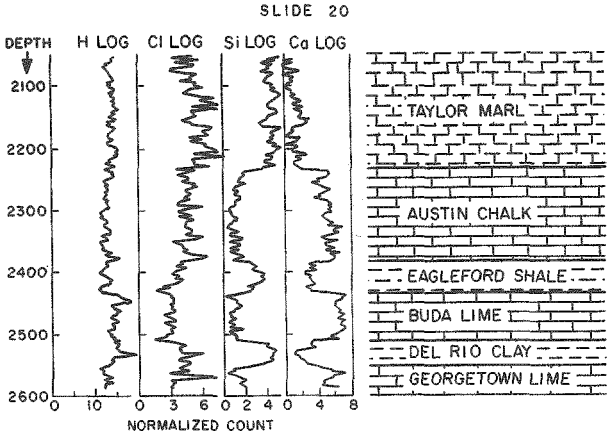

SLIDE 22

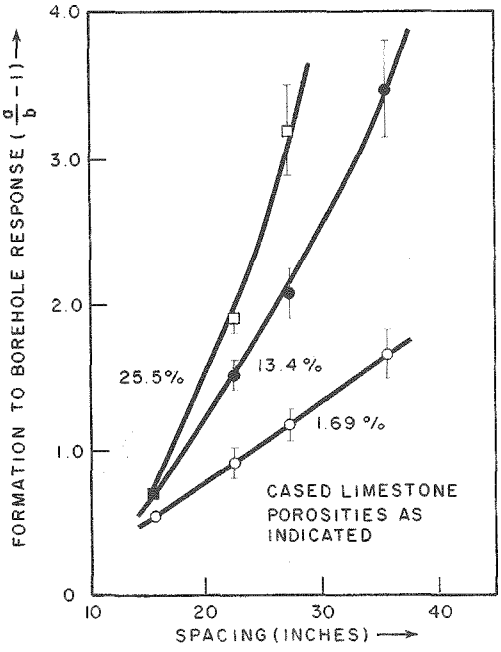

^{252}Cf NEUTRON INDUCED RADIATIVE CAPTURE GAMMA RAYS FOR HIGH ENERGY DETECTOR CALIBRATION

Jacob I. Trombka, E. Eller, and G. A. Oswald*

Laboratory for Space Physics
NASA - Goddard Space Flight Center
Greenbelt, Maryland

M. J. Berger

S. M. Seltzer

Center for Radiation Research
National Bureau of Standards
Washington, D. C.

High energy gamma ray sources produced by prompt neutron radiative capture were developed in order to study the variation of pulse height, the shape of pulse height distribution, and resolution as a function of energy for scintillation detectors. The system as described below has also been used to calibrate the gamma ray spectrometers which will be flown aboard Apollo 15 and 16.

Spectral distribution of gamma rays in the 3 to 12 Mev energy region using a 3 in. x 3 in. NaI(Tl) detector have been studied for a number of nuclear species such as: Nickel with lines at 8.999 and 8.533 Mev; Mercury – 5.967, 4.842, 4.740, and 3.289 Mev; and Hydrogen – 2.223 Mev. The neutron excitation of these samples was carried out by placing these samples in a neutron moderator near a ^{252}Cf source ($\sim 2\ \mu g$).

Methods for inferring photon spectra from the pulse height spectra have been developed and are to be used to interpret the gamma ray measurements carried out during the Apollo 15 and 16 flights. Detailed knowledge of the response of the flight detectors as a function of energy is required to perform the analysis. In the energy region above 3 Mev, it is extremely difficult to obtain response functions for truly monoenergetic gamma rays. Therefore the following approach has been taken: Monte Carlo calculations have been carried out to determine the nature of these response functions in the 3 to 12 Mev region. These spectra have been compared with the experimentally determined spectra obtained using the ^{252}Cf system described above. These comparisons form a basis for predicting the shape of the pulse height spectrum for gamma rays of any energy in this range.

INTRODUCTION

High energy gamma ray sources produced by prompt neutron radiative capture were developed in order to study the dependence of pulse height, the shape of the pulse height spectrum, and resolution as a function of energy for scintillation detectors. This type of calibration is required in order to obtain the photon energy spectrum from an analysis of the pulse height spectrum.

Radioactive sources are available to study the energy dependence up to about 3 MeV, but above this range no radioactive isotopes with a significant half life exists. The source that is needed in our particular application must be portable because it will be used in the calibration of the scintillation detectors to be flown aboard Apollo 15 and 16. The gamma ray pulse height spectra obtained during these flights will be used to infer the elemental composition of the lunar surface (1-4). The information contained in the photon spectrum is more directly interpretable in terms of elemental composition than is the pulse height spectrum. Methods for performing this analysis are described in References 5 and 6.

An excellent monoenergetic (6.13 MeV) gamma ray source using the ^{13}C (α, n) ^{16}O reaction has been developed at the Oak Ridge National Laboratory (7). Our problem requires calibration up to about 10 MeV. Thus the possibility of producing high energy gamma rays by neutron radiative capture has been investigated. Various energies can be obtained by changing the nuclear specie irradiated. Pure monoenergetic emitters cannot be obtained, therefore experimental measurements of polyenergetic spectra were obtained. Monte Carlo calculations† were then carried out to obtain theoretical shapes of the response functions characteristic of the given detector for the various energies in the polyenergetic sources. The polyenergetic spectrum was then synthesized and compared with the experimental measurements. In this way we have been able to construct a library

*Presently at the University of Cincinnati. Work at Goddard Space Flight Center on University Cooperative Program.

†The method used combines a photon Monte Carlo program with an equally detailed electron Monte Carlo program (8, 9). The entire photon-electron cascade set up in the NaI detector is followed by random sampling, in order to account for the escape of energy from the detector in the form of scattered photons, annihilation radiation, bremmstrahlung, electrons and positron. This method has previously been used in calculations of the response of Si detectors to high-energy electrons (10). Details of the response function calculations for NaI will be published elsewhere.

of response functions as a function of energy up to about 12 MeV for NaI(Tl) detectors.

DESIGN OF THE EXPERIMENT

A one microgram ^{252}Cf neutron ($\sim 2 \times 10^6$ neut/sec) was used to excite gamma emission from various samples placed near the source. Since the process of neutron production is by fission, the neutrons are produced at high energies and must be thermalized in order that the capture interaction probability be maximized.

Figure 1 is a drawing of the experiment configuration for performing the measurement.

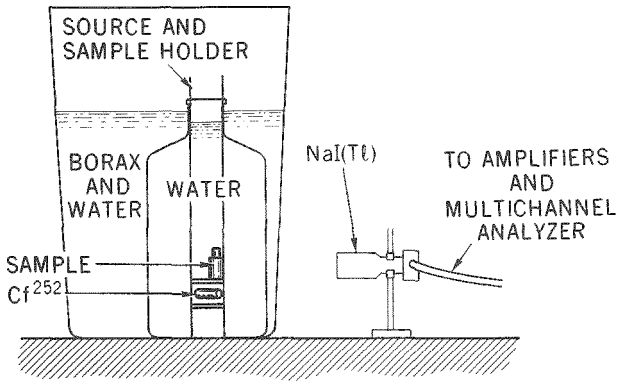

FIGURE 1. Experimental Configuration For Radiative Capture Spectral Measurements

The ^{252}Cf is placed in the center of a water moderator. The moderator is then surrounded by a water-boron thermal neutron shield. This shield prevents a large flux of neutrons outside the containment system. This shield is not only needed for radiological safety purposes but also reduces the neutron induced gamma ray emission from the detector and surrounding media. The shielding problem is a rather critical factor in obtaining meaningful spectral measurements. These considerations led to the design shown in Figure 1.

There are two other major gamma ray sources contributing to the background. The first source consists of fission gamma rays emitted from ^{252}Cf. The second source consists of gamma rays emitted subsequent to neutron capture and inelastic scattering in the moderator and containment materials. Attempts made to reduce the fission gamma ray background by using gamma ray shields were unsuccessful. It was found that the shielding material produced sufficiently intense high energy gamma rays to decrease the signal to background ratio significantly from that obtained without the shield.

The fission gamma ray background in the lower energy region considered was the major source of interference. Because of this background problem only measurements in the photopeak and first and second escape peak area were possible.

The sensitivity and spectral information found in Reference 11 was used to select the samples for irradiation in this program.

EXPERIMENT RESULTS

Figures 2 and 3 show HgO and NiO prompt capture pulse height spectra using a 3"×3" NaI(Tl). The background spectrum is superimposed on

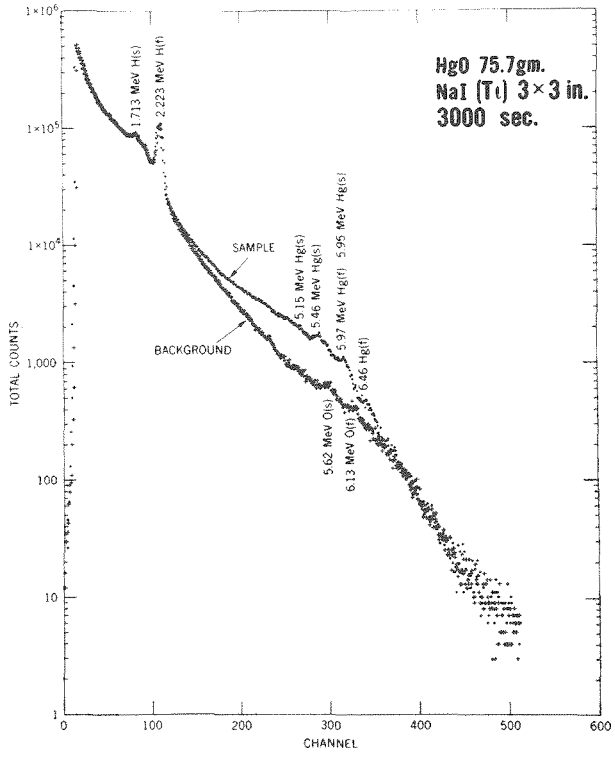

FIGURE 2. Comparison of Background with HgO, 3000 Sec Each, Using a 3" × 3" NaI(Tl) Detector

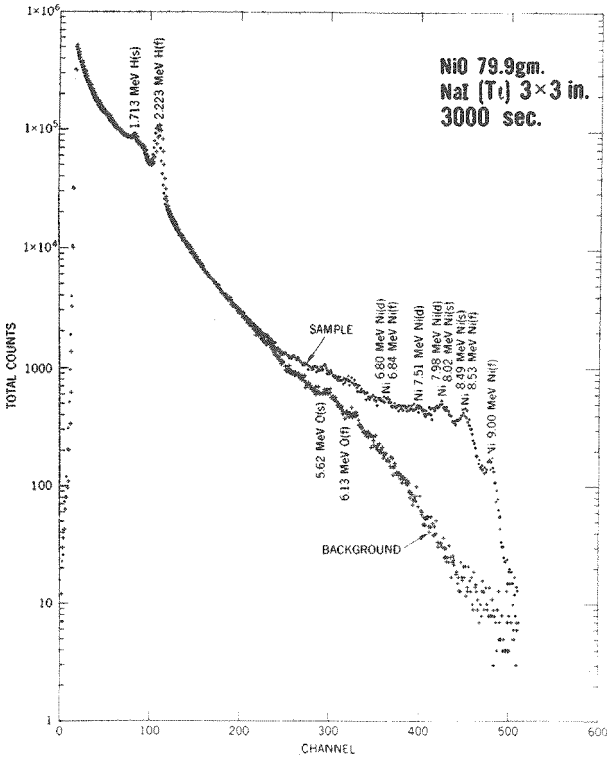

Figure 3. Comparison of Background with NiO_5 3000 Sec Each, Using a 3" × 3" NaI(Tl) Detector

both figures. The measurements shown were performed over 3000 second accumulation time. Background spectra were obtained by performing the measurement without the sample present. The 2.223 hydrogen line with the first and second escape peak can be easily seen. The oxygen (6.13 MeV) lines are less obvious. The major lines of Hg and Ni are indicated. The photopeak (f), single escape (s), and double escape (d) peaks are also indicated. Below about 4 MeV, the sample and background spectra merge and it was therefore difficult to obtain information concerning the pulse height spectrum below this energy. The Compton continuum for these high energy gamma rays are rather small, therefore the contribution in this lower energy region is not too great (see Figure 4).

COMPARISON WITH THEORY

A typical calculated response function for a 10.83 MeV gamma ray incident upon a 3" × 3" NaI(Tl) crystal is shown in Figure 4. The Monte Carlo calculation yields directly only the distribution of the amount of energy left in the detector. This distribution must be further smeared by a Gaussian that represents the intrinsic resolution of the detection system. The intrinsic resolution is a quantity that must be obtained experimentally and is determined by such processes as electron to photon conversion in the scintillator, the light collection on to the photocathode, the photon to electron conversion in the photocathode, and finally the amplification process in the photomultiplier dynode string. The results depicted in Figure 4 includes this Gaussian intrinsic resolution effect.

In most of the literature the full width at half maximum (FWHM) of the Gaussian intrinsic resolution function has been assumed to be proportional to the square root of the energy. A careful analysis of our experimental results plus a study of other pulse height spectra found in the literature indicate that the FWHM is proportional to the two thirds power of the energy. This has been found to be the case from 10 Kev up to 20 MeV. For the results shown in Figures 4 and 5, we have used the power law.

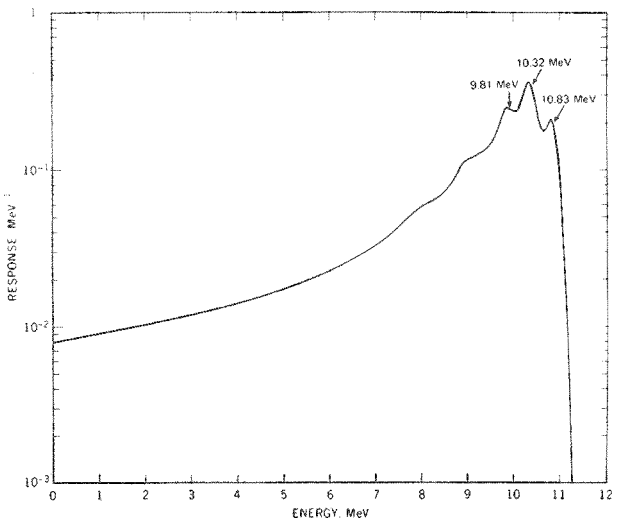

Figure 4. Response of a 3" × 3" NaI(Tl) Detector to a Narrow Parallel Beam of 10.83 MeV Gammas Incident Along the Crystal Axis

Figure 5 shows a comparison between the high energy capture lines of Ni at 8.999 MeV and 8.533 MeV as measured (i.e., difference between background and sample pulse height spectrum, Figure 3) and as calculated using Monte Carlo methods. The capture gamma ray spectrum and

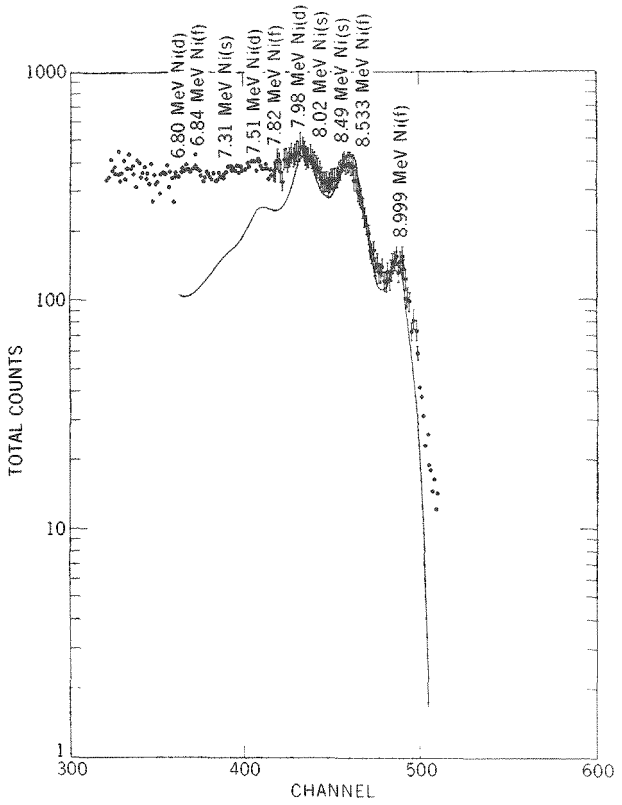

Figure 5. Comparison of Monte Carlo Calculations with Experimental Data for the Two Highest Energy Ni Lines

the relative intensity compared to the 8.999 MeV is shown in Table 1 (11).

In this particular calculation, we were only interested in the higher energy lines. The Monte Carlo calculation included only the two highest energy lines with relative intensities as shown in Table 1. Thus the comparison should only be made above 8 MeV. There should be and there is a divergence between the experimental and theoretical below this energy. The experimental measurement is higher than the calculated value. The large error in the experimental measurement indicated in Figure 5 is due in great part to the difficulty in determining the exact magnitude of the background.

TABLE 1

Relative Intensity of Ni Capture Gamma Ray Spectrum

Energy in MeV	Relative Intensity
8.999	1.00
8.533	0.45
8.121	0.083
7.819	0.22
7.697	0.033
7.536	0.12
6.837	0.29
6.584	0.047
6.105	0.050
5.817	0.056
5.695	0.024
5.312	0.027
4.859	0.028

The comparison thus between measurement and calculation show good agreement.

SUMMARY

A method using ^{252}Cf neutron source to excite high energy gamma rays has been developed. This method can be used to calibrate gamma ray detectors in the energy region above 3 MeV. Further, using the measured spectra to determine the deviation from linearity of the energy and the intrinsic resolution parameters as a function of pulse height for the given detection system, theoretical (Monte Carlo) calculations can then be carried out to obtain detail information on the shape of the pulse height distribution in the region up to 15 MeV. The results of the measurements and calculations show good agreement.

BIBLIOGRAPHY

1. Arnold, J. R. "The gamma spectrum of the moon's surface." Proceedings Lunar and Planetary Exploration Colloquium, 1958.

2. Arnold, J. R., A. E. Metzger, E. C. Anderson, and M. A. Van Dilla. "Gamma Rays in Space, Ranger 3." J. Geophys. Res. 67/12, 4878 (1962).

3. Vinogradov, A. P., I. A. Surkow, G. M. Chernov and F. F. Kernozov. Measurements of Gamma Radiation of the Moon's Surface by the Cosmic Station Luna 10. Geochemistry No. 8, p. 891, V. I. Vernadshy Institute of Geochemistry and Analytical Chemistry, Moscow, USSR (1966).

4. Adler, I. and J. I. Trombka. "Gamma Ray Spectroscopy from Lunar Orbit." Geochemical Exploration of the Moon and Planets. Springer-Verlag, Berlin, Heidelburg, New York, p. 51-58 (1970).

5. Trombka, J. I. and R. L. Scmadekech. A Numerical Least Square Method for Resolving Complex Pulse Height Spectra. NASA Special Publication 3044 (1968).

6. Adler, I. and J. I. Trombka. "Data Processing and Analysis." Chapt. 5, Geochemical Exploration of the Moon and Planets. Springer-Verlag, Berlin, Heidelberg, New York (1970).

7. Dickens, J. K. and R. D. Boybarz. A Monoenergetic 6130 keV Gamma-Ray Source for Detector Calibration. Nuc. Instr. and Meth. 85, p. 143-145 (1970).

8. Berger, M. J. "Monte Carlo Calculation of the Penetration and Diffusion of Fast Charge Particles." Methods in Computational Physics, Vol. 1, Academic Press Inc., New York, p. 135-215 (1963).

9. Berger, M. J. and S. M. Seltzer. Protection Against Space Radiation, pp. 285-322, NASA Spec. Publ. No. 169 (1968).

10. Berger, M. J., S. M. Seltzer, S. G. Chappell, J. C. Humphreys and J. W. Motz. Response of Silicon Detectors to Monoenergetic Electrons with Energies Between 0.15 - 5.0 MeV. Nuc. Instr. and Methods, 69, pp. 181-193 (1969).

11. Duffey, D., A. El-Kady and F. E. Seuftle. Analytical Sensitivities and Energies of Thermal-Neutron-Capture Gamma Rays. Nuc. Instr. and Methods, 80, pp. 149-171 (1970).

NEUTRON TECHNIQUES IN GROUND WATER EXPLORATION

Vasilii I. Ferronsky

International Atomic Energy Agency
Vienna, Austria

The interest of many countries in using ground water has especially risen during the last years, in line with the increased pollution of surface water. An increased consumption of ground water for irrigation in arid countries can also be observed, and many types of brines are used for industrial purposes. Mineral waters are employed for balneological and therapeutical purposes, and thermal waters for development of energetics.

The paper describes the use of neutron sources for different kinds of neutron well logging, for exploration of aquifers and their properties under different geological conditions. Examples for the use of penetration neutron logging in the investigation of unsaturated and saturated zones in the upper layer of soils in arid and humid areas are given. Different aspects of neutron techniques to be applied in investigations of recharge of ground water through unsaturated zones for hydrogeological observations are presented. Some factors influencing the finding of an optimal network for observations of regime of moisture in unsaturated zones are described. Reference is made to different types of moisture gauges, with neutron sources which are used for these purposes.

The activities of the International Atomic Energy Agency to promote development of neutron methods in ground water exploration are also mentioned.

1. INTRODUCTION

As is known, water is an indispensible attribute for the life and activities of man on the earth. Therefore, the problem of investigation of water has always been of interest, both in practical and scientific aspects. Water is one of the simple chemical compounds of hydrogen and oxygen, and forms of its presence in nature seem to be rather simple to understand. Nevertheless water has kept a few secrets to itself which man failed to reveal up to now, one of it being its origin on earth. The solving of this problem is the principal basis for understanding other regulations of nature connected with the distribution of water on the surface and inside the earth. The knowledge of the abovementioned regularities would be a valuable scientific basis for exploration of different types of underground water, the consumption of which is growing continuously.

Presently a number of hypotheses exist concerning the origin of water. One of them is its meteoric origin, explaining the presence of water by the capture by the earth of a comet containing enormous ice masses. This melted ice started to create the earth's hydrosphere.

Another hypothesis, spread out widely in the last years, explains the formation of the hydrosphere by means of fusion and de-gasification of light components from the planet during heating, by the decay energy of radioactive elements. At this time, it is assumed that the earth was created by condensation of cold nebula under gravitation forces.

However, it is necessary to recall that a number of facts have been observed through the analysis of which it is not difficult to contradict the abovementioned hypotheses (1).

When analysing the data of the isotopic composition of different types of waters (atmospheric, oceanic, surface and underground waters) one can find one more interesting fact: in different types of underground waters, including deep water of ancient sedimentation basins, water of oil and gas formations, mineral, thermal and pore waters and liquids included in magmatic rocks and minerals, the concentration of heavy isotopes does not exceed the one in modern ocean waters (2). In all the abovementioned types of water the concentration of deuterium is practically not exceeding the means of 0,0156 at.%, and the concentration of oxygen-18 appears to be within the limits of 0,2005 at.%. These means of deuterium and oxygen-18 are characteristic for ocean water. The exclusion of these regularities appears to exceed the concentration of oxygen-18 in thermal waters, and also in waters which have been subjected to strong heating. But this can easily be explained by oxygen exchange of water with water-bearing rocks or by the so-called oxygen shift.

It is interesting to note that many authors counted the thermal waters always to the juvenile waters, as the isotopic composition data as a rule correspond with those of modern waters of infiltration origin. It has to be pointed out that the fact of identical isotopic composition of different ancient underground waters with modern oceanic waters and the absence of increased concentrations of heavy isotopes in deep underground waters is in contradiction to the hypothesis of gasification of water vapour from deep earth layers. This latter process must lead to significant fractionation of water along the depths and to enrichment of more deep water with heavy isotopes.

It must therefore be stated that at present there are no sufficiently well-founded hypotheses on the origin of water on the earth. The topic of this symposium does not include a discussion of this problem. But it is necessary to stress that the absence of a sufficiently reliable solution of this problem leads to difficulties in developing a general theory for ground water formation, which has a direct relation to the choice and use of techniques for ground water exploration, and also to the interpretation of results of geophysical measurements.

2. NEUTRON METHODS AND FIELD OF THEIR APPLICATION IN GROUND WATER EXPLORATION

Activities in the field of industry and agriculture have developed in such a way that the absence of one or the other kind of raw material is constantly noted. Water is one of the most important types of raw material, the consumption of which is constantly growing, and its field of use increasing steadily. The main natural reservoir of different types of water, above all fresh water, is the earth crust of continents, where the water was accumulated for centuries. It is not so long ago that the exploration of underground water had the main purpose to identify sources for domestic and industrial supply. This purpose has now been expanded considerably. Underground water has a much higher specific weight in the common balance of waters used for irrigation in agriculture in arid areas. It plays an important role as a raw material including different chemical elements, the discovery of which led to the industrial development of countries which have otherwise poor mineral resources. It is possible to assume that the storage of mineral resources in underground water in sedimentation basins is practically unconfined. Mineral and thermal waters have formerly been widely used in many countries for balneological purposes, and later for energetic needs. This important reason for underground exploration leads to the needs for new methods of geological exploration.

Presently, neutron methods can be counted to the more universal and perfect methods for investigation of different types of underground waters, taking into account their physical basis. Their application however depends on many additional factors connected with differences in tasks to be solved and also, more, on the different geological conditions in the investigations. Moreover, during investigation of ground water for practical purposes it is as a rule necessary to have not only data about the qualitative volume of water in water bearing formation, but more additional data about the water-bearing formations themselves, to solve the task of practical use of underground water. In this connection practically neutron methods have been used in combination with other investigation methods.

Bearing in mind the different tasks to be solved during the ground water exploration, the application of neutron sources can be derived from two main groups:

The first group of methods includes the use of neutron sources for investigation of deep ground water located in deep layers. The conditions for such deep ground water exploration are such that it is practically only possible to investigate them in wells. In this connection neutron sources are used for different types of neutron logging in wells. There are a number of factors which determine their application as follows: depth of investigation and temperature increase with depth; presence of casings and mud; presence of annulus and needs of cementation of the space; differences in diameter of the well; complicated geological structure and different degree of mineralization of underground water.

Taking into account the abovementioned factors and bearing in mind the limitation in the resolution of neutron methods it follows from the physical basis of distribution of neutrons and their interaction with the surrounding media, that different

modifications of neutron logging for deep hydrogeological wells are developing. As a rule, in the exploration of ground water neutron methods are used in combination with other methods of investigation of wells: with gamma-gamma logging, with electrical and acoustic methods, with flowmeter and with tracer methods.

The second group of methods includes the use of neutron sources for investigation of shallow ground water located in unconsolidated deposits in saturated and unsaturated zones. This group of methods includes the tasks connected with the measurement of moisture in surface layers in unsaturated zones of soils for hydrometeorological and agricultural purposes and for investigations of subsoil waters in unsaturated and saturated zones for irrigation purposes.

The specific conditions for solving these tasks are a relatively free access to the waters to be investigated in the surface layers. Here the technical solution of the task is considerably easy and conditions for application of neutron sources are improved, and more precise quantitative data about the content of water in soils are received.

In the practical solution of the above-mentioned tasks neutron sources can be applied as follows: penetration neutron logging, which does not require the boring of a hole, and also different kinds of neutron moisture gauges and tracers with subsequent use of neutron sources.

The reason for using neutron methods in combination with other nuclear and electrical methods of investigations should be stressed here, namely, that the hydrogeological investigations also have the aim to provide extensive information on aquifers and water-bearing soils.

3. APPLICATION OF NEUTRON SOURCES FOR EXPLORATION OF DEEP GROUND WATER

Neutron sources for investigation of deep ground water are applied in logging of hydrogeological wells. The neutron logging with isotopic sources has developed in the form of modification of thermal and epithermal neutron-neutron logging, neutron-gamma logging and activation logging on aluminium, chlorine, natrium, manganine, oxygen, and spectrometric neutron gamma logging.

In principle, the neutron logging consists of recording the scattered neutron radiation emitted by a fast neutron source in a sonde which is moved about in the well. Here, use is made of the dependence of the anomalous cross-section for the slowing-down of fast neutrons to thermal energies in hydrogen atoms. Neutron logging gives a diagram showing mainly the distribution of the moisture content of the rocks in the given well section, and also the content of those elements which are anomalous neutron absorbers.

The physical and theoretical principles governing the interaction of neutrons with a medium of various chemical compositions, the resolving power of the neutron method for determining moisture content in relation to the sensitivity and range required and the factors governing choice of the optimum sonde parameters are well known (3,4). The slope of the curve of the relationship between neutron response and moisture content of the medium depends on the distance between the radiation source and the neutron detector. For short sondes, these quantities are directly proportional, while for long sondes they are in inverse semi-logarithmic dependence. For sondes of medium length (10 - 20 cm) the dependence of the radiation recorded on hydrogen content undergoes inversion (reversal of the sign), and the method becomes insensitive to variations in the moisture content. Inversion sondes are used for identifying rocks containing elements which are anomalous neutron-absorbers, and, in particular, water formations containing mineralized water.

Short sondes are highly sensitive to variations in hydrogen content. They permit low-activity radiation sources to be used and have the highest resolving power in relation to the size of formation. But they have the smallest range and, if they have drilling mud around them in a well, they give practically no information on the formation. These sondes have found a use in penetration logging whereas only the long sondes are used in well surveys.

In neutron logging the other factors affecting the moisture content parameter are well design, mud, cement plug in the annulus, cavities, and so on. These factors which are associated mainly with the drilling and well construction practices,

cause serious interferences and reduce the accuracy and precision of the results.

Depending on the radiation being recorded, we distinguish between thermal-neutron logging, epithermal-neutron logging, and neutron-gamma logging.

The neutron-gamma logging method consists essentially in recording the capture gamma radiation, which occurs as a result of the absorption of thermal neutrons from the fast-neutron source by the atoms of the rock-forming elements. The yield of capture gamma radiation in a homogenous medium is proportional to the density of thermal neutrons and, therefore, depends on the slowing-down properties of the medium, i.e. on its hydrogen content. But since here the gamma quanta are recorded, there is also a dependence on the density of the medium and the number of gamma quanta per neutron capture. The presence in the medium of chlorine - anomalous neutron absorber and anomalous gamma emitter - increases the yield of capture gamma radiation (approximately 2.4 gamma quanta per neutron capture). In hydrogeological studies this property is used for delineating the extent of fresh and saline chloride waters and for stratification of chloride water in the water-bearing formation. Neutron-gamma logging is used mainly for differentiating a section in respect of moisture content. Its advantage over thermal-neutron and epithermal-neutron logging lies in its greater radius of sphere of the rocks volume measured and, consequently the diminished effect of the well conditions on the measurement results. The latter consideration is especially important in the study of high-density sections and of cased and cemented wells. In the study of porous sections, it is profitable to use thermal-neutron logging when the section contains fresh formation water and epithermal logging when it contains highly mineralized water.

Unlike ordinary neutron logging, pulsed neutron logging studies the non-stationary neutron field in the well. By studying this field, we cannot only investigate the space-energy distribution of neutrons, as in the different versions of neutron logging, but also the time distribution of neutrons in the well.

For the purpose of studying the non-stationary processes of interaction of neutrons with matter, a pulsed neutron source of pulsating action - a so-called impulse generator - is used. The neutrons are emitted periodically by the generator during a short time interval ΔT, which is called the duration of the pulse. Neutrons are recorded between the neutron pulses during a certain time Δt, called the time "window". The time interval between the end of the neutron pulse and the beginning of recording is called the delay time t_d. The measuring channel is set at a given value of t_d, and the thermal neutrons or the gamma-quanta are recorded periodically after each pulse, which follows at a frequency varying from a few pulses per second to hundreds of cycles per second, depending on the generator type. By measuring with different delay times, we can study the time distribution of the neutron field in the well $n = f(t_d)$.

If the neutron source acts in pulse operation the process of slowing down and diffusion of neutrons can be divided in point of time. In the first $10 - 10^2$ /usec the predominant process of neutron-matter interaction is the process of slowing down. The diffusion of the thermal neutrons occurs in the time interval from $10^2 - 10^4$ /usec. This process is governed by the diffusion parameters of the medium in the well and, in the formation, by the diffusion coefficient of the thermal neutrons $D = \frac{v}{3\Sigma_s}$ (where Σ_s is the macroscopic scattering cross-section and v is the neutron velocity at a given temperature) and their average lifetime $\tau = \frac{1}{\Sigma_a v}$ (where Σ_a is the macroscopic capture cross-section for thermal neutrons in the medium). Table I gives the values of D and τ for different rocks, minerals and salts contained in water (5).

Pulsed neutron logging differs from stationary neutron logging in that its readings depend mainly on the diffusion parameters of the formation and, in particular, the average lifetime of neutrons which, as is seen in Table I, depends on what the formation contains in the nature of anomalous neutron absorbers - chlorine, boron, iron, potassium, etc. An important advantage of the pulse method over the ordinary method is that well conditions have very little effect on the measurement results, especially in gamma radiation recording in pulsed neutron-gamma logging.

TABLE I

NEUTRON DIFFUSION PARAMETERS OF MINERALS AND ROCKS

Minerals and rocks	Chemical composition	τ, msec	D, 10^5 cm^2 sec
Kaolin	$Al_2O_3.2SiO_2.2H_2O$	0.36	0.8
Montmorillonite	$Al_2O_3.4SiO_2.2H_2O$	0.55	1.2
	$Al_2O_3.4SiO_2.3H_2O$	0.46	0.97
	$Al_2O_3.4SiO_2.4H_2O$	0.40	0.81
	$Al_2O_3.4SiO_2.5H_2O$	0.35	0.68
	$Al_2O_3.3SiO_2.6H_2O$	0.33	0.55
Clay	Al_2O_3 - 29.7% SiO_2 - 45.0% $CaCO_3$ - 10.0% Fe_2O_3 - 4.08% H_2O - 11.0%	0.31	0.40
Clay marl	Clay - 75% $CaCO_3$ - 25%	0.44	1.9
Marl	Clay - 50% $CaCO_3 + CaMg(CO_3)_2$ - 50%	0.53	2.8
Quartz	SiO_2	1.1	2.7
Orthoclase	$K(AlSiO_3O_8)$	0.30	3.1
Calcite	$CaCO_3$	0.63	2.2
Dolomite	$CaMg(CO_3)_2$	0.96	1.9
Gypsum	$CaSO_4.2H_2O$	0.25	0.6
Anhydrite	$CaSO_4$	0.36	2.7
Magnetite	Fe_3O_4	0.04	1.1
Rock salts	NaCl	0.006	1.7
Water	H_2O	0.20	0.36
Naphthenic hydrocarbons	C_nH_2N	0.19	0.34

The use of neutron sources is profitably for lithological differentiation of the geological section together with other nuclear and electrical methods and for differentiation of the clay content sections in particular. Neutron response is linked with clay content, since the clay materials contain crystallized water as well as all the elements which readily absorb thermal neutrons, such as potassium, iron and also boron, the compounds of which are absorbed on the clay material. As a result, in neutron logs with long sondes an increase in the clay content of the formation will be accompanied by a diminuition in the response owing to the increased hydrogen content and neutron-absorbing elements. The method most sensitive to variations in the clay content is thermal neutron logging. However, the dependence of the thermal neutron response on clay content is not unambiguous, since hydrogen content varies also with porosity. For a more reliable lithological differentiation of the section, it is advisable to combine thermal neutron logging with gamma-gamma logging. The gamma-gamma response of a sandy clay section is to all intents and purposes a function of porosity and is independent of clay content. Another method of obtaining reliable differentiation of a sandy clay section is pulsed neutron logging. When the well is filled with fresh water - base mud and the formation contains fresh water, it is advisable to use pulsed neutron-neutron logging, since this method, unlike pulsed neutron-gamma logging, is free of background. Pulsed neutron-neutron logging, in measurements with time delay, enables us to differentiate a section in respect of its clay content on the basis that the clay materials are strong thermal-neutron absorbers and, therefore, the lifetime of the neutrons in the formation, as determined from the pulsed neutron-neutron response, will depend on clay content. The higher the clay content, the shorter will be the neutron lifetime and the lower the pulsed neutron-neutron response.

The role of neutron logging in combination with other nuclear logging for identification of water-bearing formations is irreplaceable. By differentiating sandy clay sections in respect to clay content, it is possible to identify likely water formations; the latter are high-porosity non-clay sand and sandstone formations. In the case of sandy clay sections in which the formation radioactivity is due to its clay content, water-bearing formations can be identified unambiguously by a combined use of neutron and gamma logging. As in the case of differentiation of sections, it is useful here to use thermal neutron logging with a 40 - 50 cm sonde. In sections in which water-bearing formations are sandstones or pebbles with high radioactivity of the fragmental material, the combination of thermal-neutron and gamma logging is not sufficient. But water-bearing formations with good reservoir properties may be missed if they are plugged with unfiltered mud that penetrates into formation. The gamma-gamma logs as well as the gamma logs do not obviously distinguish such formations from a formation with high clay content, and show them as unsaturated. Furthermore, the better the filtration properties of the formation, the greater is the probability of its being plugged with mud. If the formation consists of quartzite sandstones it can be identified by pulsed neutron-neutron logging, which has a considerably higher range.

In a section consisting of carbonate rocks, the water-bearing horizons may be associated with highly porous, cavernous of fissured formations. The first two types of water-bearing rocks can be identified on neutron logs on the basis of increasing formation porosity. In carbonate sections, it is most advantageous to use neutron-gamma logging with a 60 cm sonde, which is somewhat less sensitive to porosity variations than thermal-neutron logging but which is, as was pointed out above, more resistant to disturbances due to the well conditions.

The most difficult problem of all is to identify water horizons in fissured formations, especially in crystalline rocks. Fissured formations can be identified by methods using radioactive tracers - solutions of salts and elements with anomalous nuclear properties. A solution of the most easily accessible salt, NaCl, may be used for this purpose in freshwater sections. A better result may be obtained with KCl, which has a higher solubility in water than NaCl. The solutions of boron salts are still more effective and widely applicable. Their neutron-absorbing power can be increased if we use salts enriched in the ^{10}B isotope.

In case of fissured formations, in which the volume of the porous space is very small, only pulsed neutron-gamma

logging provides a suitable recording method. Unlike neutron-neutron methods, this method can be used where the well is filled with a solution that absorbs neutrons and, therefore, shields the neutron detector. The main advantage of this method over the radioisotope methods is that the well background can be eliminated if the timing is suitably chosen. Pulsed neutron-gamma logs obtained with sufficiently long delay times are not sensitive to the well conditions if the lifetime of neutrons in the mud contained in the well is shorter than in the formation. Obviously, this condition is best satisfied when a solution containing the neutron-absorbing elements is pumped into the formation.

The porosity of water-bearing layers may be determined by neutron logging, in sections composed of sands and carbonates. If the formation porosity is higher than 20% it is better to use thermal neutron-neutron logging for fresh formation-water and epithermal neutron-neutron logging for saline water, with 40 - 50 cm sondes. Neutron-gamma logging with 60 cm sonde is the best method for low-porosity formations.

As we know, hydrodynamic methods are used for determining the filtration properties of a formation. The radioactive logging methods, like the other methods, give only indirect information on the infiltration properties of the formation. The hydrodynamic methods are, however, too laborious. In order to use radioactive logging data to evaluate the filtration properties, it is desirable to find some suitable means of correlating the results of hydrodynamic studies with those of radioactive logging. In sections composed of carbonate rocks with a granular type of porosity, we observe a relationship between permeability and formation porosity, as determined by the neutron method. Accordingly, we can find the critical value of porosity below which the formation does not produce water. In complicated cases, where no univalent correlation exists between the radioactive logging data and formation porosity, as determined by hydrodynamic studies, a multivalent correlation is established by regression analysis.

Apart from hydrodynamic studies, the pumping of air or gas into the formation has been tried as a method of obtaining the reference data on formation porosity. By experimental studies on formation models, it was found that there is a close relationship between permeability and the coefficient of displacement of water by air. On the basis of these studies a method may be suggested for studying water-bearing layers, which consists in pumping air or gas into formations and determining the coefficient of displacement of water by air or gas, using neutron logs. The neutron response may be calibrated in advance in units of air saturation of pore space of the water-bearing formation occupied by air. For each formation two neutron logs are taken - one before pumping air and one after. Then, the air saturation of the formation with the best filtration properties is determined.

The degree of mineralization of water in the formations may be determined by neutron logging. The method which is most sensitive to the mineralization of water saturating a formation, is pulsed neutron-neutron logging. This method may be used for determining the average lifetime of neutrons in the formation. If the formation porosity has been determined by an independent method or by core analysis, and if the average lifetime of a neutron in the formation skeleton, as calculated from the latter's chemical composition is known, then we can determine the average lifetime of neutrons τ_w in the formation water. The dependence of τ_w on the NaCl content of the water is illustrated by the data in Table II.

TABLE II

NaCl %	τ_w, /usec
0	205
0.1	202
0.5	190
1.0	177
3.0	139
5.0	114
10.0	76.8
15.0	57.1
20.0	45.0
25.0	36.5

As can be seen from these data, the parameter τ_w is highly sensitive to variations in the NaCl content of the water.

Formations with mineralized water can be differentiated from freshwater formations in wells if the mineralization exceeds 2% in respect of NaCl at 20% formation

porosity. In this case, the difference in the values of $\tau_{form.}$ will be about 10%. It is most advisable to use pulsed neutron-neutron logging for identifying mineralized water and determining its mineralization in cased wells which have been idle long enough for the zone into which mud filtrate has penetrated to absorb the filtrate. In complicated cases, where the composition of the skeleton is not known and the average lifetime of neutrons in the formation skeleton τ_{sk} cannot be determined with sufficient accuracy, the mineralization of water can be determined by the so-called "time-measurements" method. For this purpose, pulsed neutron-neutron logs are run immediately after the well is cased, when the formation is filled with the mud filtrate, the average lifetime of neutrons in which is known and equal to $\tau_{filt.}$ The average lifetime of neutrons in the formation τ_{form} is determined. But it is necessary to know the porosity in order to solve the problem. Therefore, pulsed neutron-neutron logging is always accompanied by neutron and gamma logging.

Survey of the technical conditions of wells includes studies to detect defects in the casing and in the cement column. For detecting defects in the casing or the cement column use is normally made of radioisotopes, which may be replaced with boron or saline-water solutions which absorb neutrons intensively. The best method for the detection of defects in a well using these substances is pulsed neutron logging.

4. THE USE OF NEUTRON SOURCES FOR SHALLOW SUBSOIL WATER EVALUATION.

A wide spectrum of practical tasks connected with the evaluation of shallow subsoil water in unsaturated and saturated zones is to be found in the field of irrigation and engineering geological investigations. Hydro-reclamation studies in areas which it is planned to irrigate or drain involve a large number of problems connected with construction and operation of irrigation systems and with forecasting water and salt balance in the areas in question. The most complicated ones of these problems are those which involve the determination of the drainage capacity of the unsaturated zone. Inaccurate calculations here may lead to the swamping and salination of the areas under irrigation in arid regions, and to intensive erosion by water and wind in areas being drained in humid regions.

Penetration neutron logging together with other nuclear logging is profitable for solving the abovementioned problems. The technological process of obtaining long diagrams while making holes provided the penetration logging to be very effective from the technical as well as economical point of view. In penetration logging special hydraulic equipment has to be used for operation of the sonde which is screwed with column of rods. (6).

In hydro-reclamation and engineering geological studies, penetration neutron logging is used for determiming the lithological composition and structure of the geological section in unsaturated and saturated zones, for establishing the physical characteristics of soils (moisture, porosity) for determining the level of subsurface water and stratification of water-saturated soils, for investigating the water-spreading zones in experimental inudation, etc.

In studying the lithological structure of loose deposits it is advantageous to use the neutron logging in addition to the gamma and gamma-gamma logging. On the diagrams of the moisture content of soils, obtained by neutron logging, the boundaries of abrupt variations of properties often coincide with the boundaries of the individual litho-genetic types of soils. The sands in the section under study have a much lower bulk weight than the clay deposits; the moisture content of the sands is also lower than in the clays in the unsaturated and saturated zones with the required degree of accuracy. By calibrating the sonde it is possible to record the neutron logs in units of moisture content.

The comparison of the quantitative data of the moisture content obtained by penetration neutron logging and by conventional sampling methods shows, that these data are in sufficiently good agreement with regard to the absolute value. There is also good agreement as regards the general pattern of variation in the moisture content with depth. However, we do observe a divergence between individual data, which is sometimes as much as 5 - 7% of the absolute value of volumetric moisture content. These divergencies are due to namely considerable natural inhomogeneity of moisture content as between individual types of deposits. Since the volume of the

soil in moisture determination by thermal neutron logging exceeds the volume of the sample in laboratory studies by three orders of magnitude, the representativeness of the comparable methods is widely different. Therefore, the spread in the absolute values of moisture content is quite understandable.

It may be noted that in the neutron logging sondes used, the distance between the detector and the neutron source is chosen as short as possible. For design considerations the minimum distance is 5 cm. This design of the sonde (called "short"), enables to conduct measurements in the pre-inversion sector of the curve $I_{nn} = f(w)$. Here we observe a linear dependence between the neutron radiation being recorded and moisture content in the 0 - 35% volumetric moisture content range. According to the experimental data, if the sonde length is decreased to 1 - 2 cm, the dependence remains linear up to 60% volumetric moisture content.

From the diagrams of moisture content and bulk weight it is not difficult to plot the diagrams of porosity, degree of moisture saturation for the unsaturated zone and bulk weight of soil skeleton. These diagrams may be derived by calculation using the elementary formulas of soil science.

In reclamation studies of areas which it is intended to irrigate or drain, a very important problem is to find the spatial distribution of the physical properties of soils in order to evaluate the drainage capacity of the unsaturated zone. This problem is solved with the help of penetration logging data. Owing to the high efficiency and mobility of the equipment, it is possible to obtain a set of logs for the given section at pre-determined horizontal distances. Using these diagrams, we can plot, for the section, the spatial distribution of moisture content, bulk weight and porosity.

The position of water-bearing layers in a given section may, in general, be found from neutron logs and gamma logs. In sandy clay deposits, where the ground water level lies in the sand, reliable data on the position of the level may be obtained from one neutron log. But if the groundwater level lies in clay soils, the surface of this water has no clear boundary in the natural position. This phenomenon is due to the existence of a high-lying boundary for the capillary rise of water. In this case, the boundary of the ground water level is taken arbitrarily on the basis of the degree of water saturation of the soil pores. It is customary to regard soils as fully water-saturated when the coefficient of water saturation is close to one.

In studying the movement of saline water front in areas to be irrigated, we can use thermal and epithermal neutron logging. The difference in intensities of the thermal and epithermal neutron radiation gives the degree of salination of soils and water on the basis of chlorine content.

The filtration properties of soils in unsaturated zones of areas to be irrigated are studied under field conditions by experimental filling of wells, shafts and pits with water. Penetration neutron logging was used to determine the water dispersion zone after the experimental filling of a pit. A pit 4 x 4 m in area and 2 m in depth was filled with water and the water level maintained for several days. Before filling, thermal neutron logs were taken along the line passing through one of the pit's axes every 2 m in the horizontal plane. The spatial distribution of the natural moisture content in the section was plotted from these diagrams. During the dispersion of water in the unsaturated zone after the pit was filled, logging was conducted again and the spatial distribution of the moisture content in the section was replotted. After filtration from the pit became steady, the final picture of water dispersion was obtained from the thermal neutron logs. It showed a zone of complete soaking, a zone of intense capillary wetting of the soil and a zone of high wetting.

Qualitative estimation of the water content of soils and subsoil layers in the unsaturated zone is successfully carried out with the help of neutron moisture gauges, of which there are many different types constructed by a number of firms. At the present time these gauges are the most reliable means to give us certain information on moisture of soil in situ.

Two techniques are used in practice to determine the moisture content of soil by neutron moisture gauges. The first is based on the recording of thermal neutrons and is used when there are no strong absorbers of thermal neutrons in the soil. The second is based on the recording of epithermal

neutrons and is used in determining the moisture content of soil with a high salt concentration.

There are many publications in which detailed consideration is given to the theoretical aspects of using the neutron gauges for moisture content determination and to the influence on the results by factors such as the density and chemical composition of the medium and the probe parameters (4, 7). It is shown in these studies that the neutron method can be used to determine moisture content to within ± 1%. The soil volume measured can be as much as several thousand cubic centimeters, depending on the probe parameters and on the measurement conditions.

Numerous practical and scientific tasks are solved with the use of neutron moisture gauges for investigation of soil moisture in hydrogeology, hydrometeorology, agriculture and engineering geology. The gauges are also used for investigating the processes of seepage and leakage of water from irrigation canals and reservoirs.

During the measurement of moisture by neutron moisture gauges and during the investigation of the special distribution of moisture it is necessary to take into account that information, content and representation of the moisture data obtained are affected by the following properties of the soil: (1) the variation range of the parameter; (2) its space variability; and (3) time variability (presence of disturbances, anomalous absorbers and scatterers, effect of moisture content). The most important characteristics of the neutron method of determining the moisture content of soils include: (1) measurement range; (2) nature of measurement (linear, non-linear); (3) total error of measurement; (4) volume of one measurement (sphere of measurement) and the nature of the average of the parameter of this volume; (5) time for one measurement (series of measurements); (6) arrangement of the network and the time conditions of observations; (7) total number of observations; (8) protection from disturbances.

The total error of the neutron method of determining moisture content depends on: (1) natural variations of the properties being measured from point to point; (2) influence of impurities, mutual influence of density and moisture content, calibration errors; (3) instrumentational errors; (4) technological errors.

The influence of the abovementioned factors and their taking into account during the measurement of moisture by neutron moisture gauges can be achieved on the basis of methods of mathematical statistics and information theory which can serve as a tool for the evaluation (8).

* * *

The problem of using neutron sources for underground water exploration is one of the questions which are the subject for international co-operation, being implemented through the IAEA. The more active actions of hydrologists from different countries in the field of using nuclear methods in hydrology started in connection with the establishment of the International Hydrological Decade (1964 - 1974). The Co-ordinated Council of IHD, UNESCO established a working group on nuclear methods in hydrology for practical implementation of this co-operation. The technical and scientific secretary for this working group is provided by the IAEA.

Scientific and practical aspects of using the neutron sources for underground water exploration found their reflection in the following IAEA publications which were completely or in part prepared by the working group: "Guidebook on Nuclear Techniques in Hydrology" (9); "Nuclear Logging in Hydrology" (10); "Nuclear Moisture Gauges" (7).

Three symposia on nuclear methods in hydrology were organized also, during which questions of using neutron sources for underground water exploration were discussed together with others. The proceedings of these symposia have also been published by the International Atomic Energy Agency (11, 12, 13).

REFERENCES

1. A.E. Ringwood. "Chemical evolution of the terrestrial planets." Geochim. Cosmochim. Acta 30, 41-104 (1966).

2. V.I. Ferronsky et al. Isotope Hydrogeology. (In preparation) (1970).

3. E.M. Filippov. Applied Nuclear Geophysics (Prikladnaja jadernaja geofizika), Izd. Akad. Nauk SSSR, Moscow (1962

4. V.I. Ferronsky et al. Radioisotopic Methods in Engineering Geology and Hydrogeology (Radioisotopnie metody issledovanija v inženernoj geologii i gidrogeologii). Atomizdat, Moscow (1968).

5. V.I. Ferronsky and Ja. N. Basin. Methods of nuclear logging in hydrogeology. Report to IAEA Working Group on the use of nuclear techniques in hydrology. IAEA, Vienna (1969).

6. V.I. Ferronsky. Penetracionno-karotažnye metody inženerno-geologicheskih issledovaniy (Penetration logging in engineering geology). Izd.Nedra, Moscow (1969).

7. International Atomic Energy Agency. Neutron Moisture Gauges. Technical Reports Series No. 112, IAEA, Vienna (1970).

8. V.T. Dubinchuk. Nuclear methods for determining density and moisture content - evaluation of the information obtained and its representativeness. Report to IAEA Working Group on the use of nuclear techniques in hydrology. IAEA, Vienna (1970).

9. International Atomic Energy Agency. Guidebook on Nuclear Techniques in Hydrology. Technical Report Series No. 91, IAEA, Vienna (1968).

10. International Atomic Energy Agency. Nuclear well logging in hydrology. Technical Reports Series (in printing) IAEA, Vienna (1970).

11. International Atomic Energy Agency. Radioisotopes in Hydrology (Proc. Symp. Tokyo, 1963) IAEA, Vienna (1963).

12. International Atomic Energy Agency. Isotopes in Hydrology. (Proc. Symp. Vienna, 1966) IAEA, Vienna (1967).

13. International Atomic Energy Agency. Isotope Hydrology. (Proc. Symp. Vienna, 1970) IAEA, Vienna (1970).

Session IV

INDUSTRIAL USES OF NEUTRON SOURCES

RADIOISOTOPE NEUTRON ACTIVATION FOR ON-STREAM PROCESS ANALYSIS

John R. Rhodes

Columbia Scientific Industries
Austin, Texas

The high penetration of neutrons and gamma rays makes nuclear techniques well-suited to on-stream analysis in industrial conditions. The availability of neutron-emitting radioisotope sources, particularly ^{252}Cf, makes possible the manufacture of relatively inexpensive, rugged and reliable process analyzers. Progress in development of techniques and instrumentation is reviewed.

Early work was limited to laboratory demonstrations of the activation of fluorine, vanadium, manganese, selenium, silver, and indium in flowing solutions. More recently, parts-per-million sensitivity has been reported for on-stream determination of sodium, magnesium, aluminum, chlorine, cobalt, copper, and hafnium in solutions using a non-recirculating loop system designed for industrial process analysis. The practicability of recirculating systems for slurry analysis has also been demonstrated and the development of instruments for on-stream monitoring of fluorine, barium, and silicon in ores reported.

Current work is reported herein on the use of ^{252}Cf for on-stream determination of low cobalt levels in process solutions; copper, silver, and gold in ores; and calcium in cement raw mix.

INTRODUCTION

Neutron activation is a widely used and rapidly developing laboratory technique for elemental analysis (1, 2), but applications in the more severe industrial environment are more recent and, as yet, much fewer. Neutron techniques have considerable potential in this area since they possess certain very marked advantages over conventional methods, particularly in on-stream analysis. The relatively high penetrating power of both the incident neutrons and emitted gamma rays makes measurements feasible on flowing streams carried in standard steel containers or on moving bulk materials transported by ordinary conveyor belts. Special presentation cells with thin and/or transparent windows are not necessary. Also the high penetration (up to a few inches) minimizes errors due to heterogeneity in analysis of coarse granular solids and slurries with variable particle size. The weight of material being measured, whether a continuous or a batch sample, can often be made large enough to be representative of the process stream at that time, thus removing a very important source of error in process analysis of heterogeneous materials. In addition the recent availability of ^{252}Cf, a neutron source having extremely high specific output, should greatly increase the degree of utilization and speed of acceptance of the technique.

APPARATUS

An activation analysis system consists basically of a shielded source where samples can be reproducibly positioned for neutron irradiation, a sample transfer system where the time delay between irradiation and counting can be controlled, and a counting space where the irradiated samples are located for measurement of characteristic gamma-rays of interest, normally using a shielded lithium-drifted germanium or thallium-activated sodium iodide gamma-ray spectrometer.

In on-stream analysis the sample is continuously moving between irradiation and measurement, and optimization of flow rates and residence times with respect to wanted and unwanted radioactivity has to be considered. Simplified theoretical formulae for detector count rate as a function of residence times in the different loop components, flow rate, time, half-life, source strength and detector efficiency have been compared for both open and closed loop systems (3).

The sample to be analyzed may be solids on a conveyor belt, or a liquid or slurry in pipes. In general it is preferable to route a sample of the plant stream to a separate analysis loop so as to better control the analysis conditions, although some experiments have been performed directly on a conveyor belt. (3, 4).

Both closed and open analysis loops have been considered (3, 5, 6) and Figure 1 shows a schematic of a possible closed loop arrangement. If preferred, samples from the process stream can be introduced continuously, with a continuous bleed-off (not shown in the Figure). Naturally this would complicate the analysis somewhat, but is perfectly feasible.

slurry loops can easily be envisaged, such as where two samples could be recirculating in separate parts of the system at the same time, one being activated whilst the other is counted.

Figure 2 shows a typical schematic of the electronic system and Figure 3, a photograph of a process slurry analyzer.

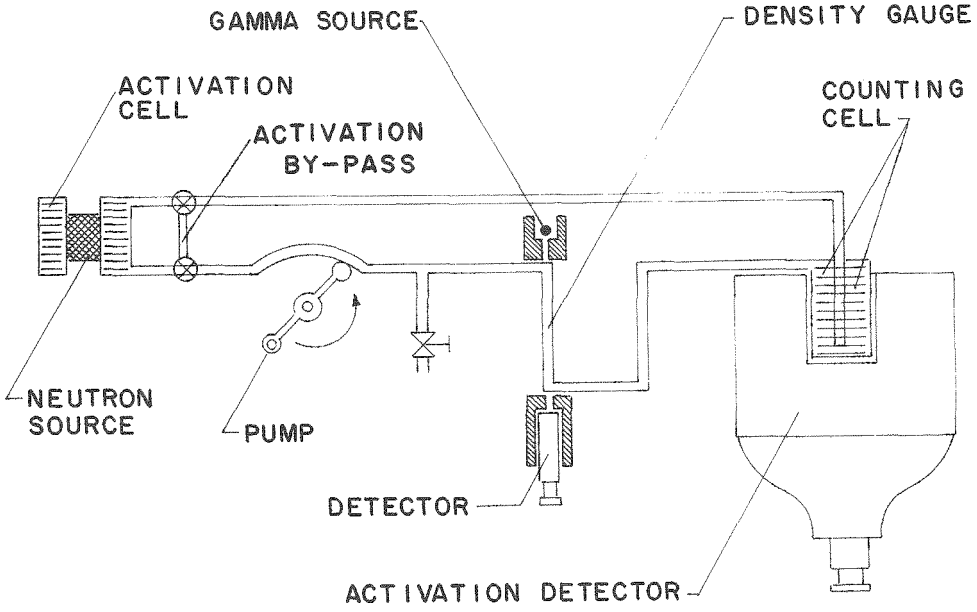

FIG. 1 SCHEMATIC SHOWING PRINCIPLE COMPONENTS OF CLOSED LOOP SLURRY PRESENTATION SYSTEM

The ancillary measurement of solids content is required for slurry analysis, since the information required is element content of the solids, not of the slurry.

The choice of loop parameters such as activation and counting cell volumes, and flow rate, depends on the mechanical properties of the material to be analyzed (e.g., the settling rate of solids in a slurry) as well as on the nuclear properties (e.g., neutron and gamma-ray energy, and half-life). A good deal of research into optimization of these parameters is being conducted at this time. One of the results of this has been the installation of an activation cell by-pass in the Columbia Scientific facility (Figure 1), to allow short-lived activity to decay and so improve detection sensitivity for longer-lived radioisotopes. Another has been the careful design of the activation and counting cells so as to preserve a constant cross sectional area of flow, equal to the cross sectional area of the connecting tubing. More sophisticated

NEUTRON SOURCES

Of the available neutron sources (nuclear reactors, accelerators and radioisotopes), the use of reactors is ruled out for process control, unless one happens to be on site.

One of the main problems with accelerator neutron generators is the need to change targets frequently or, with sealed tubes, the expense of buying a new tube. In laboratory analysis this is acceptable because a typical irradiation time is about one minute per sample and the total duration of tube operation may be only one hour per day. However, on-stream analysis often demands 24-hour continuous operation, and changing neutron targets or tubes every few days is clearly unacceptable. A further disadvantage of neutron generators using the normal (d,T) reaction is that the resulting 14 MeV neutrons are energetic enough to make the water in the analysis loop strongly radioactive by the $^{16}O(n,p)^{16}N$ reaction.

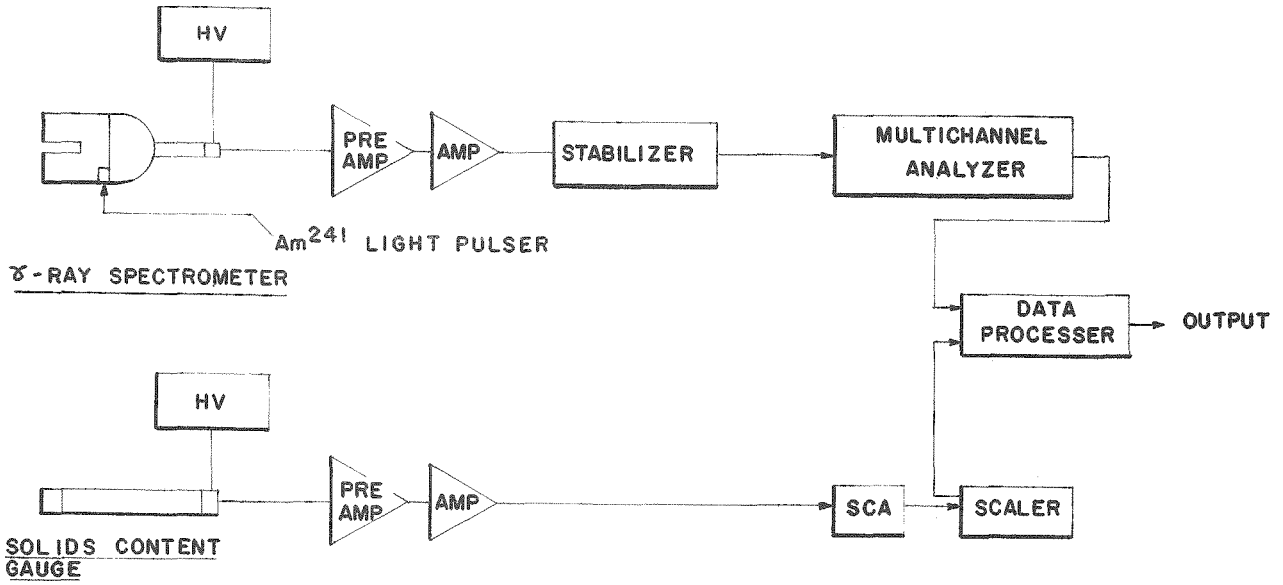

FIG. 2 BLOCK DIAGRAM OF ELECTRONIC UNITS

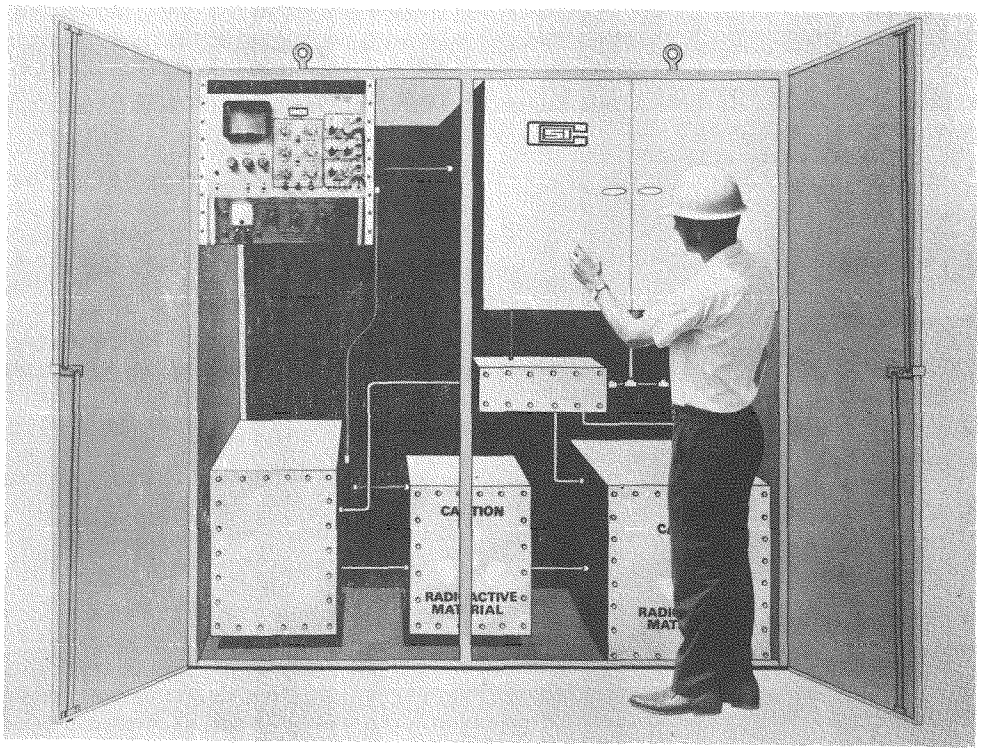

FIG. 3 PROCESS ANALYZER, SHOWING MODULAR ARRANGEMENT

Radioisotope sources are, for all practical purposes, stable, and can be chosen to have an effectively unlimited life. Thus they are very well-suited to industrial conditions. Radioisotope (α,n) sources produce neutrons with a continuous range of energies up to about 10 MeV, the most probably energy being about 4 MeV. Until now the highest outputs available have been only a few times 10^7 n/sec., using several tens of curies of an α-emitter such as ^{241}Am, ^{228}Th, or ^{210}Po, intimately mixed with a Be target. ^{124}Sb-Be (γ,n) sources give similar outputs of much lower energy neutrons. In spite of the short half-life (60 days) of ^{124}Sb, the isotope is relatively cheap and an on-stream analyzer using this source has been developed. (7). Even where outputs of specific (α,n) or (γ,n) sources above 10^8 n/sec are technically feasible, the price is comparatively high, or the physical size of the source is so great that the neutron flux per unit volume of sample irradiated is relatively low.

These problems have reduced the attractiveness of the technique and slowed its acceptance by Industry.

The recent availability of ^{252}Cf spontaneous fission sources, whose specific neutron emission is several orders of magnitude greater than that of (α,n) and (γ,n) sources, promises to open up the whole field of on-stream neutron activation analysis. A 1 mg source emits 2.34×10^9 n/sec, will cost a little over $10,000, and can be encapsulated in a cylinder 1 inch long x 0.4 inch diameter. The half-life is 2.65 years.

DETECTION SYSTEMS

The usual measurement system is a gamma-ray scintillation spectrometer as shown in the schematic in Figure 2. A three-inch diameter x three-inch thick NaI(Tl) crystal has been found to be a suitable compromise between detection efficiency and cost and is now widely used. Larger crystals, in particular five-inch diameter x four inches thick, are also in use. In many cases there is a trade-off in cost of sodium iodide against cost of neutrons.

For industrial conditions thermal stability of the system gain is most important. Water cooling of the photomultiplier can be used, or if the gamma-ray spectrum is particularly simple, it can be counted in toto, thus reducing considerably the need for gain control. The recent availability of ^{241}Am α sources embedded in the NaI(Tl) crystal has provided a convenient means of stabilizing the gamma-ray spectrum. The peak due to ^{241}Am α particles can be made to appear at any convenient pulse height equivalent to a γ-ray energy below about 6 MeV. The peak is rather sharper than a corresponding γ-ray peak and has no associated Compton distribution. A single channel analyzer window can be locked onto this peak to provide continuous automatic stabilization.

Ge(Li) detectors, with resolutions one to two orders of magnitude better than NaI(Tl) have not yet been used in industrial analyses. Their main disadvantage is the need for cryogenic cooling at all times but the latter is not at all impractical in an industrial environment; liquid nitrogen is now a very common commodity and thermoelectric or other coolers are quite practicable.

APPLICATIONS

REVIEW

There have been very few reported applications of radioisotope neutron activation analysis of flowing sample streams, although the technique was demonstrated as early as 1962 by Anders (8) who activated fluorine, silver, and selenium in aqueous solutions using a small ^{226}Ra-Be source (1.3×10^5 n/sec). Although count rates were so low as to necessitate irradiation and counting times of about six hours, the feasibility of rapid on-stream analysis using stronger sources was clearly envisaged.

Gluck et al. (9) in 1961 studied on-stream production of intrinsic radiotracers for industrial process control. Although this is not the same as continuous process analysis, the work is useful for the design studies made on optimum volumes of activation and counting cells and on the functional relationship between flow rate, mean residence time in the irradiation cell, and mean delay time between irradiation and counting, for an open loop system. The sensitivities for determination of manganese, indium, vanadium, and silver in aqueous solution were studied experimentally using 10 and 50 Ci ^{210} Po-Be sources. Sensitivities for some sixty other elements were calculated and tabulated.

Recently Downs and Davis (7) have described an on-stream activation and detection system for industrial process monitoring and radiotracer production. The instrument comprises an open loop for solution transport, a 7.2 kilocurie ^{124}Sb-Be (γ,n) source and a 3 inch x 3 inch NaI-Tl) gamma-ray scintillation spectrometer. Detection sensitivities were investigated for seven elements (sodium,

magnesium, aluminum, chlorine, cobalt, copper and hafnium) in solution and were found to be in the range 0.1 p.p.m. (Hf) to 60 p.p.m. (Mg). Sensitivities for another 65 elements were calculated.

Slurry transport imposes further constraints on the design of activation analysis loops. Flow velocities of 2 to 10 feet/sec in the analysis cells and connecting pipes are required to keep the slurry in suspension and, under some conditions, it is necessary to use continuously-stirred activation and counting cells. Thus, reduction of the volume flow rate to increase the specific activity (7, 9) is not always possible. Also, the use of long lengths of pipe for time delay may unacceptably increase frictional losses, and consequent head pressures.

It has been shown that recirculating loops can be used to avoid some of the problems of slurry transport, provide steady flow conditions for the analysis and, in certain cases, enhance the signal (3, 5, 6). Using the closed loop system, longer-lived activity can be allowed to build up to levels orders of magnitude greater than would be possible in an open loop, especially if the flow rate has to be kept high to maintain slurries in suspension.

Starnes (5) has set up a small recirculating slurry loop designed primarily for determination of fluorine and barium in fluorite and barytes slurries. The source used is 3 Ci of ^{241}Am-Be and the detector, a 3 inch x 3 inch NaI(Tl) crystal. Re-entrant, baffled activation and counting cells each of volume 3 liters are connected by 0.5 inch bore plastics tubing.

Fluorine is activated by the $^{19}F(n,\alpha)^{16}N$ reaction (gamma-ray energies 6 to 7 MeV, half-life 7.14 seconds). Barium is activated by the $^{137}Ba(n,n')^{137m}Ba$ reaction (gamma-ray energy 0.66 MeV, half-life 2.6 minutes).

With flow in one direction the delay between irradiation and counting is about 4 seconds, which allows the fluorine determination to be made. With the flow reversed the delay is about 50 seconds allowing the ^{16}N activity to decay and the barium determination to be made.

The solids content of the slurry (about 35% w/w) is monitored continuously with a ^{137}Cs gamma-ray density gauge.

Figure 4 shows a calibration curve obtained using various fluorite ores at different solids contents.

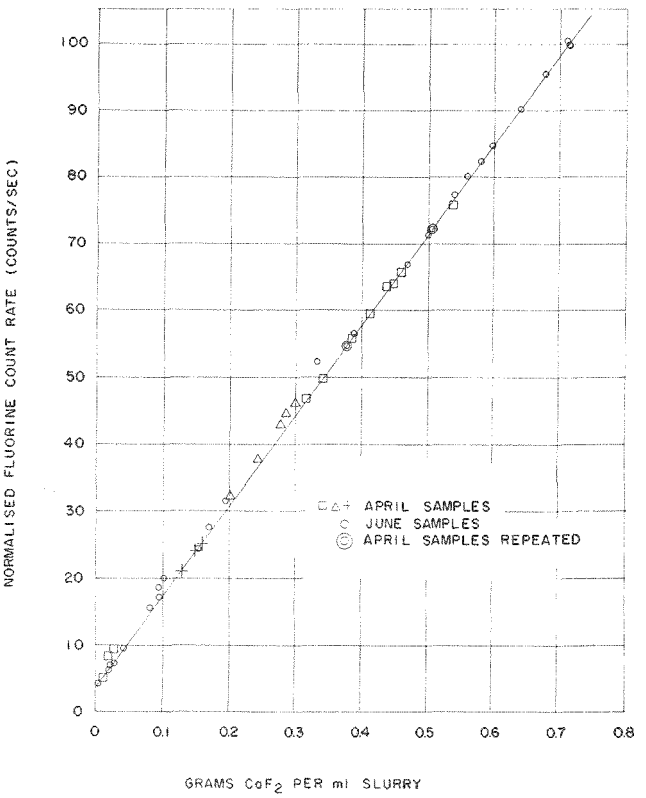

FIG. 4 CALIBRATION CURVE FOR FLUORINE DETERMINATION

CURRENT WORK

Using the on-stream analysis facility shown schematically in Figures 1 and 2 and described in reference (10), we have completed preliminary investigations of the determination of cobalt in solutions; copper, silver and gold in ore slurries; and calcium in cement raw mix slurries. This work is part of an evaluation of the potential uses for ^{252}Cf in on-stream analysis being performed under the auspices of the U. S. A. E. C. loan program. The weight of ^{252}Cf used was 400 µg, with a total output of 8 x 10^8 n/sec at the time of the experiments.

Cobalt in Solution. Cobalt is an important catalyst and occurs in certain organic and aqueous process streams in concentrations from 10 to 10^4 p.p.m. For the purpose of this test a suitable simulated solution was cobalt nitrate in water, and solutions containing up to 800 p.p.m. Co were made up. The preferred nuclear reaction for activation of cobalt is by thermal neutrons as follows. $^{59}Co(n,\gamma)\ ^{60m}Co$; γ-ray energy 1.33 MeV, half-life 10.5 mins.

Each solution was recirculated for 30 minutes and 5-minute counts taken after 1 minute and 20 minutes. Figure 5 shows the calibration curves obtained. Background under the 1.33 MeV peak was estimated by counting windows on each side of the peak. The slope of the calibration obtained after 20-minute irradiations was 7.8 net counts per p.p.m. cobalt. Since the standard deviation on the net count was 200 in 5 minutes, the detection limit (1 standard deviation) is 25 p.p.m. cobalt. For the measurements taken one minute after irradiation started, the corresponding detection limit (one standard deviation) is 40 p.p.m. cobalt.

Ore Analysis. Activation of a typical ore matrix indicated that the main source of background is due to the 1.78 MeV γ-rays from $^{27}Al(n,\gamma)\ ^{28}Al$ (and, to a lesser extent, from $^{28}Si(n,p)\ ^{28}Al$). Figure 6 shows the spectrum obtained from a natural ore sample, counting for the last 5 minutes of a 7-minute recirculating activation. The ore sample contained 12.7% Cu, 3.1 oz/ton Ag (90 p.p.m.) and 0.03 oz/ton Au (0.9 p.p.m.). Peaks due to activation of copper and silver are seen, but none due to activation of gold. The ^{28}Al peak is prominent and its Compton continuum is a major source of background under the lower energy peaks. The ^{56}Mn peak is also prominent and could be due to small quantities of manganese in addition to the relatively large amount of iron known to be present.

An ore matrix simulating the average elemental composition of sedimentary or igneous rocks was made up by mixing powdered chemicals as follows: SiO_2, 58.0%, Al_2O_3, 14.0%; $CaCO_3$, 10%; Fe_2O_3, 5.5%; Na_2CO_3, 4.5%; K_2CO_3, 4.2%; MgO, 3.0% and TiO_2, 0.8%.

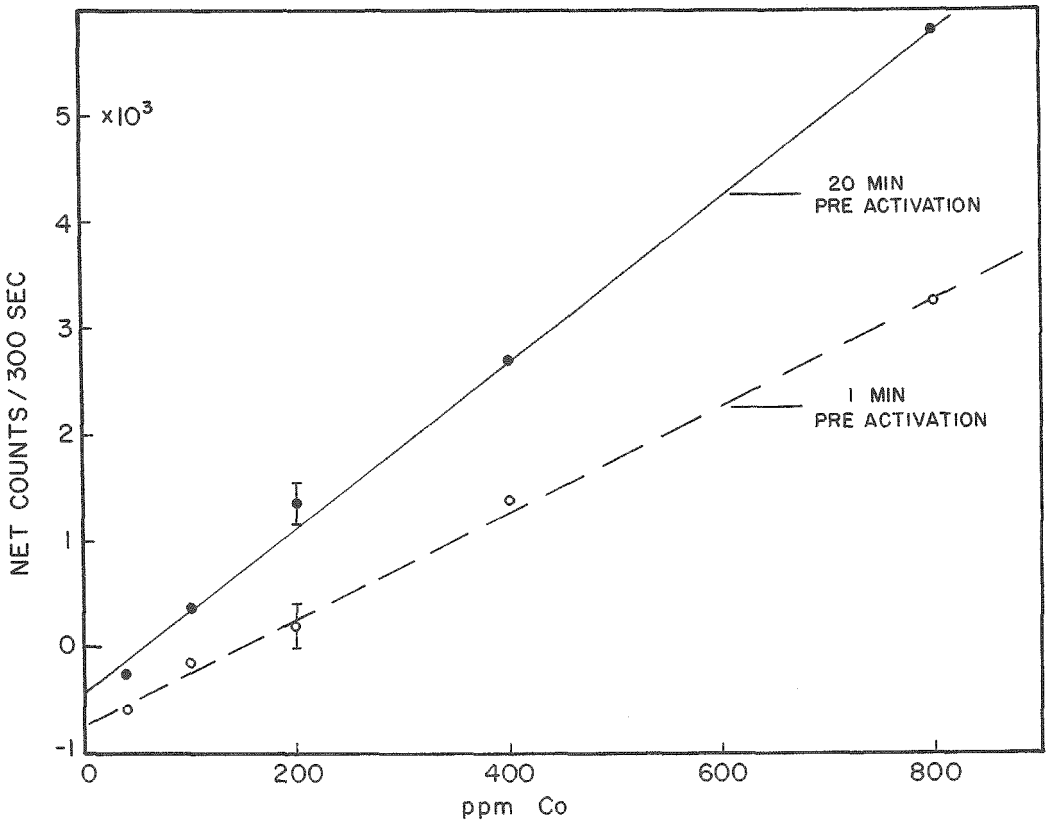

FIG. 5 CALIBRATIONS FOR DETERMINATION OF COBALT IN SOLUTION

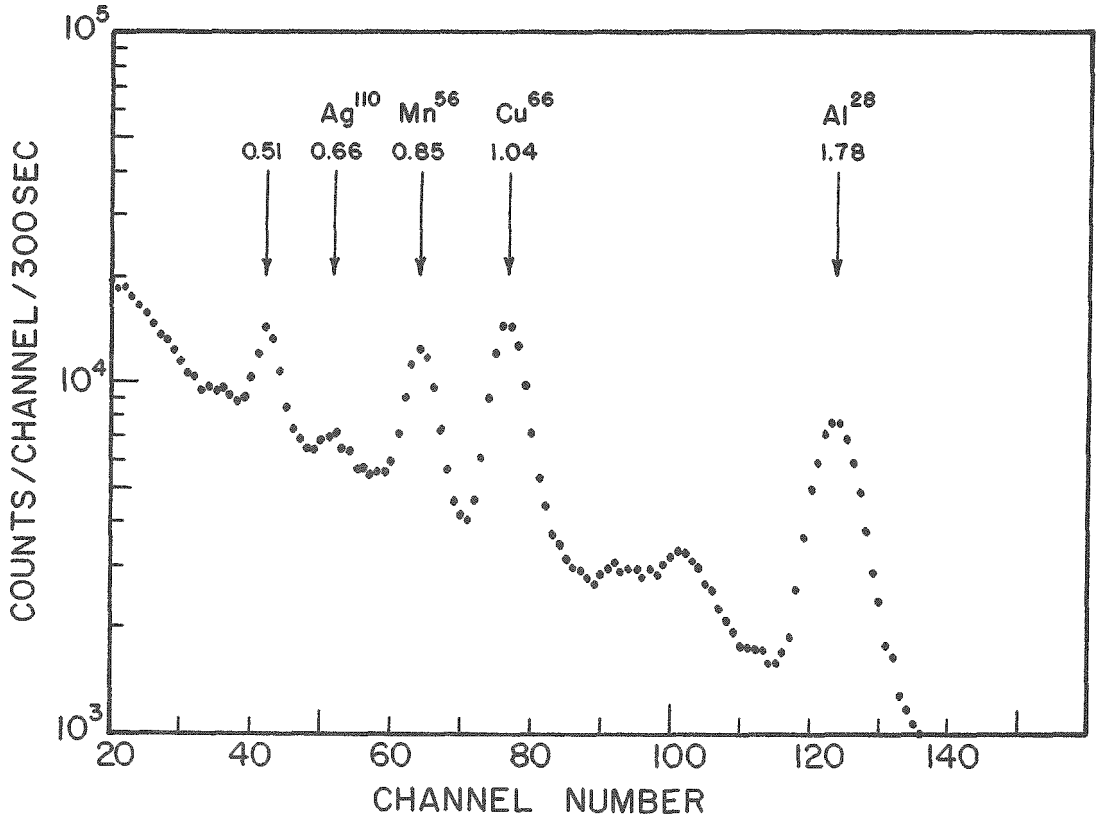

FIG. 6 SPECTRUM FROM RECIRCULATING AQUEOUS SLURRY OF NATURAL ORE SAMPLE

The sensitivity for determination of silver in ores was estimated by recirculating the simulated ore matrix spiked with known quantities of Ag_2O. The preferred reaction is $^{109}Ag\ (n,\gamma)\ ^{110}Ag$, γ-ray energy 0.66 MeV, half-life 24.5 seconds. The activation and counting schedule for each sample was 2 minutes' recirculating activation with a 50-second count started 50 seconds after commencement of the activation. The calibration curve obtained of net count in the 0.66 MeV γ-ray peak against Ag_2O content is shown in Figure 7. The net count was obtained by subtracting background as before. The slope of the calibration curve was 5.8 net counts per p.p.m. Ag_2O. The standard deviation on the net count, in the range 0 to 1000 p.p.m. Ag_2O, was 170 counts which is equivalent to 30 p.p.m. Ag_2O, or 1 oz/ton.

Copper is activated by $^{65}Cu(n,\gamma)\ ^{66}Cu$ which decays by emission of 1.04 MeV γ-rays with a half-life of 5.1 minutes. Simulated ore matrix samples spiked with CuO were activated and counted as follows. Ten minutes of recirculating activation was followed by 20 minutes of recirculating decay (using the activation cell by-pass). Five-minute counts were taken beginning 1 minute after commencement of activation, and 5 and 14 minutes after commencement of the decay cycles. Net counts were obtained for the 1.04 MeV copper peak.

Figure 8 shows the three calibration curves obtained for copper determination. The relative slopes and standard deviations are tabulated below.

Conditions	Net Counts Per % CuO	Std. Dev., % CuO
1-6 min count	3350	0.13
15-20 min count	2800	0.09
24-29 min count	1100	0.20

The earliest count shows a relatively high background due to ^{28}Al activity (note that net counts are plotted in the figure). The count begun after 5 minutes' delay shows near optimum sensitivity due to the more rapid decay of the ^{28}Al activity, but the last count gives poorer sensitivity because the ^{66}Cu has decayed too.

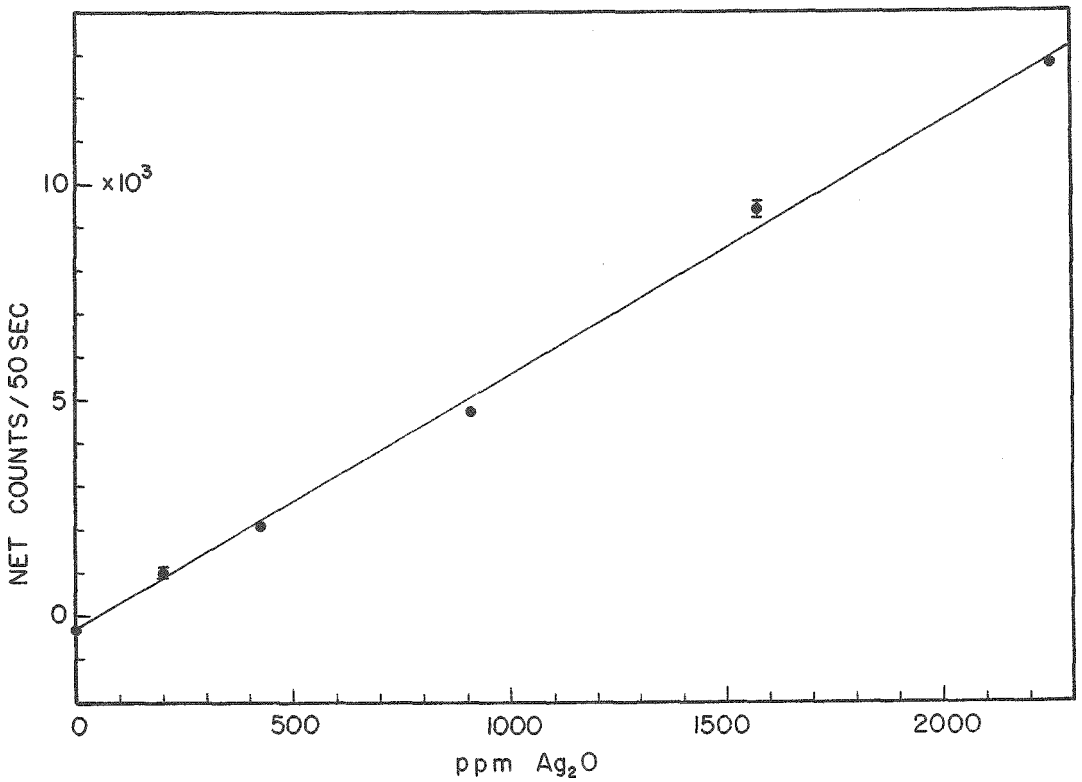

FIG. 7 CALIBRATION FOR SILVER IN ORE SLURRIES

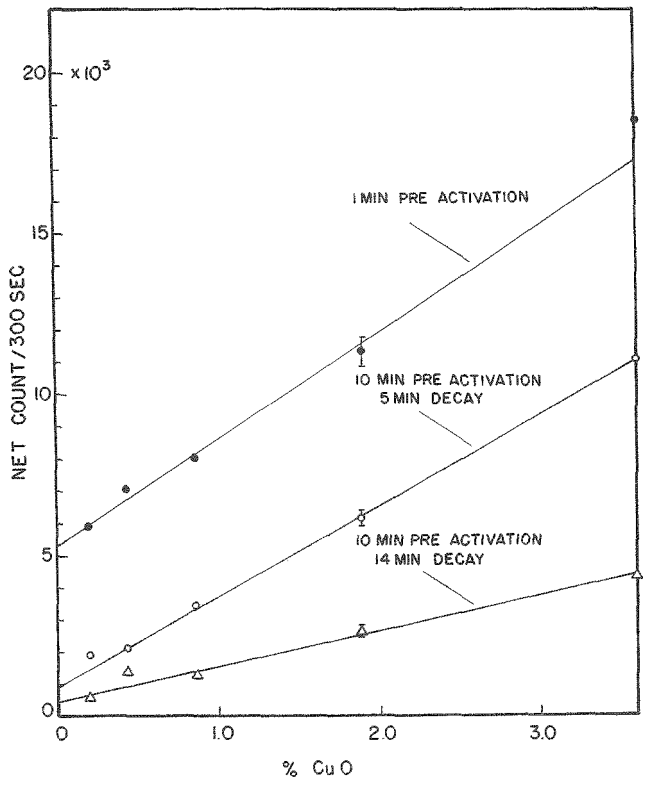

FIG. 8 CALIBRATIONS FOR COPPER IN ORE SLURRIES

The preferred reaction for gold determination is ^{197}Au (n,γ) ^{198}Au, γ-ray energy 0.41 MeV, half-life 2.7 days. The advantage of the long half-life is that long activation, decay and count times can be utilized to increase sensitivity. Naturally times of the order of a day are unrealistic, since if this time were available classical methods could be used. Artificial ore slurries spiked with up to 5500 p.p.m. gold were recirculated for just over 20 minutes each and a ten-minute count started after 10 minutes. Measurement of the 0.41 MeV γ-ray peak produced a linear calibration with a standard deviation of 400 p.p.m. gold.

Calcium in Cement Raw Mix. One of the most important potential applications of on-stream neutron activation is to the determination of "basicity ratio" in iron ore processing and cement manufacture. This involves determination of calcium and silicon, and also possibly iron, aluminum and magnesium. The key to this analysis is to assess the feasibility of the calcium determination. In spite of interference from our light pulser peak (equivalent energy 2.8 MeV) we have made a preliminary study of determination of calcium using the reaction ^{48}Ca (n,γ) ^{49}Ca (γ energy 3.1 MeV, half-life 8.8 minutes).

Using a simulated cement raw mix slurry (12.5% solids comprising 80.5% $CaCO_3$, 14.0% SiO_2, 4% Al_2O_3 and 1.5% Fe_2O_3) the statistical accuracy for counting the 3.1 MeV peak was estimated to be 1.0% $CaCO_3$ (assuming the pulser peak to be absent) in a 5-minute count after a 24-minute recirculating activation. This is considered to be extremely promising and we plan to make further investigations after modifying our detector to remove the pulser peak from the vicinity of the ^{49}Ca γ-ray energy.

Sensitivity. The sensitivity required of the above analyses in process control depends on the process. For cobalt determination the sensitivity reported here is adequate in some processes, but in others it must be ten times better. In silver ore assay a precision of about 0.1 oz/ton is required. Ore grade copper ore contains a few tenths of one percent but in copper ore processing the tailings must be analyzed with at least 10% precision, and they contain less than 0.1% copper. Sensitivities of better than 0.1 p.p.m. gold are required in gold ore analysis but for determination of gold in electroplating bath solutions, another important application, the sensitivity obtained in this work is almost adequate.

If the signal can be increased without increase in background, a proportionate increase in sensitivity results; if both signal and background increase together the sensitivity increases with the square root of the signal. It is usually possible to avoid greater rates of background increase by judicious choice of irradiation and delay times. Whether or not the signal can be increased without a corresponding background increase depends on the analysis. It is likely to be possible in the case of cobalt determination, where the matrix is dilute nitric acid, but in ore analyses, production of ^{28}Al and ^{56}Mn will always present problems.

Assuming that the ^{252}Cf source weight (i.e. output) is limited to 4 mg by cost of isotope and bulk of shielding; that the total of irradiation, decay and count times is limited to about one hour; and that for slurry analysis the solids content can be increased by a factor of four to 50% by weight, we expect the following sensitivities to be obtainable: cobalt in solution, about 1 p.p.m.; silver in ores, about 5 p.p.m.; copper in ores, about 0.02% to 0.01% depending on the matrix; gold in ores, about 5 p.p.m. (and in solution, about 20 p.p.m.); calcium in cement raw mix, better than 0.1% $CaCO_3$ at 80% $CaCO_3$ (counting statistics only).

CONCLUSIONS

Although only preliminary results have been obtained so far, it is quite clear that, with the availability of ^{252}Cf, neutron activation will have wide application in on-stream industrial process analysis. The absence of heterogeneity effects represents a significant advantage for neutron activation over other methods used for ore analysis.

Activation of the matrix is an important factor reducing sensitivity, particularly in ore analysis, and high sensitivities reported without allowing for this will not be attained in practice.

REFERENCES

1. Coleman, R. F., and Pierce, T. B. "Activation Analysis, A Review." The Analyst, 92, 1 (1967).

2. "Guide to Activation Analysis." Ed., W. S. Lyon, D. Van Nostrand Co., Inc. (1964) New York.

3. Rhodes, J. R., Berry, P. F., and Sieberg, R. D. "Nuclear Techniques in On-Stream Analysis of Ores and Coal." ORO-2980-18 (Final Report) 1968.

4. Gray, A. L., and Metcalf, A. "Industrial Applications of Neutron Activation." Modern Trends in Activation Analysis, 86, (1965).

5. Starnes, P. E., Mintek, U.K. (Private communication).

6. Ashe, J. B., Berry, P. F. and Rhodes, J. R. "On-Stream Activation Analysis Using Sample Recirculation." Modern Trends in Activation Analysis, NBS Special Publication 312, Vol. II, 913 (1969).

7. Downs, W. E. and Davis, M. W. "Characteristics of an On-Stream Analysis System Using a Multikilocurie ^{124}Sb-Be Neutron Source." Nuclear Applications, Vol. 7, 466 (November 1969).

8. Anders, O. U. "Activation Analysis for Plant Stream Monitoring." Nucleonics, 20 2, 78 (1962).

9. Gluck, P., et al. "Studies on On-Stream Production of Short-Lived Intrinsic Radiotracers for Industrial Process Control." Batelle Memorial Institute Report B.M.I., 1606 (1962).

10. Rhodes, J. R. Californium-252 Progress No. 5. U. S. A.E.C., 29 (November 1970).

USE OF A SEALED TUBE NEUTRON GENERATOR FOR QUALITY CONTROL IN EXPLOSIVES BY FAST NEUTRON ACTIVATION ANALYSIS (FNAA)

Stanley Semel and Samuel Helf

Feltman Research Laboratory
Explosives Division
Picatinny Arsenal
Dover, New Jersey

Two years of experience with a Kaman Nuclear sealed tube neutron generator for FNAA is reviewed. The history of the neutron output for the first sealed tube used with this system for 70 hours of operation is described and the operational experience is briefly discussed.

The analysis for total nitrogen content via the $^{14}N(n,2n)^{13}N$ reaction for a variety of organic explosives is described. Data are given for nitrocellulose, TNT, HMX, and Octols. It is shown that high accuracy and precision, comparable to wet chemical analysis is obtained using dual-axis rotation during irradiation and careful choice of reference standard. Comparison of accuracy and precision is also made with a single-axis rotation method.

Application of FNAA to the analysis of binary mixtures containing two compounds of different nitrogen content is also described. The total nitrogen content of a sample is first measured by activation and then related to composition of the mixture. This method is applied to Octol compositions, containing varying proportions of TNT (18.50% N) and HMX (37.84% N). A technique is described for the simultaneous irradiation of nine Octol samples and one reference standard using single-axis rotation. The precision of duplicate assays for 378 plant samples is given and discussed.

INTRODUCTION

The recent availability of high output sealed tube neutron generators, based on the $^{3}H(d,n)^{4}He$ reaction, makes the technique of neutron activation analysis more attractive as a practical tool for process and quality control applications. The chief advantages of this design over the more classical differentially-pumped Cockcroft-Walton type of generator are elimination of the high vacuum system maintenance and even more important, elimination of the need for frequent tritium target changes and handling. In this laboratory, a Kaman Nuclear model A 711 sealed tube neutron generator (1) has been used for two years, primarily for the fast neutron activation analysis (FNAA) for gross elements in explosives, propellants and related high energy materials.

A physical layout (not to scale) of the laboratory facility is shown in Fig. 1. The concrete block walls of the cell housing the generator tube and associated components are 1.7 meters thick. The system also includes a Kaman Nuclear dual-axis rotator assembly for simultaneous transfer and irradiation of a reference and unknown sample, and a dual-scintillation detector system designed for simultaneous counting of activated samples. Automatic transfer of samples between load station to the rotator assembly in front of the target and back of the count station is accomplished pneumatically by means of two 1.2 cm. (i.d.) polyethylene tubes which loop down at both ends of the system and pass underneath the concrete shielding through a pipe duct. Total one-way traverse distance for the samples is approximately 9 meters.

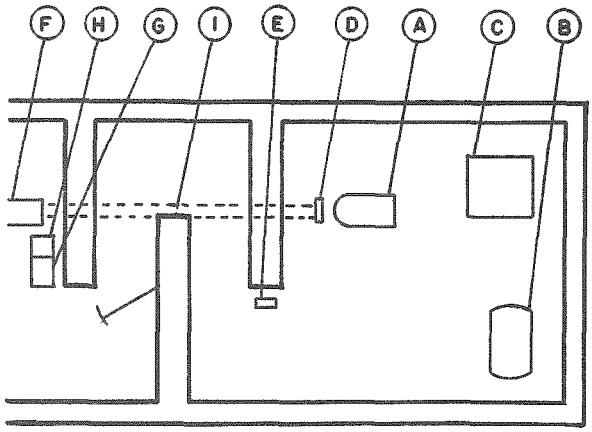

FIG.1 NEUTRON GENERATOR FACILITY

A. SEALED TUBE NEUTRON GENERATOR
B. 200 KV POWER SUPPLY
C. CLOSED-LOOP REFRIGERATION SYSTEM
D. DUAL-AXIS SAMPLE ROTATOR ASSEMBLY
E. PROTON RECOIL NEUTRON FLUX MONITOR
F. SAMPLE LOAD STATION AND DUAL CRYSTAL COUNTING ASSEMBLY
G. CONTROL CONSOLE FOR NEUTRON GENERATOR
H. PROGRAMMED TIMER FOR SAMPLE TRANSFER SYSTEM
I. POLYETHYLENE SAMPLE TRANSFER TUBING

OPERATIONAL HISTORY

The first sealed tube used with this system was operated for 70 running hours, mostly at maximum neutron output conditions, before replacement. Of this total operating time, approximately 50 hours were used for short-run activation analyses up to 3 minutes each. The other 20 hours were used for special radiation effects experiments of 14 MeV neutrons on materials. In one of these latter experiments the generator was operated continuously for a period of nine hours. During this run, the beam current remained stable but there was a slight gradual decrease in relative neutron output as measured by a proton-recoil flux monitor.

"Absolute" neutron yields were measured periodically by means of pellet activation techniques. Teflon and hexaiodobenzene pellets are preferred for such measurements because of the convenience in preparing or pressing pellets to any desired dimension and weight and also because of the relatively long half-lives of the radioactive products. The pertinent nuclear reactions and properties for these two materials are given in Table I.

TABLE I

Nuclear Data for
Neutron Yield Measurements

	Teflon $(C_2F_2)n$	Hexaiodobenzene C_6I_6
Reaction	$^{19}F(n,2n)^{18}F$	$^{127}I(n,2n)^{126}I$
Cross Section[a], mb.	67(2)	1350(3)
$T_{1/2}$	109.8 min.	13.1 days
E_γ, MeV	0.511 (annihilation)	0.667

[a] for 14.8 MeV neutrons at 0°.

Neutron yield and flux measurements have been standardized by mounting the pellets 15.0 cm. directly in front (0°) of the target cap and irradiating for 30 minutes at maximum generator output conditions (180 KV, 4.0 ma). The pellets are counted on a lead-shielded 10 x 10 cm. NaI(Tl) scintillation detector assembly. Photopeak efficiencies are periodically checked experimentally using ^{22}Na and ^{137}Cs standards (for the 0.511 and 0.667 MeV photopeaks respectively) prepared in the same physical geometry as the pellets from calibrated reference solutions.

Neutron yield determinations at various operational running times for the first sealed tube are given below:

Hours	Neutrons/sec
15	8.5×10^{10}
41	4.7
45	5.7
47	6.2
49	5.7
68	6.8

Each 4π neutron output listed is the average value obtained from activation of both a teflon and hexaiodobenzene pellet. Agreement between the two pellets was within $\pm$ 10% or better. The differences shown from period to period are therefore significant to within this limit. The relatively large increases in yield at 45 and 68 hours of operation are real and occurred after the metal dome surrounding the sealed generator tube was reflushed several times with fresh SF_6 insulating gas. It is postulated that formation of gaseous breakdown products in the insulating gas with time may result in a reduction of the effective ion beam current on the target.

The neutron flux distribution very close to the target was found to be asymmetric and experiments with teflon pellets gave results similar to those described in detail by other workers (4,5) for Cockcroft-Walton accelerators. At distances greater than 2.5 cm. in front of the target, the neutron flux was symmetrical.

After 70 hours of running time operation of the generator became erratic and it was no longer possible to maintain a stable beam current. The first sealed tube was replaced and the initial yield on the second tube was determined as 8.0×10^{10} neutrons/sec.

ANALYSIS FOR TOTAL NITROGEN CONTENT

Control of purity in explosives is often as important as in pharmaceutical and biological products. Low concentrations of impurities can not only affect performance, but even more critically, can influence safety in handling. As in other chemical industries, process and quality control requires the testing of large numbers of samples. Wet chemical and non-nuclear instrumental techniques, although generally highly accurate and precise, suffer from the usual disadvantage of slowness. For some developmental

programs of new products, the more conventional analytical techniques have the added disadvantage of being destructive with regard to the sample. This limitation can be severe when sample quantity is restricted and tests other than chemical analysis are required.

Almost all explosives and propellants, particularly those of organic composition, contain nitrogen, usually in high proportions. A rapid non-destructive method for total nitrogen content as a measure of purity is therefore attractive. Fast neutron activation via the $^{14}N(n,2n)^{13}N$ reaction provides such a method by radioassay of the 10 min. positron annihilation radiation (0.511 MeV) from ^{13}N. Application of this technique to explosives has been discussed by Rison et al (6) but data is given for only two samples of hexahydro-1,3,5-trinitro-s-triazine (RDX). For samples weighing 50 mg. these authors report an absolute error of -0.3% nitrogen.

From previous published work on FNAA as applied to gross elemental analysis in the percent range, the conditions for optimum precision and accuracy can be summarized as follows:

(1) Reference standard and sample to be analyzed should be as similar as possible in composition to minimize interferences from activation of other elements (6,7).

(2) Reference standard and sample should be as similar as possible with respect to weight, volume and density to minimize geometry counting errors and to eliminate the need for gamma and neutron self-shielding corrections (8,9).

(3) Simultaneous irradiation of both reference and sample to eliminate neutron flux correction.

(4) Dual-axis rotation of reference and sample during irradiation to insure a uniform neutron dose to both. [For certain samples, e.g. metals, where the element to be assayed is not uniformly distributed, an even more complex rotation has been found necessary (10)].

These conditions are being used routinely at this laboratory for total nitrogen content assay of "pure" homogeneous high energy compounds (see Experimental for details). Some representative results are given in Table II. Included are four samples of nitrocellulose of different degrees of

TABLE II

Total Nitrogen Content in "Pure" Explosives by High Precision FNAA

Sample	% Nitrogen Chemical Analysis	% Nitrogen FNAA[b]
Nitrocellulose	12.60	12.57 ± 0.05
Nitrocellulose	12.18	12.12 ± 0.10
Nitrocellulose	13.11	13.03 ± 0.07
Nitrocellulose	13.23	13.23 ± 0.06
TNT	18.50[a]	18.50 ± 0.06
HMX	37.84[a]	37.78 ± 0.06

[a]theoretical value for pure compound

[b]values listed are the mean of at least four determinations ± 1σ (std. dev. from the mean)

nitration and one sample each of the high explosives TNT (2,4,6-trinitrotoluene) and HMX (1,3,5,7-tetranitro-1,3,5,7-tetrazacyclooctane). The nitrocellulose samples were supplied from plant production lots and the listed nitrogen contents under "Chemical Analysis" were determined by a nitrometer technique; these values are usually precise to within a few hundreths of 1%. The TNT and HMX were from highly purified laboratory samples and the nitrogen contents listed are calculated values for the pure compounds. Precision and accuracy as indicated by the FNAA data for these compounds are excellent and most likely represent the optimum that can be achieved by this technique.

Rison et al (6) demonstrated that 50 mg. of explosives, of composition similar to those discussed in this study, could be handled safely with a pneumatic transfer system. For the work described here, sample size varied from 0.5 g. for the nitrocellulose samples to 2.3 g. for the TNT and HMX. The explosive nature of the materials can pose a special problem for these relatively larger quantities. During pneumatic transfer the polyethylene vials containing the samples approach speeds of 15 meters/sec. and come to rest against a metal stop at both irradiation and count stations. However, because of the wide overhead loops in the polyethylene transfer tubing at each end of the system, the samples are slowed down

considerably before coming to rest. The hazard from shock initiation is therefore reduced to a minimum. In over 1000 irradiations with explosives of the type tested no detonation occurred. It should be cautioned, however, that the handling techniques described in this paper are for the very shock-resistant secondary explosives and propellants. For low shock-resistant explosives such as lead azide, mercury fulminate or other initiating agents, more stringent handling conditions would have to be utilized.

ANALYSIS OF BINARY MIXTURES

Neutron activation is also being used routinely for the assay of binary mixtures containing two compounds of different nitrogen content. This method has been applied extensively to Octol compositions which contain varying proportions of TNT and HMX. The mixture is normally manufactured by dispersing finely-divided crystalline HMX in hot molten TNT and cast loading the melt into ammunition items. The finished product is designed to contain a specific HMX content in the 60-80% by weight range. Because HMX is not soluble in the molten TNT, non-uniformity of composition can result and hence the need for quality control by chemical analysis.

The conventional assay technique is an extraction procedure whereby a 5 g. sample of Octol is treated with hot benzene to remove the TNT and the insoluble HMX is determined gravimetrically. Analysis time per sample is approximately 3 hours and each sample is assayed in duplicate. For this particular product, in addition to a decrease in analysis time, a non-destructive method is especially desirable because of other physical tests that are also required on each sample.

By FNAA, the total nitrogen content of a sample is first determined and then related to composition of the mixture. Since Octols contain no ingredients other than "pure" TNT (18.50%N) and "pure" HMX (37.84%), the following linear relationship is derived from the calculated nitrogen content of each ingredient:

$$\% \text{ HMX} = 5.171 \text{ N} - 95.66$$

where N is the nitrogen content of the mixture in % by weight.

For Octol containing 60-80% HMX, a 0.2% change in nitrogen content is equivalent to approximately a 1% change in HMX content. Determination of HMX content to an accuracy of $\pm$ 1% is considered acceptable for a rapid non-destructive method. A study was made of various FNAA techniques with regard to accuracy and precision for the assay of Octol samples. Three synthetic samples were carefully prepared from purified HMX and TNT containing 60, 70 and 80% HMX respectively. These were analyzed by the following activation methods using an 80/20 (80% HMX) Octol as the reference standard in all cases:

- Dual-axis rotation with sequential counting.
- Dual-axis rotation with simultaneous counting.
- Single-axis rotation with sequential counting.

For single-axis rotation a special lucite wheel was fabricated, designed to hold up to 12 small snap-cap polyethylene vials (see Experimental). In this series of experiments, however, only one sample and the reference standard were irradiated on the wheel as for dual-axis rotation analyses. The results of these experiments are presented in Table III. Chemical analysis by extraction is also included for each sample as another basis for comparison.

Analysis by dual-axis rotation again yielded excellent results; agreement with calculated values for total nitrogen was 0.1% or less in all cases. The corresponding average absolute errors in HMX content for the three samples were 0.45 and 0.26% respectively for sequential and simultaneous counting as compared to 0.31% for chemical analysis. Differences between the two modes of counting for dual-axis rotation are not considered significant and the choice of counting arrangement is arbitrary for ^{13}N radioassay in these samples. It should be noted, however, that for simultaneous counting, great care must be exercised in the precise balance of the two single-channel analyzers for the 0.511 MeV photopeak window.

Predictably, analysis by single-axis rotation is not comparable in accuracy to dual-axis rotation. The mean absolute error was 0.24% and 1.24% for total nitrogen and HMX content respectively. Dual-axis rotation, however, despite its undeniably greater

TABLE III

Comparison of Various FNAA Techniques for
Assay of Synthetic Octol Samples

Sample	Calc.	% Nitrogen[a] Dual-Axis Rotation; Sequential Counting	Dual-Axis Rotation; Simultaneous Counting	Single-Axis Rotation; Sequential Counting	Chemical Analysis % HMX[b]
70/30	32.03	32.16 ± 0.09 (70.65 ± 0.47)	32.07 ± 0.16 (70.18 ± 0.82)	32.35 ± 0.14 (71.58 ± 0.70	70.59 70.70 (70.65)
60/40	30.11	30.19 ± 0.09 (60.42 ± 0.49)	30.19 ± 0.11 (60.42 ± 0.60	30.27 ± 0.17 (60.88 ± 0.87)	59.13 60.63 (59.88)
80/20	33.98	34.03 ± 0.13 (80.28 ± 0.70	33.94 ± 0.14 (79.82 ± 0.75)	34.22 ± 0.16 (81.27 ± 0.85)	79.99 80.68 (80.33)

[a]Mean of six determinations on each sample ± 1σ (std. dev. from the mean); Value in parenthesis is corresponding % HMX ± 1σ

[b]Two determinations on each sample; mean given in parenthesis

accuracy and precision, is limited to only one sample and reference standard per irradiation. It is the preferred method in this laboratory where speed is not essential - but when the number of Octols to be analyzed is large, multiple sample irradiation on the lucite wheel with single-axis rotation is used. The precision of this latter technique for six plant samples of Octol is shown in Table IV. In this series each irradiation consisted of six Octol samples, an 80/20 Octol reference standard and a blank vial mounted on the lucite wheel. The FNAA results were again compared with chemical analyses for HMX content. The mean 1σ precision for 10 determinations on each of the six samples was ± 1.30% HMX and the average difference between FNAA and chemical analysis was 0.84% HMX.

TABLE IV

Precision of Single-Axis Rotation FNAA for
Assay of Octol Plant Samples

Sample	FNAA[a] %N	FNAA[a] % HMX	Chemical Analysis[b] % HMX
1	30.11 ± 0.29	60.02 ± 1.42	59.04, 59.07 (59.06)
2	30.60 ± 0.22	62.56 ± 1.15	63.50, 63.60 (63.55)
3	31.94 ± 0.33	70.02 ± 0.94	70.25, 70.29 (70.27)
4	31.97 ± 0.44	70.16 ± 1.87	70.06, 70.14 (70.10)
5	32.23 ± 0.25	71.00 ± 1.27	69.94, 69.81 (69.88)
6	32.29 ± 0.22	71.28 ± 1.14	69.40, 69.79 (69.60)

[a]Mean of 10 determinations on each sample ± 1σ (std. dev. from the mean)

[b]Two determinations on each sample; mean given in parenthesis

For routine quality control on large numbers of Octols, each sample is assayed twice and for one irradiation, the lucite wheel is loaded with nine samples, a reference standard and a blank vial. Agreement between duplicate assays for 378 plant samples analyzed in this manner is summarized in Table V. For 48% of the samples, the difference in HMX content for duplicate runs was 1% or less and 2% or less for 87% of the samples. The chief advantage of multiple sample single-axis rotation is speed.

TABLE V

Precision of Duplicate Assays for HMX Content in Octol Plant Samples by Single-Axis Rotation FNAA[a]

Difference in % HMX[b]	No. of Samples	% of Total No. of Samples
0.00 - 0.50	95	25.1
0.51 - 1.00	85	22.5
1.01 - 1.50	80	21.2
1.51 - 2.00	69	18.3
2.00 - 2.51	31	8.2
2.51 - 3.00	11	2.9
3.01 - 3.50	1	0.3
3.51 - 4.00	4	1.1
4.01 - 4.50	2	0.5
	Total - 378	

[a]Nine plant samples, one reference std. and one blank irradiated simultaneously and counted sequentially

[b]Between duplicate analyses on same sample

EXPERIMENTAL

FNAA BY DUAL-AXIS ROTATION AND PNEUMATIC TRANSFER OF SAMPLES:

Samples were contained in special polyethylene vials specifically designed to fit the Kaman Nuclear dual-axis rotator assembly. These vials are 4.5 cm. long and 1.0 cm. o.d. with an internal volume of 2.3 cm^3. When filled, a vial contains approximately 0.5 g. of nitrocellulose and 2.3 g. of TNT, HMX or Octol.

A 12.60% N nitrocellulose was used as the reference standard for all samples of this material (Table II). TNT and HMX were compared against "pure" samples of each other respectively. For assay of Octol samples a synthetic 80/20 Octol was used as the standard in all determinations.

Nitrocellulose samples were irradiated for three minutes; TNT, HMX and Octols for 1 minute. Sequential counting was accomplished in a 7.6 x 7.6 cm. NaI(Tl) well - crystal detector assembly and a single -channel pulse height analyzer to measure the 0.511 MeV annihilation radiation using a 20% window. A one-min. count time was usually sufficient to exceed 10^4 counts. Simultaneous counting was performed by means of the dual 7.6 x 7.6 cm. flat NaI(Tl) crystal detector assembly in conjunction with the Kaman Nuclear programmed timer system for automatic sample transfer. The signal from each detector was fed to an individual single-channel pulse height analyzer. The 0.511 MeV photopeak (20% window) was carefully matched in each detector-analyzer pair with a ^{22}Na source.

FNAA OF OCTOL SAMPLES BY SINGLE-AXIS ROTATION:

The lucite wheel fabricated for this purpose is 1.2 cm. thick and 13.8 cm. in diameter. A concentric groove, 1.2 cm. wide and 0.7 cm. deep is located on one face of the wheel close to the rim. This groove is designed to hold standard No. 3 snap-cap polyvials (Olympic Plastics Corp.), 2.3 cm. long, 0.9 cm. o.d. with a usable volume of 1.5 cm^3. Approximately 1.5 g. of Octol can be contained in a vial. As many as 12 vials can fit on the wheel for a single irradiation.

For assay of Octols, the wheel is mounted 7.5 cm. in front of the target cap and rotated at $\sim$ 100 r.p.m. Up to nine plant Octol samples are loaded onto the wheel with an 80/20 reference standard and one blank vial. Following a 3-min. irradiation, a "cooling" period of 3 min. is allowed after which the samples are removed for sequential counting in the well-crystal detector system. A blank correction for this analysis is important and a typical counting sequence is sample-sample-blank-reference -sample-blank-sample-sample-blank, etc. Each vial is counted for 1 min. and all counts are corrected for ^{13}N decay taking the time for the first sample as zero.

CHEMICAL ANALYSIS FOR HMX CONTENT:

5.0 g. of Octol sample is treated with 30 ml. of HMX-saturated benzene at 90°C. The mixture is then filtered through a tared crucible and the residue is washed with more HMX-saturated benzene. The crucible is then dried at 100°C and the HMX content is calculated.

CONCLUSIONS

The use of a sealed tube neutron generator is a convenient source for gross element activation analysis, in particular for routine laboratory and plant quality control applications. The elimination of vacuum system maintenance and tritium target changing is a decided advantage.

Total nitrogen content in organic explosives and related materials can be determined by FNAA to an absolute accuracy comparable to wet chemical or combustion analysis, i.e. to within less than 0.1% N. This is accomplished by dual-axis rotation of the sample and a carefully selected reference standard during neutron irradiation. The optimum reference standard is one of similar composition, density, weight and volume to the sample being analyzed. Rapid pneumatic transfer of organic explosives of low mechanical shock sensitivity poses no special safety problems.

For large numbers of individual samples, a multiple sample irradiation system with single-axis rotation can be used for more rapid analysis. Precision and accuracy by this method are not as good as compared to a dual-axis rotation technique. Absolute accuracy for total nitrogen is in the order of 0.2%. This method is useful only for those reactions where the half-life of the product is long enough to allow for sequential counting of multiple samples from a single irradiation.

ACKNOWLEDGEMENT

The authors are grateful to Burt Hashizume for assistance with the neutron activation experiments and to Jerome Haberman for performing the chemical analyses of the Octol samples. The support given for this work by J.D. Hopper of the Applied Chemistry Branch is also gratefully acknowledged.

REFERENCES

1. Kaman Nuclear Division, Kaman Sciences Corp., Garden of Gods Road, Colorado Springs, Colorado.

2. S. Takanobu et al. "The $^{19}F(n,2n)^{18}F$ Reaction as a 14-MeV Neutron Flux Monitor". J. Inorg. Nucl. Chem. 30, 1-4 (1968).

3. Neutron Cross Sections, Brookhaven National Laboratory Report No. 325, Second Edition, Supplement No. 2, P. 53-0-19, May 1966.

4. H.F. Priest, C.F. Burns, and G.L. Priest. "Neutron Flux Distribution from a 14 MeV Neutron Generator". Nucl. Instr. and Methods 50, 141-146 (1967).

5. G. Oldham and D.M. Bibby. "Neutron Flux Distribution Around the Target of a 14 MeV Neutron Generator". Nuclear Energy Nov/Dec 1968.

6. M.H. Rison, W.H. Barber, and P.W. Wilkness. "Fast Neutron Activation Analysis for Nitrogen in Explosives and Propellants". Radiochemica Acta 7, 196-198 (1967).

7. J.T. Gilmore and D.E. Hull. "Nitrogen-13 in Hydrocarbons Irradiated with Fast Neutrons". Anal Chem. 34, 187-189 (1962).

8. G.H. Anderson and J.A. Algots. "The Effect of Sample Bulk Density on the Determination of Nitrogen by Fast Neutron Activation Analysis". J. Radioanalytical Chem. 3, 261-264 (1969).

9. S.S. Nargowalla et al. "Solutions of Blank Problems in 14-MeV Neutron Activation Analysis for Trace Oxygen". Anal Chem. 41, 168-171 (1969).

10. H.F. Priest, F.C. Burns, and G.L. Priest. "An Irradiation, Transfer, and Counting System for Neutron Activation Analysis of Short-Lived Components in Inhomogeneous Samples". Anal. Chem. 42, 499-503 (1970).

APPLICATION OF NEUTRON CAPTURE GAMMA RAYS USING A ^{252}Cf NEUTRON SOURCE TO INDUSTRIAL PROCESS STREAM ANALYSIS

Dick Duffey

University of Maryland
College Park, Maryland

Peter F. Wiggins

U. S. Naval Academy
Annapolis, Maryland

Frank E. Senftle

U. S. Geological Survey
Washington, D. C.

An examination of the neutron capture gamma ray method using a ^{252}Cf neutron source indicates that this technique may be feasible for process stream analysis and control of certain elements. Simulated laboratory experiments were made on iron in taconite and magnetite, and copper and nickel in their respective ores. Satisfactory analyses were obtained for 500-1000 g samples in a combined irradiation and counting time of 100 minutes. For large industrial size samples this time could be shortened. Based on these experiments, a set of guidelines are given for the use of the neutron capture gamma method in an industrial plant.

INTRODUCTION

The application of conventional neutron activation and detection of delayed gamma rays to on-stream analysis can be applied to many industrial processes. Rhodes (1) has recently reviewed the delayed gamma techniques which have been tried with both radioisotope and accelerator type neutron sources. Ashe et al (2), using a taconite ore slurry, have demonstrated the advantages of a recirculation or 'closed loop' system compared to a single pass or 'open loop'. Rhodes points out that for either system, because of the neutron and gamma ray penetration, a sample several inches thick is observed. Thus, errors due to heterogeneity and variable particle size are reduced as compared to some other analytical methods, X-ray fluorescence (3), for instance. Although slow neutrons diffuse but a few inches into a sample, fast neutrons penetrate much deeper and it is conceivable that a much larger sample can be observed if high energy neutrons are used.

To obtain a maximum flux of high energy neutrons, an accelerator using a tritium target is generally used to produce 14 MeV neutrons. Although this is an attractive high flux neutron source, 14 MeV is above the threshold energy for many fast neutron reactions which mask the radionuclides produced by (n,γ) reactions in many of the elements of low abundance. Hence, it would be convenient to have a high yield source of 2-3 MeV neutrons, an energy which is below the energy threshold for most fast neutron reactions (unless one specifically desires to produce a fast neutron reaction in a given element). Monte Carlo calculations of 2 MeV neutron penetration in a 50 percent saturated soil indicates that most of the moderation takes place throughout the first 1 to 1 1/2 feet of soil and drops off almost exponentially at greater depths (see Figure 4, ref. 4).

In principle one could use a deuterium target in the accelerator and produce 3 MeV neutrons, but the flux would be reduced lower than that obtained for 14 MeV neutrons by a couple orders of magnitude for the same accelerating voltage. Alternatively, the high neutron yield of ^{252}Cf makes this isotope an attractive source of neutrons. ^{252}Cf has an average neutron energy of 2.3 MeV and its energy distribution peaks at about 1 MeV. For industrial use ^{252}Cf sources which emit 10^9 to 10^{10} neutrons per second can be adequately handled with proper personnel shielding. Delayed neutron activation as described by Rhodes (1,2) but using a ^{252}Cf neutron source will have some distinct advantages over a 14 MeV accelerator, namely, (a) less interference from fast neutron reactions and, (b) minimum maintenance.

An alternative method for process control is radiative neutron capture which results in prompt gamma emission. Christell and Ljung-

gren (5) have suggested that a low energy capture gamma ray method be used for measuring boron in a process stream. When a ^{252}Cf source is placed in or adjacent to any material, high energy capture gamma rays are produced which can be measured with a Ge(Li) detector placed nearby the process stream, and thus can provide a technique for on-line analysis. The current work has been directed primarily towards the base metal ores, particularly iron, copper, and nickel ores. Extension to other industrial elements such as silicon, sodium, and aluminum also appear feasible.

It is the purpose of this paper to examine the feasibility of using high energy capture gamma rays for process control.

TECHNIQUE

When neutrons are absorbed by a nuclide, capture gamma rays are emitted almost instantaneously; some with an energy up to ∿11 MeV. Tabulations of the relative sensitivity of most of the elements and the principal gamma ray energies have been made (6). About a dozen industrially important elements have high sensitivities and respond particularly well to the capture gamma ray technique.

The number of prompt photons detected following neutron capture in a specific nuclide is given by:

$$n = (WN/A)\ \sigma\ \phi\ k\ \varepsilon\ f\ t$$

where n is the number of impulses in a given spectral peak detected in a time, t, W is the mass of element in the sample, N is Avogadro's number, A is the atomic weight, ϕ is the neutron flux, σ is the cross section, k is the isotopic abundance, ε is the total efficiency (including counting geometry) of the detector for a given spectral peak, and f is the number of photons emitted per neutron absorbed. A similar expression can be written for the delayed gamma rays but this must be multiplied by a build-up and decay factor both of which may be considerably less than one. As pointed out by Isenhour and Morrison (7) for equal values of ϕ, ε, and f, the capture gamma ray method should give better sensitivities than the delayed gamma method, but there are several practical problems which have to be evaluated. While f for both methods is generally the same order of magnitude, ε is much less for the capture gamma compared to the delayed gamma method.

Capture gamma spectra are more complicated than delayed gamma spectra. To obtain the required resolution a relatively low efficiency Ge(Li) detector, rather than the more efficient NaI(Tℓ) detector must be used for capture gamma ray work. However, it should be pointed out that this may only be a short term disadvantage. Although the best Ge(Li) detectors currently available have only about 20% of the efficiency of a NaI(Tℓ) detector, the efficiencies are constantly being improved. Nevertheless, the low efficiency of Ge(Li) detectors is currently the most serious disadvantage. Computer methods to enhance the spectra are currently being developed for NaI(Tℓ) detectors (8), which may extend the use of scintillation counters to high energy capture gamma ray work.

An additional drawback to the neutron capture method is the vulnerability of the Ge(Li) detector to neutrons. The detector-to-source distance must be great enough to ensure that the flux through the detector will not produce substantial radiation damage. In general, this critical distance is large enough to reduce the counting geometry to a relatively low value compared to that which can be used to count delayed gamma rays.

The source-detector separation will depend on the size, shape, and water content of the sample, type of shielding, size of source, etc. In water the detector can be put 18-20 inches from a 100 μm ^{252}Cf source for an extended time without undue damage to the crystal.

In spite of these disadvantages, there are certain advantages of the high energy neutron capture gamma ray method.

1) The irradiation and counting times are not controlled by the decay constants and no delay times are needed to reduce interference from other elements. One need only to use a time necessary to acquire the required counting statistics.
2) Because of the higher energies of capture gamma rays compared to delayed gamma rays, the interference from photopeaks (E < 3 MeV) can be eliminated by working in the high energy end of the capture gamma ray spectrum.
3) Elements can be determined whether or not they go to stable nuclides or to β emitting radionuclides after neutron capture.

As the half life of a radionuclide is not a factor in determining the capture gamma

ray spectrum, one cannot enhance the signal-to-noise ratio by using a closed loop recirculation system as is sometimes done with the delayed gamma ray method. In an industrial process one is generally confronted with a continuously changing sample. Thus, if the ^{252}Cf source is placed into the stream, the capture gamma ray spectrum will be an average of the sample which has passed by the source during the counting period. If the material in the stream flow rapidly varies locally in composition, and the variation is important, a holding tank must be placed in the flow system to reduce the flow rate past the sample and thus obtain a more representative sample. Stewart (9) has used this system successfully to monitor the carbon content in iron ore sinter and also in coal ash.

A sketch of a possible arrangement for slurry analysis is shown in Figure 1. The source-sample-detector geometry is constant and calibration can be obtained from several slurries of known concentration. If the holding tank is relatively large such that the source has about a foot or so of slurry on all sides, then besides having an enhanced sensitivity because of the large sample, little shielding for personnel safety will be needed because of shielding by the sample. Nevertheless, personnel monitoring and controlled access must be maintained to assure safety at all times.

It should be re-emphasized that if it is required to make an on-line analysis in short periods of time on a continuing basis, the poor geometry and counting efficiency of a Ge(Li) detector will preclude a statistical meaningful answer. However, if counting periods of an hour or greater are tolerable to yield concentration trends in large volumes of process feed material, the capture gamma ray method would appear to be a possibility. The following experiments were made as a preliminary investigation to see if a useful system might be developed.

EXPERIMENTAL ARRANGEMENT

Although in actual practice a large sample would be available in a typical holding tank in a process stream, tests on large samples were not made as facilities were not available to make full scale measurements. However, if good capture gamma spectra could be obtained on small samples in a reasonable counting time, better counting statistics could be obtained on the larger samples. For this reason measurements were made on about 500-1000 gram samples in a simulated holding tank.

The ^{252}Cf neutron source used for this work was double encapsulated in stainless steel and had a yield of 3×10^8 neutrons per second ($\sim$120 µg). The source, inserted in the end of a phenolic rod, was placed in and near one side of a 19 x 22 x 26 inch plastic tank filled with water (see ref. 10 for details). A plastic petri dish containing the sample was placed outside of the tank just opposite the source. Thus, the samples could be conveniently changed without immersion in the water. A 30 cm^3 Ge(Li) detector with suitable boron and lead shielding was placed on the opposite side of the water tank. This arrangement simulated the detector outside a holding tank and the gamma ray emission penetrating 33 inches (width of water tank plus paraffin shield) of slurry and shield. In spite of the unfavorable counting conditions relatively good spectra were obtained in 100-200 minutes.

It would be helpful to make a calculation of the results which might be expected from an arrangement such as shown in Figure 1, but this is not possible because the neutron flux decreases rapidly with sample thickness and the mean flux is unknown. However, from experimental data on small samples it is possible to get some approximate figures by making some assumptions. Consider a holding tank about the same dimensions of the plastic laboratory tank and containing an ore slurry with a volume ratio of ore-to-water of 0.5. Assume a marginal nickel ore of about 1 percent nickel with a density of 200 lbs/cu. ft. The approximately 6 cu. ft. tank will, therefore, contain about 2 cu. ft. or 400 lbs. of ore at any one time assuming a homogeneous flow of slurry through the tank. In the laboratory, under similar, but not exactly the same conditions, 2-3 lbs. samples of one percent nickel ore gave 20.4 counts per lb. in the 7.98 MeV nickel peak in one hour which would be equivalent to be 8170 counts per hour for a 400-lb. sample in a holding tank. Should the ore grade change from 1 percent nickel to 0.9 percent the counts in the same time would drop to 7350, a change which could be used to give a semiquantitative analysis of the change in grade. Depending on the particular problem and the required resolution the irradiation-counting time could conceivably be shortened to several minutes by using multiple detectors, large plastic or NaI(Tℓ) scintillators, etc.

METALLURGICAL PROCESSES AND RESULTS

IRON

Iron, because of the immense production of steel, is handled in large quantities from crude iron ores and process streams to finally fabricated shapes. Although much ore is high enough in grade for blast furnace use directly, recently lower grades have been enriched near the mines for shipment and use. The taconite operations of Minnesota are an example where an ore is mined, crushed, enriched by electromagnetic separation, and the iron concentrate compacted into pellets at the mine site for shipment (11). At the steel mills, the ore is reduced in a blast furnace, and steel is made in an open hearth, Bessemer, or electric furnace. In all these operations it is necessary to know the amount of iron and certain impurity concentrations.

On-line determination of iron by neutron activation and a delayed gamma ray spectrum analysis is not feasible because of the lack of suitable decay products. The thermal neutron reactions for iron are:

$$^{54}Fe(n,\gamma)^{55}Fe \xrightarrow[\text{Electron Capture}]{2.7y} {}^{55}Mn \text{ (Stable)}$$

$$^{56}Fe(n,\gamma)^{57}Fe \quad \text{(Stable)}$$

$$^{57}Fe(n,\gamma)^{58}Fe \quad \text{(Stable)}$$

$$^{58}Fe(n,\gamma)^{59}Fe \xrightarrow[\beta^-,\gamma]{49d} {}^{59}Co \text{ (Stable)}$$

Both ^{55}Fe and ^{59}Fe have half lives which are too long for practical application. However, as previously indicated, iron is easily detected by neutron capture gamma ray analysis. Figure 2 shows the capture gamma ray spectrum of Fe_2O_3. Note the three peak sequence; 7.64 MeV - full peak, 7.13 MeV - single escape, and the relatively large 6.62 MeV - double escape peak. These peaks are actually doublets and are the most prominent sequence in the iron spectra. The 6.62 MeV peak is the most prominent peak for nominal size Ge(Li) detectors. If the ore contains substantial quantities of aluminum or cobalt some interference may be experienced from their capture gamma rays at 6.7 MeV. In this case one of the other iron peaks can be used. At the lower energies, the double escape peaks of 6.26 MeV, 5.00 MeV, and 4.90 MeV are also prominent. The 5.12 MeV energy line is a combination of the escape peaks of chromium and probably oxygen. The chromium peak is presumed to stem from the chromium of the stainless steel capsule.

Typically taconite ore may be 32% iron, and the shipped pellets 63% iron (11). A spectrum from crude taconite and the magnetite concentrate is shown in Figures 3 and 4. A correlation of the taconite and magnetite analyses and those of synthetic mixtures of Fe_2O_3 and sand are shown in Figure 5 for the three most prominent lines. The linearity suggests an obvious application to on-line analysis of iron process streams. In addition, there are many other products in the steel mills, particularly where silica, alumina, and later lime are added to the melt, which are amenable to process control by a neutron capture gamma ray method.

COPPER

The mining of copper ores is one of the largest operations in the United States. In 1968 the U. S. produced about 170 million short tons of ore averaging about 0.6% Cu, which was about a fifth of the worlds production (12).

Typically the mined copper ore is initially handled in much the same manner as the iron ore. The process streams are solid chunks of rock in trucks or rail cars, crushed materials on belts or in bins, water slurries or pulps, molten metals and slags, water solutions, and again flue gas streams of wastes. The flotation concentrates are typically from 20 to 30% copper, the smelter matte from 30 to 45% copper, and the converter product 98% copper (13). The converter slag might analyze 2% copper and 47% iron oxide (14). A copper electrolyte in the electrolytic refining might contain 30 to 50 g of copper per liter (15). Copper in these concentrations is easily analyzed either by thermal or fast neutrons. The thermal neutron reactions are $^{63}Cu(n,\gamma)^{64}Cu$ and $^{65}Cu(n,\gamma)^{66}Cu$, neither of which is as sensitive as the fast neutron reaction $^{68}Cu(n,2n)^{62}Cu$ (16). Rhodes (1) using 14 MeV neutrons from an accelerator and the latter fast neutron reaction made some tests in a process pilot plant. However, as he points out a 15 minute delay time was needed to allow the decay of the ^{28}Al formed from the silicon in the ore. More recently Dibbs (16) using the same reaction has noted zinc to be a significant source of interference. As an alternative to these methods the neutron capture gamma ray technique may be used. Although some interference may be expected, this method appears particularly promising.

Figure 6 shows the prompt gamma ray spectrum of copper in CuO. The full, single, and double escape peaks at 7.91 MeV, 7.40 MeV, and 6.89 MeV, respectively, are the most sensitive for copper (6). The strong double escape peak at 6.62 MeV is close to an intense iron peak and is not recommended for analytical purposes. The only peaks due to other elements which occur within 15 keV (the typical resolution of a 30 cm^2 Ge(Li) detector) of the 6.89 MeV copper line are the full peaks of cobalt and chromium. Of these only the cobalt peak has a significant sensitivity and this element does not generally occur in copper ores. The capture gamma ray method, therefore, appears to be a feasible method to make on-line analyses in process streams involved in the copper metallurgical process. Test analyses of copper in various ores such as from Ducktown, Tennesse, have been successfully made in the laboratory on 500 g samples (Figure 7) and could easily be repeated on much larger samples such as in a holding tank in a process stream in a mill. As shown, the analysis was satisfactory for an industrial process.

NICKEL

Nickel production in the world is also large and about half of the output is from Canada (12). At Sudbury, Ontario, the ore is beneficated by flotation from about 1% Ni and 1% Cu and smelted to a nickel concentrate of 73% Ni and 6% Cu. Further metallurgy and electrolytic refining gives a 99.9% Ni product.

Nickel, like iron, is not easy to analyze by a delayed gamma ray method using short irradiation periods and a low neutron flux. The thermal neutron reactions for nickel are:

$$^{58}Ni(n,\gamma_1)^{59}Ni \xrightarrow[\text{Electron Capture}]{8 \times 10^4 y} {}^{59}Co \text{ (Stable)}$$

$$^{60}Ni(n,\gamma_1)^{61}Ni \text{ (Stable)}$$

$$^{61}Ni(n,\gamma_1)^{62}Ni \text{ (Stable)}$$

$$^{62}Ni(n,\gamma_1)^{63}Ni \xrightarrow[\beta^-]{92y} {}^{63}Cu \text{ (Stable)}$$

$$^{64}Ni(n,\gamma_1)^{65}Ni \xrightarrow[\beta^-,\gamma_2]{2.56h} {}^{65}Cu \text{ (Stable)}$$

The activation products are stable or long lived with the exception of ^{65}Ni. However, because of the low abundance of the parent the yield of this radionuclide is not high and hence, the sensitivity is poor.

The neutron capture gamma ray yield for nickel on the other hand is very good. As shown in the prompt gamma spectra of Figure 8 for pure nickel, there are a multiplicity of rather intense lines. The single, and double escape peaks at 8.49 MeV, and 7.98 MeV are the most prominent. Senftle et al (17) have demonstrated the use of the 7.98 MeV line for nickel analyses of ores. Chromium, which has a single escape peak at 8.00 and 7.97 MeV could offer some interference if the chromium content of the ore was high. In this case it would be more judicious to choose one or more of the other strong lines in the nickel spectrum for on-line analysis. The linearity with nickel content is shown in Figure 9 for two lines. The analysis of a typical ore (Thompson, Manitoba) agreed satisfactorily with the chemical analysis.

OTHER ORES AND APPLICATIONS

The neutron capture gamma ray method is not limited to iron, copper, and nickel ores. As pointed out by Duffey et al (6) all the transition elements, e.g. titanium, vanadium, chromium, manganese, and cobalt, have intense lines in the prompt gamma ray spectra. In addition, gold, mercury, chlorine, and ytterbium are also very sensitive.

Other elements have moderately intense lines, e.g. aluminium, sodium, silicon, sulphur, potassium, zinc, arsenic, and silver. Some of these may be of importance in process control in other industries such as silica and alumina in the ceramics of concrete industry.

PRACTICAL APPLICATION

The specifications of any neutron capture gamma ray device must be dictated by the type of sample and process stream to which it is applied. However, some broad principles can be given which may help in the design of such a device for plant operation.

1. As the neutron emission from a ^{252}Cf source is isotropic, the source should be located within the stream, i.e., surrounded by an aqueous solution, suspension of solids, or dry pulp.
2. The average energy of the neutrons from ^{252}Cf is 2.3 MeV. If the process stream material is dry, the neutrons, which must be moderated to near-thermal energies before capture, must travel a foot or more before maximum moderation is achieved. Beyond the point of maximum moderation the near-thermal flux is controlled by the fast

component and drops off exponentially. At a distance of about 30 inches or more from the source the thermal flux will be attenuated to several orders of magnitude below the source strength. Thus for dry material a large sample extending over 30 inches on all sides of the source is recommended.

If the process stream material is damp or an aqueous slurry, the appropriate sample size will be smaller depending on the water content. For instance, in water the maximum occurs at less than an inch from the source and is a thousandth of the source strength at distance of about 6 inches (18).

Thus, the size of holding tank or tube in the process stream will depend on the water content of the sample.

3. As was indicated in the above, the area around the irradiation point in a plant must be shielded for personnel protection. To a large extent the process stream itself acts as a shield and reduces the necessity for massive shielding. However, while it is necessary to place the detector as close to the process stream as possible, adequate shielding must be provided to prevent radiation damage to the detector by the neutrons.
4. If the method is to be used for rough analysis of truck or rail car loads it is recommended that the ^{252}Cf and detector be built into a fixed probe which can be forced as a unit into a bulk sample by an automatic servo device.
5. Iron and stainless steel have very intense lines in the prompt gamma spectra. If the pipes or troughs holding the process streams are of this material, interference may be encountered. To reduce such interference plastics may be substituded, but polyvinyl chloride should be avoided because of the response of chlorine. An evaluation of the best construction materials for neutron capture gamma ray analysis has been reported by Senftle et al (10).

In summary, the use of neutrons from ^{252}Cf as an analytical probe with measurement of the penetration high energy capture gamma rays offers a feasible method of analysis of certain elements in bulk materials in process industries.

ACKNOWLEDGEMENTS

The authors wish to thank their colleagues R. Moxham and A. Tanner for their constructive suggestions and P. Philbin for his assistance. Thanks are also due to N. Stetson of the U. S. Atomic Energy Commission for making the ^{252}Cf source available for these experiments.

REFERENCES

1. J. R. Rhodes. "Applications of Neutron Activation To On-Stream Analysis." Isotopes and Radiation Technology 6, 359-368 (1969).

2. J. B. Ashe, P. F. Berry and J. R. Rhodes. "On-Stream Activation Analysis Using Sample Recirculation." Modern Trends in Activation Analysis, Ed. J. R. DeVoe and P. D. LaFleur, Natl. Bur. Stds. Spec. Pub. 312, Vol. II, 913-917 (1969).

3. C. L. Lewis, R. A. Hall, J. W. Anderson and W. H. Tumm. "The On-Stream X-Ray Analysis Installation at the Lake Dufault Mine." Can. Mining and Metall. Bull. 61, 513-518, (1968).

4. F. Senftle, P. Philbin and P. Sarigianis. "Distribution of Neutrons From a ^{252}Cf Source in Soil at Depth and Just Below the Air-Ground Interface." Nucl. Appl. and Tech. 7, 576-583 (1969).

5. R. Christell and K. Ljunggren. "Continuous Determination of Boron in a Process Stream Using Low Level Neutron Source." Atompraxis 10, 259-263 (1964).

6. D. Duffey, A. El-Kady and F. Senftle. "Analytical Sensitivities and Energies of Thermal-Neutron-Capture Gamma Rays." Nucl. Instr. and Methods 80, 149-171 (1970).

7. T. Isenhour and G. Morrison. "Modulation Technique for Neutron Capture Gamma Ray Measurements in Activation Analysis." Anal. Chem. 38, 162 (1966).

8. J. Trombka, F. Senftle and R. Schmadebeck. "Neutron Radiative Capture Methods for Surface Elemental Analysis." Nucl. Instr. and Methods 87, 37-43 (1970).

9. R. F. Stewart. "Nuclear Measurements of Carbon in Bulk Materials." Instr. Soc.

Amer. Trans. 6, 200-208 (1967).

10. F. Senftle, A. Evans, D. Duffey and P. Wiggins. "Construction Materials for Neutron Capture Gamma Ray Measurement Assembly Using ^{252}Cf." Nucl. Appl. and Tech. 10, 204-210 (1971).

11. O. Lee. "Taconite Beneficiation Comes of Age at Reserve's Babbitt Plant." Min. Eng. 1-5 (1954).

12. Minerals Yearbook. U. S. Bureau of Mines, 1968 edition, Vol. I and II, p. 463; p. 769 U. S. Government Printing Office.

13. G. Hayward. Outline of Metallurgical Practice. 3rd ed., p. 24, Van Nostrand Company, Inc., New York, N. Y., (1964).

14. Ibid, p. 70.

15. A. Butts. Copper. Amer. Chem. Soc. Monograph, Reinhold Pub. Co., Inc., p. 176, New York, N. Y. (1954).

16. H. Dibbs. "The application of Neutron Activation Analysis to the Determination of Copper in Minerals." Can. Inst. Min. Trans. 73, 102-108 (1970).

17. F. Senftle, P. Wiggins, D. Duffey and P. Philbin. Unpublished Data.

18. D. Magnuson. Thermal Neutron Flux Distribution From a ^{252}Cf Spontaneous-Fission Neutron Source. USAEC Report CONF-681032, TID-4500 (Jan. 1969); Californium-252 Symp. Proc., J. Barker, ed.

Process Control Arrangement Using Neutrons Of ^{252}Cf For Capture Gamma Rays

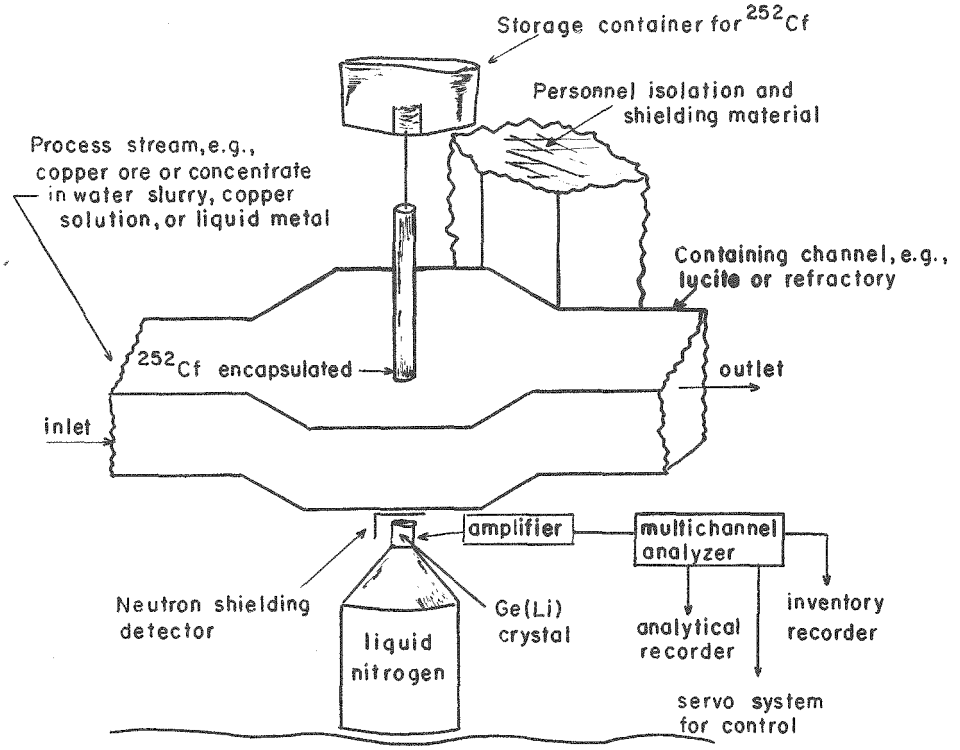

Figure 1 - Relative arrangement of source and detector with respect to the process stream in a possible industrial situation.

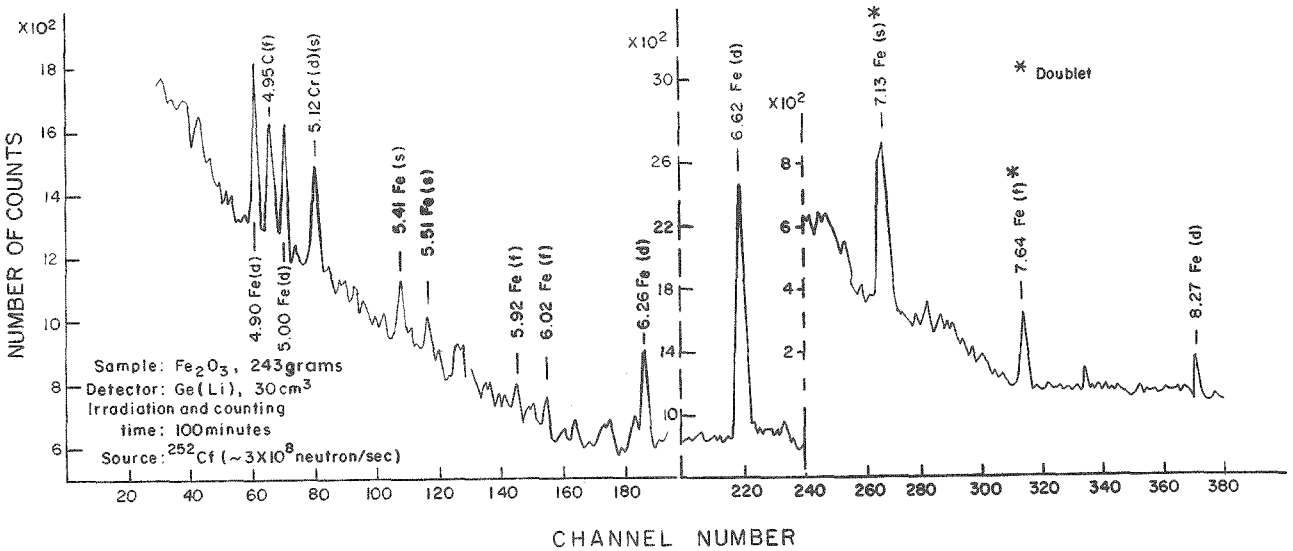

Figure 2 - High-energy-capture gamma spectra of iron oxide showing prominent iron lines. f, s, and d stand for full, single, and double escape peaks, respectively.

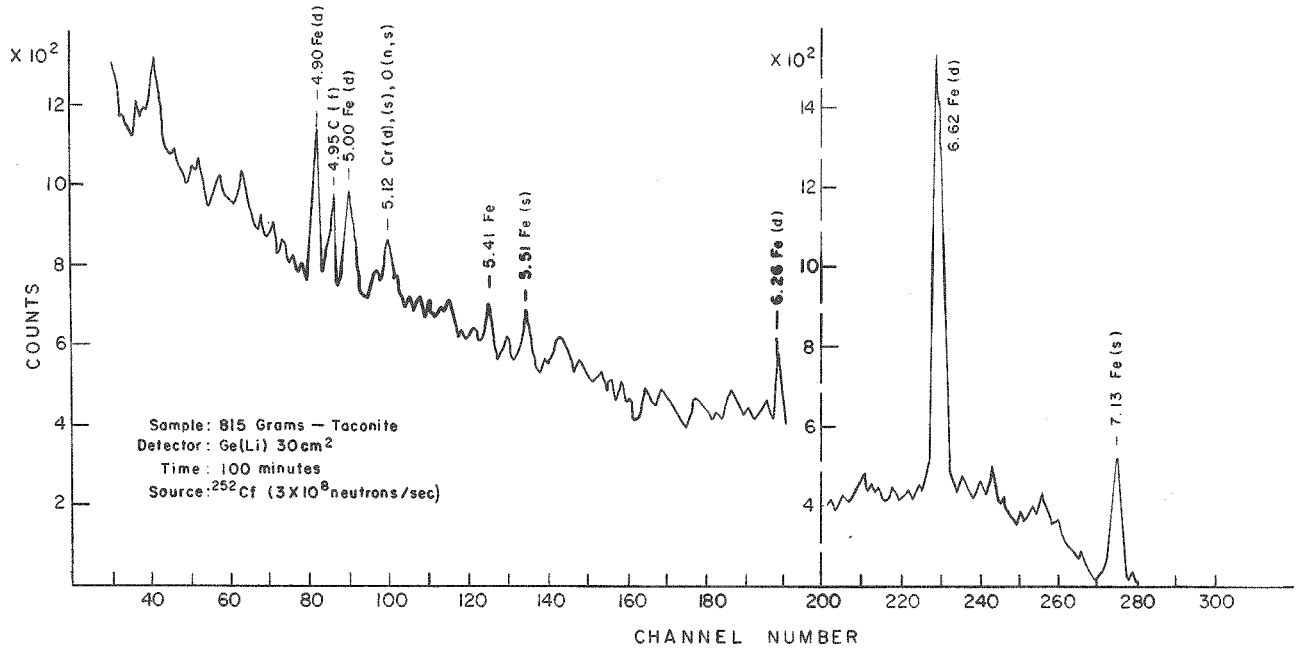

Figure 3 - High-energy-capture gamma spectra of taconite. f, s, and d stand for full, single, and double escape peaks, respectively; (n,s) is an inelastic scattering reaction.

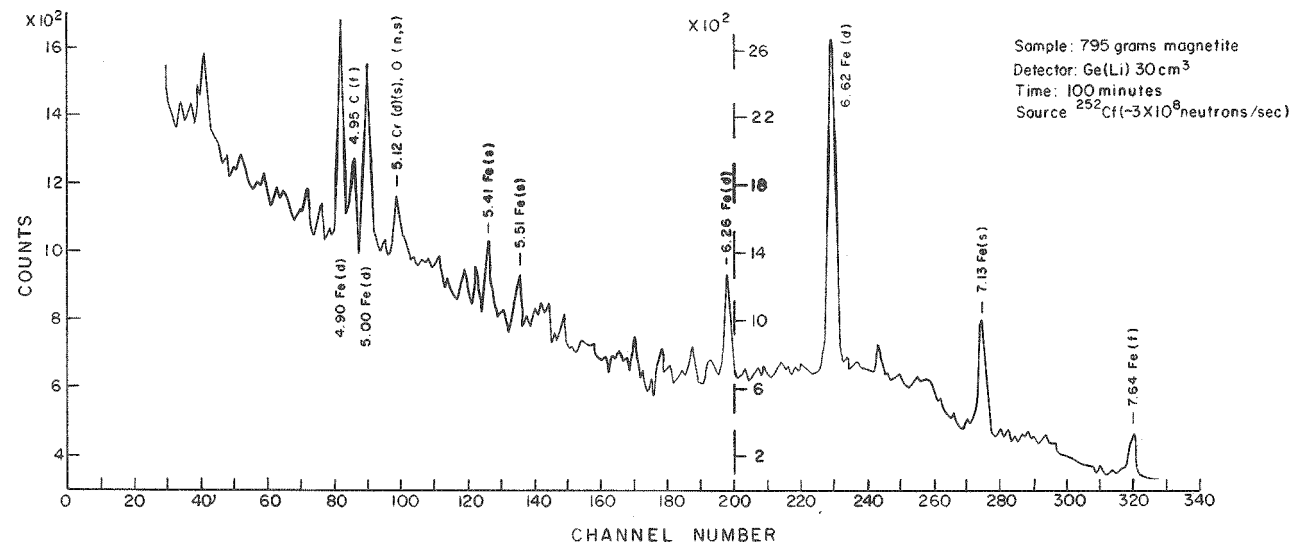

Figure 4 - High-energy-capture gamma spectra of magnetite concentrate. f, s, and d stand for full, single and double escape peaks, respectively; (n,s) is an inelastic scattering reaction.

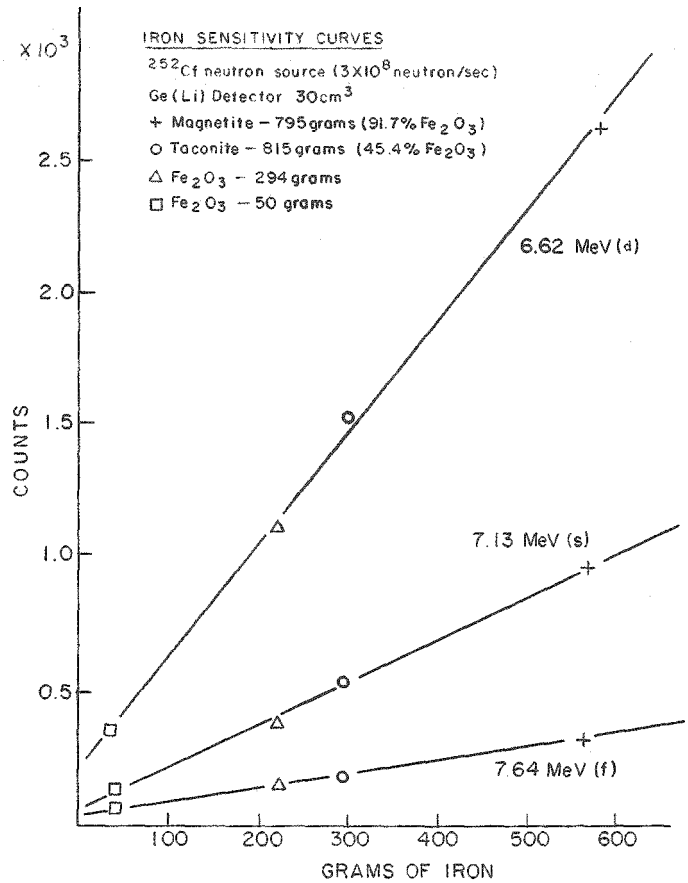

Figure 5 - Sensitivity curves for the full(f), single(s), and double(d) escape peaks of iron for Fe_2O_3, taconite, and magnetite.

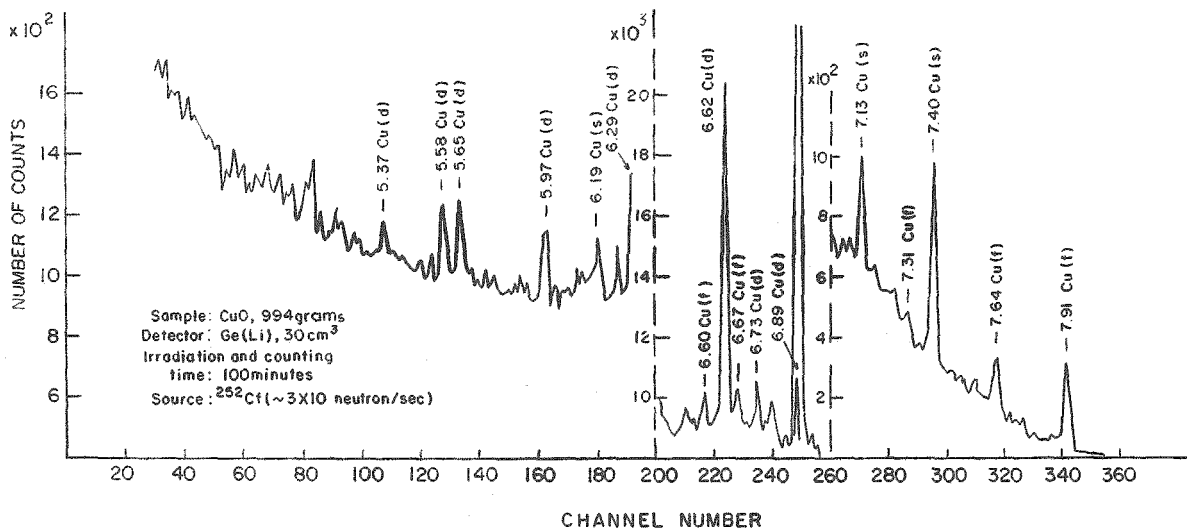

Figure 6 - High-energy-capture gamma ray spectra of CuO showing the prominent peaks of copper. f, s, and d stand for full, single, and double escape peaks, respectively.

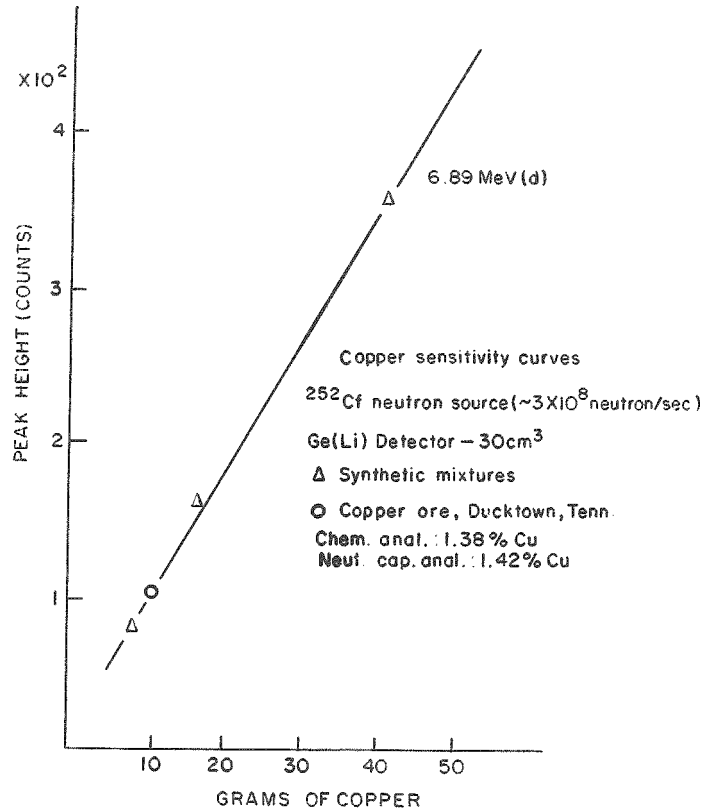

Figure 7 - Copper-calibration curve showing analytical data for a copper ore.

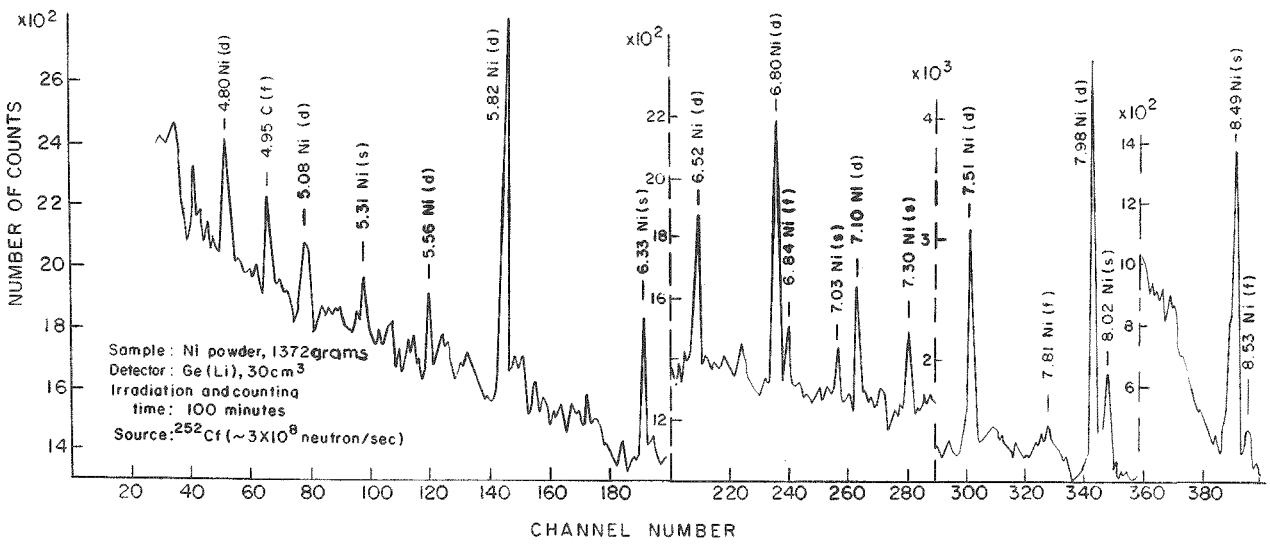

Figure 8 - High-energy-capture gamma ray spectra for nickel powder. f, s, and d stand for the full, single, and double escape peaks, respectively.

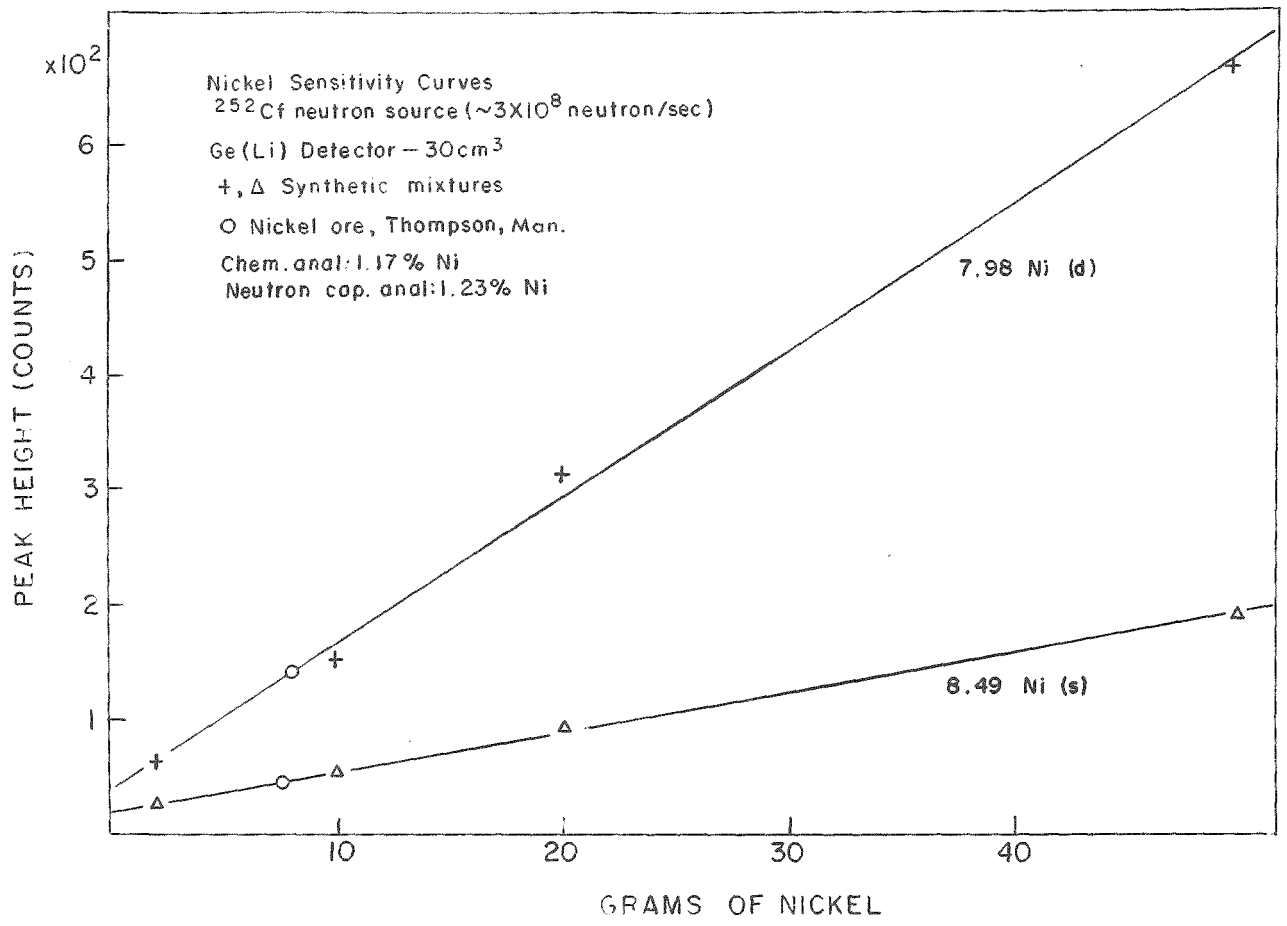

Figure 9 - Calibration curves for the single and double escape peaks of nickel showing analytical data for a nickel ore.

FAST PROCESS MEASUREMENT FOR MANGANESE IN STEELS BY NEUTRON ACTIVATION ANALYSIS

Steven J. Aron, Jr.

Republic Steel Corporation
Electromechanical Research Center
Nucleonics Division
Cleveland, Ohio

A 1120.9 microgram source of californium-252, emitting 2.6 x 10^9 neutrons per second, was used for neutron activation analysis of manganese in steels.

With the aid of specially made steels limiting curves were developed to define the limit of matrix effect errors inherent in the analysis. By means of these limiting curves it is possible to determine the concentration of manganese in either high or low alloy steels with an accuracy of ±3% of the actual content.

Low alloy bar stock and basic oxygen furnace samples were analyzed using standards as time bases. This method greatly simplifies the manganese measurement. In the case of the basic oxygen furnace steels obtained from molds, the neutron activation method is demonstrated to be a fast and accurate process measurement tool. The accuracy of the method is comparable to present analytical techniques and is accomplished in approximately 2 minutes.

INTRODUCTION

With the great emphasis on fast, productive steelmaking furnace operations has come the need for increasingly faster ways of analyzing steels prior to tapping. Conventional methods take five to ten minutes. This includes taking the sample and preparing it for analysis. The use of 1 milligram of Cf-252, on loan from the U.S.A.E.C., has been considered for rapid nuclear activation analysis of steel samples from the furnace. This report covers work recently conducted for analyzing manganese content of samples. It outlines the various theoretical considerations relating to interferences, matrix effects, limiting curves, and time independent activation analysis. Experimental work with steel samples is also described, with results presented to show the utility and accuracy of high strength Californium-252 sources for rapid activation analysis of manganese in steels.

THEORY

NUCLEAR REACTION

Analysis for manganese in steels is accomplished by means of the following nuclear reaction:

$$Mn^{55}(n,\gamma)\ Mn^{56}$$

Where Mn^{56} decays according to the scheme shown in Figure 1 (1).

INTERFERENCES

The following reaction produces an interference in the determination of manganese:

$$Fe^{56}(n,p)\ Mn^{56}.$$

The threshold energy for this reaction is 2.95 Mev (2). This is an important interference since it determines the lower concentration limit for the analysis of manganese in steels as described in this report. No attempt is made to correct for this effect by using a cadmium difference method since a fast and simple determination is our primary objective. Fortunately, this interference has been found to be much smaller when employing a Cf-252 neutron source compared to other conventional isotopic sources since Cf-252 has a lower average neutron energy (3). For the concentration range of interest (0.3 - 10.0% manganese) the error introduced by this reaction is less than the statistical error encountered in the analysis.

Other elements which were found to be of importance are copper and aluminum. By means of the reactions,

$Cu^{65}(n,\gamma)\ Cu^{66}$; $T_{1/2}$ = 5.2 min.

and

$Al^{27}(n,\gamma)\ Al^{28}$; $T_{1/2}$ = 2.3 min.

these elements can produce radiations which add to the background of the 0.85 Mev manganese photopeak. When present in normal amounts ($\lesssim$ 0.05% Cu and $\lesssim$ 0.05% Al), they do not significantly affect the analysis for manganese. Simple electronic checks can be provided in a gaging system to ascertain if these elements are present in larger amounts. If this is found to be the case, then corrections can be made to obtain an accurate manganese measurement.

MATRIX EFFECTS AND LIMITING CURVES

Matrix effects can seriously affect the overall accuracy of any manganese analysis by neutron activation. In order to determine the magnitude of these effects the following two sets of steel samples were specially made and are referred to in this report as the limiting steels:

1. 0-10% Mn (in 1% increments); 90-100% Fe (Low Alloy)

2. 30% Cr; 0-10% Mn (in 1% increments); 30-40% Fe; 30% Ni (High Alloy).

These steels were chosen based upon a mathematical study of the neutron activation problem. The main considerations were the thermal neutron absorption cross sections of chromium, manganese, iron, and nickel (4). By performing a neutron activation analysis for manganese using the samples in the above listed steels, it was possible to generate what is referred to in this report as limiting curves. These curves were developed separately for two activation positions from the Cf-252 source to investigate matrix errors with average neutron energy. The first position was at 10 inches from the source and the second at one inch from the source. It is estimated that essentially all steels should fall between the limiting curves and thus the maximum matrix error is specified by them.

TIME INDEPENDENT ACTIVATION ANALYSIS

Since it was desired to make the manganese determination in about two minutes, it was necessary to monitor the activation and waiting times of the sample very accurately. This was accomplished by using standards as time bases. The standards used were wafers of quick mount material sufficiently doped with pure manganese powder to act as a statistically accurate measure of the activation and waiting times of the sample. To serve as time bases, the standards were activated simultaneously with the samples. In order to show the time independence of this method the following simple and non-rigorous derivation is given.

It is well known in activation methods that the number of gamma ray emissions P_{sa} that result after thermal neutron activation of a sample for a time t_a, waiting for a time t_w, and counting for a time t_c, is (5):

$$P_{sa} = E^{sa}_{act}\ \phi_o V_{sa}(1-e^{-\lambda t_a})e^{-\lambda t_w}\frac{(1-e^{-\lambda t_c})}{\lambda} \quad (1)$$

where E^{sa}_{act} = the thermal neutron macroscopic cross section

ϕ_o = the thermal neutron flux

V_{sa} = the volume of the sample

λ = the disintegration constant.

(Note: t_a, t_w, and t_c are the same for the standard and the sample.)

Rewriting equation (1) for the standard and dividing into the above equation for the sample, one obtains:

$$\frac{P_{sa}}{P_{st}} = \frac{E^{sa}_{act}\ V_{sa}}{E^{st}_{act}\ V_{st}} \quad . \quad (2)$$

This equation readily reduces to the following,

$$C_{Mn} = \text{constant x Relative Count} \quad (3)$$

where Relative Count = $\frac{P_{sa}}{P_{st}}$

and C_{Mn} = concentration of manganese.

Equation (3) shows that the concentration of manganese as determined by this method is time independent. Moreover, it states that a linear relationship should exist between manganese concentration and the relative count. For the range of 0.3 - 2% manganese this is verified and is presented in the experimental results.

EXPERIMENT

STEEL SAMPLES

There were three sets of steel samples analyzed in this study. The first set of steel samples, previously mentioned, were used to generate the limiting curves to investigate matrix effects. The second set of steel samples were machined from low alloy bar stock material. The last set consisted of steel samples obtained from molds by sampling various heats from a basic oxygen furnace. All samples had the configuration of right circular cylinders with a diameter of 2 inches and a length of 1.5 inches. These dimensions were chosen for the following reasons.

1. It was desired to make the activity measurement as insensitive to length as possible to minimize sample preparation (6).

2. Standard NaI (Tl) crystals with 2 inches diameter were readily available.

3. The same samples could later be used to investigate manganese in steels using the X-ray fluorescence method of selective excitation (7).

NEUTRON ACTIVATION AND COUNTING

A standard and a steel sample were placed together in a holder and lowered into the neutron moderator assembly (see Fig. 2) at a distance of one inch from the Cf-252 source. The activation time was held to approximately 1 minute ±15 seconds. Because standards were used as time bases, it was not necessary to know the exact times. After removing the sample from the moderator the waiting time varied anywhere from 20 seconds to several minutes. Again, it was not necessary to monitor the waiting times when standards are used. Dual counting chambers were not available at the time, therefore, the activity of the sample was first measured for 1 minute in a lead enclosed counting chamber as seen in Figure 3. Immediately after counting the sample, the standard was counted for an equal length of time. This sequential counting of standard and sample introduced a constant counting error of 0.4%. Thus it did not affect the overall accuracy of the analysis. In practice, a dual counting chamber will be used with the scaler of the standard set at a preset count to provide a stop signal for the sample scaler. In this way the standard serves as a time base and provides for automatic division to obtain the relative count. The relative count was determined in this report by dividing the 0.85 Mev manganese photopeak count of the sample by the gross count of the standard. Once the relative count is known, the concentration of manganese is easily found by either a simple equation, graph, or an analog voltage.

A block diagram of the detector and associated electronics is shown in Figure 4.

DATA AND RESULTS

The data and results for the limiting steel samples activated at a distance of 10 inches from the source are given in Table I. For the same samples activated at 1 inch from the source the data and results are presented in Table II. Both sets of data are seen graphically in Figures 5 and 6.

Data and results for the bar stock and basic oxygen furnace samples activated at 1 inch from the source are found in Table III. Using the accurately known manganese concentrations of the 1% and 2% samples and repetitive measurements, a least squares fit for the data of Table V was obtained. This is shown in Figure 7.

DISCUSSION OF RESULTS

HIGH AND LOW ALLOY LIMITING STEELS

Figure 5 shows that the matrix errors present in the activation analysis of high and low alloy steels at 10 inches from the source are ±8% of the manganese concentration. By activating the same samples at 1 inch from the source the matrix errors are reduced to ±3% of the manganese content as seen in Figure 6. This reduced error results from irradiation with higher average

energy neutrons at the 1 inch position and the smaller variation of the elements' neutron cross sections at the higher energy. For a steel of unknown composition, therefore, matrix errors will limit the accuracy of the analysis to ±3% of the manganese concentration.

LOW ALLOY BAR STOCK AND BASIC OXYGEN FURNACE STEELS

The least squares fit to measurements of accurately known low alloy limiting steels yields the following equation:

$$C_{Mn} = \text{Relative Count} - 0.052 \qquad (4)$$

where C_{Mn} is the manganese concentration in per cent. Equation (4) is used together with the data of Table III to determine the manganese concentrations of the low alloy bar stock and basic oxygen furnace steels. Table III shows the important result that the manganese concentrations obtained by neutron activation techniques differ from those found by conventional methods by approximately ±0.02% manganese in the range 0.3% - 2.0%.

MEASUREMENT ERRORS

There are three principal sources of measurement error:

1. the $Fe^{56}(n,p)\ Mn^{56}$ interference reaction;
2. the statistical error present in any nuclear measurement; and
3. the electronic system error.

It has been noted from previous work (3) that the iron interference reaction produces a manganese percentage error of approximately +0.01%. This was true for manganese concentrations in the range of 0 - 2%.

Experimentally, the maximum statistical error at the 95% confidence level is $\leq$ ±3% of the manganese content. This error decreases as the manganese concentration increases beyond 0.3%. Typically, the statistical error is $\leq$ ±0.02% manganese.

The electronic system error is estimated to be less than ±0.01% manganese.

CONCLUSIONS

1. A one milligram Californium-252 source can be used for activation analysis of manganese in steels and matrix effect errors can be minimized by a suitable choice of sample irradiation position.
2. In samples of unknown alloy content manganese can be determined to an accuracy of ±3% of the concentration.
3. For low alloy bar stock and basic oxygen furnace steels, a 2 minute activation analysis is accurate to ±0.02% manganese.
4. The neutron activation analysis of manganese in steels is a fast and accurate process measurement tool comparable to present analytical techniques.

REFERENCES

1. K. G. A. Porges, A. Devolpi, and R. N. Larsen. "Electronic Design of an Absolute Counting System for Mn^{56}". Nuclear Instruments and Methods. 29, No. 1, 157-169 (1964).
2. K. H. Beckurtz and K. Wirtz. Neutron Physics. Springer Verlag, New York (1964).
3. S. J. Aron and D. J. Brisbin. "Neutron Activation Analysis of Manganese in Steels Using a Californium-252 Neutron Source". Republic Steel, ERC Report 1832 (1970) (not published).
4. L. V. Groshev, V. Lutsenko, A. M. Demidov and V. I. Pelekhov. Atlas of Gamma Ray Spectra From Radiative Capture of Thermal Neutrons. Pergamon Press, New York (1969).
5. W. J. Price. Nuclear Radiation Detection. McGraw Hill Book Company, New York. 311-363 (1964).
6. S. J. Aron and D. J. Brisbin. "Time Independent Neutron Activation Analysis of Manganese in Steels". Republic Steel, ERC Report 1840 (1970) (not published).
7. S. J. Aron. "Non-Dispersive X-Ray Fluorescence Analysis by Selective Excitation" Ph.D. Thesis. Case Western Reserve University (1969).

TABLE I

LIMITING STEELS ACTIVATED AT 10 INCHES FROM THE SOURCE

Sample	Relative Count (Normalized)	% Manganese *
S-356	0.005	0
S-357	1.102	1.0
S-358	1.963	2.0
S-359	3.037	3.0
S-360	3.860	4.0
S-361	4.623	4.8
S-362	5.531	5.8
S-363	6.256	6.7
S-364	7.234	8.1
S-365	7.900	9.0
S-366	8.764	10.1
S-368	0.005	0
S-369	0.496	0.5
S-370	1.825	2.1
S-371	2.575	3.0
S-372	3.476	4.1
S-373	4.272	5.1
S-374	4.805	6.1
S-375	5.681	7.1
S-376	6.396	8.3
S-377	6.980	9.2
S-378	7.560	10.2

* Wet Chemical Analysis

Note: S-356 - S-366 are Mn, Fe Binary Samples

S-368 - S-378 are Cr, Mn, Fe, Ni Samples

TABLE II

LIMITING STEELS ACTIVATED AT 1 INCH FROM THE SOURCE

Sample	Relative Count (Normalized)	% Manganese *
S-357	1.075	1.0
S-358	2.012	2.0
S-359	2.891	3.0
S-360	3.686	4.0
S-361	4.428	4.8
S-362	5.237	5.8
S-363	5.953	6.7
S-364	7.201	8.1
S-365	7.814	9.0
S-366	8.727	10.1
S-369	0.554	0.5
S-370	2.011	2.1
S-371	2.721	3.0
S-372	3.649	4.1
S-373	4.488	5.1
S-374	5.286	6.1
S-375	5.913	7.1
S-376	6.815	8.3
S-377	7.615	9.2
S-378	8.371	10.2

* Wet Chemical Analysis

Note: S-357 -S-366 are Mn, Fe Binary Samples
S-369 -S-378 are Mn, Fe, Ni, Cr Samples

TABLE III

RESULTS OF NEUTRON ACTIVATION ANALYSIS OF MANGANESE IN LOW ALLOY STEELS

SAMPLE	RELATIVE COUNT	C_{Mn}(%) *NAA	C_{Mn}(%) **	DEVIATION (%)
S-418	0.371	0.32	0.32	0
S-413	0.396	0.34	0.36	-0.02
S-396	0.458	0.41	0.39	0.01
S-390	0.510	0.46	0.48	-0.02
S-406	0.564	0.51	0.50	0.01
S-427	0.734	0.68	0.67	0.01
S-391	0.797	0.74	0.74	0
S-386	0.848	0.80	0.80	0
S-389	0.983	0.93	0.94	-0.01
S-395	0.971	0.92	0.90	0.02
S-385	1.095	1.04	1.03	0.01
S-425	1.192	1.14	1.12	0.02
S-412	1.404	1.35	1.34	0.01
S-394	1.565	1.51	1.52	-0.01
S-426	1.695	1.64	1.63	0.01
S-415	0.730	0.68	0.70	-0.02

*Neutron activation analysis

**Determined by wet chemistry, emission spectroscopy, and/or X-ray flourescence analysis

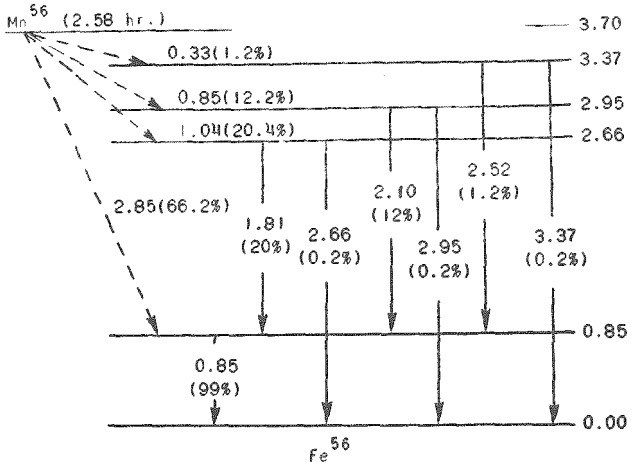

FIG.1 MANGANESE-56 DECAY SCHEME

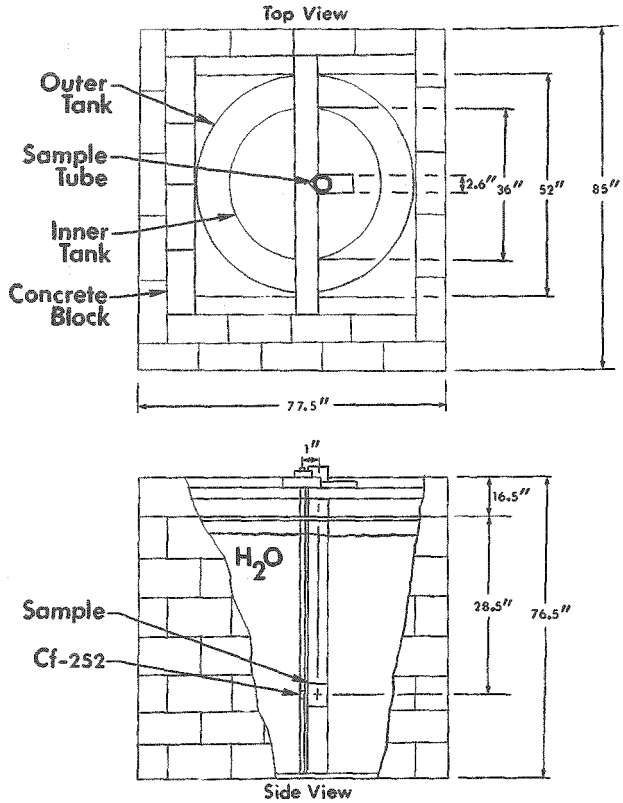

FIG. 2 NEUTRON MODERATOR ASSEMBLY

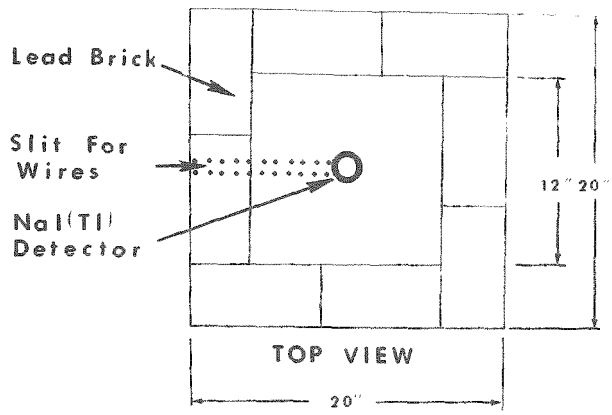

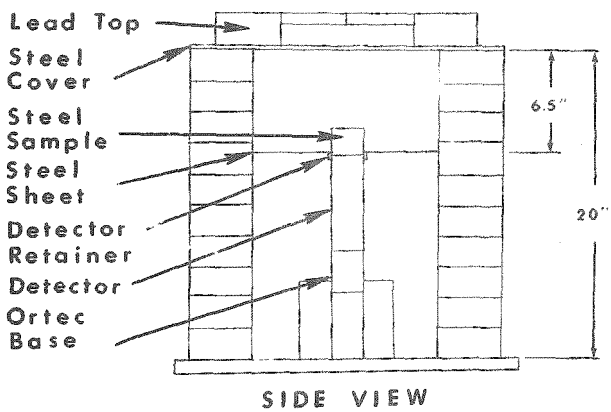

FIG. 3 COUNTING CHAMBER

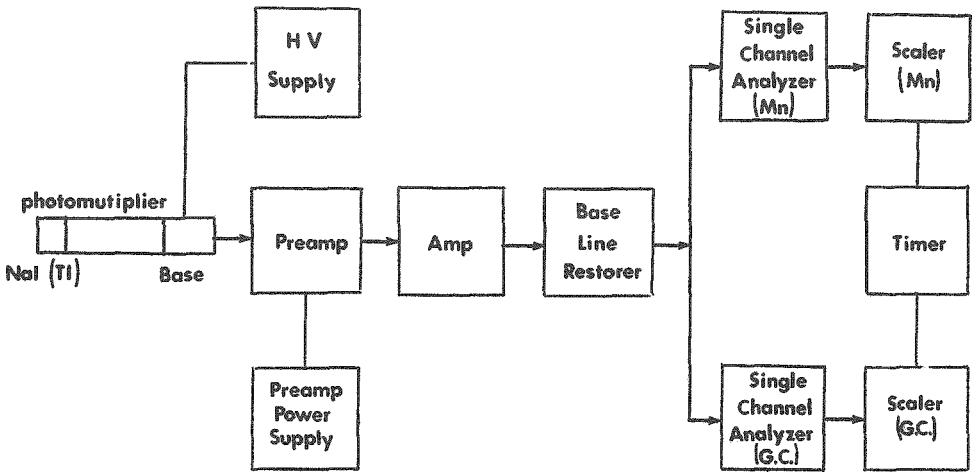

FIG.4 BLOCK DIAGRAM OF ELECTRONICS

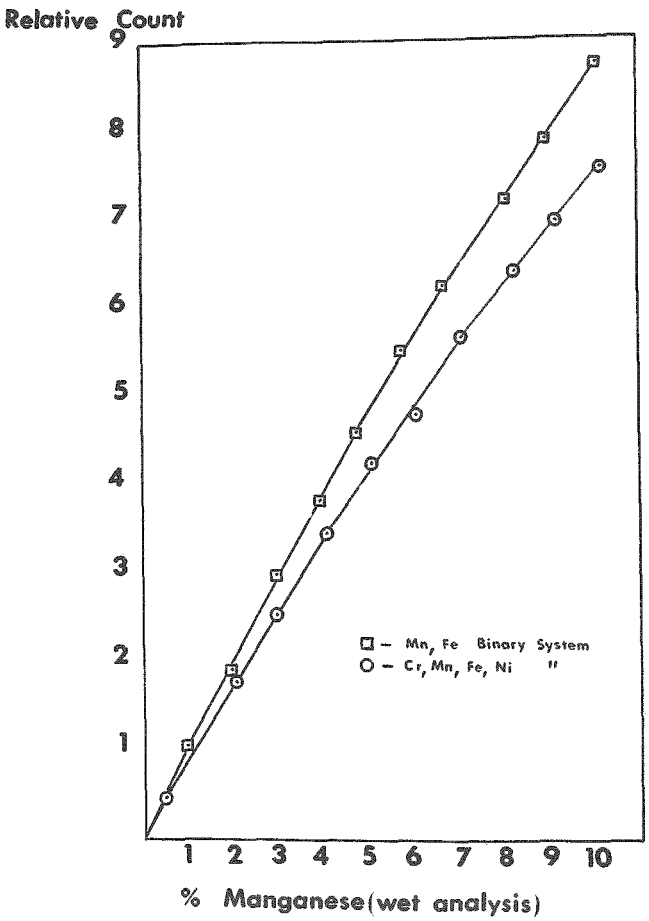

FIG. 5 ACTIVATION OF LIMITING STEELS (10 INCHES)

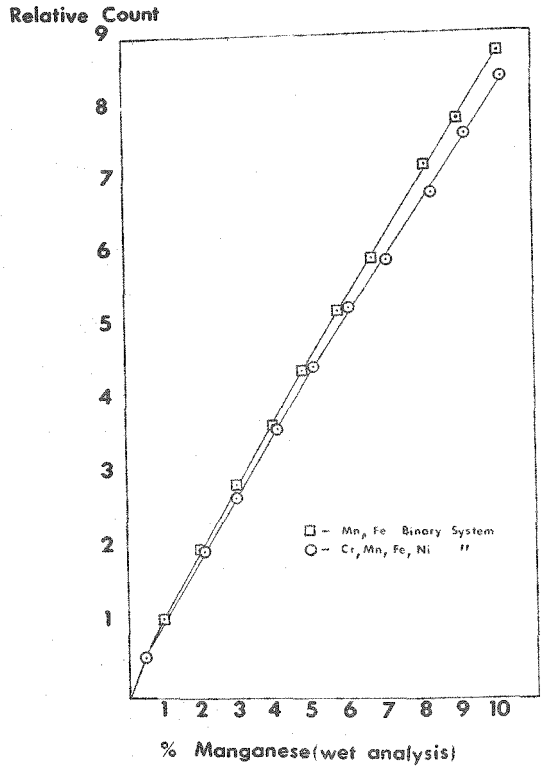

FIG. 6 ACTIVATION OF LIMITING STEELS (1 INCH)

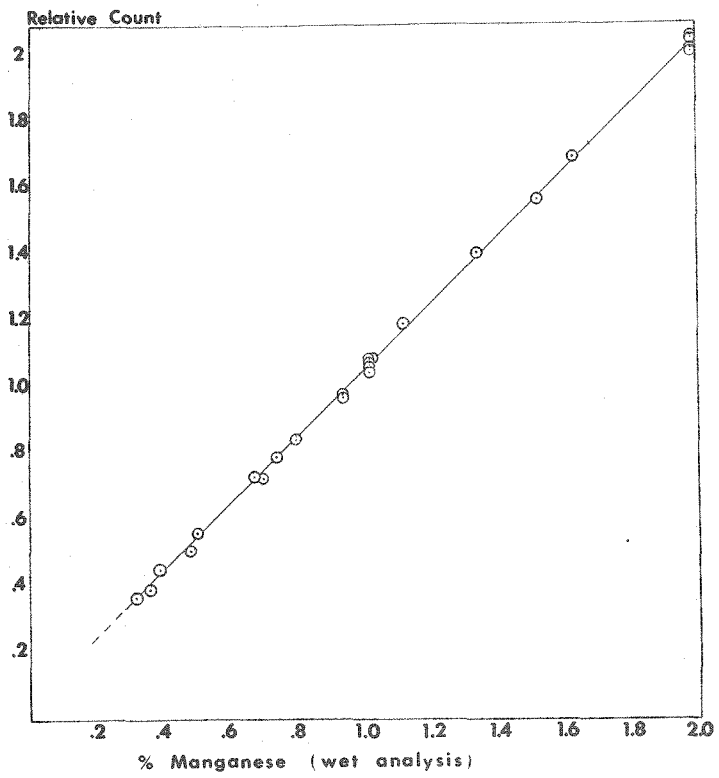

FIG.7 ACTIVATION OF LOW ALLOY STEELS

A PROMPT GAMMA-RAY COAL ANALYSIS SYSTEM

Daniel R. Parsignault, Henry H. Wilson, and R. Mineski

American Science and Engineering
Cambridge, Massachusetts

S. L. Blatt

Department of Physics
Ohio State University
Columbus, Ohio

A system designed to measure the prompt γ-rays produced by the interaction of thermalized neutrons from a californium-252 source with the constituents of coal is described. The system operates at a total counting rate of 1 Megahertz, with an energy resolution of ~5% at 5 Mev. Such high counting rates allow for the determination of the sulfur content of coal with an error of less than 2%, in a few minutes. To obtain this accuracy in this short time period, a NaI(Tl) detector surrounded by a plastic anti-Compton shield together with a sophisticated electronic system rejecting pile-up events is used. The γ-spectra are collected in a mini-computer which analyzes them, while monitoring and adjusting the system continuously.

INTRODUCTION

The determination of the sulfur in metallurgical coal has been done, up to now, by a wet chemical analysis method. This method requires an elaborate sampling technique, involving tedious sample preparations and chemical analysis. Furthermore, such a technique is time consuming, necessitating up to 24 hours for the results to be known. It has been recognized for sometime that another technique, the prompt activation analysis technique, should be most advantageous in coal analysis. However, up until recently the full advantage of this method of analysis could not be used due to limits in the nuclear technology. With the advent of fast electronics, better γ-ray detectors, and minicomputers, this technique can now be exploited to its full advantage. Its advantages over the chemical analysis method are speed, large sample sizes, high reliability and accuracy, and it can be incorporated in an automated processing scheme. In this paper we describe such a system which is presently being tested in the laboratory and will be installed and tested in an actual plant in the near future.

THE (n, γ) REACTION

The irradiation of matter with neutrons generally results in the radiative capture of the low energy neutrons (thermal neutrons). A thermal neutron incident on a nucleus of mass M_A produces a nucleus of mass M_{A+1} in a highly excited state. This excited nucleus will then decay through one of the three possible channels: charged particle emission, electromagnetic radiation emission, or fission. In the case of the very light elements ($A < 20$), the emission of a charged particle is preponderant. For the very heavy elements ($A > 200$), the fission process competes very favorably with the γ-ray emission. However, in most other instances the charged particle emission or the fission process is energetically forbidden or greatly retarded by the Coulomb barrier, and the principal mode of decay is the emission of one or several γ-radiations.

The energy balance for such a radiative capture reaction is:

$$E_n + M_n + M_A = M_{A+1} + (Q + E_n)$$

where E_n = initial neutron energy

Q = energy of the reaction (for most isotopes between 2 and 12 MeV).

In a time of the order of 10^{-14} sec, the energy Q is dissipated (except for the small nucleus recoil energy) in a single or several electromagnetic radiations as the nucleus M_{A+1} returns to its ground state, or to a long-lived isomeric state.

In most of the light elements (A < 100), the γ-ray spectra are relatively simple, and the presence of a given isotope can be implied by identification of its characteristic signature; i. e., the presence of one or several characteristic γ-rays of well defined energy. Several compilations of thermal neutron-capture γ-ray spectra for most elements are available (1, 2), the most recent having been made by Rasmussen et al. (3) and by Duffey et al. (4).

MEASUREMENT OF THE SULFUR CONTENT OF COAL

The mode of interaction between thermal neutrons and nuclei discussed briefly in the proceeding section can be used, in principle, to perform an analysis of the constituents of a given bulk material. The sample is bombarded by a flux of neutrons, and the resulting γ-ray spectrum is recorded. Each element will emit one or several γ-rays which are peculiar to that element. By knowing the cross-sections for the nuclear interaction process with the different elements (i. e., the probabilities of interaction), and the efficiency of detection of the γ-rays, the percentages of each of the elements making up the bulk material can be determined to very high accuracy. The precision of the analysis depends only on the number of counts obtained for each typical γ-ray, and the precision to which the cross-sections are known.

The great possibilities of such a method of analysis have long been recognized, and actual experiments demonstrating its feasibility have been performed (e. g., Stewart (5)). However, because of physical constraints in the available detectors and nuclear electronics, which limited the maximum counting rates and energy resolution, the method had been limited until now to sample analysis which require long measurement periods. In order to take full advantage of the technique, one must have the capability to perform a rapid analysis of a large sample (typical: 1 - 2 tons).

In the rapid measurement of neutron-capture radiations for the determination of the amount of sulfur present in coal, large numbers of γ-rays in the energy range 3 - 6 MeV must be detected over a relatively short period of time, in the presence of an intense background of neutrons. These conditions dictate the need for a detection system capably of good energy resolution (better than 5%) at very high total counting rates (total counting rates > 1 MHz). The system proposed here is designed to meet these requirements through the following general approaches:

1. The basic detector type and geometry are selected to provide a monoenergetic γ-ray response which has a high proportion of the counts in a single, narrow peak. Such a response reduces the total number of counts needed for a given accuracy of analysis, thereby permitting lower basic counting rates.

2. The number of pulses which are distorted due to pileup is reduced drastically by the use of fast electronics. This allows total counting rates up to about 1 MHz while preserving the basic resolution provided by the detector.

3. Losses due to analog-to-digital conversion dead-times are minimized by requiring analysis of only the undistorted pulses in the energy range of interest.

DESCRIPTION OF THE SYSTEM

The proposed system incorporates 3 separate units: a neutron source, a γ-ray detector and an electronic processing unit. During the laboratory testing of the system, the neutron source is located at the geometrical center of a 500 lb. barrel of coal. When installed in a coal processing plant, the neutron source will be located in the middle of the coal bin, and the detector in

close proximity to it. The electronics processing the output signals from the γ-ray detectors can be located away from the detector by as much as 150 feet.

THE NEUTRON SOURCE

In using prompt (n, γ) reactions as the method of analysis of bulk materials, one does not need the high neutron fluxes necessary in the conventional activation analysis method. Such low neutron fluxes do not produce any appreciable radioactivity in the irradiated material, and thus allow it to be industrially processed after its irradiation.

In this particular application, we use a 12μg ^{252}Cf radioactive source for laboratory purposes, and we plan to use a 300μg ^{252}Cf source in the field. This relatively stronger source will allow for a typical measurement on the sulfur content of coal to be made in a few minutes (typically, 5 minutes) and with an error of less than 2%.

THE DETECTOR

A schematic diagram of the detector assembly is shown in Figure 1. It consists of a central detector, an active shield, and a passive shield.

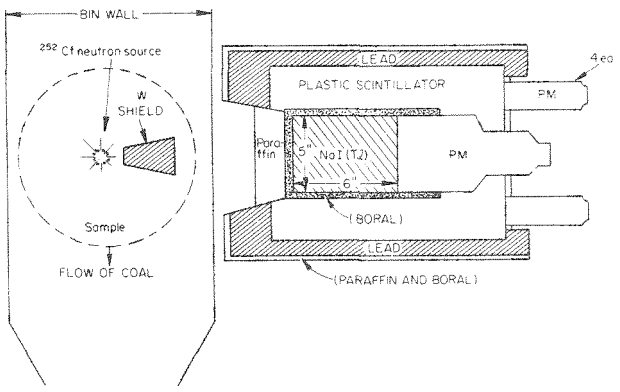

Figure 1. Source-Detector Configuration (Not to Scale)

The central detector consists of a 5" x 6" NaI (Tℓ) crystal optically coupled to a 5" fast, high-gain photomultiplier tube. The intrinsic energy resolution of this detection system is better than 5% at 5 MeV.

The active shield is a plastic cylinder 16" x 16", almost surrounding the central detector. This shield is further enclosed in an Al cylinder to make the system light-tight. Four PM tubes, having similar characteristics as the central PM, are used to view the events in the plastic detector.

The passive shield consists of a Pb ring 5" thick in the front, and ~1" of Pb on the sides. A 1/8" thick Boral (Boron carbide with Al) surrounds the whole system. Furthermore, Boral is used between the plastic shield and the Na (Tℓ) crystal. Work is presently in progress to optimize this passive shielding.

THE ELECTRONIC SYSTEM

The block diagram of the electronics unit is shown in Figure 2. Linear pulses from the central NaI (Tℓ) detector are applied to three channels: A, B, and C. Channel A performs a rough pulse height selections, discriminating against events below a certain threshold. The output of this channel triggers a pulse generator which opens a linear gate in Channel C which in turn presents the shortened detector pulses to the PHA for analysis. The function of Channel B is to detect pilup conditions for time intervals less than 200 ns. The discriminator passes all pulses, down to the lowest level which could cause pileup distortion, to the pileup gate. The pileup gate produced a veto command, to inhibit an output from Channel A, when it detects the occurrence of successive pulses within a 200 ns time interval. Channel A output signals are also inhibited when a pulse is received from one of the detectors coupled to the plastic scintillator shield. The function of the plastic shield is to detect γ-rays which have interacted by the Compton process with the NaI crystal, and the 511 KeV annihilation γ-ray radiations. Thus, the linear gate in Channel C is opened to accept valid signals only

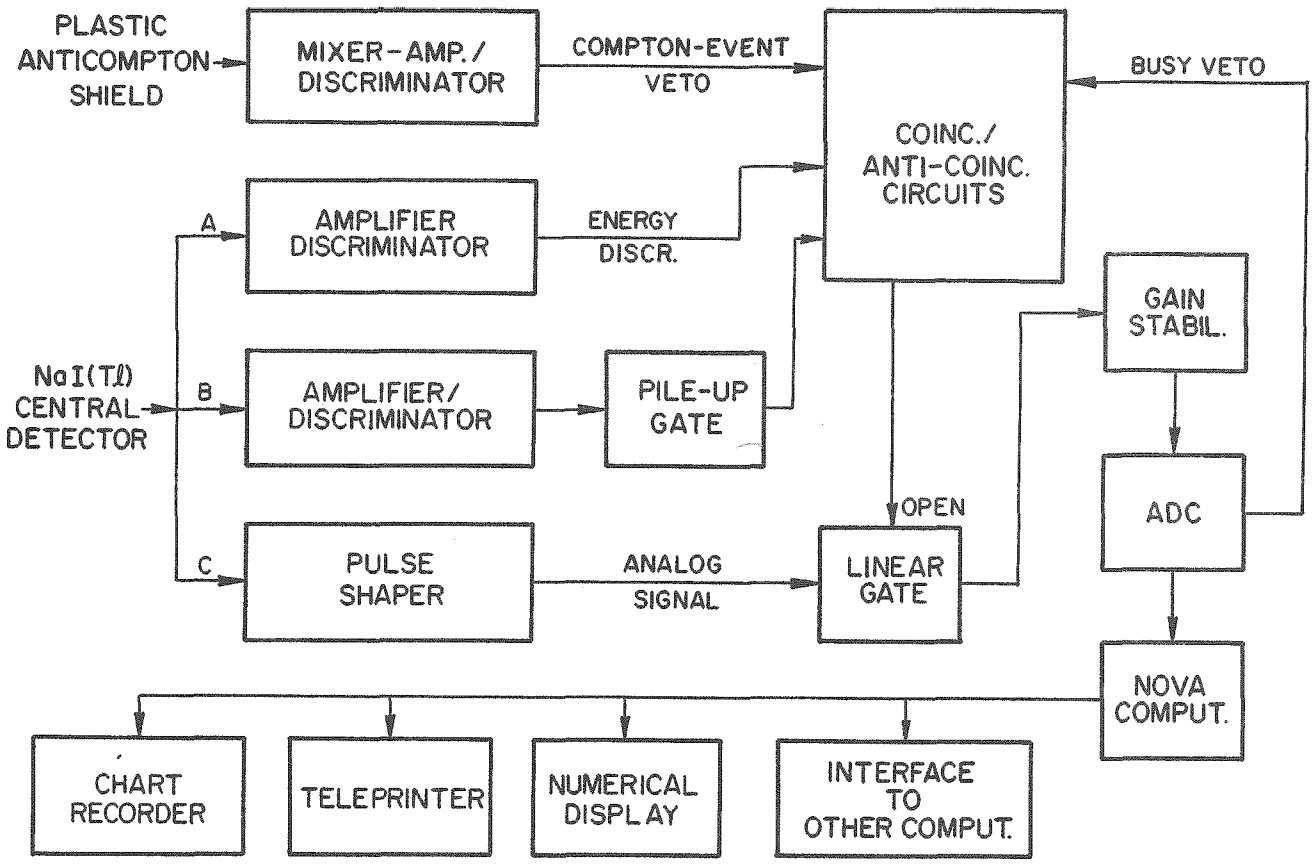

Figure 2. Electronics Block Diagram

after it has been established that there is no pileup (below 200 ns), and that the detector pulse is not coincident with a signal from the plastic shield. Channel C utilizes fast electronics and a pulse-shortening technique to prevent the occurrence of pileup for time intervals down to 200 ns.

In this linear branch of the circuit, a filter network is used to shorten the pulses to about 100 ns at the baseline, while preserving the linearity of the total pulse area.

Figure 3 shows input and output waveforms for a typical matched filter. In Figure 3a the decay time constant of the output signal is approximately 200 ns. By proper modification of the circuit parameters a baseline width of 100 ns is readily achieved. Figure 3b illustrates the effectiveness of this circuit in eliminating pileup at the output for the case of two input pulses spaced 200 ns apart.

With the high gain photomultipliers employed, there is enough information in the first 100 ns of the anode pulse to obtain excellent resolution in the 5-MeV region. The shortened linear pulses reduce the time-region within which pileup could occur from about 4 μs (with conventional processing) down to 200 ns. The fast linear gate assures that interferring pulses arriving beyond the 200 ns time window do not get through to the stretcher, where the pulses are integrated and shaped to the pulse-height analyzer requirements.

PRELIMINARY RESULTS

Figure 4 shows a typical spectrum taken

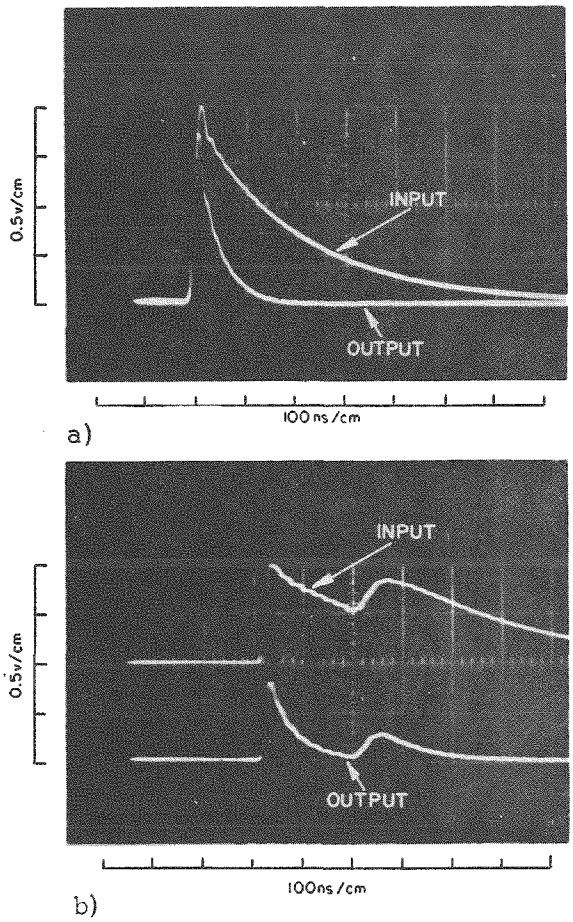

Figure 3. Matched Filter Response

with a 12 μg ^{252}Cf source (2.8×10^{7} neutrons/sec) irradiating a 500 lb. sample of coal ob tained through the courtesy of the U. S. Steel Corporation, from its Robena Slope Facility coal processing plant. Since such a neutron source results in a counting rate at the detector of approximately 60 - 70 KHz, a 1 MHz total counting rate was obtained by placing in close proximity to the NaI detector, a 1 mc ^{60}Co source.

Only the energy region of interest, between ~4 MeV and 7.8 MeV, is shown in Figure 4. The main peaks corresponding to the (n, γ) reactions with the different elements comprising the coal are indicated in the figure together with an energy calibration curve corresponding to these peaks. A high resolution energy spectrum, obtained with a Ge (Li) detector confirmed these peak assignments.

A note concerning the 6.8 MeV γ-ray peak: in the particular run when these data were taken, the Boral sheet surrounding the detector had been removed. Thus, slow neutrons were allowed to interact with the NaI (Tℓ) crystal. This broad peak at 6.8 MeV correspond to the absorption of the total binding energy of the last neutron in Na (6.96 MeV), I(6.8 MeV) and Tℓ (6.64 MeV).

The percentage of sulfur contained in the coal sample can be determined from the area under the photopeak of sulfur, at 5.42 MeV, after the Compton background and the small Cl peak at 5.72 MeV has been subtracted.

Since for a 5" x 6" NaI (Tℓ) crystal, the first escape peak intensity of 5 MeV γ-rays is about 80% of the full energy peak intensity, it would seem then a large amount of information is lost by the use of an anti-Compton shield, which eliminates it from the spectrum. However, the intensity of the first escape peak of S alone can be obtained from the "coincidence" spectrum, i.e., the spectrum recorded in the NaI detector which is in coincidence with events in the plastic shield. In such a spectrum, only first and second escape peaks plus the Compton γ-rays distribution appears. This "coincidence" spectrum is taken simultaneously with the normal "anti-coincidence" spectrum, and each one of the spectra is stored in different blocks of the on-line computer memory.

Finally, we would like to point out several problems which are being solved at present. The first problem is a change in the coal bulk density which could introduce apparent changes in the sulfur peak intensity. The bulk density of the volume being sampled can be monitored by a radioactive source placed on one side of the volume and a γ-ray detector directly opposite to the source, which will record any change in γ-ray intensity from the source, i.e., a change in bulk density.

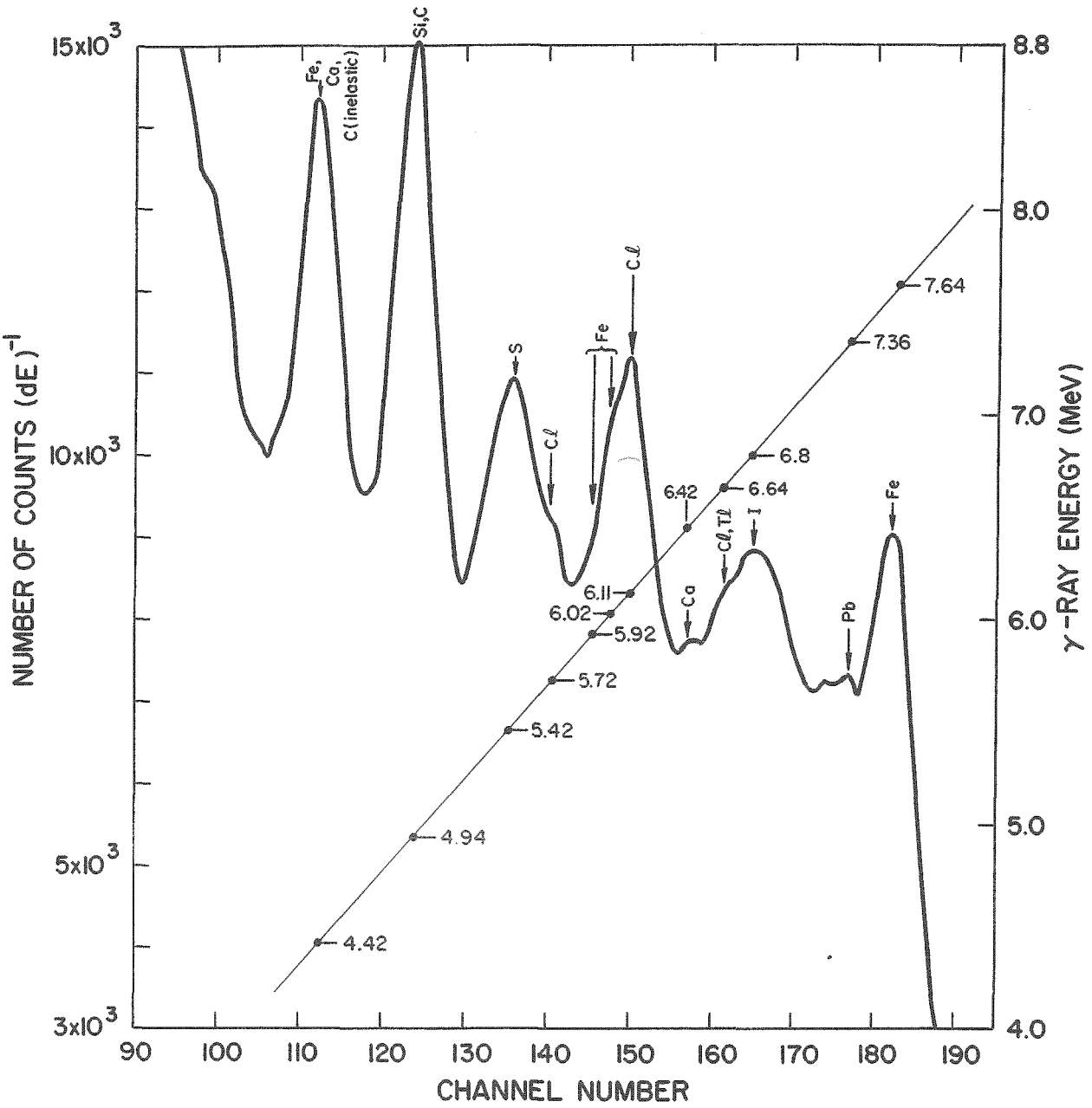

Figure 4. Neutron-capture γ-ray spectrum (4 MeV < E < 8 MeV) resulting from the irradiation of a coal sample with a ^{252}Cf neutron source.

The second problem, much more complex, is the change in the neutron thermalization rate due to a change in moisture in the coal. This can be done using the information contained in the peak at 2.23 MeV corresponding to the formation of deuterium. The intensity in this peak is proportional to the hydrocarbon and H_2O content of the coal. The correction for the change in the thermal neutron flux is done on-line, using the mini-computer.

CONCLUSIONS

Laboratory results obtained with the above described system indicate that the determination of the sulfur content of coal

can be performed within a matter of minutes and on large coal samples, using the prompt γ-ray activation technique. Such measurements should yield the sulfur content of coal with an error inferior to 2% (ASTM standard) in a time period under 5 minutes. Using the same system, the same measurement should also yield, in principle, the percentage of moisture and possibly the total ash content of the same coal.

REFERENCES

1. G. S. Bartholomew and L. A. Higgs. Atomic Energy of Canada Report AECL 669 (1958).

2. L. V. Groshev, V. N. Demidov, A. M. Lutsenko, and V. I. Pelekhov. Atlas of Gamma-Ray Spectra from Radioactive Capture of Thermal Neutrons. (Atomizdat, Moscow, 1958); Eng. Transl. by J. B. Sykes; The Pegramon Press, London (1954).

3. N. C. Rasmussen, Y. Hukai, T. Inouye, and V. J. Orphan. Thermal Neutron Capture Gamma-Ray Spectra of the Elements. Clearinghouse for Federal Scientific and Technical Information, Springfield, Va., AD 688 955 (1969).

4. D. Duffey, A. El-Kady and F. E. Senftle. Analytical Sensitivities and Energies of Thermal-Neutron - Capture Gamma Rays. Nucl. Instr. and Meth. 80, 149 (1970).

5. R. F. Stewart. "Nuclear Measurement of Carbon in Bulk Materials," I. S. A. Trans. 6, 200 (1967).

OPTIMIZATION OF SOURCE-COLLIMATOR GEOMETRY FOR A NEUTRON RADIOGRAPHIC FACILITY UTILIZING A ^{252}Cf SOURCE

Kenneth D. Kok
Joseph W. Ray

Battelle Memorial Institute
Columbus Laboratories
Columbus, Ohio

The optimization of a neutron radiographic facility requires the maximum possible resolution on the radiograph for the shortest possible exposure. These effects are functions both of the collimator source geometry and the detector-recorder combinations. Several source-collimator geometries were studied utilizing a single detector-recorder combination.

The BMI ^{252}Cf neutron radiographic facility allows both horizontal and vertical movement of the neutron collimator with respect to the source. Experimental runs were made utilizing collimators with 7.5 inch and 15 inch lengths and 15:1 length to diameter ratios to determine the peak thermal flux at the collimator inlet, the thermal flux at the collimator outlet, and the gamma dose rate at the collimator outlet.

Air gaps were then added to the collimator so that the source was farther from the collimator inlet with little addition of moderating material, thus increasing the neutron-to-gamma ratio at the exit aperture.

Optimum source-collimator geometries can be selected using these data to either maximize the flux or the neutron-to-gamma ratio, depending on the particular radiographic application.

INTRODUCTION

Neutron radiography has been used for several years as an increasingly important means of nondestructive testing. The wide application of neutron radiography has been limited by the lack of a small intense neutron source. Californium-252 provides this needed source of neutrons. The problem has now become the application and optimization of ^{252}Cf as a neutron source for neutron radiography.

Since most radiographic applications call for maximum resolution in a minimum amount of time, the optimum neutron-radiography facility will provide both, within the limits of the neutron-source intensity. These effects are functions of collimator-source geometry and the detector-recorder combinations. This paper deals with source-collimator-geometry studies.

APPARATUS

SOURCE

The source used for these studies contained 946 micrograms of ^{252}Cf, with a neutron-emission rate of $2.385 \times 10^9 \pm 3$ percent neutrons per second, on August 21, 1970. Since the source is constantly decaying, all fluxes referred to in this paper have been normalized to the source strength on that date.

The source is mounted on a transfer assembly which can be moved vertically in a support stand. The whole apparatus is positioned in the pool-shielding facility at the Battelle Research Reactor (BRR).

COLLIMATORS

Two collimators have been constructed for use in these geometric-optimization studies. The first is 7.5 inches long with a 0.5 x 0.5-inch entrance aperture and a 4 x 5-inch exit aperture. The second is 15 inches long with a 1 x 1-inch entrance aperture and a 8 x 10-inch exit aperture. Thus both collimators have 15:1 length-to-diameter ratios. Each collimator is also equipped with a removable 0.020-inch cadmium liner.

Either collimator can be adjusted both vertically and horizontally with respect to the source. This permits the selection of an infinite number of source-collimator geometries.

EXPERIMENTAL MEASUREMENTS

Dysprosium foils were used as flux monitors, since the cadmium ratio for dysprosium is so large (~500) that only bare foils were required. Gamma measurements

Work performed under AEC Contract AT(38-1)-593.

at the collimator outlet were made with ^{7}LiF thermaluminescent dosimeters.

INLET FLUX

The thermal-neutron flux at the collimator entrance aperture was measured for the 7.5-inch collimator. The source was positioned in contact with the collimator and then moved away in 0.25-inch steps. The resulting flux profile is shown in Figure 1. The peak thermal flux was 9.6×10^{6} $n/cm^2/sec$. As expected, the neutron flux increases when the collimator-to-source distance is first increased, and finally the flux begins to fall off with increasing source-to-collimator separation. The relatively constant flux in the 0.25 to 1.0-inch range is caused by the combined effects of the cadmium absorber in the collimator and the increasing amount of water surrounding the source.

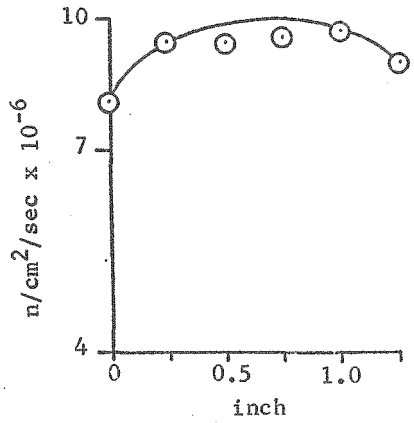

FIG. 1 COLLIMATOR-INLET NEUTRON FLUX AS A FUNCTION OF VERTICAL SOURCE-TO-COLLIMATOR DISTANCE

The source was also positioned in the plane of the collimator inlet and the source-to-collimator separation increased horizontally. Because of the physical size of the apparatus, the minimum distance between the center of the collimator inlet and the source is 1.0 inch. The flux profile obtained in this case is shown in Figure 2. The flux continues to decrease as the separation increases.

These results indicate that the peak outlet flux should occur with the source in a position directly under the collimator and 0.25 to 1.0 inch away.

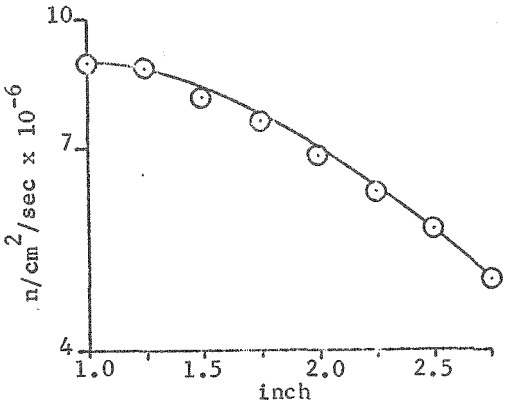

FIG. 2 COLLIMATOR-INLET NEUTRON FLUX AS A FUNCTION OF HORIZONTAL SOURCE POSITION

OUTLET FLUX

Thermal-flux measurements were made at the collimator outlet of both the 7.5 and 15-inch collimators. In order to move the source away from the collimator to minimize the flux depression caused by the cadmium liner, a series of air gaps were introduced at the collimator inlet (1). Four series of runs were then made with each collimator. First, horizontal and vertical source-to-collimator distances were varied with a constant air gap, and then air-gap size was varied for constant vertical and horizontal source positions. All data are presented as the ratio of neutron flux to source neutron-emission rate (n/cm^2/source n). This ratio will remain constant through the source life since it is geometry dependent only. The purpose of these runs is to determine where the peak flux-to-source ratio occurs.

Constant Air Gap. A 2-inch air gap was positioned at the inlet of each collimator and the thermal flux was measured at the outlet. Figures 3 and 4 show the flux-to-source ratios obtained for the 7.5 and 15-inch collimators, respectively, for a variable vertical source-to-collimator distance. For the 7.5-inch collimator, the peak flux per source neutron of 5.6×10^{-6} occurs at a source-collimator separation of 0.5 inch, while the ratio for the 15-inch collimator is relatively constant at 2.7×10^{-6} n/cm^2/source n.

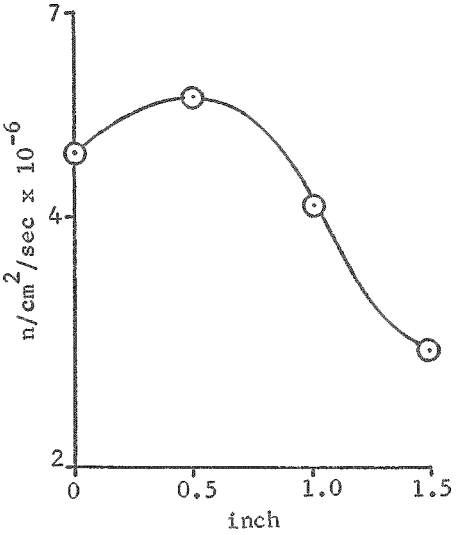

FIG. 3 COLLIMATOR-OUTLET FLUX PER SOURCE NEUTRON AS A FUNCTION OF VERTICAL SOURCE-TO-COLLIMATOR DISTANCE FOR A 7.5-INCH COLLIMATOR WITH A 2.0-INCH AIR GAP

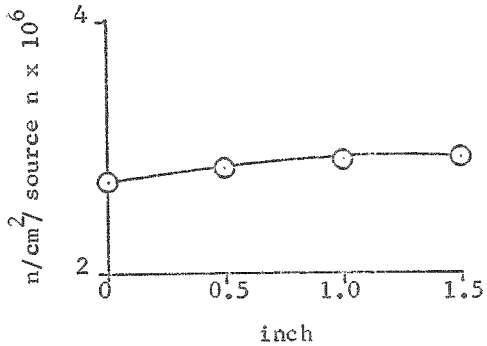

FIG. 4 COLLIMATOR-OUTLET FLUX PER SOURCE NEUTRON AS A FUNCTION OF VERTICAL SOURCE-TO-COLLIMATOR DISTANCE FOR A 15-INCH COLLIMATOR WITH A 2.0-INCH AIR GAP

Figures 5 and 6 show the flux per source neutron for a variable horizontal source-to-collimator distance for the 7.5 and 15-inch collimators, respectively. The flux per source neutron is 5.8 x 10^{-6} for the 7.5-inch collimator, while the peak is only 3.2 x 10^{-6} for the 15-inch collimator.

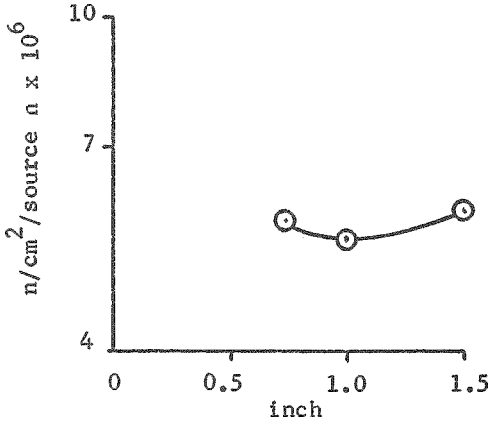

FIG. 5 COLLIMATOR-OUTLET FLUX PER SOURCE NEUTRON AS A FUNCTION OF HORIZONTAL SOURCE-TO-COLLIMATOR DISTANCE FOR A 7.5-INCH COLLIMATOR WITH A 2.0-INCH AIR GAP

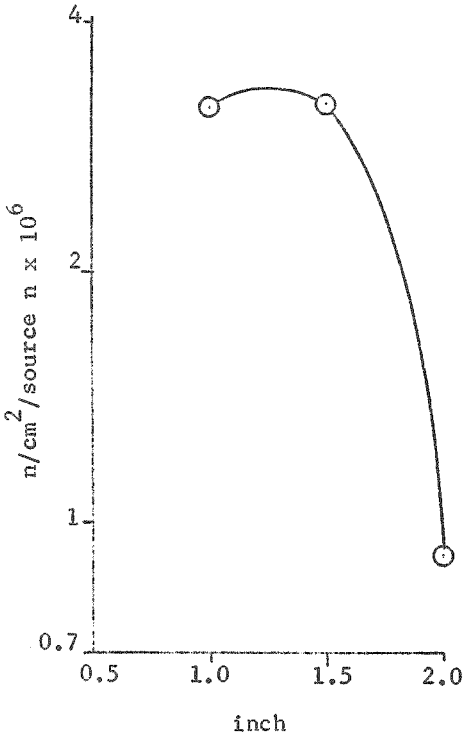

FIG. 6 COLLIMATOR-OUTLET FLUX PER SOURCE NEUTRON AS A FUNCTION OF HORIZONTAL SOURCE-TO-COLLIMATOR DISTANCE FOR A 15-INCH COLLIMATOR WITH A 2.0-INCH AIR GAP

Variable Air Gap. The second set of experiments to determine the optimum source-collimator geometry were made by changing the length of the air gap and keeping the source-to-collimator and/or air-gap distance constant. Figures 7 and 8 show the results for the 7.5- and 15-inch collimators, respectively. In both cases, the peak flux per source neutron with the source in the vertical position occurs with the 1-inch air gap. The maximum is 5.5 x 10^{-6} n/cm^2/source n for the 7.5-inch collimator and only 2.9 x 10^{-6} n/cm^2/source n for the 15-inch collimator.

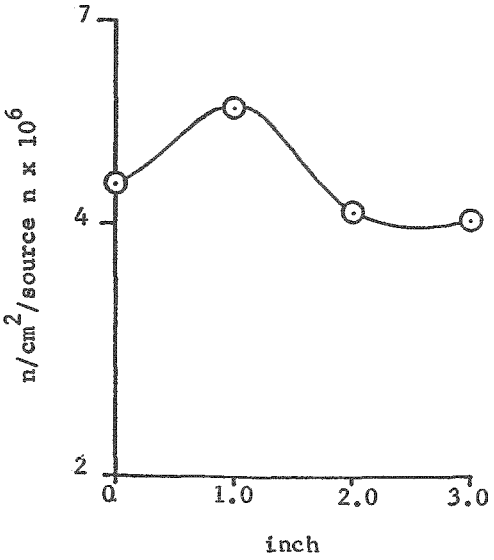

FIG. 7 COLLIMATOR-OUTLET FLUX PER SOURCE NEUTRON AS A FUNCTION OF AIR-GAP LENGTH FOR A 1-INCH VERTICAL SOURCE POSITION USING A 7.5-INCH COLLIMATOR

Figures 9 and 10 show the results for 7.5- and 15-inch collimators, respectively, for a variable air gap with the source held in a tangential position. The peak flux-to-source neutron ratio for the 7.5-inch collimator of 9.2 x 10^{-6} n/cm^2/source n occurs with no air gap, while the peak of 3.1 x 10^{-6} n/cm^2/source n occurs with the 2-inch air gap for the 15-inch collimator.

GAMMA DOSE RATE

Another important parameter for a neutron-radiography application is the gamma contamination in the neutron beam. The gamma dose rate was measured using ^{7}LiF thermoluminescent dosimeters. From these data and the previously determined neutron-flux data, the thermal neutron-to-gamma ratio in the beam for the various geometries can be determined. These data are presented in Figures 11 through 18. The best measured neutron-to-gamma ratio is 1.8 x 10^4 n/cm^2/mr for the 7.5-inch collimator with the source 1 inch vertically below a 2-inch air gap. The results for the 15-inch collimator are essentially the same, although the peak is only 1.2 x 10^4 n/cm^2/mr for the source 1 inch vertically below the 2-inch air gap.

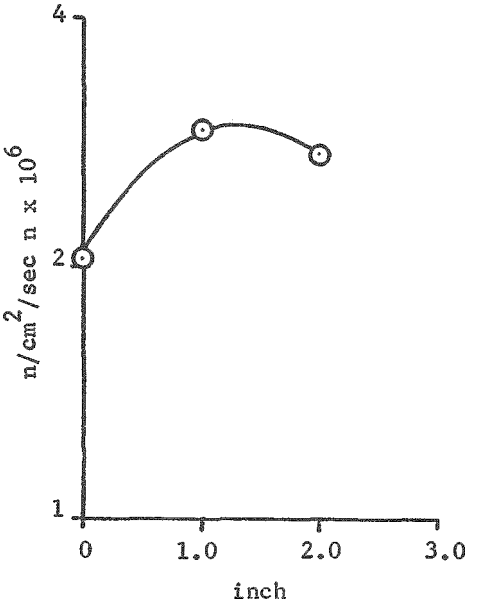

FIG. 8 COLLIMATOR-OUTLET FLUX PER SOURCE NEUTRON AS A FUNCTION OF AIR-GAP LENGTH FOR A 1-INCH VERTICAL SOURCE POSITION USING A 15-INCH COLLIMATOR

ANALYSIS

The peak thermal flux in an infinite water moderator with this ^{252}Cf source was found to be 2.5 x 10^7 n/cm^2/sec.

The introduction of the 7.5-inch collimator into the moderator region at this peak flux gave a collimator inlet flux of 9.4 x 10^6 n/cm^2/sec, or a reduction of 40 percent.

The outlet flux for this source configuration was only 1.1 x 10^4 n/cm^2/sec, which is a decrease of 2 orders of magnitude in the collimator.

EFFECT OF COLLIMATOR LENGTH

The two collimators used in these studies had 15:1 length-to-diameter ratios

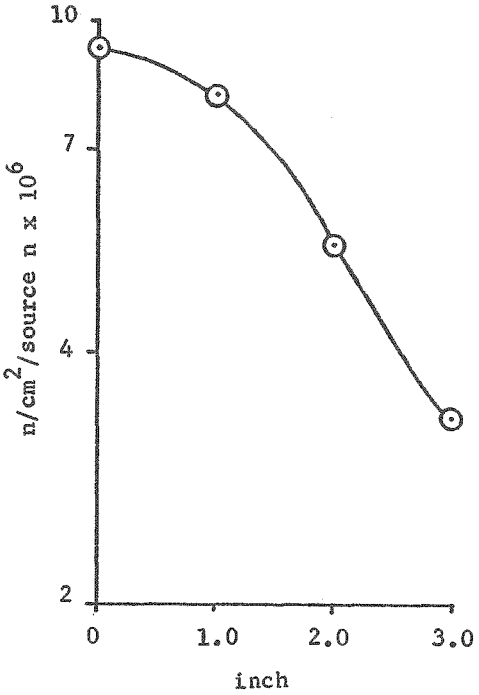

FIG. 9 COLLIMATOR-OUTLET FLUX PER SOURCE NEUTRON AS A FUNCTION OF AIR-GAP LENGTH FOR A 1-INCH HORIZONTAL SOURCE POSITION USING A 7.5-INCH COLLIMATOR

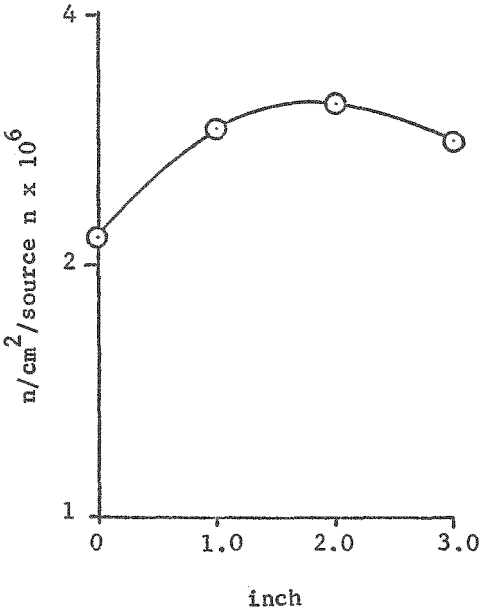

FIG. 10 COLLIMATOR-OUTLET FLUX PER SOURCE NEUTRON AS A FUNCTION OF AIR-GAP LENGTH FOR A 1-INCH HORIZONTAL SOURCE POSITION USING A 15-INCH COLLIMATOR

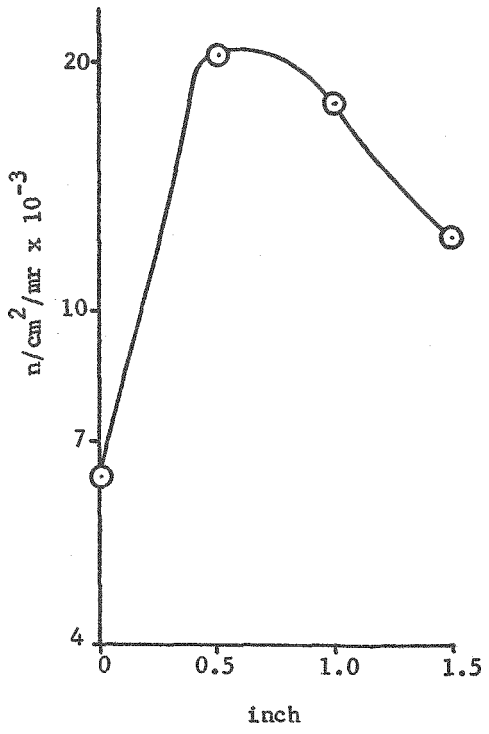

FIG. 11 COLLIMATOR-OUTLET NEUTRON-TO-GAMMA RATIO AS A FUNCTION OF VERTICAL SOURCE-TO-COLLIMATOR DISTANCE FOR A 7.5-INCH COLLIMATOR WITH A 2.0-INCH AIR GAP

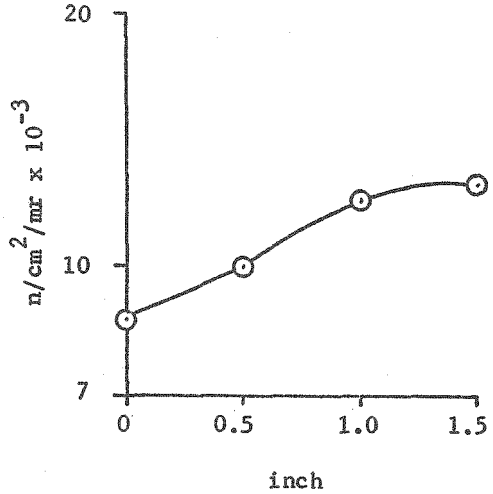

FIG. 12 COLLIMATOR-OUTLET NEUTRON-TO-GAMMA RATIO AS A FUNCTION OF VERTICAL COLLIMATOR-TO-SOURCE DISTANCE FOR A 15-INCH COLLIMATOR WITH A 2.0-INCH AIR GAP

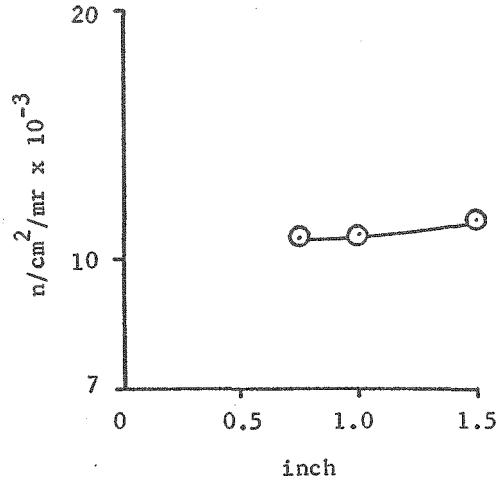

FIG. 13 COLLIMATOR-OUTLET NEUTRON-TO-GAMMA RATIO AS A FUNCTION OF HORIZONTAL COLLIMATOR-TO-SOURCE DISTANCE FOR A 7.5-INCH COLLIMATOR WITH A 2.0-INCH AIR GAP

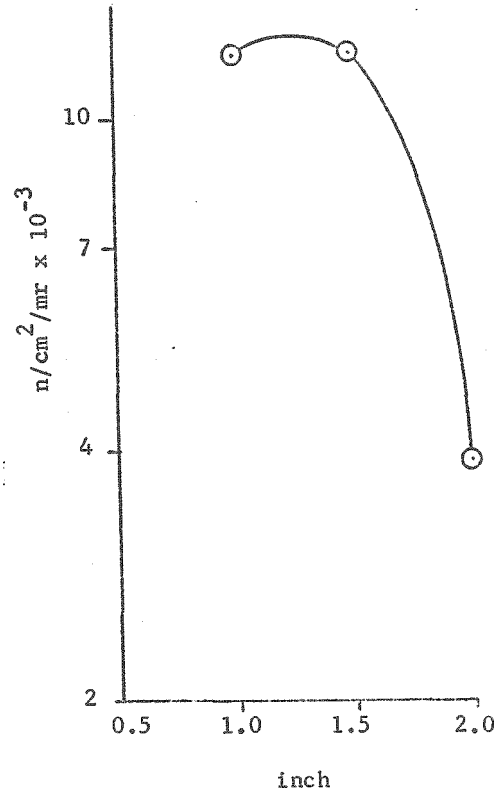

FIG. 14 COLLIMATOR-OUTLET NEUTRON-TO-GAMMA RATIO AS A FUNCTION OF HORIZONTAL COLLIMATOR-TO-SOURCE DISTANCE FOR A 15-INCH COLLIMATOR WITH A 2.0-INCH AIR GAP

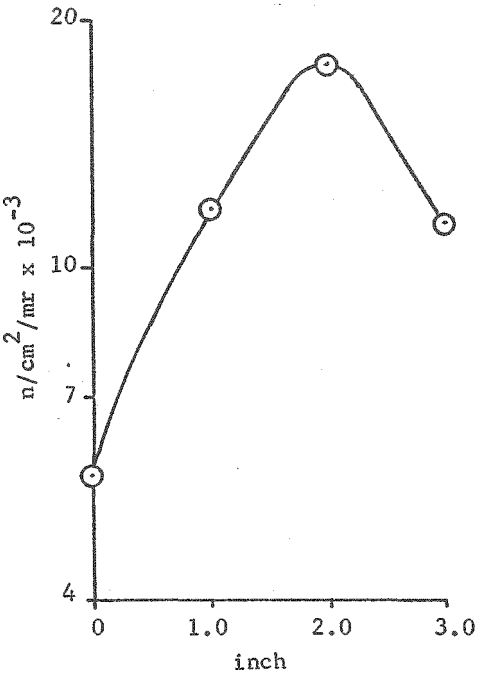

FIG. 15 COLLIMATOR-OUTLET NEUTRON-TO-GAMMA RATIO AS A FUNCTION OF AIR-GAP LENGTH FOR A 1-INCH VERTICAL SOURCE POSITION USING A 7.5-INCH COLLIMATOR

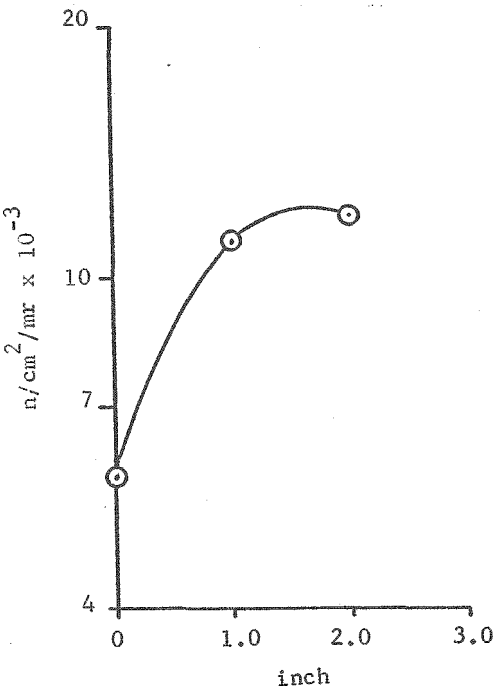

FIG. 16 COLLIMATOR-OUTLET NEUTRON-TO-GAMMA RATIO AS A FUNCTION OF AIR-GAP LENGTH FOR A 1-INCH VERTICAL SOURCE POSITION USING A 15-INCH COLLIMATOR

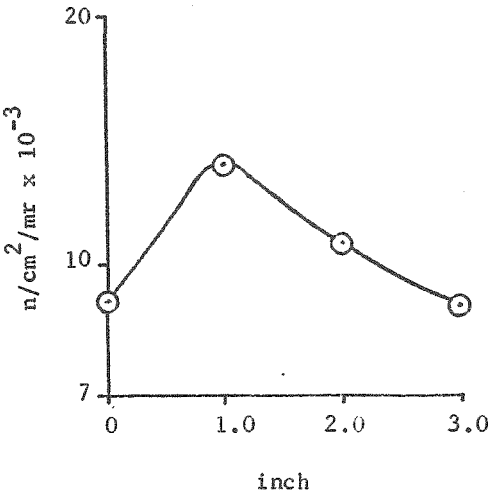

FIG. 17 COLLIMATOR-OUTLET NEUTRON-TO-GAMMA RATIO AS A FUNCTION OF AIR-GAP LENGTH FOR A 1-INCH HORIZONTAL SOURCE POSITION USING A 7.5-INCH COLLIMATOR

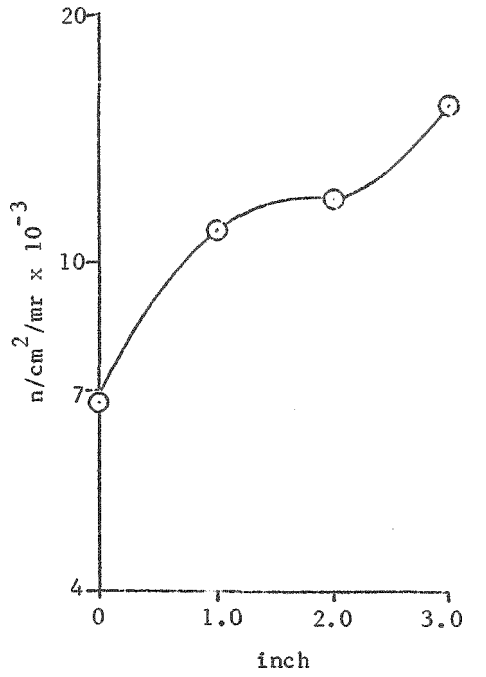

FIG. 18 COLLIMATOR-OUTLET NEUTRON-TO-GAMMA RATIO AS A FUNCTION OF AIR-GAP LENGTH FOR A 1-INCH HORIZONTAL SOURCE POSITION USING A 15-INCH COLLIMATOR

with two lengths, one 7.5 inches and the other 15 inches. It is interesting to note (see Figures 11 through 18) that the neutron-to-gamma ratio is essentially independent of collimator length, for a given test configuration, i.e., a constant air gap and source-to-collimator distance. This indicates that an increased length (substitution of the 15-inch unit for the 7.5-inch one) caused the same decrease in gamma dose rate as it did in neutron flux.

The decrease in the ratio of flux per source neutron, in changing from the 7.5-inch collimator to the 15-inch collimator, was 25 percent.

One effect of increasing collimator length, which is apparent in a radiograph but not from the flux or gamma dose considerations, is the decrease in beam divergence over a specified area. This effect will be seen as the image recorder is moved away from the object being radiographed. Therefore, the purpose of the radiograph may dictate the collimator length rather than the neutron-to-gamma ratio and the available neutron flux.

EFFECT OF AIR-GAP LENGTH

Generally, the effect of the addition of the air gap was an increase in the ratio of flux per source neutron. This result confirms the effect of the cadmium liner perturbation on the neutron flux around the source.

The neutron-to-gamma ratio also increased in every case of additional air-gap length. This increase was due both to an increase in the neutron flux owing to perturbation removal and a decrease in the gamma dose rate owing to increased distance between the collimator and the source.

EFFECT OF SOURCE POSITION

Moving the source either vertically or horizontally with respect to the collimator inlet revealed an increase in the ratio of flux per source neutron owing to the presence of the reflector peak near the neutron source. It can also be seen from the decreasing neutron-to-gamma ratio that the thermal-neutron flux decreases more rapidly in the water surrounding the source than does the gamma dose.

In general, a higher neutron flux and a better neutron-to-gamma ratio is obtained with the source in the horizontal position.

CONCLUSION

The optimum collimator-source geometry selected from these experiments, when considering neutron-to-gamma ratio as a limiting criteria, is the 7.5-inch collimator with a 2-inch air gap and the source located 0.5 inch vertically below the collimator. If a 15-inch collimator is required, because of beam divergence considerations, the optimum geometry would call for the 2-inch air gap and the source 1 inch from the collimator either vertically or horizontally.

1. Californium-252 Progress, 2, 20 (1970)

NEUTRON RADIOGRAPHY USING CALIFORNIUM-252 FOR AIRCRAFT NDT APPLICATIONS

Warren E. Dungan

General Dynamics
Convair Aerospace Division
Fort Worth Operation
Fort Worth, Texas

Neutron radiography research using a 1 milligram californium-252 isotope in a water-moderated tank facility is described. The research was conducted to determine the suitability of using californium-252 for the radiographic inspection of a variety of aerospace materials and components. Conventional direct-exposure techniques using X-ray film with gadolinium metal conversion screens in spring-loaded cassettes were used to obtain several 5 in. by 7 in. neutron radiographs of several items. Image quality indicators, defective pyrotechnic devices, rubber O-rings in sealed metallic valves, boron-fiber laminates, water droplets and sealants in honeycomb structure, and adhesive bonded metallic lap-shear specimens were inspected with varying degrees of success using a 5-in. square beam of thermal neutrons. Detailed measurements of field distributions were made to arrive at suitable shield configurations and beam geometries. Estimates of facilities and shipping costs are given. Thirteen illustrations include sketches of the shipping container and neutron radiography facility, plots of thermal-neutron flux profiles, exposure times for film, film-density grids, and several positive prints of neutron radiographs. It is concluded from the results presented that californium-252 is suitable for the design and fabrication of an inexpensive, cheaply operated facility for exploratory nondestructive test applications of many products using thermal-neutron radiography.

INTRODUCTION

Neutron radiography has advanced within the past decade from a mere laboratory curiosity to an accepted method of nondestructive testing. The need for expensive equipment, such as reactors requiring highly trained operators, to provide the necessary intense neutron sources has prevented more widespread use of the technique on routine NDT problems. The recent availability of californium-252 with its prolific output of neutrons has suggested that this source may have many uses, one of which is neutron radiography.

This report is part of a more extensive document (1) describing the research in neutron radiography performed at the Fort Worth operation of General Dynamics' Convair Aerospace Division over the past year using a nominal 1 milligram source of ^{252}Cf. The research was performed as part of the market evaluation program for ^{252}Cf being supported by the AEC to aid in setting future production levels. This report includes a description of the source and shipping procedures. The preliminary measurements performed to determine shield requirements and neutron facility conditions are outlined in some detail.

Several neutron radiographs obtained with a simple water-moderated facility are shown as positive prints. These results support the conclusion reached during the study, i.e., a useful exploratory radiography device may be fabricated and operated cheaply using ^{252}Cf to provide acceptable neutron radiographs of a variety of aerospace materials.

CALIFORNIUM-252 SOURCE DESCRIPTION AND SHIPPING PROCEDURES

Source SR-CF-106, supplied on loan to General Dynamics by the AEC, contained a total of 916.9 micrograms as calculated by the Savannah River Laboratory on 19 December 1969. The effective half-life of 2.646 years has reduced this activity about 30 percent within the past year so that the initial 2.23×10^9 neutrons per second emission rate is less than 1.7×10^9 neutrons per second at this writing. The emitted neutrons have the fission distribution in energy with an average at about 2.35 MeV. The gamma emission rate is about 1.3×10^{10} photons per second per milligram. The source is contained in a double stainless-steel capsule with external dimensions 1.3 in. long by 0.37 in. diam; a threaded cap at one end accommodates a handling tool.

The information contained in this article was developed during the course of work under Contract AT(38-1)-506 with the U. S. Atomic Energy Commission using californium-252 source SR-CF-106.

The source was shipped to Fort Worth from Savannah River Laboratories in a steel-shelled cylindrical cask filled with paraffin and polyethylene (Fig. 1). A centrally-located 2 3/4 in. diam by 3 1/4 in. long lead cylinder containing the source served to reduce the prompt gamma rate at the exterior surface. The total surface dose rate of the cask with source was about 600 millirem per hour. Shipment was made in a van via sole use of vehicle at a cost of about $520. The cost of the cask for material, fabrication, and checkout is estimated at $870.

PRELIMINARY SURVEY MEASUREMENTS

After receipt of the source at General Dynamics, several preliminary measurements were made to verify integrity of the source, to compare shielding calculations with experimental data, and to provide design data for the neutron radiography facility. Several dose measurements made with Health Physics survey-type instrumentation verified the 600 millirem per hour total surface dose rate for the shipping cask. A number of gamma measurements made with thermoluminescent detectors (TLD from Edgerton, Germeshausen and Grier - EGG TL-23) showed the dose to be approximately in inverse proportion with distance to about 6 ft from cask. Replacing the lead insert in the cask with polyethylene increased the leakage rate about 50 percent.

A series of contamination tests was made to verify the integrity of the source against leakage of poisonous products. The source was removed from the cask, using hot cell facilities, and was given a series of washings with alcohol in an ultrasonic cleaner. The alcohol was evaporated from planchets which were subsequently counted for beta, gamma, or alpha activity. Due to the absence of any significant counting level it was concluded the sources were not leaking.

Several neutron-flux measurements were made with the source following the attachment of a four-foot perforated aluminum handling tube to the threaded cap. Neutron-detecting foils including 10-mil dysprosium, 20-mil indium, 30-mil magnesium, 30-mil aluminum, and 250-mil sulfur were mounted on the periphery of a motor-driven disk. The source was mounted 10 cm from the disk in air inside the hot cell. The detectors were exposed for over two hours, and the foils subsequently were counted with the General Dynamics foil-counting system (2). The neutron-flux results calculated from the foil activations are given in Table I.

Before attempting to assemble a system for neutron radiography several nuclear measurements were made to estimate shielding requirements and to select a suitable neutron radiography collimator configuration. The source was mounted vertically in an aluminum guide tube which was centrally located in a 36-in. square, stainless steel, water-filled tank. Neutron- and gamma-dose measurements were made with various alternating thicknesses of lead and 6-percent borated polyethylene shielding. Two measurements were made with the source placed adjacent to the inside tank wall to provide supplementary data. Instrumentation included a neutron rem counter, a fast-neutron detector (FND) filled with 90 percent argon - 10 percent methane, a Geiger-Muller counter, and Ludlum scaler-ratemeters. The removable BF_3 detector of the rem counter was used for some relative measurements. The instruments were calibrated with a 10-curie Pu-Be source, ^{60}Co, and ^{137}Cs. Results of the neutron and gamma dose-rate measurements are given in Table II.

Several gamma spectra obtained with an Ortec Model 8001-10 Ge(Li) crystal system and a Hewlett-Packard 1024-channel analyzer system showed a smooth spectrum decreasing exponentially with energy for the source mounted in air. Mounting the source centrally in the water tank created two capture peaks at 1.2 and 2.2 MeV without shielding. A third peak at 510 keV (annihilation energy) became apparent with added lead and borated polyethylene shielding.

The thermal-neutron environment in the water surrounding the source was mapped to a distance of 30 cm in increments of 2 cm using bare and 20-mil cadmium-shielded foils of indium, gold, dysprosium, and silver-manganese. Two 16-hour exposures of the foil sets were made, and the foils were counted with General Dynamics system. The data were reduced, and fluxes were calculated using a program with a Hewlett-Packard 9100 B desk calculator; the results are plotted in Figure 2.

NEUTRON RADIOGRAPHY FACILITY CHARACTERISTICS

The neutron radiography facility sketched in Figure 3 includes the previously

described 36-in. stainless steel tank filled to a depth of 36 in. with demineralized water. The tank exterior is shielded with 2 in. of lead and 3 in. of 6-percent borated polyethylene. This shielding is sufficient to reduce the total dose rate at the exterior surface to about 2 millirem per hour with the source centrally located in the tank. Removable aluminum sheets cover the tank top to prevent contamination by dirt and evaporation of water.

A 20-in.-long, closed aperture, aluminum, beam tube shielded externally with 1/4 in. lead and 1/4 in. boral is suspended vertically from two steel angle supports at the tank top. The tube is divergent with a 1-in. square input aperture and a 5-in. square exit port. The lead and boral extend to within 3 in. of the collimator entrance to permit an air gap at the input. The source tube is within the aluminum guide tube which is mounted in tangential geometry 2 in. from the collimator as defined by Figure 3. An adjustable collar at the source tube top permits locating the source vertically at a desired position. A conservative estimate of the cost for materials and fabrication of the facility is $5000.

The direct method of neutron radiography, in which the sample and cassette containing the film and converter screen are exposed to the beam simultaneously, was used for approximately 100 radiographs taken over the past year with the source. Three exposures using 20-mil indium foil for the transfer screen were unsuccessfully attempted by the indirect method. This technique consists in exposing a metallic screen together with the sample and transferring the neutron-activated metal to film following exposure. The procedure records on the film the activation profile which is proportional to the transparency of the sample. The indirect technique is required in the presence of a high, film-fogging gamma background such as encountered in inspecting radioactive material. The intensity of the 918 microgram source was not sufficient for the indirect technique using an indium screen to be useful; other more sensitive screens such as dysprosium or europium were not investigated.

Four types of x-ray film were used and are in order of increasing speed - Kodak* AA, T, M, and R. Gadolinium conversion screen 0.5 - 1.0 mils in thickness was used in 5 in. by 7 in. spring-loaded cassettes with magnesium faces. The faster films are more grainy than the slower films, and for fine resolution and sharpness the relatively slow type M or even the slower type R are required. Exposure periods varied from a few hours to two or three days depending on film type, opacity of object, and intensity of beam. The latter was held nearly constant during most of the exposures with the source located at the 2 in. position adjacent to the inlet end of the beam-tube collimator as shown in Figure 3. This standard position optimized the thermal-neutron flux output from the source and provided adequate beam collimation with little gamma interference at the beam exit. This information was determined from a series of nuclear measurements at the exit port with the source position varied vertically.

A few nuclear measurements were made with 1/2 in. bismuth inserts in the beam to increase the neutron-gamma ratio. Although the gamma component of the beam was reduced about 80 percent, the thermal-neutron flux was also reduced about 20 percent and no definite improvement in neutron radiographic quality was apparent.

During the course of the investigation, extensive measurements of the nuclear beam characteristics were made with gold and dysprosium foils to obtain thermal-neutron data and thermoluminescent (TLD) dosimeters for gamma-dose data. The TLD were enclosed in sintered boron carbide shields to reduce their neutron sensitivity to a negligible amount. The thermal-neutron flux at the beam exit averages about 1.0×10^4 neutrons cm^{-2} sec^{-1} and the gamma-dose rate is 127 mR hr^{-1} resulting in a neutron-to-gamma ratio of 2.9×10^5 neutrons cm^{-2} mR^{-1} suitable for quality neutron radiography.

The uniformity of the neutron field in the beam tube was determined by exposing a sheet each of type T and AA film to obtain two radiographs with no samples in the exit beam. Subsequent density measurements over the film area were made with a Photovolt Corporation Model 52 densitometer having a 0.175 in. diam light aperture. Figure 4 is a sketch of the grid system used on the T-type film with densities identified. The horizontal and vertical precision is given, and the minimum and maximum values are noted. The spread and precision on the AA-type film was similar to the results for the T-type shown. A plot of film density versus exposure time for a series of exposed T films is shown in Figure 5.

*Trademark of Eastman Kodak Co., Rochester, N.Y.

APPLICATIONS OF NEUTRON RADIOGRAPHY

The following items were successfully neutron radiographed with the 918 microgram ^{252}Cf source facility.

1. General Dynamics and Argonne National Laboratory image quality indicators
2. Defective shielded, mild detonating cord tips
3. Elevon rate-selector valve from B-58 aircraft
4. Boron-fiber epoxy laminates
5. Aluminum honeycomb containing water droplets
6. Leading-edge section of the F-111 aircraft horizontal stabilizer
7. Adhesive-bonded aluminum lap-shear specimens

An image quality indicator (IQI) of the type used consists of several materials with different neutron and gamma attenuation properties included with each radiograph as a small device to check unexpected variations in beam characteristics for different exposures. The General Dynamics' IQI is shown in Figure 6, while the Argonne Lab IQI is shown in Figure 7. Figures 8 through 13 are positive prints of neutron radiographs of the items noted above. The defects, O-rings, boron fibers, water droplets, and adhesive bonds are noted in the illustrations.

CONCLUSIONS

The research reported in this document leads to the following conclusions.

- Californium-252 is a useful neutron emitting isotope that can be utilized for exploratory studies in neutron radiography. The isotope properly encapsulated is easily adapted to a simple, safe, and inexpensive water-tank facility with a nominal amount of shielding.
- Quantities of ^{252}Cf approximating a milligram provide a usable neutron beam for laboratory-type, off-line neutron radiography utilizing conventional direct exposure techniques with divergent collimators.
- Exposure areas approximating 36 $in.^2$ requiring times on the order of a few hours per exposure are practical for inspecting for defects in moderately opaque materials. Exposure times may be reduced by using sources in excess of 1 milligram or more efficient conversion methods than film.
- Fine resolution and excellent contrast require relatively long exposures of several hours with fine-grained film.
- Neutron radiographs of a variety of objects common to the aerospace industry are readily made using ^{252}Cf.
- The achievement of portability and economy in a neutron radiography device is more likely realized by using ^{252}Cf than by any other known method.

REFERENCES

1. W. E. Dungan. Neutron Radiography Research Using Californium-252 for Aerospace Nondestructive Testing Applications. General Dynamics' Convair Aerospace Division, Fort Worth Operation Report ERR-1079 (31 December 1970).
2. J. Romanko and W. E. Dungan. "Specification and Measurement of Reactor Neutron Spectra." Neutron Dosimetry, Vol. 1, IAEA, Vienna (1963).
3. J. P. Nichols. "Design Data for ^{252}Cf Neutron Source Experiments." Nuclear Applications, Vol. 4 (June 1968).

TABLE I

Neutron Flux in Air at 10 cm from 918-microgram ^{252}Cf Source

Detector	Thermal Flux, n/(cm^2-sec)	Fast Flux, n/(cm^2-sec)
Bare Dy/Cd-covered Dy foil	1.52×10^4	
Bare In/Cd-covered In foil		1.2×10^6 above 0.85 MeV
Sulfur pellets		4.25×10^5 above 2.9 MeV
Magnesium foil		4.5×10^4 above 7.5 MeV
Aluminum foil		2.4×10^4 above 8.1 MeV
Calculated from known source strength		3.9×10^5

TABLE II

Neutron and Gamma Dose Rates from 918-microgram ^{252}Cf Source in Water-Filled Tank

Source Location	Shielding	Detector Distance from Tank Wall, in.	Neutron Dose Rate, mrem/hr Rem Counter[a]	Neutron Dose Rate, mrem/hr FND[b]	Gamma Dose Rate, mrem/hr Geiger-Muller Counter[c]	Cadmium Ratio[d]
Middle of tank	None	24	6.7	5.4	23.2	35.0
Middle of tank	▨	24	4.6	5.3	6.8	33.3
Middle of tank	▨▤	24	3.5	4.5	6.3	3.9
Middle of tank	▨▤▨	24	3.4	2.2	2.2	4.8
Middle of tank	▨▤▨▤	24	2.2	1.7	1.9	4.8
Inside surface of wall	▨▤	39.4	3.7	1.3	-	-

▨ 1 in. lead ▤ 1 in. borated polyethylene

[a] Modified Andersson and Braun counter (I. O. Andersson and J. Braun. "A Neutron Rem Counter with Uniform Sensitivity from 0.025 ev to 10 Mev." Neutron Dosimetry, Vol. II, IAEA Vienna (1963).)

[b] Radiation Counter Laboratories, Skokie, Illinois, fast neutron detector

[c] Electronic Optical Nuclear Products Corp., Brooklyn, New York, Model 5112

[d] (Bare BF_3 counts per min)/(Cd-covered BF_3 counts per min)

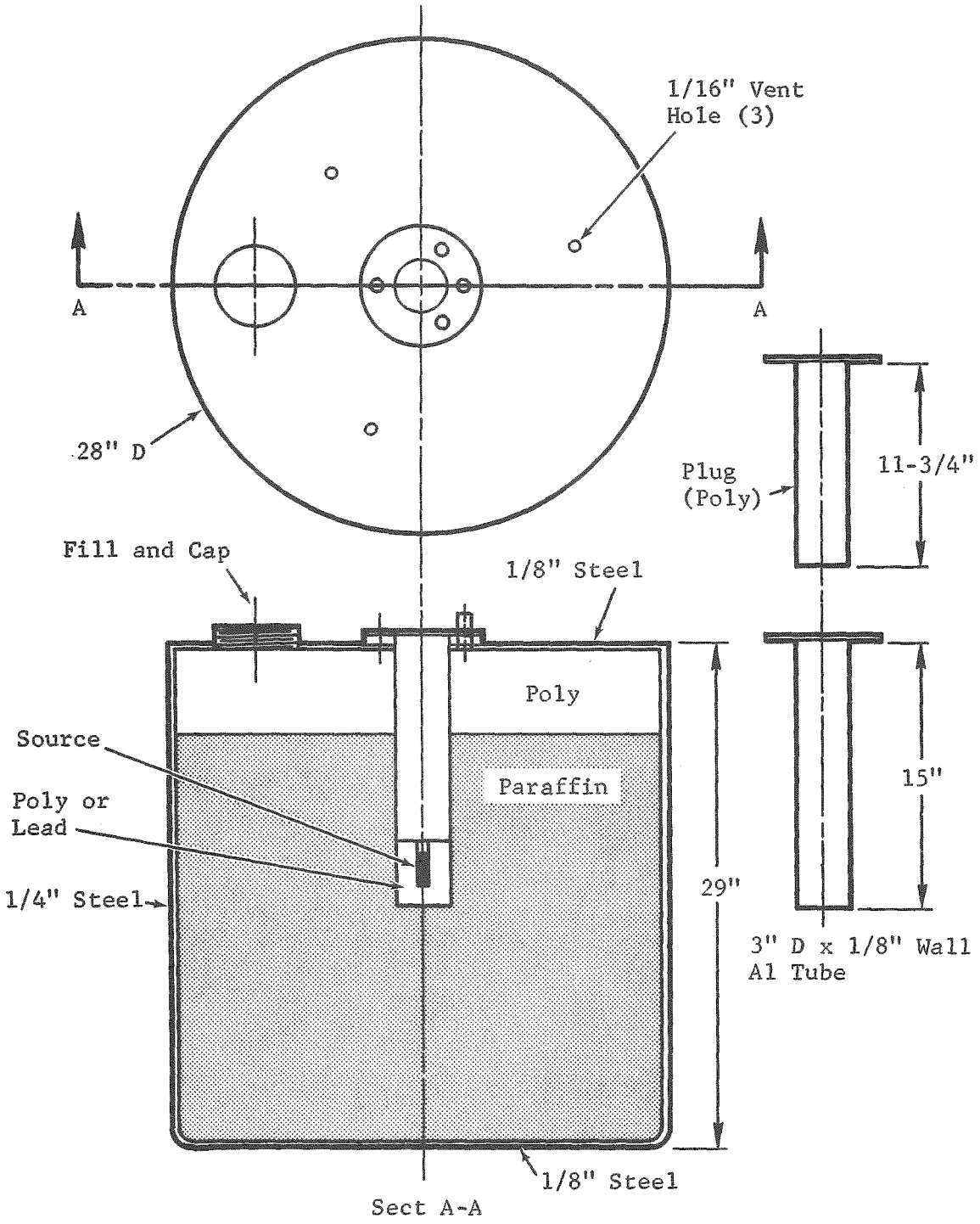

Figure 1 Neutron Source Containment Vessel

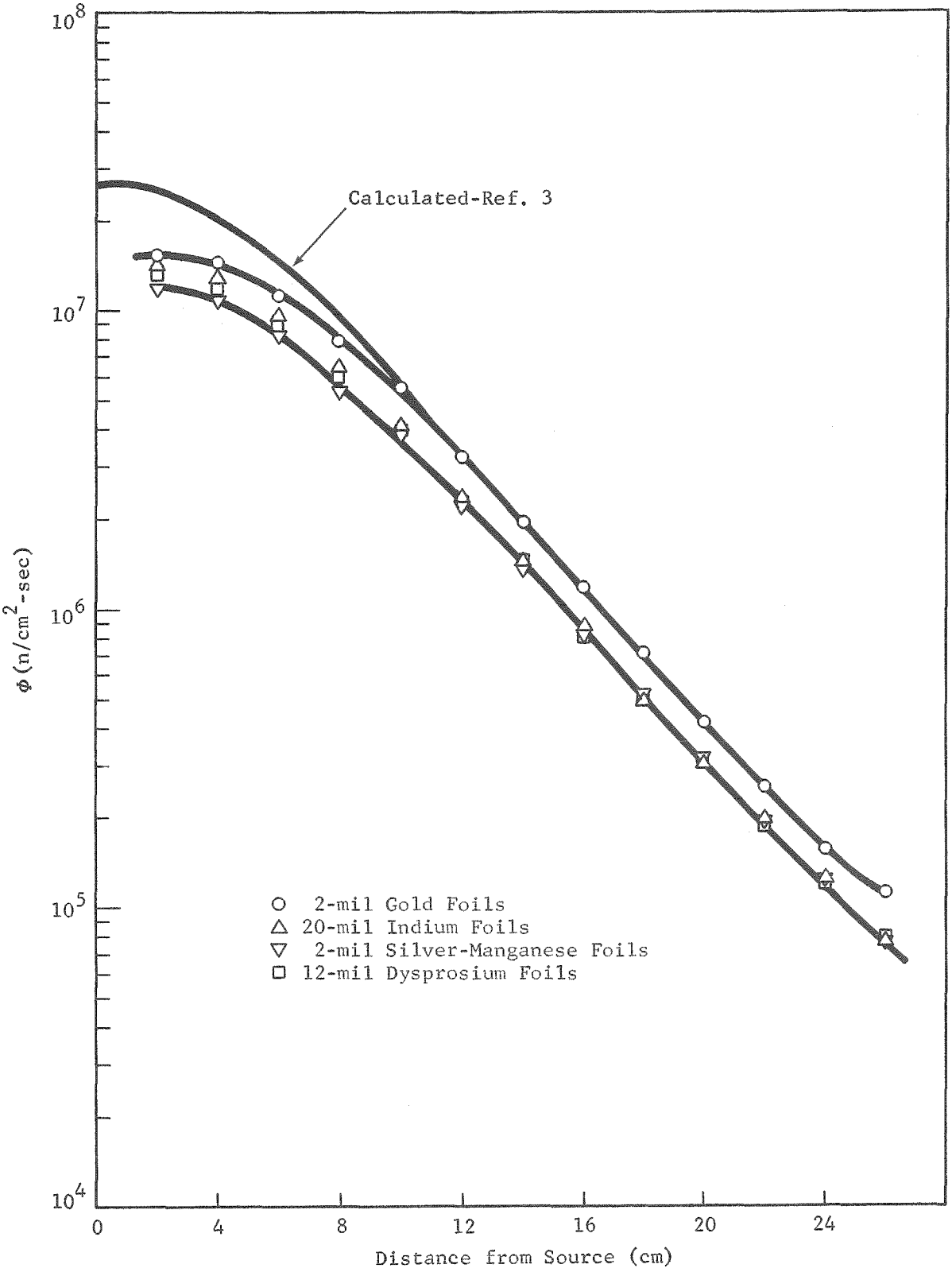

Figure 2 Thermal-Flux Distribution in Water from 918μg Cf-252

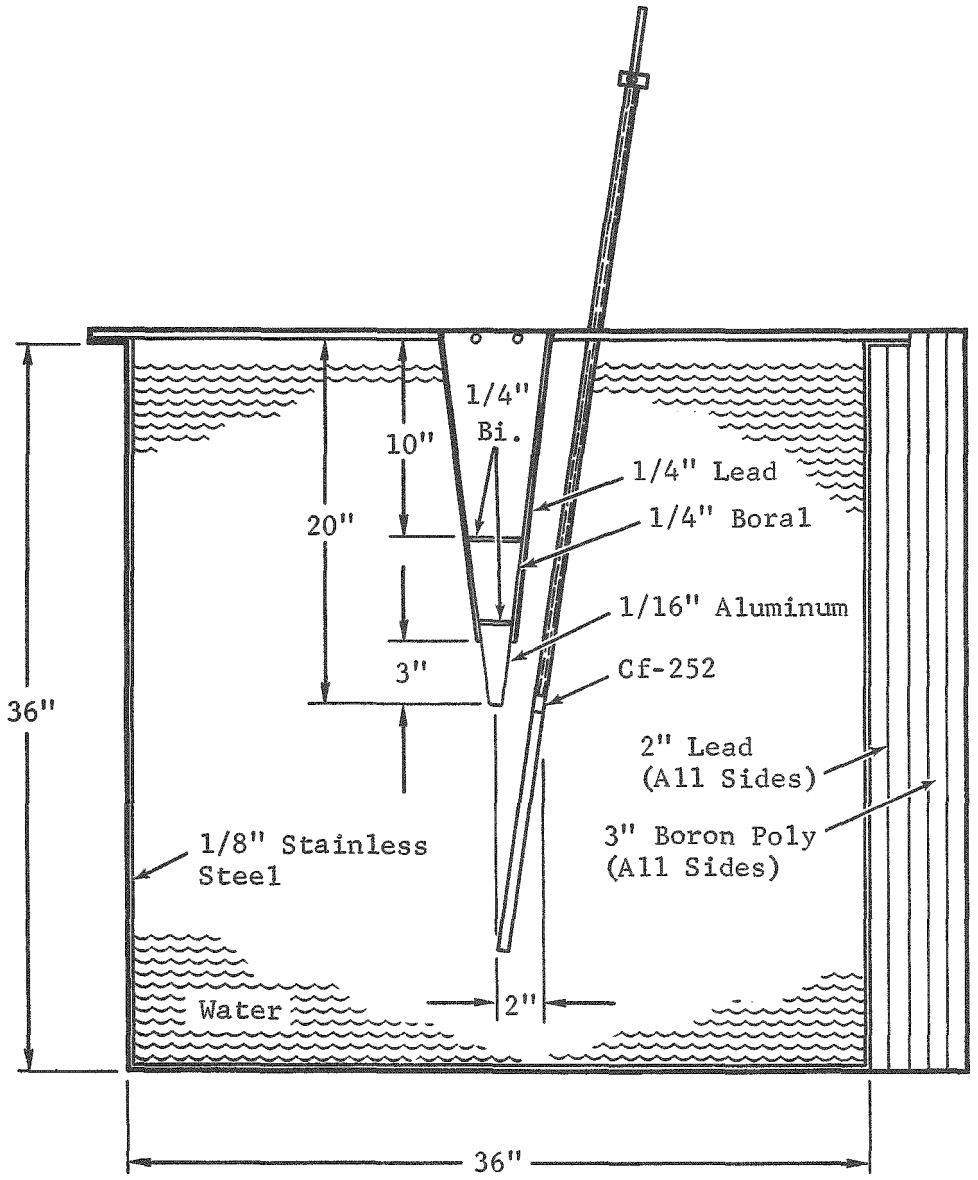

Figure 3 Neutron Radiography Facility - 918μg Cf-252

Mean $\bar{\rho}$ = 2.19 σ (%) = 2.21	2.15	2.19	2.23	2.24	2.24	2.23	2.20	2.16	2.10 (Min)
Mean $\bar{\rho}$ = 2.26 σ (%) = 2.66	2.22	2.28	2.31	2.32	2.31	2.31	2.27	2.22	2.14
Mean $\bar{\rho}$ = 2.30 σ (%) = 2.53	2.26	2.32	2.35	2.35	2.34	2.35	2.30	2.26	2.18
Mean $\bar{\rho}$ = 2.31 σ (%) = 2.59	2.28	2.33	2.35	2.37	2.36	2.34	2.33	2.27	2.18
Mean $\bar{\rho}$ = 2.36 σ (%) = 2.59	2.34	2.37	2.41	2.42	2.41	2.41	2.37	2.32	2.23
Mean $\bar{\rho}$ = 2.39 σ (%) = 3.07	2.37	2.41	2.44	2.45 (Max)	2.45 (Max)	2.43	2.41	2.32	2.23
Mean $\bar{\rho}$ = 2.39 σ (%) = 3.01	2.38	2.42	2.45	2.45	2.44	2.43	2.40	2.33	2.23

Mean $\bar{\rho}$ = 2.317
N = 63
σ (%) = 3.89
Max Variation:
2.45
2.10 = 1.17

Mean $\bar{\rho}$:	2.28	2.33	2.36	2.37	2.36	2.35	2.32	2.26	2.18
σ (%):	3.68	3.43	3.30	3.32	3.19	3.11	3.24	2.75	2.32

T-Film-16 Hour Exposure - No Bi

Figure 4 Density Distribution of Neutron Radiography Beam

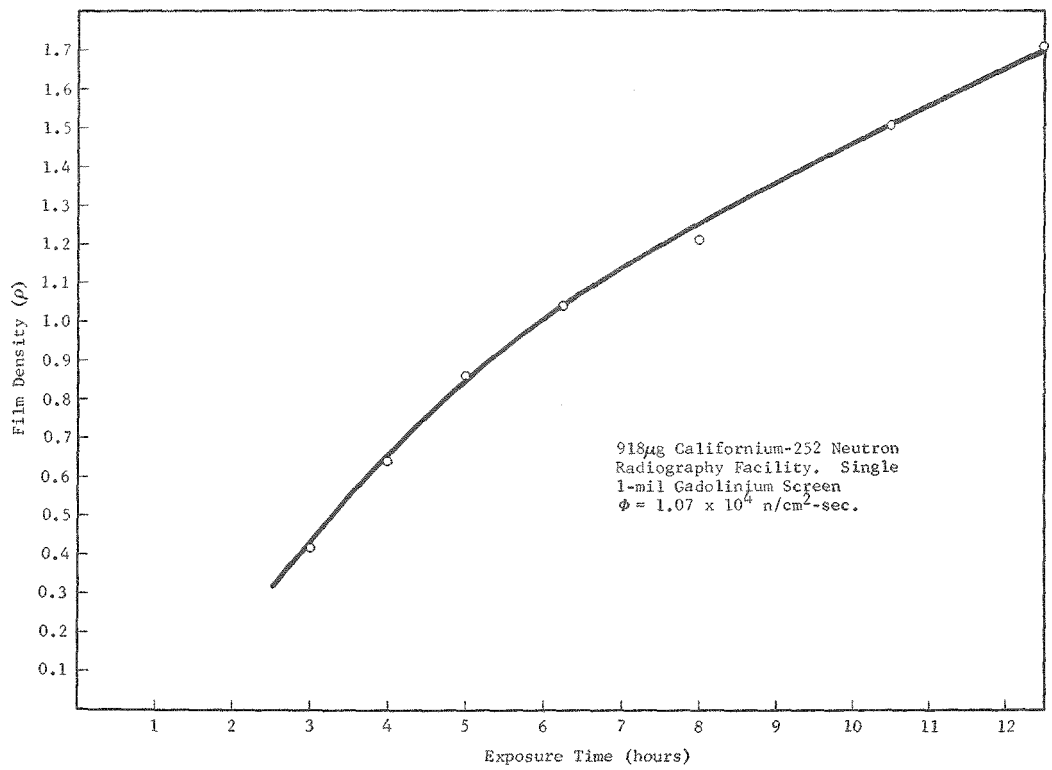

Figure 5 Kodak Type-T Film Density versus Exposure Time

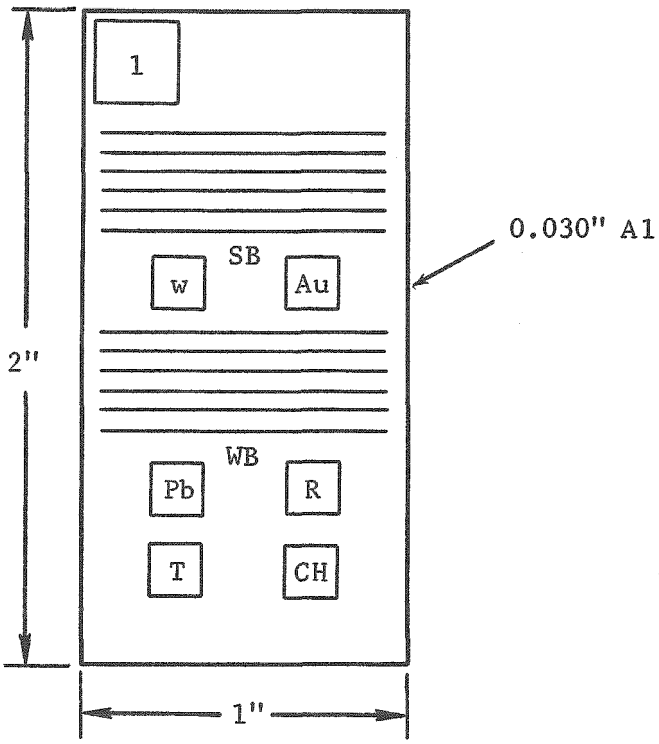

Code	Description
1	20 mil Cadmium Numeral
W	2 mil Tungsten
AU	2 mil Gold
Pb	30 mil Lead
R	30 mil Neoprene Rubber
T	40 mil Teflon
CH	30 mil Polyethylene
SB	1 mil Silica-Core Boron Fibers
WB	1 mil Tungsten-Core Boron Fibers

Figure 6 Image Quality Indicator GD/FW

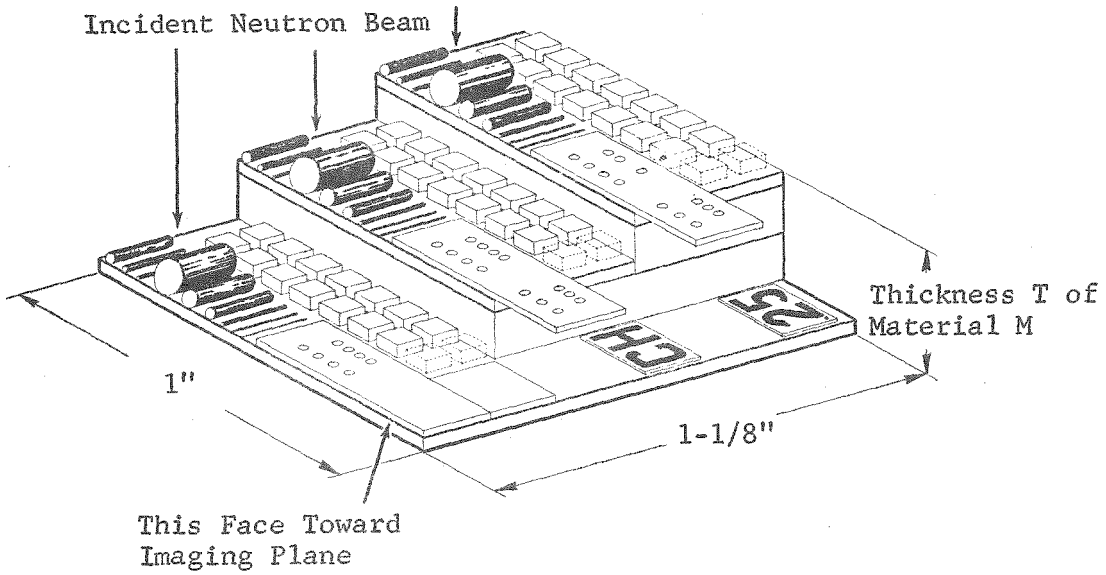

Neutron Radiography - Object 101

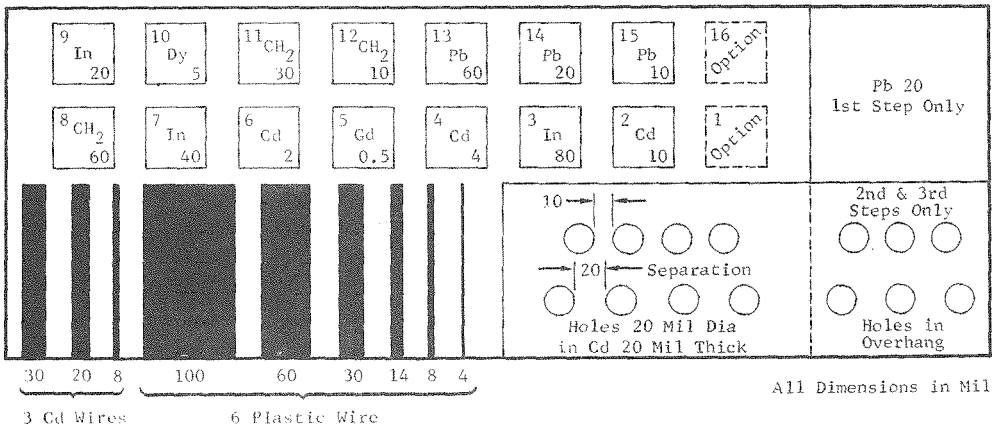

Detail of Test Strips - Three Steps

Figure 7 Image Quality Indicator (ANL)

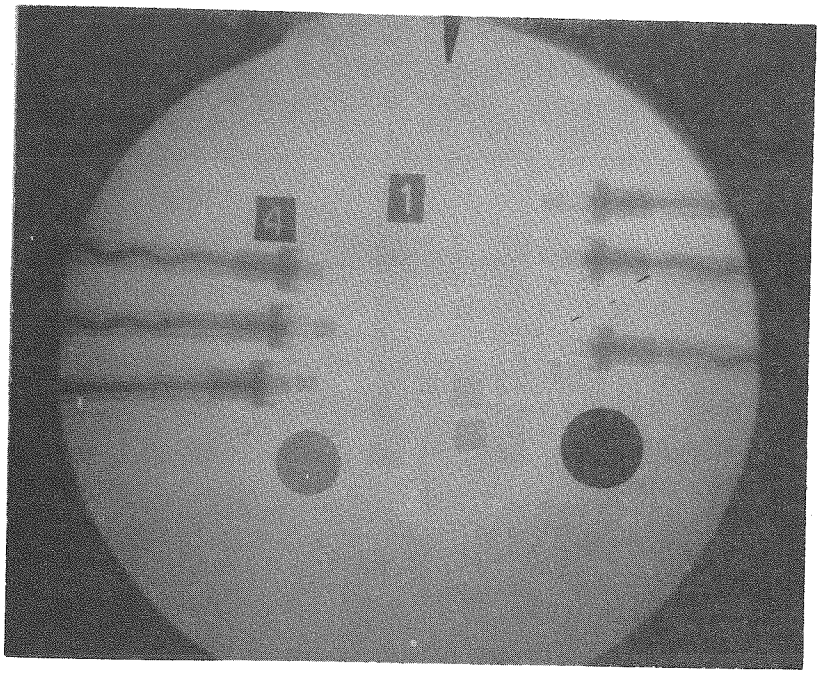

Figure 8 Neutron Radiograph of Defective SMDC Tips and GD/FW IQI with 12-mil Dysprosium Foils

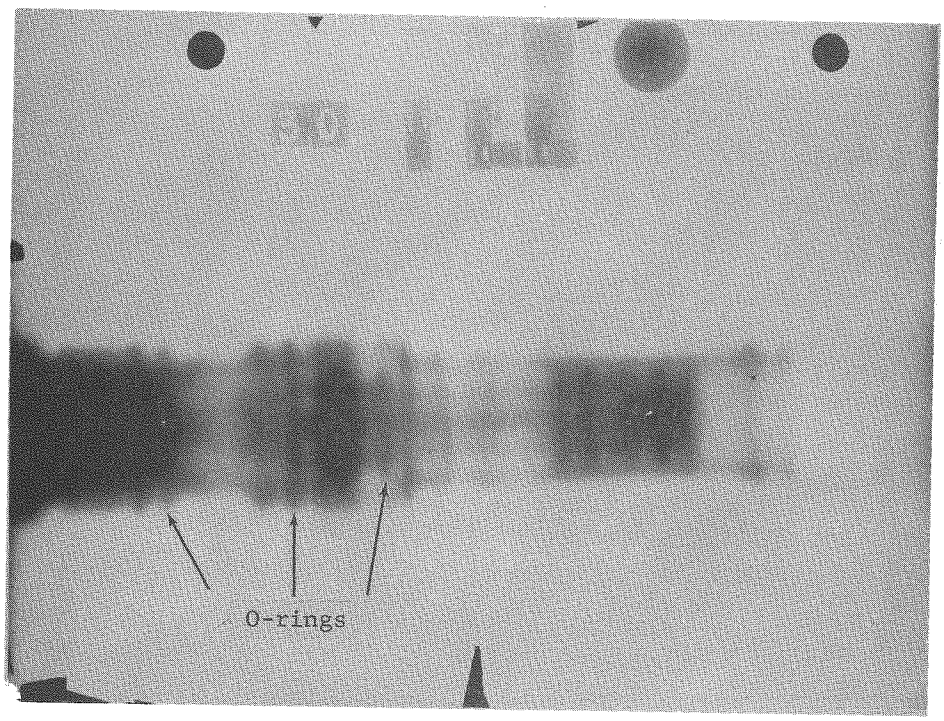

Figure 9 B-58 Elevon Rate Selector Valve Assembly - Neutron Radiograph - Cf^{252}

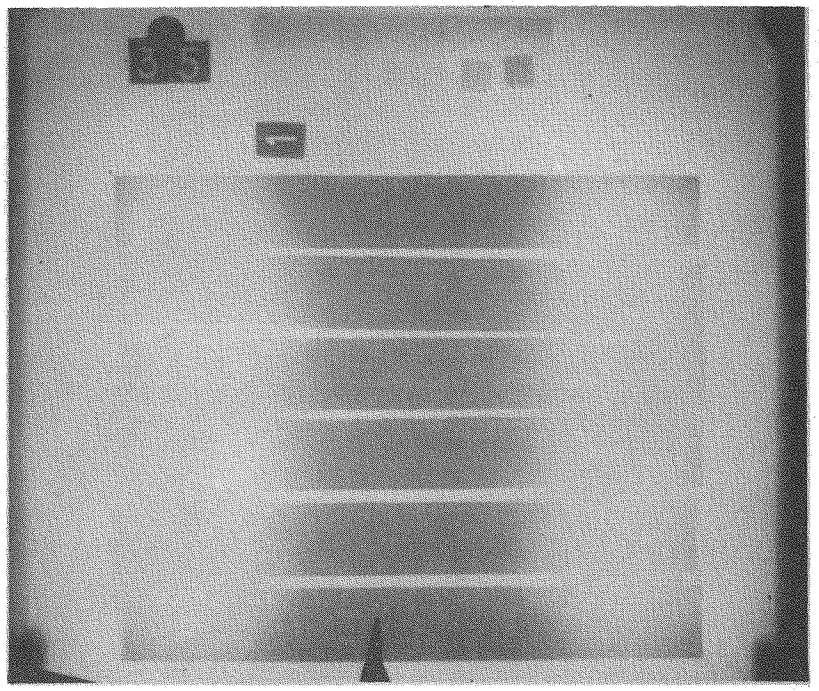

Figure 10 Boron Fiber - Aluminum Matrix Tensile Specimens - Neutron Radiograph - Cf^{252}

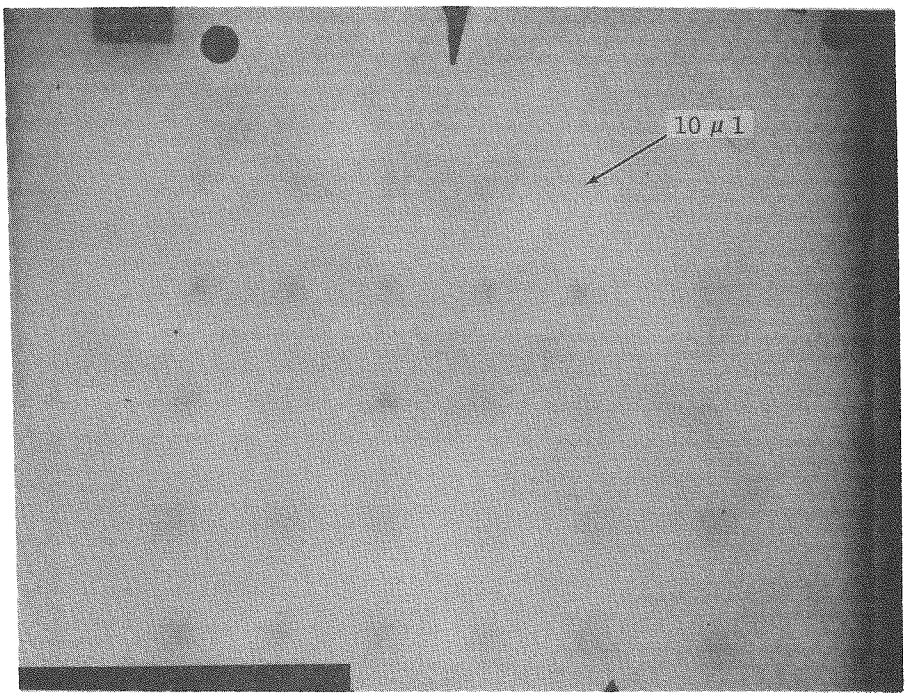

Figure 11 Aluminum Honeycomb - 3 in. Thick with Water Droplets of 5 to 200 Microliters in Cells - Neutron Radiograph - Cf^{252}

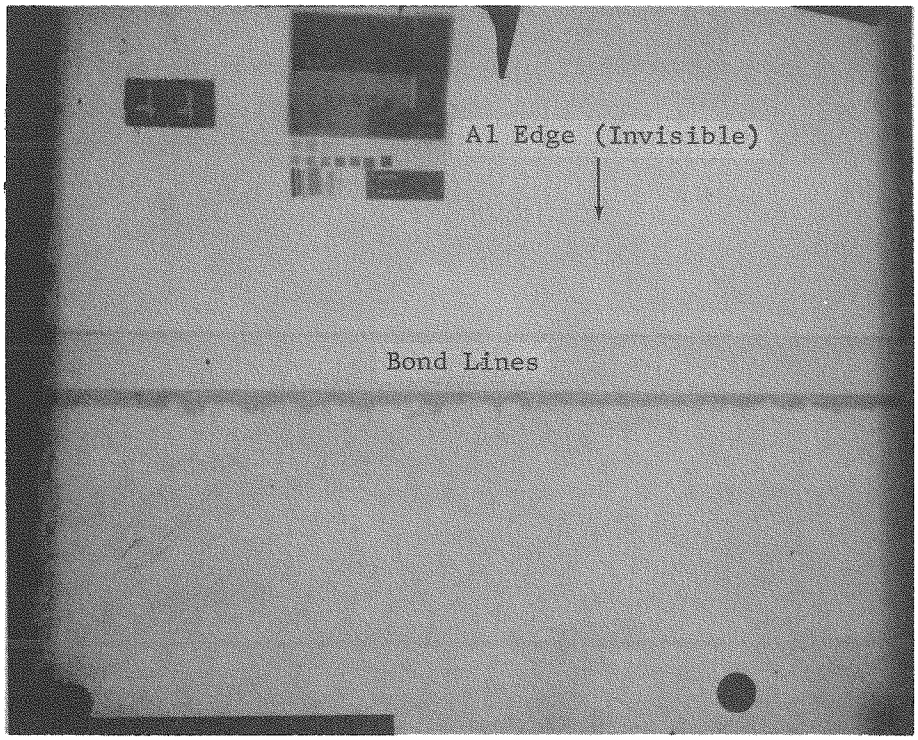

Figure 12 F-111 Leading Edge of Horizontal Stabilizer - Neutron Radiograph - Cf^{252}

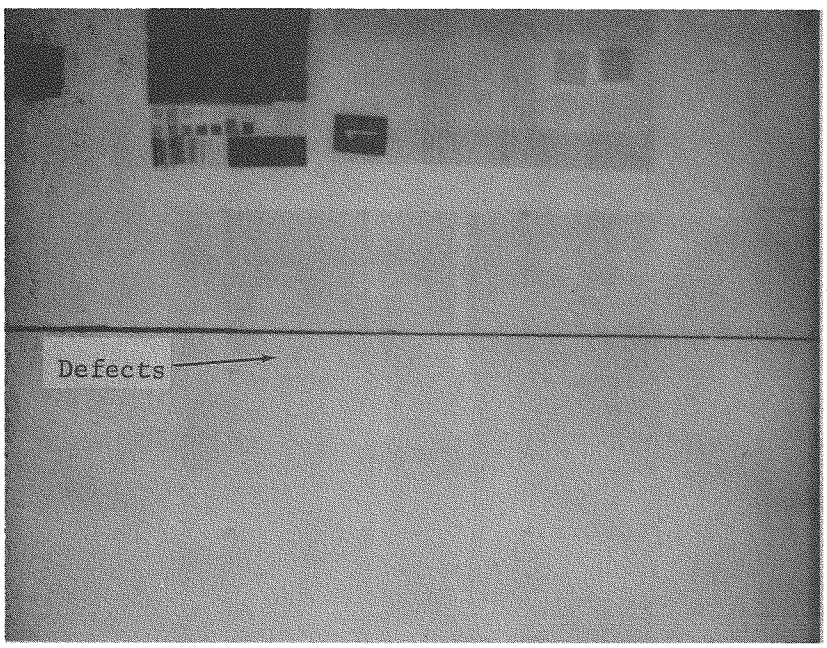

Figure 13 Aluminum Adhesive-Bonded Lap Shear Specimens - Neutron Radiograph - Cf^{252}

NEUTRON RADIOGRAPHY WITH Cf-252: The Effect of Tailoring Neutron Energy Spectra on Photography Images

Gary Don Bouchey
E. Linn Draper, Jr.
Stephen J. Gage

Nuclear Reactor Laboratory
The University of Texas at Austin
Austin, Texas

A californium-252 neutron source was used to study the effect of neutron energy spectrum, converter screen, and film type on the quality of neutron radiographs of a multielement test object. Each of four spectra was investigated with four converter screens. The neutron energy spectrum and gamma content of the beam were altered by filter insertion to enhance imaging of various portions of the test object.

INTRODUCTION

The image obtained from a neutron radiograph depends on the total neutron cross section of the object that is being inspected as well as the reaction cross section of the converter screen. These cross sections, of course, may be strongly dependent on neutron energy. None of the presently available sources can generally be used to provide monoenergetic neutrons suitable for radiography. The neutrons in a thermal nuclear reactor are created with a fission spectrum of energies and slow down through the resonance region to thermal energies. The neutrons obtained from isotopic sources such as Pu-Be, Am-Be, etc. also emit rather high neutron energy spectra which must be thermalized before use in thermal neutron radiography. Neutron generators, although they produce monoenergetic neutrons, yield such high energy neutrons that moderation is usually required before good radiographic results can be obtained with conventional screens. Finally, Cf-252, which is used for this work, produces a fission spectrum which may be moderated if desired.

Because of the variation of cross section with energy it is often possible to alter the radiographic image substantially by "tailoring" the neutron energy spectrum to suit a particular application. Several authors have used the energy dependence to advantage for radiographic applications (1,2,3).

This paper investigates the photographic results of varying the neutron energy spectrum obtained from a Cf-252 neutron radiographic assembly at The University of Texas at Austin[1] (4,5). Since considerable gamma radiation is emitted from the Cf-252 it is also necessary to consider the effect of the gamma contribution to the radiographic image. Several beam arrangements are studied. Direct exposure of the object to the source results in a beam with an energy distribution near the fission spectrum. Beams with lower energy distribution are achieved by inserting various thickness of neutron scattering materials such as lead, iron, polyethylene, water, etc. between the source and the object. Insertion of these materials particularly the heavier materials such as lead, and iron also affects the gamma contribution in the beam.

As indicated earlier, the photographic results are dependent not only on the cross sections of the materials in the object, but on the neutron reaction properties of the converter screen. Some screens

1 These investigations were conducted using a 1000 μg Cf-252 source that was provided for the University as part of the USAEC Cf-252 Market Evaluation Program.

may be effective for detecting thermal neutrons but will not record the epithermal contribution. Others may exhibit especially large resonances and be particularly effective for recording neutrons of higher energies. Four of the most common converters namely gadolinium foil, indium foil, LiF-ZnS, and organic scintillator material, are evaluated for each different beam configuration.

Each beam arrangement studied was characterized by measurement of the thermal, and epithermal neutron fluxes by means of induced activation detectors (6,7). Bare and cadmium covered gold foils were used to measure the thermal and resonance fluxes. The gamma levels were measured with a calibrated G-M detector. The gamma contribution to the photographic image was also evaluated by making identical exposures of the film without the neutron converter screen in place. Comparison of the image quality from various beam arrangements was accomplished through the use of a test object designed to allow evaluation of resolution, contrast, fast neutron, thermal neutron, and gamma contributions.

NEUTRON IMAGING STUDIES

BEAM CONFIGURATIONS

The neutron imaging studies performed in this paper were all done with a one milligram Cf-252 source, encapsulated in stainless steel. The source is normally housed in a combination shield and experimental facility designed especially for the Cf-252 source. The principal shielding material in the facility is water extended polyester resin (WEP) containing 70% water. Access to the source is achieved through four beam tubes which penetrate the cylindrical shield. The bulk of the radiography work was performed through one of the 4" stepped tubes. A cadmium lined diverging collimator was inserted into the beam tube for most the work in order to achieve the desired geometric resolution (see Figure 1). The central cavity in the shield may be left empty as shown in that figure, may be filled with water, or may be lined with a 2" layer of sodium borate. Provision is also made for inserting 4" diameter disks of variable thickness between the source and the entrance of the collimator. This allows insertion of various materials such as iron, lead, polyethylene, etc. for the purpose of tailoring the neutron energy spectrum in the beam.

Thermal Beam. For most radiographic inspection problems thermal neutrons provide the most satisfactory results. In order to achieve a thermal beam (Beam #1) from the Cf-252 source a water-filled polyethylene container with a penetration for the 4" diameter collimator was constructed to fit into the central cavity of the shield. The source was located approximately 1 inch below the collimator entrance. Offsetting the source in this matter is reported to improve the image quality and the neutron to gamma ratio in the beam (4). A second thermal beam (Beam #2) was identical to Beam #1 except that a 4" dia. x 1" disk of lead was inserted between the source and the collimator entrance.

Fast Beam. To achieve a fast neutron beam (Beam #3) the central cavity was lined with 2" of powdered sodium borate contained in a sheet metal can. The beam was extracted through the cadmium lined collimator used for the thermal beam with the source located directly in the entrance of the collimator. For some of the fast neutron experiments which required higher neutron levels the source was simply used as a point source without collimation and the object, converter and film were positioned approximately 8 inches from the source in a 10" beam port as shown in Figure 2 (Beam # 4).

FLUX MEASUREMENTS IN THE BEAMS

Neutron flux levels and an indication of the neutron energy distribution were obtained by activation of bare and cadmium covered gold (Au) foils in the Cf-252 beams. A neutron flux calibration was obtained by comparing the activation of gold in the Cf-252 beams to the activation of gold in a position of known thermal flux in the University of Texas TRIGA nuclear reactor. The reactor flux was measured by coincidence counting of gold foils. The relatively standard techniques used for the foil measurements are described in greater detail in reference (6) and (7). Gamma levels in each beam were simply measured with a calibrated β-γ survey meter and recorded in units of milliroentgens per hour. The results of the neutron and gamma measurements for each beam discussed in this paper are summarized in Table I.

TABLE I

Spectrum Characterization

SPECTRUM	THERMAL FLUX (#/cm^2-sec)	EPITHERMAL FLUX[a] (#/cm^2-sec)	CADMIUM RATIO (Au)	GAMMA DOSE RATE (mr/hr)
1 (Thermal Beam)	849	266	1.18	118
2 (Lead Filtered Thermal Beam)	3139	284	1.40	78
3 (Fast Beam	216	185	1.06	124
4 (High Intensity Fast Beam)	268,200	9117	2.67	3000

a. The values in this table correspond to Φ_{epi} where the epithermal flux $\Phi(E) = \frac{\Phi_{epi}}{E}$

NEUTRON CONVERTER SCREENS

LiF-ZnS Scintillation Screen. This screen consists of a mixture of LiF and ZnS deposited on an aluminum plate. The screen used for this work is available commercially from Nuclear Enterprises Corporation. In our experience, the lithium scintillation screen is the best screen available for low intensity thermal neutron radiography. When used with the extremely high speed Poloroid Type 57 film it allows good quality thermal neutron pictures with extremely low total neutron exposure and is exceptionally insensitive to gamma and fast neutron interferences. For improved resolution and contrast the slower Polaroid Type 51 film is recommended.

Gadolinium Screen. Gadolinium is probably the most widely used screen for high resolution thermal radiography with nuclear reactor beams. In low intensity radiography the gamma to neutron ratio is usually relatively high. For this reason gadolinium is not a very satisfactory screen for use with low intensity beams because it requires a direct exposure (i.e., the film and screen remain in direct contact during exposure in the neutron beam); thereby, resulting a considerable gamma contribution to the radiograph. Kodak Royal Blue and AA X-Ray films were used with the 1 mil gadolinium screen used for these studies.

Indium Screen. Indium is a good absorber with an exceptionally strong resonance at 1.5 ev. In-115 activates with a 54 minute half life so that indium may potentially be used as both a direct and transfer type screen. Because of the relatively high thermal cross section combined with the resonance structure indium offers potential as both a thermal neutron and an epithermal screen. Indium-115 also exhibits the following reaction: $In^{115}(n,n')In^{115m}$ at higher neutron energies making it a possible candidate for a fast neutron converter screen.[2] As with the gadolinium screen, Kodak Royal Blue and AA X-ray films were used for indium radiography.

Organic Scintillation Screen. This type of screen has been suggested previously as a possible fast neutron screen (8) using the proton recoil mechanism resulting from neutron scattering by the hydrogenous material in the screen to produce ionization. For these investigations a scintillation screen composed of PPO in a mixture of 20% butyl-methacrylate and styrene was used. A complete description of the fabrication of these screens may be found in reference (9). Type 57 and Type 51 Polaroid films are used for the work with this screen.

2. K. H. Beckurts and K. Wirtz, Neutron Physics, p. 290.

TEST OBJECT

In order to evaluate the image quality obtained from the various configurations and converter screens, a simple test object was devised. The object consisted of three thicknesses each of polyethylene, cadmium backed polyethylene, lead, and indium. It also included a 5 mil gold foil and a cadmium test piece with several holes drilled in it. These included two larger holes of 0.250 and 0.0625 inches and a set of 0.020 inch holes. The twenty mil holes were spaced as follows: 1, 2, 4, 8, 16, 32, and 64 mils. All these materials were mounted on a thin aluminum plate as shown in Figure 3.

SELF IMAGING WITH RESONANCE ABSORBERS

An intriguing concept that has been used to advantage for certain neutron cross section work and that might prove to be extremely useful for certain very specialized inspection problems is that of "self imaging" by resonance absorbers. Conceptually the idea is quite simple. Suppose it is required that we inspect a material which has a strong resonance structure in the presence of other materials which have relatively large thermal neutron cross sections. It is then conceivable that both X-radiography and thermal neutron radiography may yield poor results. In this situation it may prove advantageous to filter the neutron beam in such a way as to remove all thermal neutrons and to maximize the number of neutrons in the resonance region. Then if we use the same material (i.e., the material that is to be observed) as a neutron converter screen, the image may be considerably improved since nearly all of the activation of the screen results from absorption of neutrons at the energies of the resonance. For this reason, the film will receive considerably less exposure in regions where the same material which composes the screen is present in the object. Also since the neutrons in the beam are of epithermal energies, they will tend to penetrate other materials in the object better and the result is that the contrast between the material of interest and the other materials in the object is greatly enhanced.

In prinicple this method appears extremely promising for certain applications, unfortunately there are at least two serious difficulties that must be overcome before good results may be achieved. For the inspection of thick objects the scattering of faster neutrons into the resonance regions seriously degrades the quality of the image that may be obtained. Antiscatter grids of the type described in the literature (10) may provide a partial solution to this difficulty . This problem is not studied in this work. Instead the object was limited to the thin test piece described earlier.

The second difficulty results because of the gamma contribution that is invariably present in a radiographic beam. This problem is particularly acute for work with low intensity beams obtained from non-reactor sources. Because epithermal and fast neutrons (which tend to interact with much smaller effective reaction cross sections) are used for exposure of the film, the ratio of the neutron to gamma ray exposure of the film is significantly decreased when compared to the situation in thermal neutron radiography. If there is an abundance of neutrons and the screen activates in a way such that it may be used as a transfer screen, the gamma problem is easily eliminated. Indium self imaging for example may be demonstrated quite easily using the transfer method in a beam from a nuclear reactor. With the Cf-252 source, however, much more difficulty is encountered. One result is shown in the next section (see Figure 7) with the high intensity fast beam. Unfortunately the resolution of this picture is not very satisfactory because the screen is so close to the source.

PHOTOGRAPHIC RESULTS

The photographic results in these studies are too numerous to present in their entirety here. The results are, however, summarized in a rather subjective manner in Table II. In this presentation the resolution, gamma-ray contribution to the photographic image, and the fast and thermal neutron contributions are characterized. It must be pointed out that these results were at times difficult to interpret. Judgements about the relative effect of gammas and neutrons on the image were particularly complex. Even though interpretations of the results are based on judgements by the authors, certain useful information may be obtained. For classification of resolution, the following four categories were used:

Excellent - All hole and spacings between holes could be distinguished on the Cd test object

Good - The 0.020 inch holes could be distinguished but smaller hole spacings not visible.

Fair - The 0.0625 inch hole distinguished but 0.020 inch holes not visible.

Poor - Only the 0.250 inch hole was distinguishable.

In order to demonstrate the type of images that were obtained and to help clarify the way in which results were presented in Table II several radiographs of varying quality are included. Figure 4 shows a thermal neutron radiograph obtained with Beam #2 using the LiF-ZnS scintillation screen and Type 51 Polaroid film. This radiograph demonstrates "excellent" resolution and exhibits very little gamma contribution. Figure 5 shows a radiograph with the fast beam (Beam #3) using the gadolinium screen and Kodak Royal Blue X-ray film. The resolution in this case was good with an extremely strong gamma contribution being quite apparent. Figure 6 shows a radiograph obtained with Beam #1 using the direct exposure method with an indium screen and Kodak Royal Blue X-ray film. The resolution is poor and a strong gamma interference is present.

Finally Figure 7 demonstrated the self imaging technique. This radiograph was obtained in the high intensity fast beam (Beam #4) using the transfer exposure method with the indium screen and the Kodak Royal Blue film. Recall that resolution is relatively poor because of the positioning of the object and screen to achieve the higher neutron intensity. The object and cassette containing the screen where cadmium covered so that there is no thermal neutron contribution. Since the transfer method was used gamma rays do not contribute to the image. The result is that the indium in the object is visible, but other materials in the object are not seen. This image may be compared with Figure 6 which is a thermal radiograph with the indium screen. It is easily seen that if the objective is to inspect for indium in the presence of other materials significant advantage might be realized. Notice that the paraffin objects cause some additional moderation of the fast neutrons resulting in increased exposure. It is suggested that this sort of a technique may be extended to many materials with strong resonance structures. Particularly likely candidates might be the rare earths and a variety of metals.

CONCLUSIONS

As one might have expected, it is apparent from our results with a Cf-252 neutron source that for most nondestructive inspection problems, thermal neutron radiography is superior to fast or epithermal radiography. Gamma interference does seem to be a significant problem for neutron radiography with Cf-252 sources. One effective way of eliminating gammas in thermal radiography is the use of the LiF-ZnS screen and Polaroid high speed film (which is primarily light sensitive). This screen cannot, it appears, be used for fast or epithermal radiography, probably because of the low cross section of Li for the higher energy neutrons. Transfer type exposures could of course also be effective for reducing gamma contribution but the low neutron intensity is difficult if not impossible to overcome for reasonable sized Cf-252 sources. Finally, it is possible to insert a material such as lead which exhibits high gamma and low neutron absorption. This was not, however, found to be particularly effective. Insertion of lead certainly reduces the high energy gammas emitted directly from the source but it also decreased the neutron level, primarily by neutron scattering, and subsequently the needed exposure time. Experiments with a lithium-drifted germanium gamma-ray spectrometer placed in our beams indicated that the main gamma contribution between 0 and 3 Mev were resulting from neutron capture in hydrogen with a small contribution from boron and cadmium capture. Since the neutron capture gamma contribution is not affected significantly by lead in the beam, the decrease in direct gamma is negated by the increased capture gamma contribution. The strong capture gamma contribution also accounts for degradation of resolution that was observed for high gamma to neutron ratios.

For some applications it might be desirable to use a faster neutron spectrum in order to increase the penetration in thick objects or to enhance the contrast of certian materials. In this case the LiF-ZnS screen is not effective and the

gamma interference problem becomes acute. Use of the organic screen did not give good results either. All images obtained in the fast beams appear to result primarily from gamma contributions. Further investigation of other scintillators may, however, prove to be more effective for fast radiography. The best results using fast neutron radiography with conventional screens were achieved with Beam #3 and gadolinium and indium direct exposures. The gamma exposure of the film was still quite high in these cases, but the resolution was reasonably good. This arrangement could not be used effectively then to inspect large thickness of heavy material, but might be effective for differentiating between lighter materials. Indium and gadolinium generally gave images for other epithermal beams as well, but the resolution was generally not good because of the fogging of the film by capture gamma rays from the collimator and shielding material. The self imaging method also indicated considerable potential for special inspection problems in fields such as metallurgy. For thicker objects it will require special antiscatter grids and transfer methods with correspondingly high neutron intensities.

ACKNOWLEDGEMENTS

The authors acknowledge the support of the USAEC Savannah River Operations Office who provided the 1 mg Cf-252 source used for these studies as part of the Cf-252 Market Evaluation Program. The work of Richard R. Day in establishing our photographic procedures for developing and printing the radiographs is gratefully acknowledged.

REFERENCES

1. L. G. Miller and T. Watanabe, "Enhancing Contrast of Neutron Radiography by Energy Tailoring of Beams" , Sixth Int. Conf. on NDT, Hanover, Germany, (June 1-5, 1970).

2. J. P. Barton, "Radiographic Examination Through Steel Using Cold Neutrons", Brit. J. Appl. Phys., 16, 1833-1839, (1965).

3. M. Brown and P. B. Parks, "Neutron Radiography in Biological Media", Tenth Annual AUA-ANL Nuclear Engineering Education Conference, (February 1969).

4. J. P. Barton and M. P. Klozar, "Thermal Neutron Radiography with Cf-252 and Other Small Sources", Trans. Amer. Nucl. Soc., 12, 465, (1969).

5. J. L. Cason, "Californium-252 for Neutron Radiography" Californium-252 Progress, Its Use for Market Potential, No. 2, Jan., 1970, Savannah River Operations USAEC, Aiken, South Carolina.

6. K. H. Beckurts and K. Wirtz, Neutron Physics, Springer Verlag, New York (1964).

7. K. C. Ruzich, "Absolute Neutron Flux Spectrum Measurements, Argonaut Reactor", ANL-6990, Manual of Reactor Laboratory Experiments, pp 28.1-28.45, (January, 1965).

8. H. Berger, "Image Detection Methods for 14.5 Mev Neutrons: Techniques and Applications", Int. J. of Appl. Rad. and Isotopes, 21, 59-70, (1970).

9. R. H. Richardson, "Studies in Genetics VI", Marshall R. Wheeler, Ed., University of Texas Publication, in press, (1970).

10. P. B. Parks and M. Brown, "Antiscatter Grids for Low Energy Neutron Radiography", Radiology, 92, 178-179, (January, 1969).

TABLE II

Characterization of Photographic Results

Type of Screen	Beam #1	Beam #2	Beam #3	Beam #4[a]
LiF-ZnS	excellent resolution good thermal neutron image no fast neutron imaging no gamma contribution	excellent resolution good thermal neutron image no fast neutron imaging no gamma contribution	no image at all	not used
Gadolinium	fair resolution substantial thermal neutron imaging some fast neutron imaging strong gamma contribution	fair resolution substantial thermal neutron imaging some fast neutron imaging strong gamma contribution	good resolution some thermal imaging substantial fast imaging strong gamma contribution	not used
Indium direct	poor resolution substantial thermal neutron imaging substantial fast neutron imaging strong gamma contribution	poor resolution substantial thermal neutron imaging substantial fast neutron imaging strong gamma	fair resolution some thermal neutron imaging substantial fast neutron imaging strong gamma	not used
Indium transfer	not used	not used	not used	poor resolution no thermal contribution excellent indium self imaging no gamma contribution
Organic Scintillator	low quality gamma radiograph	low quality gamma radiograph	low quality gamma radiograph	low quality gamma radiograph

a. Scattered thermal neutrons were eliminated in this beam by encasing the object, screen, and film in cadmium

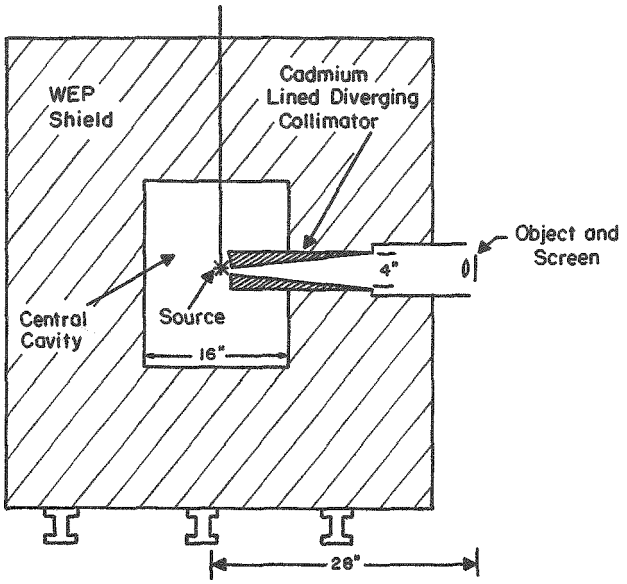

Figure 1. Diagram of the Cf-252 neutron radiography facility showing the diverging collimator.

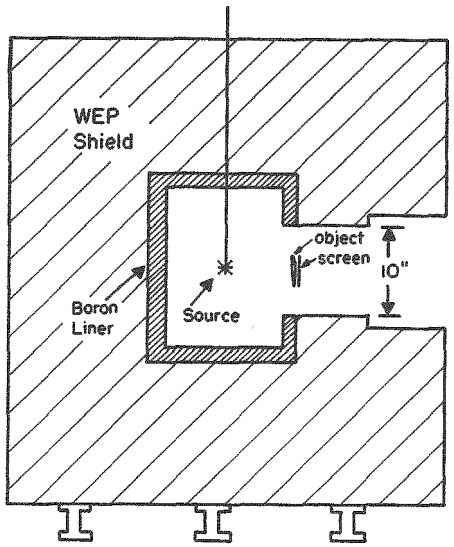

Figure 2. Diagram of the high intensity fast beam (Beam #4) arrangement.

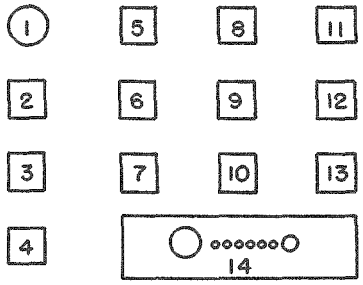

Figure 3. Diagram of the test object: (1) 3 mil gold foil, (2) 240 mil polyethylene with 30 mil cadmium backing, (3) 120 mil polyethylene with 30 mil cadmium backing, (4) 62 mil polyethylene with 30 mil cadmium backing, (5) 12 mil indium, (6) 60 mil indium, (7) 120 mil indium, (8) 324 mil lead, (9) 216 mil lead, (10) 108 mil lead, (11) 240 mil polyethylene, (12) 120 mil polyethylene, (13) 62 mil polyethylene, (14) 30 mil cadmium test object.

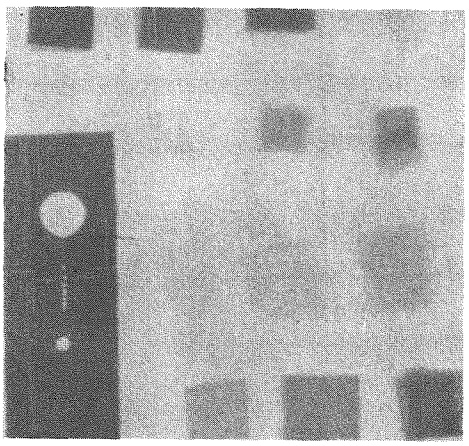

Figure 4. Thermal radiograph of the test object: LiF-ZnS screen, Polaroid type 51 film, and Beam #2.

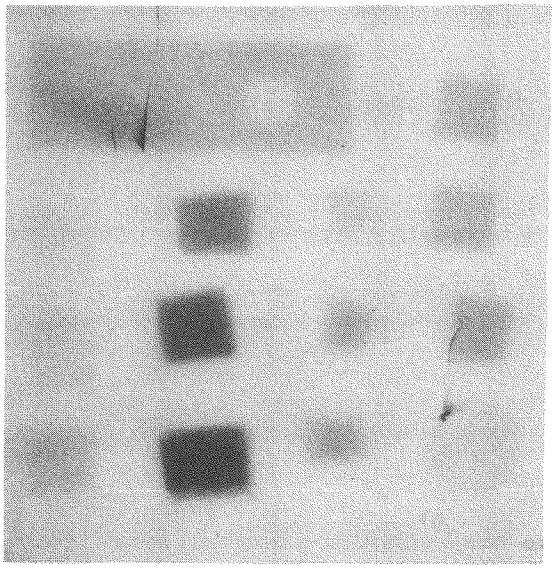

Figure 5. Fast neutron radiograph of the test object: Gd screen, Kodak Royal Blue Film, and Beam #3.

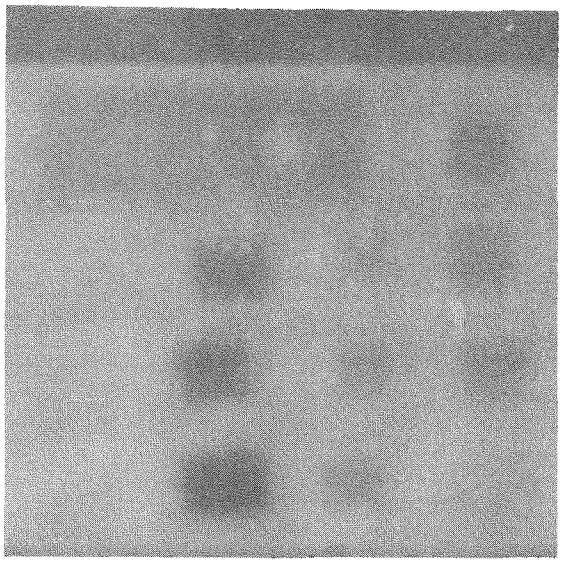

Figure 6. Thermal neutron radiograph of the test object: Indium Screen (direct), Kodak Royal Blue film, and Beam #1.

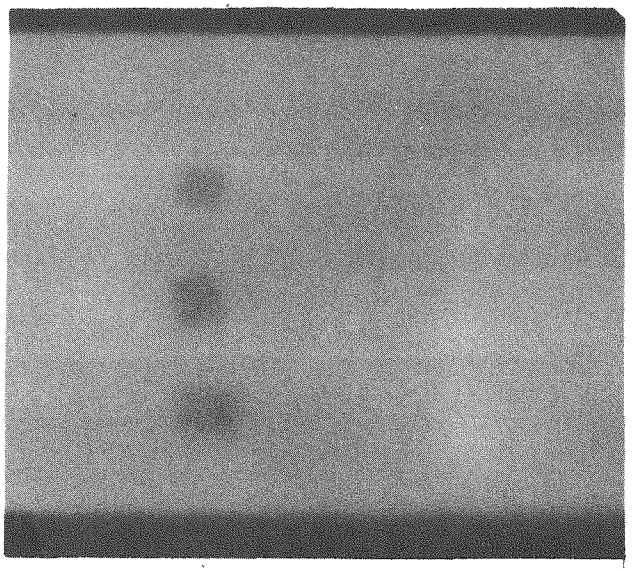

Figure 7. Fast neutron radiograph of the test object showing self imaging: Indium Screen (transfer), Kodak Royal Blue film, and Beam #4.

NEUTRON RADIOGRAPHY WITH A TRIGA NEUTROVISION SYSTEM

George T. Schnurer
Albert T. McMain

Gulf Energy & Environmental Systems, Inc.
San Diego, California 92112

The TRIGA[R] NEUTROVISION[TM] concept is reviewed, and various types of TRIGA NEUTROVISION systems are discussed. Specific information is given on a low-cost, simplified system, which has great potential for industrial neutron radiography applications. Examples of neutron radiography applications with a TRIGA system are presented. Facility housing, auxiliary equipment, staffing, and maintenance requirements are reviewed.

INTRODUCTION

As neutron radiography becomes increasingly accepted in industry as a meaningful and useful technique, more emphasis will be placed on the characteristics of the neutron source or, perhaps more properly, on the total system used to produce neutron radiographs. In perspective one might even say that the wide acceptance of neutron radiography and the availability of a neutron radiography system at moderate expense are complementary--one cannot happen without the other.

TRIGA reactors have found worldwide acceptance as versatile and highly useful research reactors. The geometric configuration and the extent of experimental facilities can be varied widely and are discussed in greater detail elsewhere (1). The suitability of a TRIGA reactor for performing neutron radiography has become readily apparent, and a number of organizations already operating TRIGA reactors are actively engaged in neutron radiography programs of their own. The NEUTROVISION system is the complete array of equipment and facilities required to perform neutron radiography, having as its focal point a TRIGA reactor. The system includes a neutron source, collimators, sample holders, and the like, which are necessary to provide an integrated capability for performing neutron radiography.

Although all TRIGA reactors have characteristics that are desirable in the neutron source of a NEUTROVISION system, a new one, the mini-TRIGA (Figure 1), is of special interest for performing neutron radiography. Of particular importance is its low cost and high degree of flexibility. This paper describes a typical NEUTROVISION system based on a mini-TRIGA as the neutron source. Typical examples of work that can be performed with such a system are also described as a means of illustrating the quality of work that can be performed with this modestly priced neutron source.

DESCRIPTION OF TRIGA NEUTROVISION SYSTEM

Gulf Energy & Environmental Systems is a world leader in research reactors, having constructed, or under construction, 49 TRIGA research reactor facilities. Of more importance, within the context of this paper, is the fact that Gulf Energy & Environmental Systems in its San Diego laboratory operates three TRIGA reactors which have been used for some time in performing neutron radiography (2,3).

Increasing requirements for a low-priced reactor neutron source with sufficient flux have developed in a number of areas of increasing importance, such as neutron activation analysis, production of short-lived

radioisotopes, and, of course, neutron radiography. Foreseeing this developing requirement, we have made a detailed review of all TRIGA reactor designs with a view toward further simplification of the reactor and significantly reducing its cost while at the same time perserving the "large reactor" capability. As a result, we have introduced a new member of the TRIGA family of reactors, called the mini-TRIGA. Although similar in appearance to the well-known TRIGA Mark I reactor, the mini-TRIGA employs fully enriched uranium-zirconium hydride fuel with a graphite reflector. This combination drastically reduces the size of the core and produces a very high flux per watt.

By taking advantage of the TRIGA's ability to be operated with only natural convection cooling of the core, thus eliminating a water-cooling system, further savings have been achieved and operation at 100 kW is still permitted for short periods. Still other simplifications have contributed to reduction in cost. Although the turnkey price varies with installation circumstances, a typical mini-TRIGA costs $175,000 in the United States, exclusive of building and pool but including all control and operating equipment as well as installation and startup.

Despite its simplicity the standard mini-TRIGA operates at steady-state power levels up to 100 kW, providing a neutron source flux of 3.5×10^{12} n/cm^2-sec at a specimen exposure thimble adjacent to the core.

A controlling factor in the design of the mini-TRIGA, which is of particular importance for a neutron radiography consideration, is that upgrading to higher performance levels can be accomplished with relatively little expense. For example, upgrading to 250 kW is achieved by simply providing another control rod and drive and adding fuel to existing unfueled grid positions.

Figure 1 illustrates a typical mini-TRIGA installation for a NEUTROVISION system. The other components and subsystems that would be required in a typical NEUTROVISION system employing a mini-TRIGA will be briefly described.

Figure 1 illustrates a setup using a portable beam tube or divergent collimator with its lower terminus near the reflector region of the reactor and with its upper end terminating approximately 3 feet above the surface of the reactor pool in a receptacle that contains the sample holder, the foil and plate holder, and suitable shielding. The collimator shown is portable and can be moved as required. For example, the collimator would most frequently be positioned in the core-reflector interface region to obtain a high neutron source and still maintain the gamma background at an acceptably low level. Figure 2 is a schematic representation showing relative positions of the source, collimator, object, converter, and film. Note that in the actual facility with a mini-TRIGA, the collimator would be oriented vertically.

Figure 3 shows a typical NEUTROVISION collimator in greater detail, identifying the pertinent points considered in the design to achieve maximum signal and reduced background. The collimator is discussed in References 3 and 4. Typically, this collimator has a maximum L/D (length to diameter ratio) of approximately 40 to 50, which is considered suitable for many general-purpose types of neutron radiographs. Inserts within the collimator source end can increase the L/D significantly. With this type of resolution and with the collimator positioned on the graphite reflector, the mini-TRIGA could deliver a flux in the range of 10^6 to 10^7 n/cm^2-sec at the photographic plate with a gamma background dose of 15 to 20 R/hr at the sample location. A higher neutron flux (by as much as a factor of 10) can be achieved by moving the source end of the portable collimator closer to the core region.

Special applications may require a smaller angular divergence of the beam mentioned above. This can be provided with this type of collimator by a variable feed aperture, which could be as simple a device as a plug that is placed at the source end of the collimator. Such a technique would permit an adjustable L/D from approximately the 40 to 50 range to as high as 120 to 1 or 200 to 1. With the collimator presently being used with the TRIGA in San Diego in a comparable type of configuration, neutron radiographs with an image size of 8 in. by 10 in. are produced. An increase in the image size to 14 in. by 7 in., or even larger, is possible with a larger beam tube. As a specific example the Aerotest Corporation, which uses a reactor having a TRIGA core with a configuration not too dissimilar to the mini-TRIGA illustrated in Figure 1, uses a collimator that can handle images up to 14 in. by 17 in. They currently use collimators that have an L/D of 125 to 1 and 250 to 1. In their case, however, the TRIGA core is operated at a power level of 250 kW, which produces a thermal neutron flux over the exposure area of the facility of

1.78×10^7 n/cm^2-sec maximum and 1.61×10^7 n/cm^2-sec average, with a cadmium ratio of 14 to 1. At the same time the gamma ray dose rate was measured to be 24.3 R/hr (5).

Although Figure 1 shows a conical collimator, it is quite feasible to use a Soller slit system. In fact, at a TRIGA reactor in San Diego that also has a below-ground configuration comparable to that of the mini-TRIGA, a Soller slit collimator has been used in a routine and completely satisfactory manner (2,6). In this instance, since the distance available from the reactor core to the sample to be radiographed was only a little more than 2 feet, a compact system was required. The samples radiographed with this system on a routine basis are fissile-heated thermionic cells. These are highly radioactive, thereby requiring the transfer method rather than the direct exposure method for taking neutron radiographs. The particular collimator that was used was fabricated from thin-walled cadmium-plated stainless steel tubes about 1/8 in. in diameter and 8 in. long. The Soller slits were arranged so that they were sufficiently separated from the object to be imaged to eliminate unwanted images of the collimator structure. The system provided for the remote, vertical insertion of the thermionic cells to be imaged. A water shutter was used to control the volume between the collimator and the object to be radiographed. The L/D was approximately 32. For this particular instance the Soller slit collimator had some definite advantages over the conical collimator. One principal advantage, of course, was the smaller size suitable for the relatively restricted space within which the work had to be done. Another more important advantage was the ability of the Soller slit system to provide a parallel neutron beam over the entire object to be imaged, thus reducing a portion of the geometric distortion inherent in the divergent collimator (3,4).

In addition to the collimator, another essential component is a beam catcher, which also includes shielding for sample-scattered neutrons. Although frequently not a separate item, another essential component is a suitable shutter mechanism to cut off the neutron beam. Quite frequently this shutter is constructed as part of the beam collimator. In addition to the foregoing, a suitable mechanism for holding the samples to be radiographed must be devised. Depending on the specific samples to be radiographed, the sample holder may be conveniently constructed as a slide-through type, somewhat analogous to a slide changer on a 35 mm projector. For certain large and bulky samples, however, this slide-through type is not appropriate.

The next essential item making up the system is a suitable array of converter foils (Figure 2), assuming the direct method is being used. These are usually 1-mil-thick gadolinium foils or they can be gadolinium-oxide plates, which are commercially available. For radiographs in which the transfer technique is necessary (as in the case of examination of highly radioactive samples), transfer foils such as dysprosium or indium are used.

It will also be necessary to have several film cassettes, which can be modified quite readily from commercially available medical X-ray cassettes by the radiography staff associated with the facility. In addition, there are commercially available vacuum cassettes, which are specifically manufactured for use in neutron radiography. With regard to film, there are a number of standard radiographic films suitable for neutron radiography with the direct foil system. Our experience has been that a good, general-purpose, high-quality film is Kodak single emulsion R film. When using the transfer technique with a dysprosium foil, we have used Kodak AA film for early results, but even here the R film is employed where possible to give superior results. With this technique the transfer foil is sandwiched between two layers of the film in the cassette after neutron activation of the transfer foil.

Thus far we have discussed a number of essential items that must be included in any NEUTROVISION system. These include the neutron source, in this case a mini-TRIGA; the collimator, which, depending on the application, can be either the conical or the Soller slit type; a suitable beam catcher and shutter; a sample holder; and a sufficient inventory of foils, film cassettes, and film.

The following components of the NEUTROVISION system are optional in that their use depends largely on the volume of neutron radiographs being processed, as well as the existence of ancillary or supporting activities. For example, if you intend to do your own photographic processing, a darkroom equipped with the normal standard photographic darkroom equipment for developing and processing film will be necessary. The amount of added equipment to be used, such as automatic film processers and enlargers, will vary with the facility requirements. In some

instances it may be advantageous to have the films processed by an outside laboratory. Another component that could be incorporated is an image intensifier converter system. This item is commercially available. A typical system might consist of a neutron-sensitive converter image intensifier that displays the neutron radiograph on a small screen that can be viewed by a TV camera or a regular camera. Work is being done using such an image intensifier converter system in conjunction with a video tape unit to provide a permanent record of the radiographs. This latter type of optional equipment can be quite useful for doing neutron radiography on nonradioactive samples.

The foregoing discussion has described a typical NEUTROVISION system using the mini-TRIGA as a neutron source. As noted earlier, other models of the TRIGA reactor are equally as adaptable for use with the system. For example, the mini-TRIGA is installed in a below-ground configuration; that is, the reactor is located in the bottom of an open, water-filled pool. Other TRIGA reactor configurations are constructed entirely above ground to permit the use of horizontal beams rather than the vertical beams previously described. Through proper design, these horizontal beams can be oriented so as to minimize contamination of the beam with gamma rays. A typical solution for producing a low-gamma-background beam with a horizontal type of arrangement is described in greater detail elsewhere (2).

Thus far we have discussed the equipment and components necessary for a complete, operable NEUTROVISION system. We will now turn our attention to the staffing requirements for running such a facility. The typical staffing requirements for a system employing a mini-TRIGA are given in Table I. The staff listed in Table I would be sufficient to operate the facility on a one-shift basis and could also provide other types of reactor service, such as activation of samples for performing neutron activation analysis. If the volume of radiographs processed by the facility should become substantial, additional NEUTROVISION technicians would be necessary, and, if multi-shift operation were required, additional licensed reactor operators would be needed. Most of the staff are typical of personnel required to operate a TRIGA reactor, independent of its application. The NEUTROVISION technician, however, is specific to a facility primarily engaged in neutron radiography.

TABLE I

Staffing Requirements[a]

Director of NUETROVISION service/reactor supervisor (1)
Senior reactor operator (1)
Reactor operator - electronic technician (1)
NEUTROVISION technician (1)
Health physicist (part-time) (1)

[a]The reactor supervisor and senior reactor operator would hold senior reactor licenses from the U.S. Atomic Energy Commission and the reactor operator - electronic technician would hold a reactor operator's license.

The NEUTROVISION technician may be a licensed reactor operator, but his primary skills are in the area of neutron radiography. Specifically, he must have the following qualifications:

1. Capable of loading and unloading samples
2. Experienced in darkroom procedures and process photography*
3. Ability to interpret radiographs
4. Sufficiently experienced in basic theory to set exposure parameters according to sample specifications

TYPICAL APPLICATIONS

Some typical applications of a NEUTROVISION system are illustrated in this section. Figure 4 is a photograph of the test block, identifying the variety of materials used. All of the neutron radiographs were taken using a below-ground configuration of a TRIGA similar to that of the mini-TRIGA discussed earlier. Figure 5a is a gamma radiograph (using an iridium source), Figure 5b is an X-radiograph, and Figure 5c is a neutron radiograph. A comparison of the radiographs with the test block gives a graphic illustration of some of the capabilities of neutron radiography. Note, in particular, the results for lead in the X- and gamma radiographs and the

*If the volume of neutron radiographs is large, the actual processing would be handled by a full-time phototechnician.

results for the Lucite in the neutron radiograph. One of the major differences in the neutron radiograph is due to hydrogen in the sample (Lucite).

Figure 6 is a neutron radiograph of two samples of the same object. One shows the presence of "Locktite" (arrow), and the other the absence of "Locktite," on an important set screw.

An interesting variation on applications of neutron radiography in examining fissile materials is that it can distinguish between different isotopic compositions, for example, between natural uranium and enriched uranium. Figure 7 compares a neutron radiograph with an X-radiograph of a test capsule containing uranium of different enrichments. It is expected that this technique will find applications in nuclear materials management, particularly in various safeguard programs.

CONCLUSIONS

A complete NEUTROVISION system has been reviewed and typical staffing requirements and applications have been discussed. Although any TRIGA reactor is suitable as the neutron source of a NEUTROVISION system, the mini-TRIGA, because of its simplicity and low cost, has been emphasized. As noted at the outset, the availability of a low-cost neutron radiography system is a prerequisite for a wide acceptance of neutron radiography as a routine nondestructive test technique. A NEUTROVISION system with a mini-TRIGA meets this requirement.

ACKNOWLEDGMENTS

The author gratefully acknowledges the assistance of the TRIGA reactor staff, in particular W. L. Whittemore, J. R. Shoptaugh, and J. E. Larsen, who provided the radiographs for the paper and made valuable suggestions during the preparation of the paper.

REFERENCES

1. G. T. Schnurer. Experimental Capabilities and Performance of TRIGA Research and Test Reactors for Neutron Applications. (paper included in these Proceedings).

2. W. L. Whittemore, G. T. Schnurer, and A. T. McMain. "Uses of a TRIGA Neutrovision System Including Examination of Radioactive Materials." Proceedings of 17th Conference on Remote Systems Technology. p. 846, American Nuclear Society (1969).

3. W. L. Whittemore, J. E. Larsen, and J. R. Shoptaugh. A Flexible Neutron Radiography Facility Using a TRIGA Reactor Source. (to be published in Materials Evaluation).

4. W. L. Whittemore. Fluxes, Beam Intensity, Collimation and Resolution for Neutron Radiography. Gulf General Atomic Report GA-9472 (1969).

5. R. L. Tomlinson (Aerotest Operations, San Ramon, California). Recent Advances in High Resolution Neutron Radiography. March 1970 (unpublished report).

6. G. T. Schnurer et al. "Uses of TRIGA Research Reactors for Engineering Research, Testing and Training." Proceedings of the Panel on Engineering Programmes in Research Reactors. International Atomic Energy Agency, Vienna, Austria (to be published).

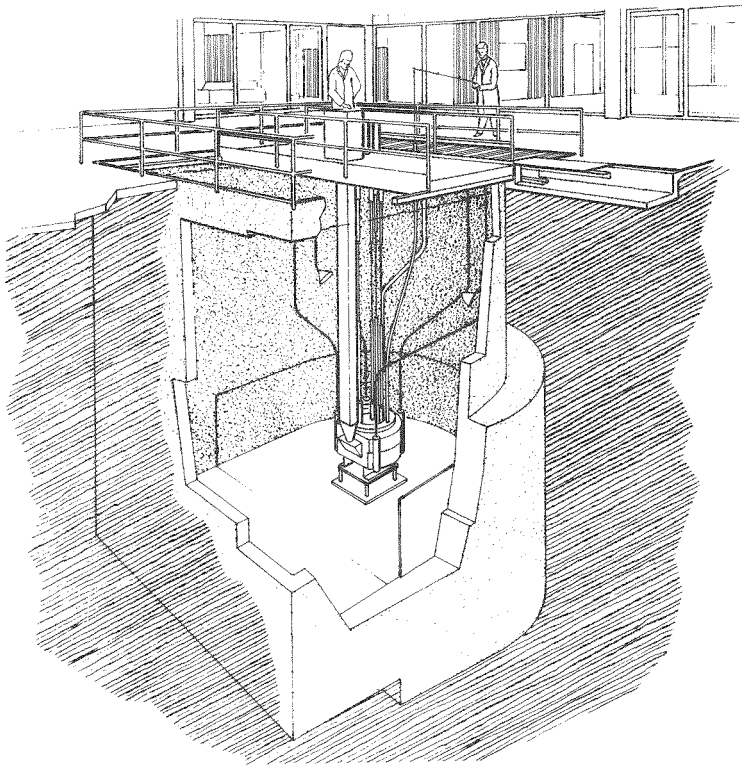

FIG. 1 NEUTROVISION SYSTEM SHOWING TYPICAL MINI-TRIGA INSTALLATION

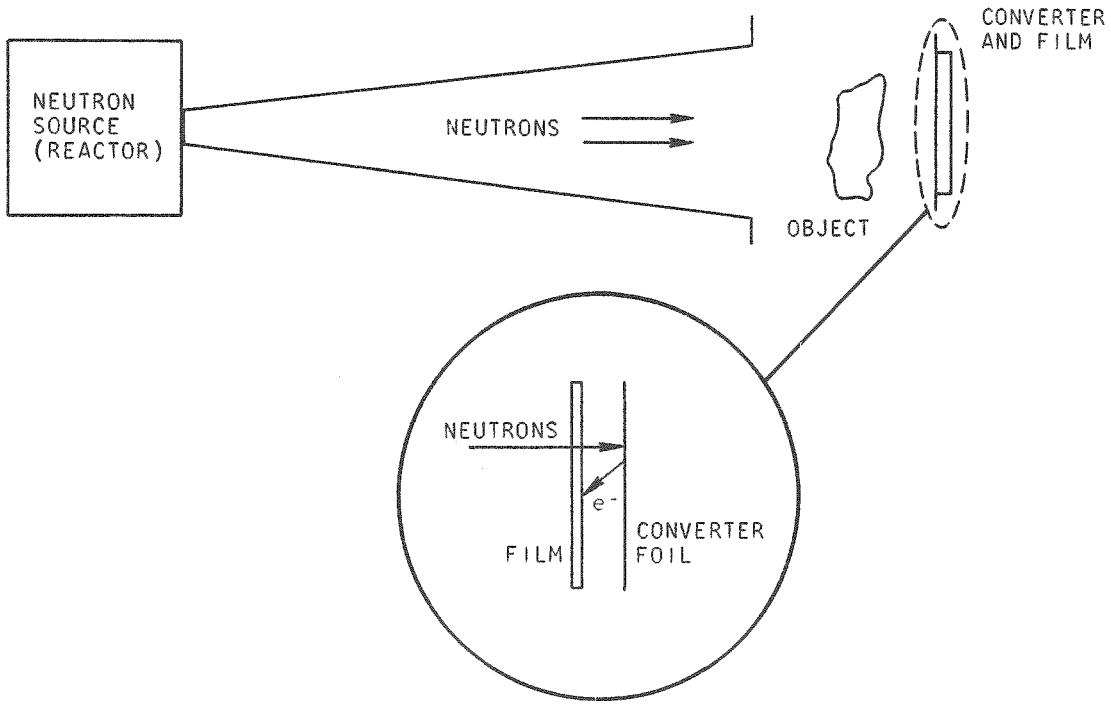

FIG. 2 SCHEMATIC SHOWING ORIENTATION OF SOURCE, COLLIMATOR, OBJECT, CONVERTER, AND FILM

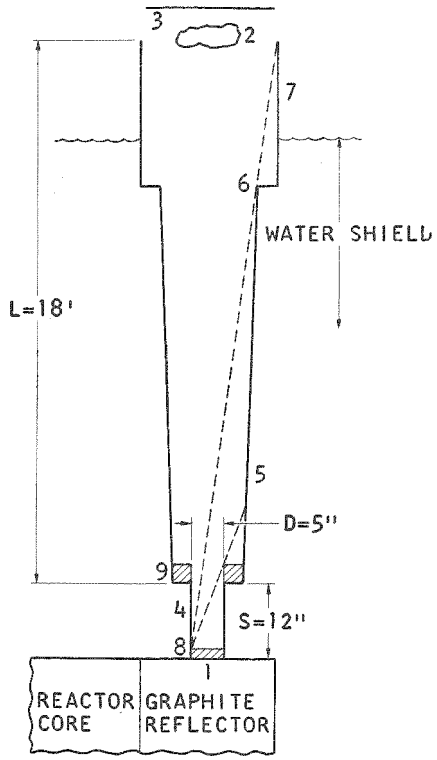

FIG. 3 SCHEMATIC DETAILS OF A NEUTROVISION BEAM PORT SHOWING THE REACTOR SOURCE (1), THE NEUTRON RADIOGRAPH OBJECT (2), THE DETECTOR LOCATION (3), SEVERAL POSSIBLE INTERNAL SOURCES OF PARASITIC RADIATION (4,5,6,7), GAMMA RAY ATTENUATORS (8,9), PRIMARY SHIELDING THICKNESS (S), AND DIMENSIONS (D) AND (L)

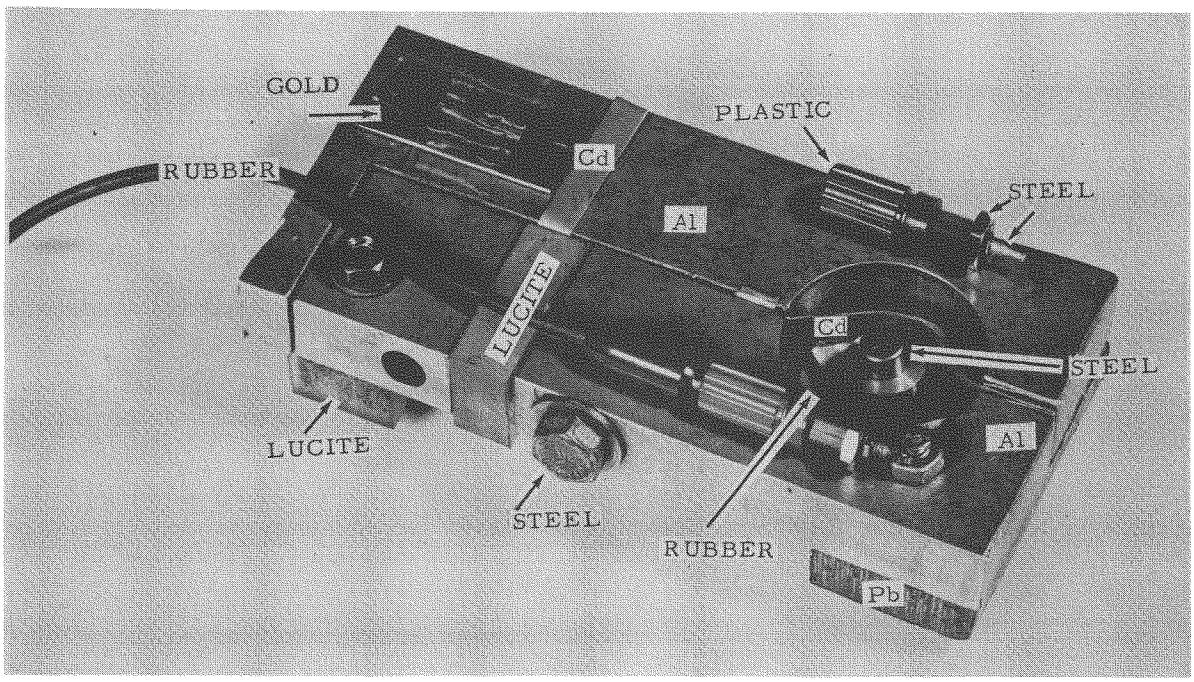

FIG. 4 TEST BLOCK SHOWING MATERIALS USED FOR RADIOGRAPHS IN FIGURE 5

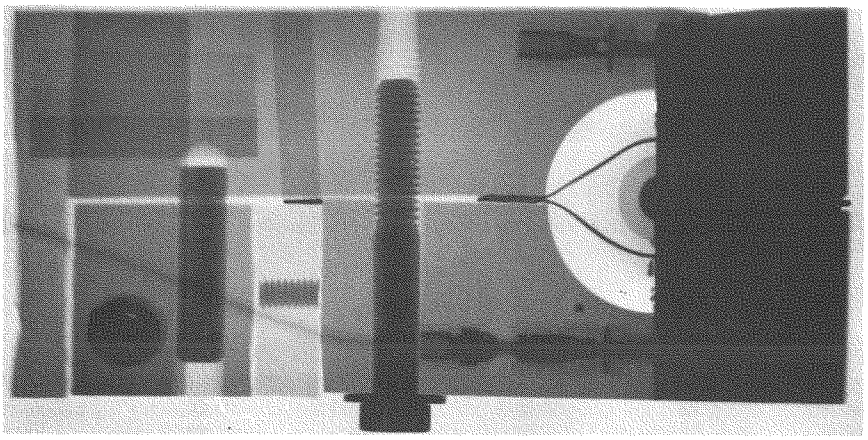

(a)

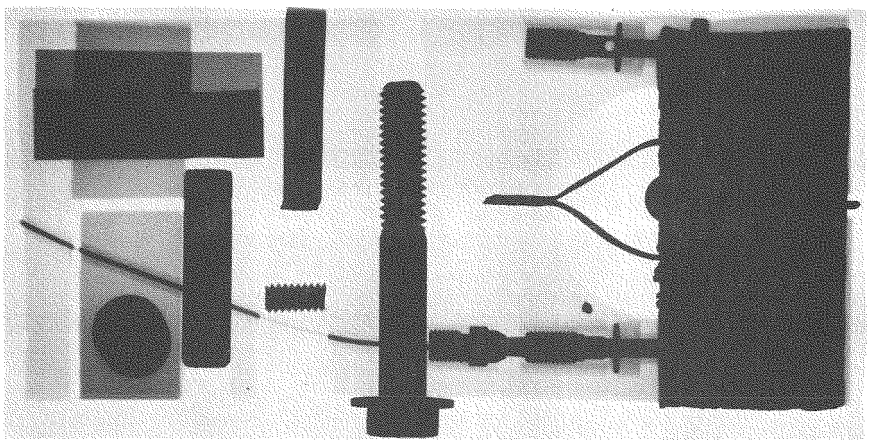

(b)

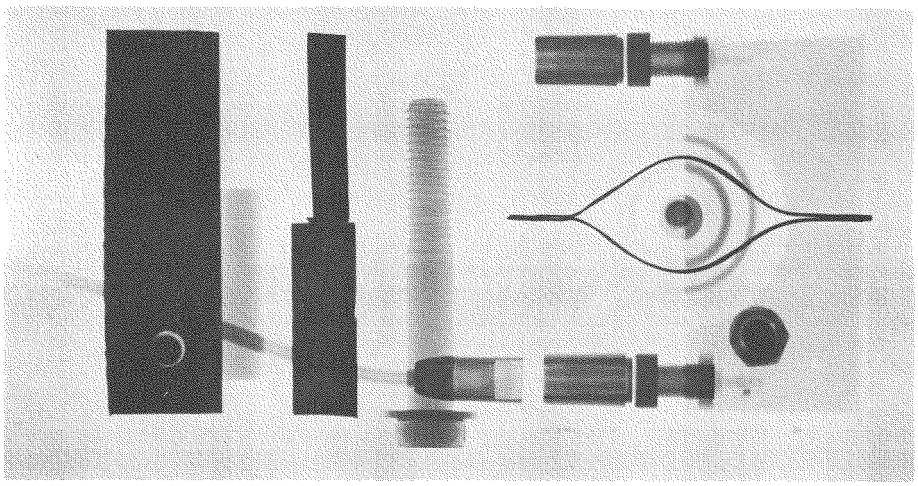

(c)

FIG. 5 RADIOGRAPHS OF TEST BLOCK: (a) GAMMA RADIOGRAPH (USING AN IRIDIUM SOURCE), (b) X-RADIOGRAPH, (c) NEUTRON RADIOGRAPH

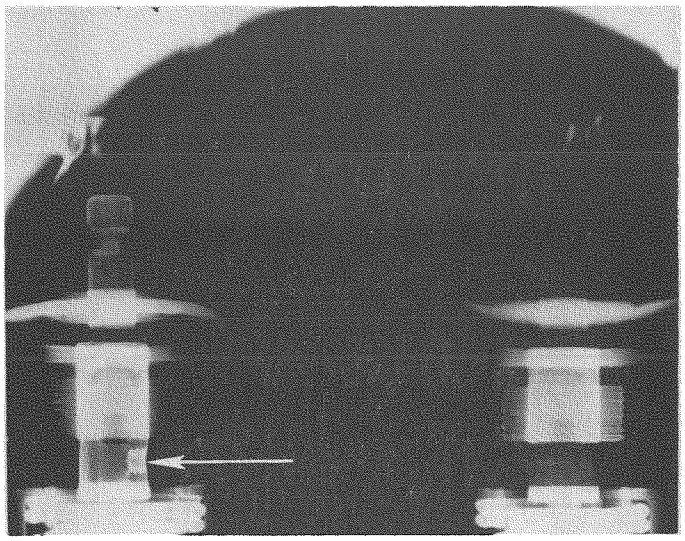

FIG. 6 NEUTRON RADIOGRAPH OF MECHANISM SHOWING PRESENCE (ARROW) AND ABSENCE OF "LOCKTITE" ON IMPORTANT SET SCREW

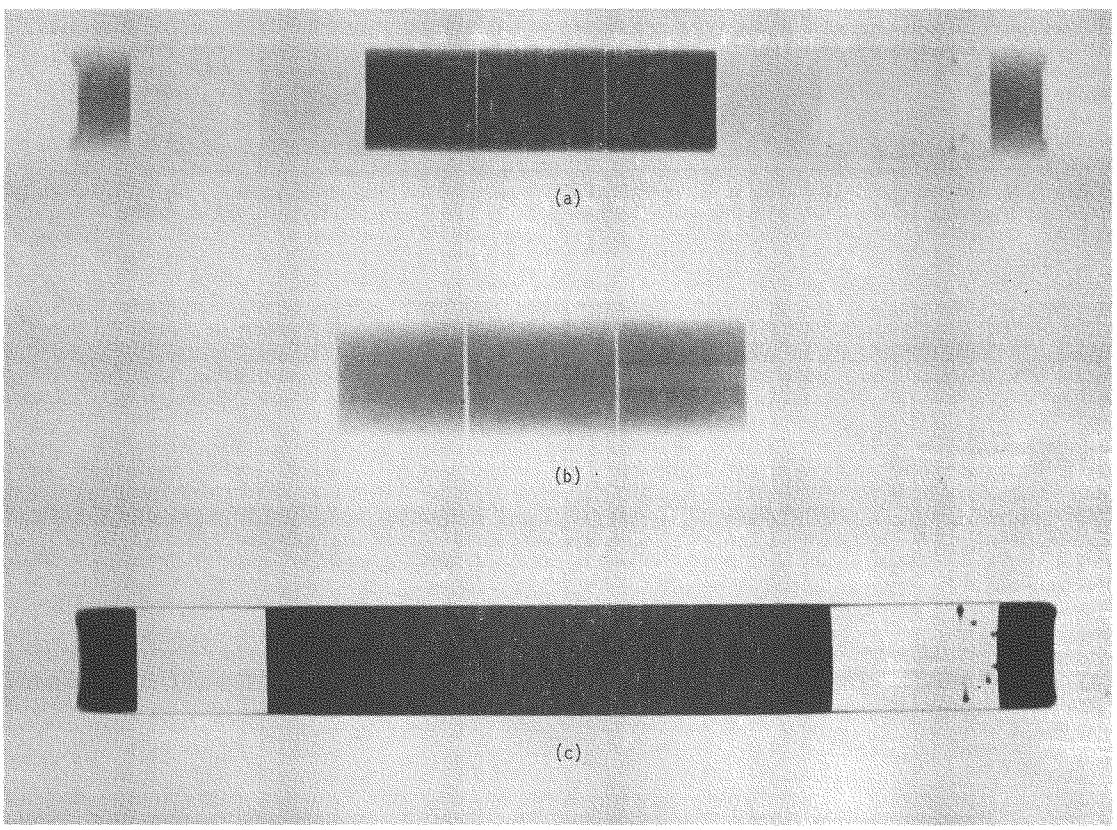

FIG. 7 NEUTRON RADIOGRAPHS (a, b) AND X-RADIOGRAPH (c) OF A SPECIMEN CONTAINING PELLETS WITH VARYING AMOUNTS OF U-235: (a) SHOWS THE NEUTRON RADIOGRAPH OF PELLETS AND CLADDING AND (b) IS A DIFFERENT PHOTOGRAPHIC TREATMENT OF (a) SHOWING THE AXIAL HOLE IN ONE HIGHLY LOADED PELLET

SMALL PULSED REACTOR FOR NEUTRON RADIOGRAPHY, AND UNDERWATER FACILITY USING EXISTING POOL REACTORS

Gerard Farny and Michel Houelle
Commissariat a L'Energie Atomique, France

A very simple inexpensive reactor neutron source has been developed for particular neutron radiography applications. The reactor is based on a solution of uranyl nitrate which is rendered momentarily critical on inward movement of a BeO reflector face, and which then shuts itself down by inherent negative reactivity coefficients. Experimental work has been performed on such an assembly built at the Service d'Etudes de Criticite, and a second assembly built at Cadarache for neutron radiography in the Rapsodie fast reactor program has been in operation for a few months. For this second facility some characteristics are: 2.2 kg ^{235}U critical mass, 93 percent enriched fuel, 2.7 seconds doubling time for 60 grams ^{235}U super criticality. At the exposure peak the power corresponds to 10^{15} fissions per second (30 kw) (5×10^{16} fissions per pulse). Repetition time is 3 hours and for the application of central void examination in fast reactor fuel a collimation ratio of 1:40 gives satisfactory results (3×10^{9} n/cm^2 on Indium converter).

The seven pool reactors of the CEA in France are now equipped with facilities for underwater neutron radiography. The facilities are proving extremely valuable for frequent inspection and measurement on experiments irradiated within the reactors. A typical facility is described which has a divergent collimator of boron carbide, a variable collimation ratio, a field of view of 60 cm vertical dimension, and can accept objects of complex shape by virtue of an ice sealed exposure system. Such facilities are somewhat complex to develop but are simple and reliable in operation.

INTRODUCTION

Although reactor based neutron radiography is now considerably used for the internal needs of the Commissariat D'Energie Atomique (CEA) in France (irradiation rigs, fast breeder fuel development, etc.) the general industrial application of neutron radiography did not get really started until the latter half of 1969. Radiography facilities vary according to their type of application and the type of reactor. They can be grouped into two categories: external beams (1) and underwater beams (2).

Two CEA laboratories have external beam reactor-based neutron radiography facilities operational for industrial work; Centre d'Etudes Nucleaires de Fontenay - aux - Roses (near Paris) and Centre d'Etudes Nucleaires de Grenoble. At the Fontenay - aux - Roses center a commercial company provides the neutron radiography service; they use the reactor Triton, and during the twelve months of 1970 they have dealt with a total of 6,000 objects.

In addition a special small reactor has been built for external beam neutron radiography, and the first part of this paper describes this design. The second part of the paper describes an available underwater facility.

1. DEMAND FOR SMALLER SOURCES

The handicap of a fixed reactor installation far from the client is realized, and it seems probable that if neutron radiography were available with the smaller source convenience of conventional X radiography, the growth would be more rapid. A truly mobile source could probably only be based on an isotopic source (such as ^{252}Cf), and at present the needs for field use neutron radiography are rare in France. By contrast we have already been asked for small installations to be integrated within a laboratory for non-destructive control. Therefore, parallel to studies being performed on accelerator sources at C.E.N. Grenoble we have designed and optimised a small, pulsed, critical assembly for which the safety, the size, and the ratio of performance to price have presented much interest.

The criticality and divergence studies, and the optimization of the apparatus have been carried out on an experimental assembly installed at the criticality laboratory Service d'Etudes de Criticite. (S.E.C.) Subsequently a first prototype has been built at C.E.N. Cadarache providing an inspection facility for nuclear fuel assemblies for the fast reactor Rapsodie.

DESCRIPTION OF THE SOURCE

Neutrons are produced during the free evolution of a divergent chain reaction within a fissile liquid medium rendered critical by the approach of a movable neutron reflector.

The general form of the reactor is shown in Fig. 1. The apparatus comprises principally:

(a) a cylindrical vessel of stainless steel, diameter 300 mm into which the fissile solution is introduced.

(b) a reflector of BeO opposite the lower face, movable vertically by a pneumatique jack.

(c) a chamber for expansion and confinement of gases released during fission.

(d) different systems for measurement of nuclear and physical parameters.

(e) a control panel.

The facility built at Cadarache also includes:

(f) a safety control rod of neutron absorber.

(g) a system for recombination of the gases.

(h) a system for cooling the solution by circulation of cold air.

In the case of the facility built at Cadarache the fissile solution is stationary within the vessel, whereas for the experimental assembly at S.E.C. each approach to criticality is commenced by raising the level of solution in the vessel using a reservoir and a pump.

A side reflector could be placed around the vessel of the S.E.C. assembly, whereas the facility built at Cadarache has no side reflectors.

OPERATION

The volume of fissile solution placed in the vessel is such that with the base reflector separated the assembly is subcritical. With the reflector raised the positive reactivity $\Delta k/k$ is of the order of 500×10^{-5} (0.5 per cent). When the conditions for operation are ready (temperature, pressure, safety, etc.) the control rod is withdrawn and the reflector is moved up. The chain reaction is started with a divergence period of the order of 2 seconds, and the fissile medium is automatically subjected to an inherent shut down mechanism (principally the effect of temperature) which stops the divergence at a peak power level corresponding to 10^{15} fissions per second (30 Kw).

The neutron population thereafter decreases until the shut down of the facility which can be effected either automatically or manually.

CRITICALITY CHARACTERISTICS

The critical mass of the uranyl nitrate solution is 2.2 Kg of ^{235}U when no side reflectors are used, and 1.5 Kg ^{235}U with side reflectors of paraffin 10 cm in thickness. Uranium enrichment used is 93 per cent, and the solution concentration is of order 90 grams per liter of ^{235}U. The power doubling time is 2.7 seconds for the nonreflected system corresponding to a super criticality of 60 grams ^{235}U, and 1.4 seconds for the reflected case corresponding to 30 grams ^{235}U above critical mass.

SAFETY CHARACTERISTICS

The development of a chain reaction of free evolution within a fissile solution of uranyl nitrate has been experimentally studied during the course of the program "C.R.A.C." devoted to examination of criticality accidents and associated phenomena. These studies have shown that the natural shut down mechanism of the chain reaction (due to temperature and gas production) stop the divergence and ensure automatic security for the system. The phenomena used constituted the maximum capable accident condition capable of affecting the installation when the total reactivity is fixed by construction. This is the case for the prototype at Cadarache with fixed fissile content at rest in the vessel, and fixed external configuration.

The lowering of the reflector totally stops the chain reaction due to a high negative reactivity change. In addition, the dropping of the safety control rod

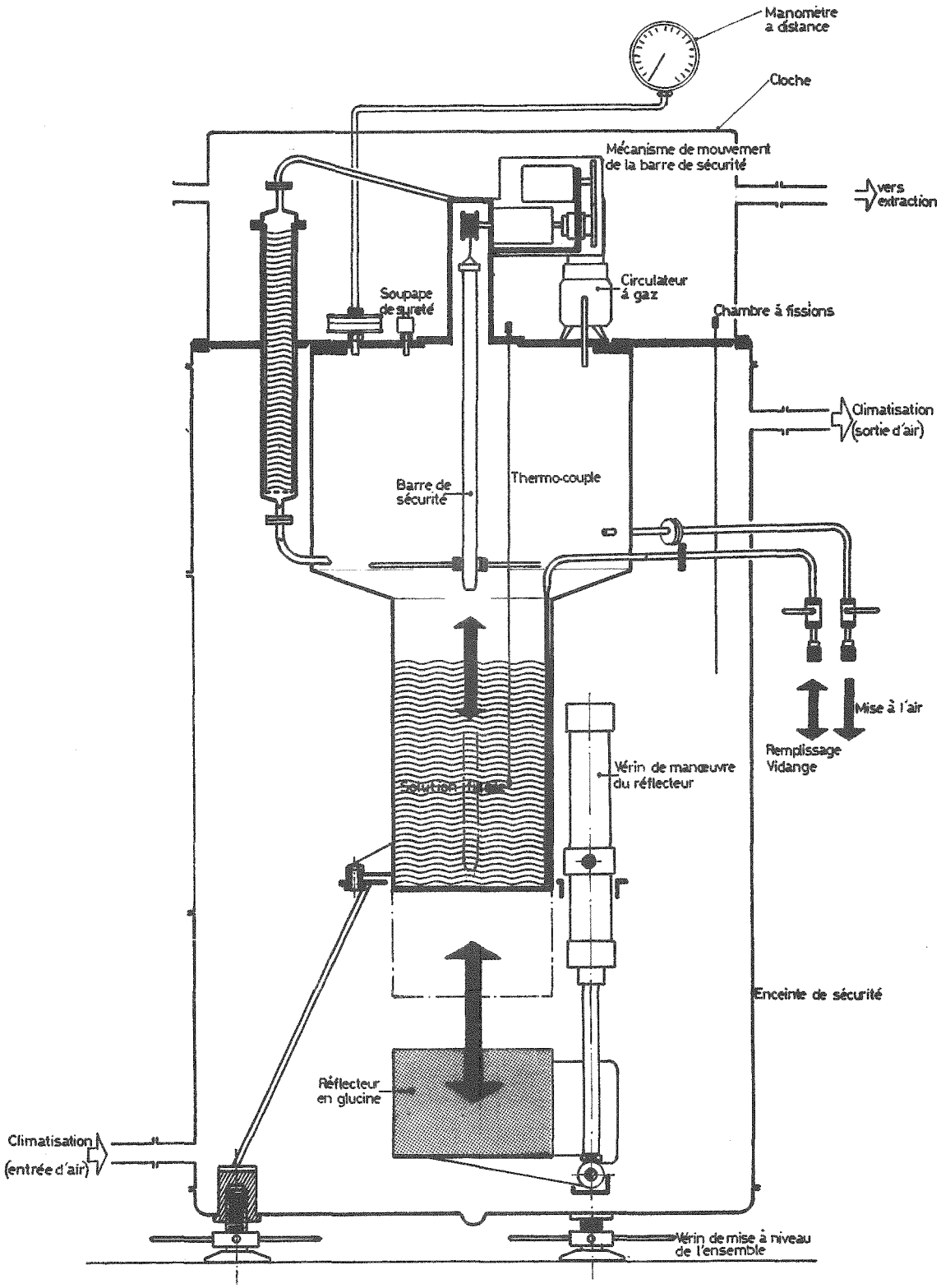

Fig. 1. Small Reactor for Neutron Radiography.

considerably augments the negative reactivity (in the case of the S.E.C. reactor there is complete emptying of the solution from the vessel). This negative reactivity is such that the assembly could undergo a large lowering of temperature without any possibility of unplanned criticality.

The biological shielding is provided by the concrete walls of the cell in which the assembly is operated.

NEUTRON RADIOGRAPHY MEASUREMENTS

Optimization of the neutron radiography design was performed on the experimental S.E.C. assembly where a number of detectors permitted precise evaluation of the effects of changes in collimation, moderator, etc.

In order to approach a permanent design we opted for a beam extended through the protection, approaching the core tangentially at a separation corresponding to the position of peak thermal flux in the moderator. This avoids having a direct view of the reactor core, and considerably limits the gamma radiation while providing a thermal neutron flux equivalent to that for an axial beam. The residual gamma flux of a few roentgens (intergrated over the pulse) is eliminated by a bismuth filter positioned in the beam tube.

A typical single pulse of the reactor produces 5.10^{16} fissions which corresponds to 3.10^{13} n/cm^2 (thermal) in the moderator and about 3.10^{8} n/cm^2 at the object for a collimator of ratio 1:100. We use metallic convertor sheets prepared in our laboratories by a method of deposition using an electron gun. The exposure of 3.10^{8} n/cm^2 for a collimation of 1:100 provides high quality neutron radiographs typically using film Defenix (equivalent to Kodak U.S.A. Type AA).

The prototype reactor built at Cadarache started operation a few months ago. A collimation ratio of 1:40 is used with Indium converter, which is sufficient for the required examination of Uranium-Plutonium fuel pins, and which leads to a neutron exposure nearly ten times higher than the example presented above. Precise examination of the central hole of the fast reactor fuel material is accomplished in this way.

SOURCE DESIGN FOR GENERAL APPLICATIONS

The proposed reactor will have side reflectors and the safety control rod will not be needed. The large negative reactivity will be provided by the retraction of the base reflector and by part, or all of the side reflectors. A cooling system based on circulation of cold liquid will permit operation at 15 minute intervals. Biological protection will be provided by concrete blocks positioned against the side reflectors. Tangential or axial beam tubes will be provided through the protection blocks. The possibility of introducing a flux trap is not excluded, although for simplicity the present systems do not have this.

Applications in addition to neutron radiography can be envisaged for this type of neutron source and these are being considered. Two possible applications are for activation analysis and for fabrication near a hospital of short half life radioelements for medical use.

2. SUBMERGED FACILITIES FOR POOL REACTOR

In France the research reactors are generally of the pool type. In these reactors are placed numbers of rigs which maintain experimental samples under controlled temperature and pressure during the irradiation. It is advantageous to examine the experiments under the pool water, thereby using the biological shield of water to protect against radiation from the capsule. The extremely high gamma emission of these capsules makes inspection by X-radiography very difficult, and in addition submergence of a suitable X-ray facility is a very expensive task. Therefore, neutron radiography finds an immediate application avoiding problems of radiation source and radiation protection. This first and important application has greatly contributed to the rapid development of neutron radiography within the C.E.A. and also to extension of the applications to industry. Such underwater neutron radiography facilities now operate for the reactors Melusine, Isis, Osiris, Pagase, Peggy, Siloe, and Triton.

The design of these neutron radiography facilities pose two principle problems: the collimation and the elimination of water throughout the trajectory of the neutrons.

In order to detail the adopted solutions we will describe the neutron radiography facility for the reactor Osiris which is similar in principle to the others mentioned above.

COLLIMATION

The form of the collimator design is illustrated in Fig. 2. One facility of the type described has been photographed before installation in the reactor pool, and this is shown in Fig. 3.

The intense source flux of neutrons permits a very good collimation to be used, and the actual length is only limited by the dimensions of the pool. The collimator length is 220 cm. The part of the rig to be inspected usually corresponds to the height of the reactor core, i.e. 60 cm. In order to avoid having to take multiple exposures the exposure field of the collimator is therefore 60 cm in the vertical dimension. The shape of the collimator is rather like a pyramid with a flattened top pointed toward the reactor neutron source. In order to compensate for eventual variations in flux at the collimator input end, the diameter of this end is made variable (from 2 mm to 16 mm) by means of a diaphragm controlled by the rod (Fig. 2, No. 8). The neutron absorbing walls of the collimator are of boron carbide which permits epithermal as well as thermal neutron radiography. Aluminum, which is effectively transparent to neutrons, is used in the construction of the apparatus. The thermal neutron flux at the object is about 10^7 n/cm^{2}sec, which is considerably greater than the ambient background neutron intensity in the water at the same distance from the core. Exposure times of about 10 minutes are typical.

ELIMINATION OF WATER

Water has a large scattering cross section for neutrons. There must therefore be no trace of water in the path of the neutrons between input diaphragm and detector screen. The collimator itself (Fig. 2, No. 1) is sealed and filled with helium. The capsules to be examined are of variable and complex geometry and this complicates the problem of water elimination. A supplementary container is used to enclose the portion of the capsule to be radiographed. (Fig. 2., No. 2). The isolation from the water in the pool above the container is accomplished by a seal of ice (Fig. 2, No. 5). A refrigeration unit (Fig. 2, No. 7) provides and maintains the ice seal during the exposure period. With the seal made, the water is forced out of the container by compressed air. The combination of collimator, object, and detector foil cassette (Fig. 2, No. 3) are held together by means of a hydraulic jack (Fig. 2, No. 6). Films of water at positions A and B (Fig. 2) are initially formed due to deformation of the aluminum structure under the water pressure at the depth of 10 meters, but these films too are eliminated by the compressed air. Thus, from the source all the way to the convertor foil, there is no trace of water during operation, and the few small thicknesses of aluminum have negligible effect on the radiographic quality. The complete facility makes possible neutron radiography of highly acceptable definition and there is no unacceptable distortion at the high or low extremities of the field of view.

OPERATION

The neutron converter foils which we have in use do not have the complete length of 600 mm. Neutron radiographs are therefore taken in a single exposure by placing three converter foils end to end. An example of a routine neutron radiograph taken with this facility is printed as Fig. 4.

For neutron radiography of this type only transfer method neutron imaging is used due to the presence of high gamma radiation both from the object and from the reactor core. Dysprosium foil is used for thermal neutron radiography and indium foil for epithermal work.

The facility is relatively complex to design and manufacture, but is very simple to operate. It typically takes about half an hour to move a capsule from the reactor core and have it set up for neutron radiography; the exposure time itself is short in comparison.

The neutron radiography of rigs is now used very frequently. For example neutron radiography may be relied upon (1) at intervals during an irradiation to make dimensional measurements of change rates, (2) to investigate a capsule malfunction, or (3) before final destructive analysis of the capsule in a hot cell facility.

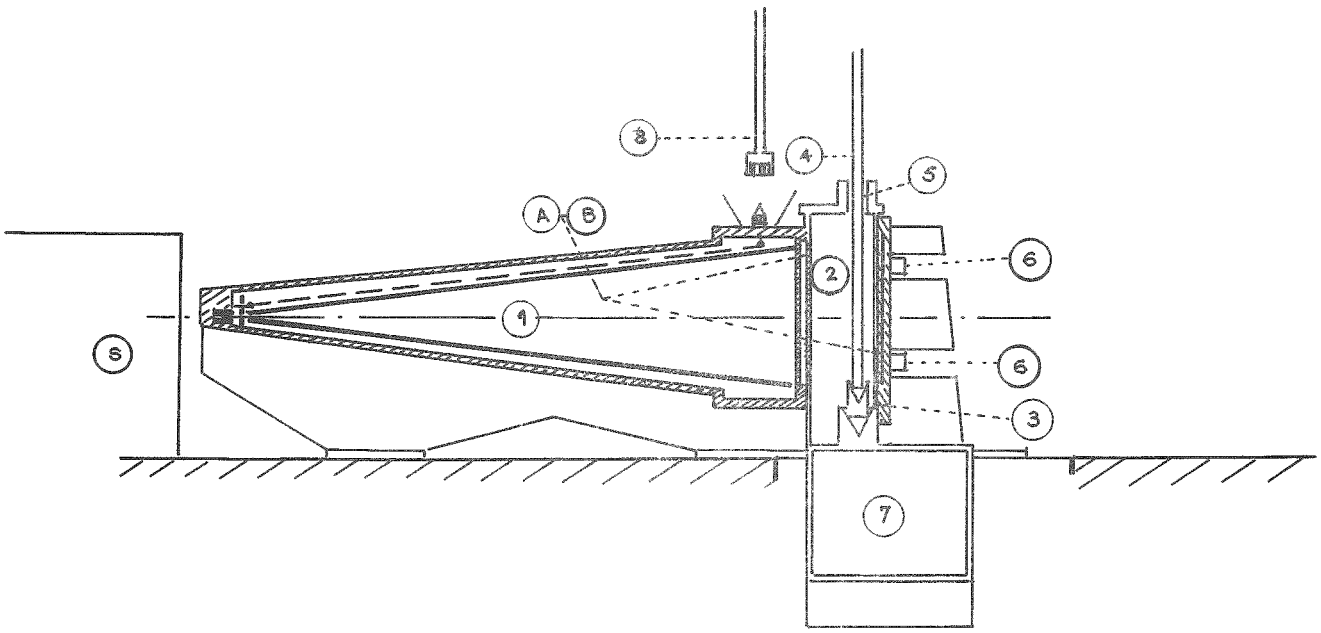

Fig. 2. Underwater Divergent Collimator System for Neutron Radiography.

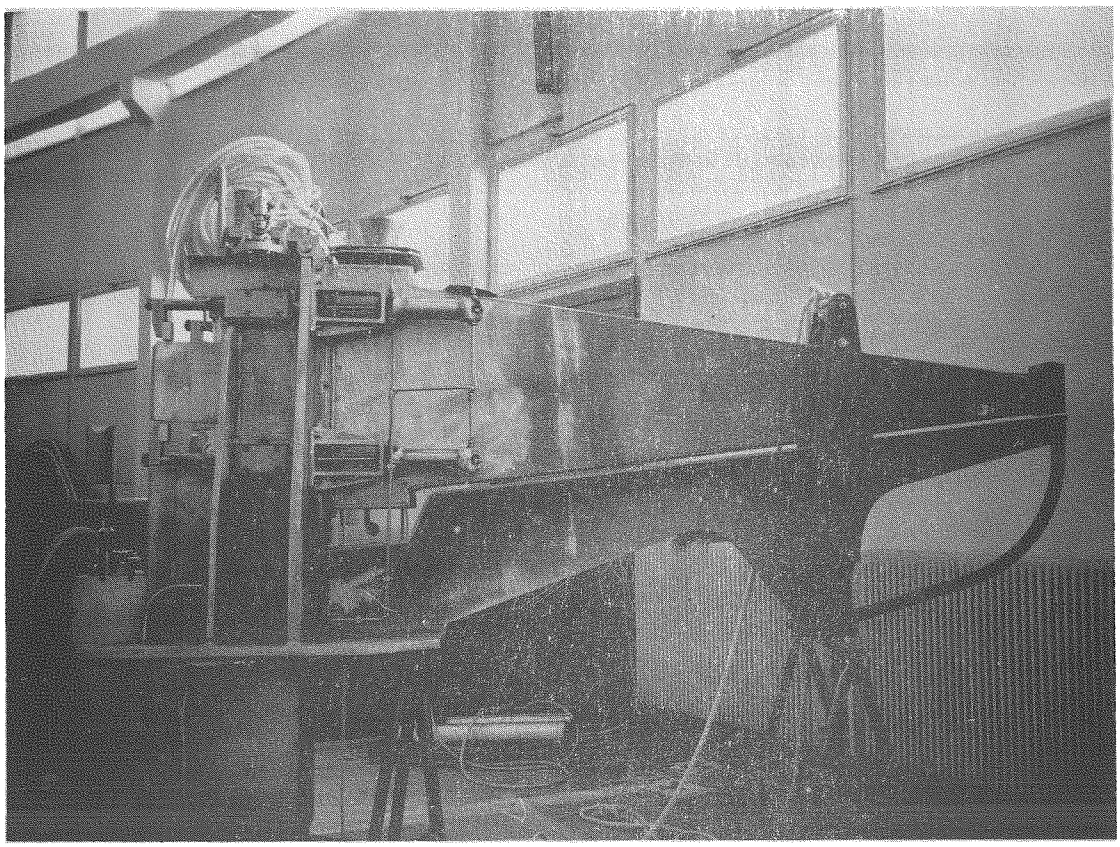

Fig. 3. A Neutron Radiography Facility Before Submergence in the Reactor Pool.

ACKNOWLEDGEMENT

We wish to offer particular thanks to Dr. J. P. Barton for the assistance he has given in the preparation of this paper.

REFERENCES

1. H. Berger, Neutron Radiography. Elsevier Publishing Company. Amsterdam (1965).

2. J. P. Barton and J. P. Perves. "Underwater Neutron Radiography Using a Conical Collimator." British Journal of Nondestructive Testing 8, 79-83 (1966).

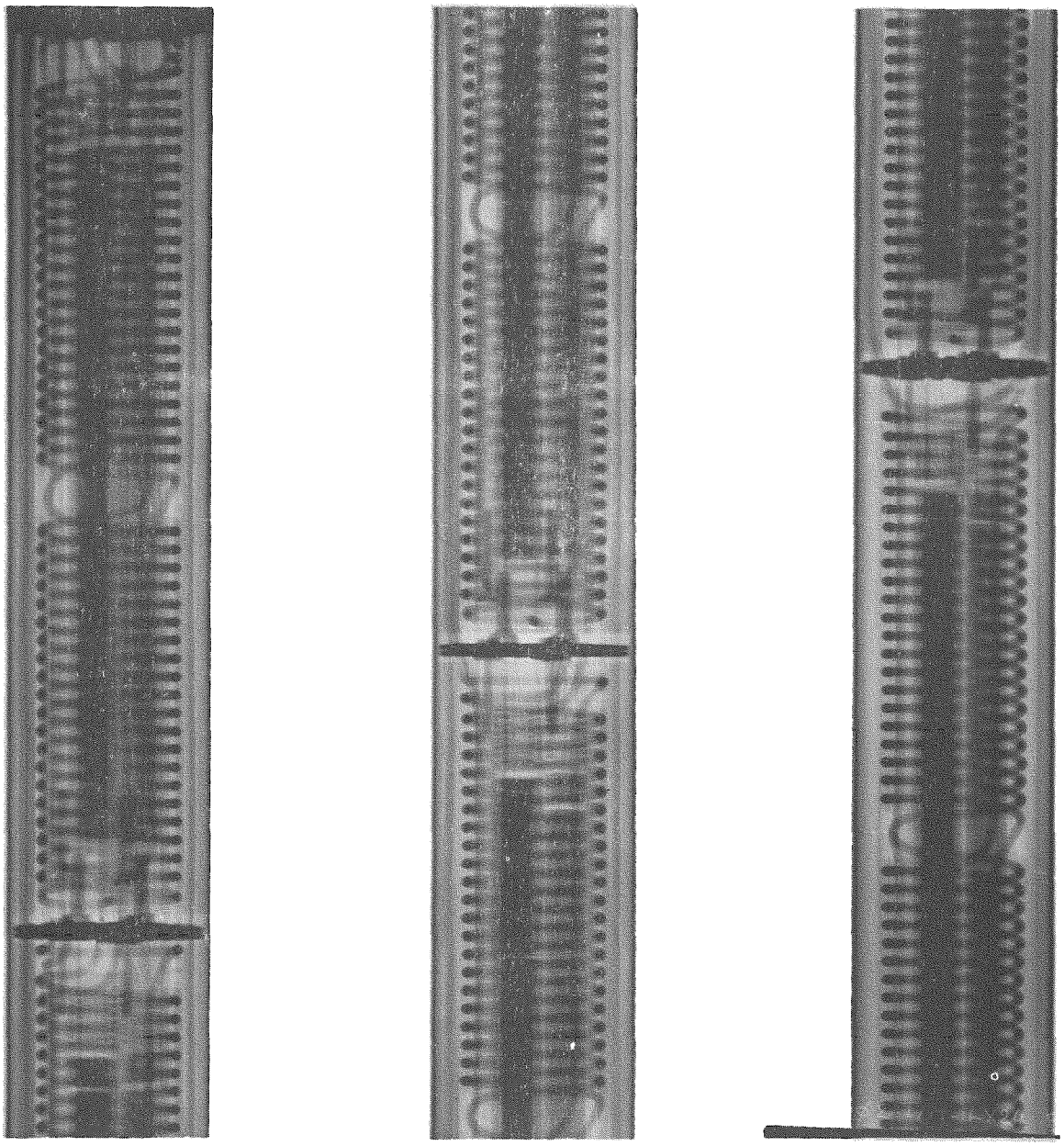

Fig. 4. A Print of a Neutron Radiograph Taken on the Underwater Facility.

^{88}Y – A NEW REPLACEMENT FOR ^{124}Sb IN A NUCLEAR MATERIALS ASSAY SYSTEM

Lorenz A. Kull and J. R. Beyster
JRB Associates
La Jolla, California

Mario E. Schillaci
Los Alamos Scientific Laboratory
Los Alamos, New Mexico

A number of neutron sources have been studied for application in nondestructive assay systems for fissionable material under the auspices of the AEC Nuclear Materials Safeguards Program. One of the assay devices which showed promise of providing useful assay data on the fissile content of low to moderate enrichment samples was designed around an ^{124}Sb-Be source. A survey of photoneutron sources shows that the ^{124}Sb-Be source is an adequate, but not the optimum choice for this assay application. From a technical standpoint, the ^{88}Y-Be source is a better source than the ^{124}Sb-Be for a fissile material assay system. However, up to now the economics of the situation have dictated that ^{124}Sb be used in building a practical device. Recent studies have shown that certain high energy accelerators in the 10^8-10^9 eV range can be used to produce high yields of radioisotopes which are not readily produced in reactors or low-energy cyclotrons at the present time. This paper presents a feasibility study showing the ^{88}Y sources could be produced at the Los Alamos Meson Physics Facility (LAMPF) at a cost which competes favorably with ^{124}Sb in the present application. Details of the source preparation are included.

INTRODUCTION

A number of relatively new techniques exist today for non-destructive assays of material to determine its fissionable material content. The interest in this technology has been fostered by the requirements of nuclear material safeguards for effective accountability and control of special nuclear material in the nuclear fuel cycle. A large amount of work performed on the initial study, the eventual development, and finally the implementation of practical fissionable material assay apparatus has been sponsored by the AEC Nuclear Materials Safeguards program (1).

Among the methods of assay which have received attention in the past year, are a class of techniques which employ isotopic neutron sources to stimulate characteristic and measurable responses from fissionable material in the samples being assayed (2, 3, 4, 5). Desirable characteristics which these devices have either already demonstrated or show potential for eventually achieving are: compact size, relatively low cost, simple operation, and low maintenance. They therefore offer attractive possibilities for eventual widespread use in the nuclear fuel cycle for the measurement of a variety of sample configurations.

One of the devices which has shown promise for providing useful data on the fissile content of low to moderate enrichment samples is designed around an ^{124}Sb-Be isotopic neutron source. This paper describes a possible replacement for the ^{124}Sb-Be source which would require little or no change in the assay apparatus itself. This replacement source, ^{88}Y-Be, should prove to be more effective for fissionable material assays than the ^{124}Sb-Be source, and could be available in sufficient quantities at economical prices in the near future.

APPARATUS DESCRIPTION

The ^{124}Sb-Be assay device is designed around a neutron source with the physical characteristics listed in Table I. The energy of the ^{124}Sb-Be neutrons is well below the neutron fission threshold of common fertile materials (for example, for ^{238}U the effective neutron fission threshold is about 1.4 MeV and for ^{232}Th it is about 2.0 MeV). On the other hand, it is high enough to provide reasonably good penetration into the sample under assay. The ^{124}Sb-Be neutrons cause fissions in the sample's fissile material. The higher

TABLE I

^{124}Sb-Be Neutron Source Characteristics

$\tau_{1/2}$	- 60 days
n/sec per Ci [a]	- 3×10^6
Average Neutron Energy [a]	- ~27 keV
γ - Exposure Rate (1 meter from an unshielded source)	- 1R/h per Ci

[a] The yield and average energy of the source neutrons depends on the amount of beryllium surrounding the ^{124}Sb source; additional beryllium around the ^{124}Sb source increases the neutron yield, but moderates the neutron energy spectrum.

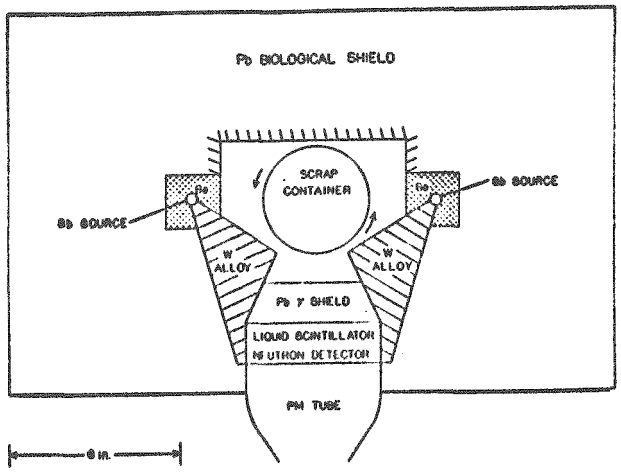

FIG. 1 ASSAY DEVICE FOR SCRAP CONTAINERS

energy prompt fission neutrons (the average fission neutron energy is about 2 MeV) are then detected with a proton recoil or similar detector which is insensitive to the lower energy source neutrons. The neutron detector's response to the source gamma rays is eliminated by the use of a pulse shape discrimination circuit which differentiates between gamma ray and neutron events in the detector. A simple conceptual design of a system for assaying low to moderate enrichment scrap containers is shown in Figure 1 (2). The layer of lead and other high-Z material surrounding the source is used to reduce the gamma background in the neutron detector and serves as a radiation shield for personnel operating the device.

Variations of this design could be utilized for the assay of fuel rods, fuel plates, and other configurations commonly found in the fuel cycle. These assay devices could be used to determine the fissile material content of a number of fertile-fissile fuel mixtures which have been used including ^{238}U - ^{235}U, ^{232}Th - ^{233}U, ^{232}Th - ^{235}U, and others.

^{88}Y VERSUS ^{124}S

A survey of photoneutron sources has shown that the ^{124}Sb source is an adequate, but not optimum choice for the assay system described above. The physical characteristics of the ^{124}Sb-Be and ^{88}Y-Be sources are compared below in Table II.

TABLE II

^{124}Sb-Be and ^{88}Y-Be Source Characteristics

	^{88}Y-Be	^{124}Sb-Be
Half-life	107 days	60 days
n/sec Ci	3×10^6	3×10^6
Average Neutron Energy	200 KeV	27 KeV
γ - Exposure Rate (1 meter from unshielded source)	1R/h per Ci	1R/h per Ci

It can be seen that the ^{88}Y-Be neutron source has a higher average neutron energy implying greater sample penetrability. The half life of ^{88}Y-Be is nearly twice as long as that of ^{124}Sb-Be so that ^{88}Y-Be source replacements are necessary about half as often. The neutron source intensities per Curie of activity and the gamma exposure rate are almost identical for both sources so

that the shielding design is the same for both sources. From a technical standpoint, the ^{88}Y-Be source is obviously a better source than the ^{124}Sb-Be for a fissile material assay system.

Why hasn't the ^{88}Y-Be source been considered up to now for assay work? The answer lies in the economics of producing these sources. The present price for producing ^{88}Y in a cyclotron facility is about $40,000/Ci. The cost of producing moderately large ^{124}Sb sources in a reactor is about $30/Ci. Therefore, up to now, cost considerations have dictated that ^{124}Sb be used to build practical assay systems of the type described above.

NEW PRODUCTION FACILITIES FOR ^{88}Y

Recent studies have shown that certain high energy accelerators in the 10^8 - 10^9 eV range can be used to produce high yields of radioisotopes which are not readily produced in reactors or lower energy cyclotrons. The Los Alamos Meson Physics Facility (LAMPF), now scheduled for operation use in January, 1973, could be used to produce a number of radioisotopes previously unavailable in large quantities. In particular, it will be able to produce ^{88}Y in batches of 10^1 - 10^2 Ci. Another accelerator which could produce reasonable quantities of ^{88}Y is the 200 MeV high current injector for the AGS accelerator at Brookhaven. The following details for producing ^{88}Y at the LAMPF facility have been worked out to illustrate the feasibility of the method.

^{88}Y and other radioisotopes can be inexpensively produced with a high energy accelerator, such as the LAMPF machine, because the accelerator can be used primarily to perform other tasks, while a beam stop of appropriate materials is activated with "used" beam. For ^{88}Y production, the activation target consists of seven pieces of zirconium dioxide, each 0.35 cm thick and about 15 cm in diameter (total thickness = 2.45 cm). The target is divided into sections for ease in handling during radiochemical processing. Typical targets in this facility will be 10 cm or more thick, so that additional radionuclides can be produced at the same time as ^{88}Y by including other materials in the beam stop.

A computer program was used to calculate the ^{88}Y yields assuming a 0.5 ma beam of 700 MeV protons irradiates the target. The thick target yields were conservatively calculated assuming a constant cross-section throughout the target thickness ($\sigma(^{88}Sr(p,n)^{88}Y) = 44$ mb). Details of the calculation are presented in another paper given at this meeting (6). The results of the calculation show that if the zirconium targets were irradiated for one ^{88}Y half life of 107 days, the calculated ^{88}Y activity would be 210 Ci/target. If the target thickness were increased by a factor of 6 (total thickness $\simeq$ 15 cm), the activity would be increased roughly by a factor of 3 (about 630 Ci).

After irradiation, the zirconium oxide target is moved from the beam stop area to a hot cell for radiochemical separation of the ^{88}Y. An ion exchange column is used to perform the separation. It is estimated that two hot cells would be required for two days to handle the 2.5 cm thick zirconium oxide target. The proposed procedure for separating the ^{88}Y is given below:

1. Dissolve in 3L of 9M HF; the added acid would contain a few mg of Y carrier and possibly 3 gm of $MgCl_2$.
2. Filter the YF_3 and MgF_2.
3. Dissolve the filter cake (this should have a volume of about 5-8 ml) in either boric acid and dilute nitric acid or in aluminum nitrate and dilute nitric acid.
4. Extract several times with a phosphate ester such as dibutyl phosphate to remove the last traces of Zr.
5. Extract the Y into tributyl phosphate by proper adjustment of pH and salting agent concentration. Wash this organic phase several times with concentrated nitric acid to remove rare earths (liable to be present as impurities in the target material), this wash step

should also give good decontamination from Sr and Rb.

6. Y is back extracted from the organic phase with water and precipitated as the hydroxide. It might be pure enough for use at this point. Otherwise -

7. Dissolve the precipitate in dilute hydrochloric acid and absorb on a cation resin, wash with dilute acid then elute the Y in a very small volume of a complexing agent such as pH adjusted ammonium lactate or alpha hydroxy-isobutyrate.

8. Mount or convert to desired form for use.

A cost estimate for the materials and labor, but not including hot cell time, is given in Table III.

TABLE III

Cost Estimate for Producing Ten - 20 Ci ^{88}Y Sources[a]

Zirconium Target (ZrO^2)	$ 50
Chemicals	50
^{88}Y separation (labor)	150
Encapsulation (labor + material)	750
Total	$1,000
Cost per Source[b]	$ 100

[a] These prices do not include the cost of hot cell time.

[b] The cost for producing only one 10 Ci source would be about $350.

The cost of hot cell time is uncertain--if the cells are not busy, there may only be a charge for labor and materials (included in the above estimate). The cost as calculated above is at least a factor of one hundred lower than the present cost of producing ^{88}Y. It is also somewhat lower than the cost of about $1,200 for producing two ^{124}Sb sources in succession (with half-lives about half that of the ^{88}Y). Not included in this comparison with the ^{124}Sb source is the cost of transporting the sources from the production site to the user location. Air freight costs for a 1500 lb shipping container range from $225 to $375 per 1000 miles. The larger cost incurred in transporting two ^{124}Sb sources compared to only one ^{88}Y source could be offset somewhat by a shorter distance between producer and user for the reactor produced ^{124}Sb. It is clear from the above discussion, however, that under some circumstances the ^{88}Y source could definitely be less expensive to use than the ^{124}Sb source.

In order to make a rough estimate of the total production of ^{88}Y required per year to show that it could be a practical alternative to ^{124}Sb, consider the following example. Assume 20 assay devices were in use and each required a new 20 Ci source every 5 months (~ 1.5 ^{88}Y half-lives). The total activity required per year would be less than 1000 Ci/year or only about 5 single targets per year. This requirement would not appear to strain the isotope production capability of the LAMPF facility. In practice, one would probably use more targets and irradiate them for shorter times in order to keep up a steady supply of ^{88}Y. This simple example points out that the LAMPF facility alone could provide adequate source replacement service to a fair number of assay units operating in the field.

It is therefore clear from the above that the LAMPF facility and possibly other high energy accelerators could produce ^{88}Y in sufficient quantities and at low enough cost to warrant using it in place of ^{124}Sb for this Nuclear Material Safeguards application. This study is just one particular example of new approaches to problems in a number of fields, which will be made possible with the advent of these new sources of radionuclides.

ACKNOWLEDGMENTS

The authors want to thank Dr. J. W. Barnes of the Los Alamos Scientific Laboratory for his help in defining the radio-

chemical procedures for separating ^{88}Y from the zirconium targets. They also wish to thank Dr. W. Higinbotham and Dr. E. Weinstock of the Safeguards Technical Services Organization at Brookhaven National Laboratory for their helpful comments and suggestions during the progress of this work.

REFERENCES

1. Proceedings of the AEC Symposium on Safeguards Research and Development. WASH-1147 Los Alamos Scientific Laboratory, Oct. 27-29, 1969.

2. J. R. Beyster and L. A. Kull. Safeguards Applications for Isotopic Sources (to be published as a TSO-BNL report).

3. G. R. Keepin, R. A. Forster, H. O. Menlove, H. A. Walter, and J. L. Parker. Nuclear Safeguards R&D. LA-4523-MS, p. 11.

4. T. Gozani and D. G. Costello. "Isotopic Source Assay System for Nuclear Materials." Trans. Am. Nuc. Soc. 13, 746 (1970).

5. S. Untermyer. "Nuclear Fuel Assay". Electrical World, 36 (1968).

6. H. A. O'Brien, Jr. and M. Schillaci. "Isotopic Neutron Sources from the Los Alamos Meson Physics Facility." Topical Meeting on Neutron Sources and Application, Augusta, Georgia (1970).

MODERATOR INVESTIGATIONS ON ^{252}Cf FOR NON-DESTRUCTIVE ASSAY OF FISSIONABLE MATERIALS

R. A. Forster
H. O. Menlove

Los Alamos Scientific Laboratory
Los Alamos, New Mexico

The Nuclear Safeguards Research Program at the Los Alamos Scientific Laboratory includes the application of radioactive neutron sources to the assay of fissionable materials. Radioactive sources provide inherent simplicity and reliability at nominal cost, although they lack some of the flexibility and high intensity of accelerator neutron sources. The source which has received the most attention is ^{252}Cf. Neutronics calculations using the DTF-IV neutron transport code have provided "tailored" neutron spectra for different moderator configurations. Folding in these spectra with appropriate sample cross sections and detector responses yields detector counting rates, signal-to-background ratios, and fissile-to-fertile reaction rates. By considering various moderators it is possible to increase substantially the signal from the sample and the signal-to-background ratios. Such calculations have provided guidance for the design of a fuel pin assay assembly to measure the fissile component in low enrichment reactor fuels. A prototype fuel pin assay system has been designed and constructed and will be evaluated in a major industrial fuel fabrication facility.

INTRODUCTION

The Nuclear Safeguards Research Program at the Los Alamos Scientific Laboratory includes application of radioactive neutron sources to the assay of fissionable materials (1, 2). Radioactive sources provide an attractive alternative to accelerator sources for neutron interrogation and assay of nuclear materials because of their inherent reliability and simplicity. They are also well suited for in-plant and field assay applications for the same reasons.

There are two basic techniques for applying radioactive neutron sources to fissionable material assay: modulated and stationary methods. In the first category, either the source or the sample is transferred (e.g., pneumatically) from the irradiation position and counting of the sample begins. Modulation or pulsing is desirable in the case of activation analysis when delayed gamma rays are counted, as well as when delayed neutron response is used as the assay signature. In the stationary methods, the neutron source, fissionable material, and detector remain in a fixed position during the assay. For example, one may use a neutron detector which is biased to count only those neutrons above a given energy (e.g., above ~ 1 MeV). Thus, if the source emits low energy neutrons or if a high energy source is moderated to produce low energy interrogating neutrons, these "source" neutrons will not be counted and the detector will respond only to high-energy fission neutrons from the sample. Another example of a stationary assay method is the resonance self-indication technique (3) in which a beam of neutrons from a moderating assembly passes through the fissionable sample and into a thin fission detector containing the same fissionable isotope as in the sample. Since the fission detector is very sensitive to the resonance absorption lines in the transmitted flux, the fission detector rate gives a measure of the amount of fissile material in the sample.

Neutrons can be produced from radioactive sources by spontaneous fission reactions, (α, n) reactions with light nuclei such as Be, Li and F, and (γ, n) reactions with Be or D. The radioactive neutron source receiving the most attention in LASL's Safeguards group is ^{252}Cf which spontaneously fissions producing neutrons with an energy distribution slightly "harder" (i.e., slightly higher average energy) than a ^{235}U fission spectrum (4). ^{252}Cf has such outstanding

Work performed under the auspices of the U. S. Atomic Energy Commission.

and advantageous features as a high specific neutron yield ($\sim 2.4 \times 10^{12}$ n/g-sec), low cost, reasonably long half-life (2.6 yrs.), and low gamma and heat outputs relative to other sources. Nearly all of the present applications of ^{252}Cf involve assemblies designed to tailor neutron spectra for a particular purpose. The effect of some common moderators on the ^{252}Cf spectrum are discussed in the next section.

MODERATORS FOR ^{252}Cf

The effects of various moderators on ^{252}Cf neutrons must be known in detail in order to design tailoring assemblies for a particular assay application. Six common moderating materials will be compared: three materials - CH_2, ZrH_2 and H_2O - have large slowing down powers ($\xi\Sigma_s$) while the remaining three - Be, C, and D_2O - have large moderating ratios ($\xi\Sigma_s/\Sigma_a$). The slowing down power is a measure of how well a moderator slows down neutrons, while the moderating ratio represents the ability of a moderator to slow down neutrons without capturing them.

Figure 1 shows calculations of the thermal flux versus radius for a ^{252}Cf source in 30-cm-radius spheres of the five moderators. These calculations were performed with the DTF-IV code and 25 group cross-sections. It can be seen that CH_2 and H_2O produce very similar thermal flux spectra, because of their similar H_2 densities. The neutron flux peaks at the center and drops off rapidly with increasing radius resulting in a rather large flux gradient at interior positions for sample irradiations. ZrH_2 yields a similar curve for thermal flux vs. radius. The moderators with the largest moderating ratios yield much flatter thermal fluxes as a function of radius because of less thermal absorption. Beryllium yields a larger flux than D_2O or C because of its larger macroscopic thermal scattering cross-section. Figure 1 shows that both Be and D_2O are more suitable than the other moderators for thermal neutron irradiations involving energy biased detectors which must be suitably displaced from the high-energy ($\bar{E}n \sim 2$ MeV) ^{252}Cf source neutrons. This is illustrated in Fig. 2 which shows a graph of calculated $^{235}U/^{238}U$ ratios, assuming equal masses, versus radius for the various moderators. These large $^{235}U/^{238}U$ ratios ($> 60,000$) show that it is possible to preferentially interrogate the fissile component (^{235}U) in low enrichment or natural uranium. Also, the $^{235}U/^{238}U$ ratio is proportional to the signal-to-background ratio for a detector biased at the ^{238}U fission threshold. At radii greater than 12 cms, Be and D_2O yield $^{235}U/^{238}U$ ratios greater than the hydrogenous moderators. Carbon does poorly because neutrons do not lose much energy per collision.

One method to increase both the thermal flux and $^{235}U/^{238}U$ ratios in the interior of an assembly of a given volume is to surround the ^{252}Cf source with a small sphere of material with a high slowing down power such as CH_2. This hydrogenous moderator softens the neutron spectrum more than would the same volume of high moderating ratio material; however, because of the small volume fraction of the hydrogenous core, the thermal neutron capture in the hydrogen is minimal. In addition, surrounding the entire moderating assembly with a layer of CH_2 increases the thermal flux throughout the assembly as well as providing exterior neutron shielding.

Figures 3 and 4 show calculations of the thermal flux and $^{235}U/^{238}U$ ratios versus radius for some moderator systems composed of CH_2 in the center and periphery, and either D_2O, C, or Be in the intermediate region. The outer radii of the three regions are 5, 20, and 30 cm respectively. The radius of the inner sphere was chosen as 5 cm to maximize the thermal flux in the outer regions of the moderator. The thermal fluxes in Figure 3 for both C and D_2O in the range 5 to 20 cms is greatly enhanced by this technique while the flux in Be remains essentially the same. At a radial position of 20 cm, the thermal flux in the CH_2-D_2O system is slightly greater than the flux at the same position in the pure Be assembly. Figure 4 shows that the largest change caused by the composite moderators is in the $^{235}U/^{238}U$ ratio. Both C and D_2O yield much larger ratios for the composite

systems while the ratio for Be remains essentially unchanged. Therefore, such composite assemblies represent a significant improvement over a one-region moderator for certain assay applications.

DESIGN OF A REACTOR FUEL PIN ASSAY SYSTEM

One application of ^{252}Cf neutron interrogation is in the assay and quality control of fabricated reactor fuels where the sample geometry and position are well known. Specifically, thermalized ^{252}Cf neutrons can be used to interrogate the fuel sample, and the resulting fission neutrons can be counted with an energy biased neutron detector and compared with standard measurements. Such a system is limited to low enrichment or low density fuel because of self-absorption of thermal neutrons in the fuel.

The preceeding moderator calculations and measurements have been used to guide the design of a ^{252}Cf moderator system for the assay of the fissile content of low enrichment fuel rods for power reactors. The moderated neutrons from the ^{252}Cf source interrogate the fuel material and prompt neutrons from the induced fission reactions are counted using energy-biased fast-neutron detectors.

Figure 5 is a schematic diagram of a cylindrical assay device showing the ^{252}Cf source located at the center and the ^{4}He gas fast-neutron detectors located near the sample holes. The ^{252}Cf source is surrounded by a 2-cm-thick tungsten * shell to take advantage of the large cross section of W for inelastic neutron scattering and also to shield the γ-rays emitted in the spontaneous fission of the ^{252}Cf. The adjacent layer of ZrH_2 (4-cm-thick) further moderates the source neutrons by virtue of its large slowing down power ($\xi\Sigma_s$) (i.e., the ZrH_2 performs the same moderator function as the CH_2 core in Fig. 3). In addition the Zr helps in reducing the fast neutron flux by inelastic scattering and aids in the shielding of γ rays. The central hydrogenous core (ZrH_2 plus ~ 20% CH_2) was held to a 6-cm-outer radius because the capture of thermal neutrons by the hydrogen becomes excessive if more hydrogen is added to the central region. The surrounding shell of D_2O (14-cm-thick) further moderates the source neutrons without significant capture of the thermalized neutrons. The outer layer of CH_2 serves primarily as a neutron reflector and also provides additional neutron shielding at the exterior of the system. The Li added to the thin layer of poly-vinyl chloride (PVC) captures a large fraction (> 80%) of the thermal neutrons prior to their leakage into the outer shield. This reduces the exterior γ-ray dose because, unlike neutron capture in B, the capture of neutrons in Li does not produce secondary γ rays.

Reentrant holes to accommodate the samples to be assayed (i.e., fuel pins) are located in the outer cylindrical layer of CH_2 at a radius of 22 cm, (cf. Fig. 5) which is roughly the position where the signal to background ratio reaches its maximum as indicated in Fig. 4.

^{4}He gas tubes were selected as the fast-neutron detectors because: (1) their favorable efficiency for detecting fission spectrum neutrons, (2) their low sensitivity to γ rays, (3) their electronic stability and simplicity and (4) they can be closely coupled geometrically with the fuel rods. To optimize the size and composition of the moderator system for maximum signal-to-background ratio in the ^{4}He detectors, it was necessary to calculate the expected response in the detector for various input neutron spectra as a function of energy bias setting in the detector. By integrating the differential scattering cross section for neutrons in ^{4}He, it is possible to obtain the probability that an incident neutron of a given energy will be counted as a function of detector bias energy. Figure 6 shows the calculated and experimental results for counting rate of a ^{252}Cf source in air as a function of ^{4}He detector bias energy. It can be seen that with the incorrect assumption of isotropic angular distribution in the ^{4}He recoils, the calculations show considerable error. However, when the measured

* The tungsten was in the form of an alloy containing 90% W, 6% Ni and 4% Cu.

angular distributions for (n, ^{4}He) scattering are used (5), the agreement between calculation and experiment is good and the signal to background rate as a function of bias energy can be calculated reasonably well, as seen in Fig. 6.

The results of the signal-to-background ratio at the sample position as a function of bias energy of the ^{4}He are shown in Fig. 7. Several different core configurations are shown for comparison. The signal-to-background is increased ~ 10% and 20% by using ZrH_2 in place of CH_2 and D_2O respectively in the core. It should be noted that the signal-to-background ratio can be further increased by enlarging the outer radius of the D_2O layer (thus increasing the volume of the assay device). However, the principle of diminishing returns enters here inasmuch as the cost of the additional D_2O and other materials increases at a much faster rate than does the signal-to-background ratio.

In the design of the fuel rod assay system, 6 sample holes are included (cf. Fig. 5) to increase the assay capacity of the device. All sample holes can be used simultaneously with negligible cross-talk (< 1%) between adjacent rods because of the shielding effect of the intervening moderator and the energy bias in the ^{4}He detectors. The detectors are biased such that the signal-to-background ratio reaches its maximum; this corresponds to a ^{4}He recoil energy of ~ 0.25 MeV or an incident neutron energy of ~ .4 MeV as can be seen in Fig. 7. The counting rate for a typical 4% enriched fuel rod is calculated to be ~ 1000 cps for a ^{252}Cf source of about 200 μg. Thus it should be possible to measure the total ^{235}U content of 6 fuel rods in less than one minute to a counting statistical accuracy of better than 1%.

The fuel rod assay system described herein has been fabricated at Los Alamos and will be evaluated in the plant production line of a major U. S. manufacturer of power reactor fuel elements.

REFERENCES

1. G. R. Keepin and R. B. Walton. "Nuclear Safeguards Applications of ^{252}Cf." Proc. Symposium on Californium 252, CONF-681032, p. 257, New York (1968).

2. G. R. Keepin, editor. Nuclear Safeguards Research and Development Program Status Report, LA-4523-MS, Los Alamos Scientific Laboratory, Los Alamos, N. M. (1970 and prior).

3. H. O. Menlove, C. D. Tesche, M. M. Thorpe, and R. B. Walton. "A Resonance Self-Indication Technique for Isotopic Assay of Fissile Material." Nucl. Applications 6, 401 (1969).

4. A. B. Smith, P.R. Fields and J. H. Roberts. "Spontaneous Fission Neutron Spectrum of ^{252}Cf." Phys. Rev. 108, 411 (1957).

5. D. I. Garber, et al. Angular Distributions in Neutron-Induced Reactions, Volume I, Z = 1 to 20. USAEC Report BNL 400, 3rd ed., Brookhaven National Laboratory, Upton, N. Y. (1970).

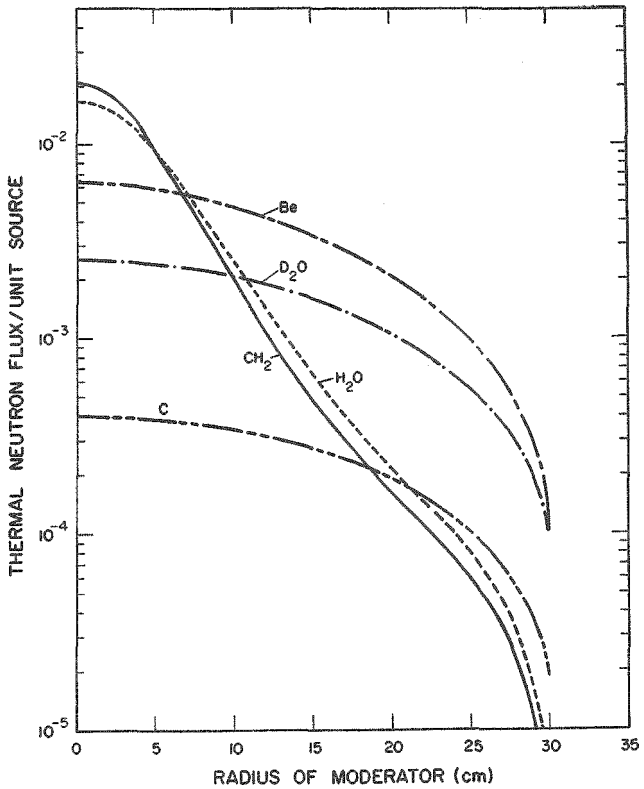

Figure 1. Calculated thermal neutron fluxes vs. radius produced by a ^{252}Cf source in a one-region 30-cm-radius spherical assembly

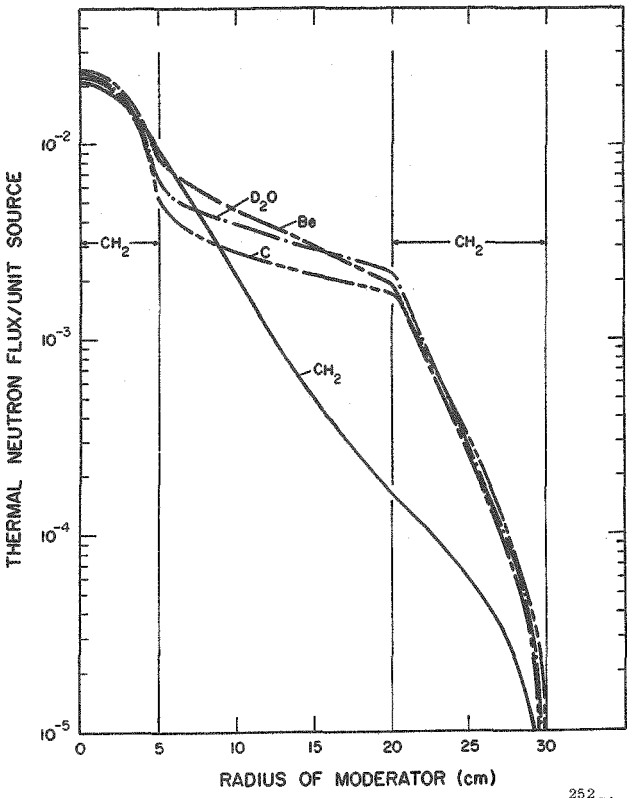

Figure 3. Calculated thermal neutron fluxes vs. radius produced by a ^{252}Cf source in a composite moderator assembly with various moderators in the middle region.

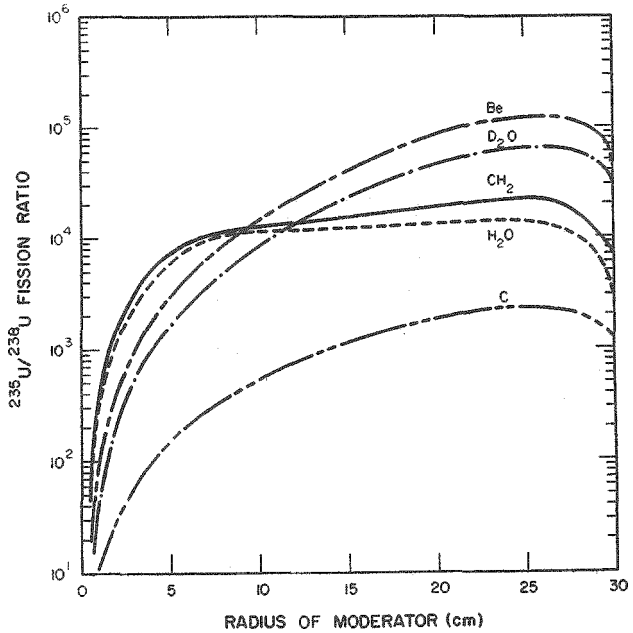

Figure 2. Calculated $^{235}U/^{238}U$ fission ratios (equal masses of both isotopes) vs. radius for a ^{252}Cf source in a one-region 30-cm-radius spherical assembly.

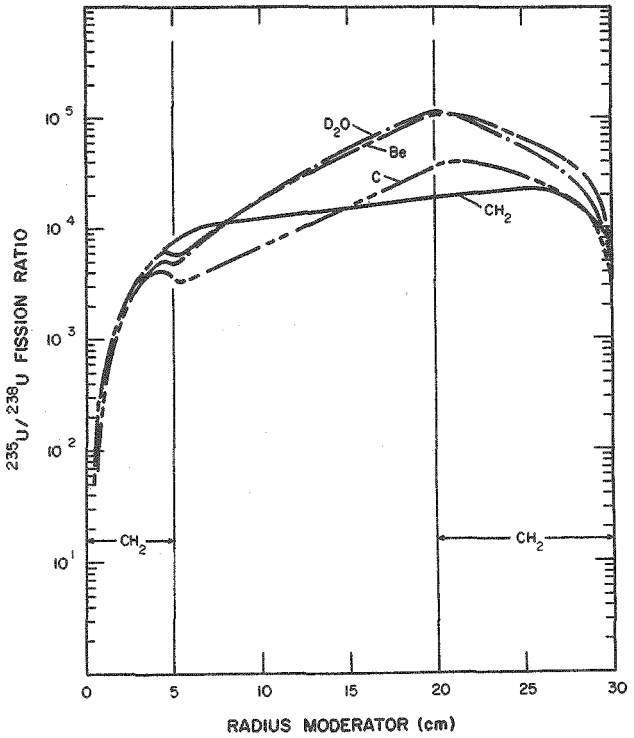

Figure 4. Calculated $^{235}U/^{238}U$ fission ratios (equal masses of both isotopes) vs. radius for a ^{252}Cf source in a composite moderator assembly with various moderators in the middle region.

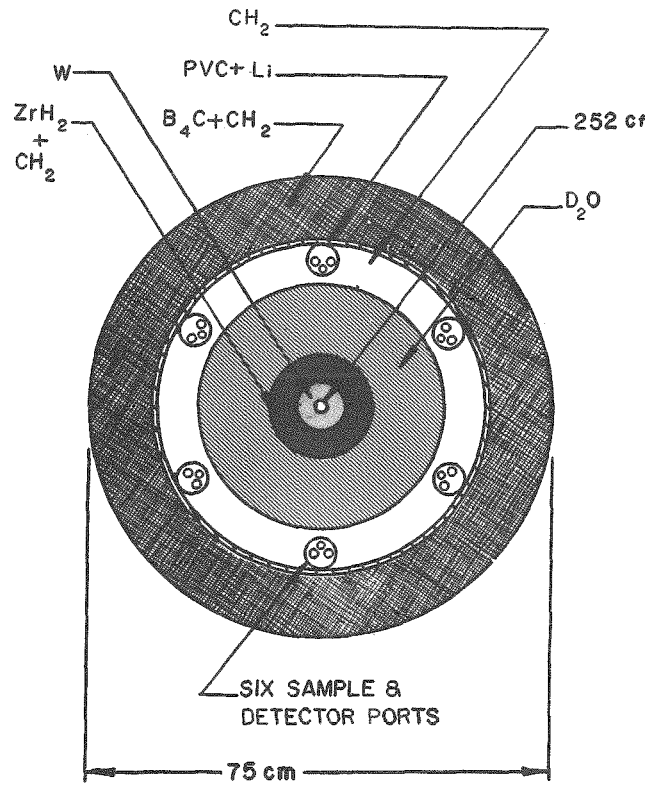

Figure 5. Schematic diagram showing a cross section of the cylindrical composite moderating assembly for the assay of reactor fuel rods.

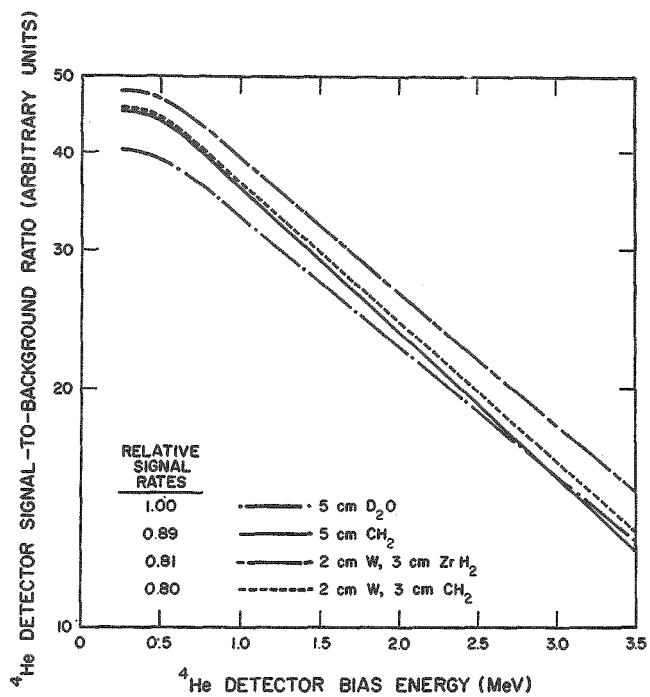

Figure 7. Calculated ^{4}He-detector signal-to-background vs. bias energy for various compositions of the inner 5 cm region surrounding a ^{252}Cf source in a composite assembly. The ^{235}U sample was located in the 10-cm-thick CH_2 shell at a radius of 22 cm with D_2O in the region from 5 to 20 cm.

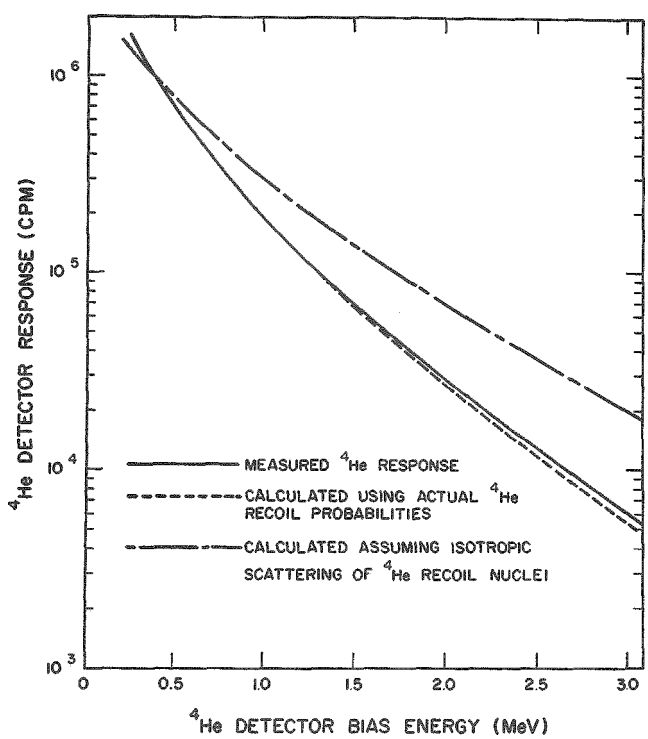

Figure 6. Comparison of experimental and calculated ^{4}He-detector responses vs. bias energy normalized at 0.4 MeV for a ~ 2×10^5 nts/sec ^{252}Cf neutron source in air located 10 cm from the detector.

APPLICATIONS OF NEUTRON SOURCE REACTIVITY EFFECTS TO LOW–POWER REACTOR EXPERIMENTS

Edmondo Pedretti

Lab. Fisica e Calcolo Reattori
Roma (Italy)

The kinetic equations describing the response of a low-power reactor to the step-insertion of an extraneous neutron source have been modified by explicitly introducing the reactivity effect due to the neutron source. Results of measurements performed by the RITMO reactor, in which both positive and negative source effects have been found, are reported. Reactor responses, calculated for both source effects, for various initial reactivities and insertion levels, are shown and compared with responses obtained experimentally. The verification of inversion levels predicted by theory is reported with the description of methods for obtaining linear divergencies and for determining negative constant terms of reactor response when the "reactor plus source" system diverges. Development of a source-drop technique for measuring negative reactivities is described and results of control means calibration are shown. Also included is a discussion of the influence that spatial effects and reactivity-dependence of kinetic parameters may have on source-drop measurements. Corrections due to source effect are specified for the source-jerk technique, for Hogan's differential method and for the transfer function of an oscillating neutron source.

INTRODUCTION

Artificial neutron sources used in nuclear reactor applications, in general have been considered as pure neutron emitters, an assumption that in many cases was justified by actual experimental conditions, such as smallness of the neutron source compared to the dimensions of the multiplying system within which the source was placed. But with the advent of fully enriched, more compact reactor cores it became apparent that the assumption of a pure emitter was not acceptable any more. Effects clearly due to the material of which the neutron source is made were pointed out by Littler (1) and investigated by this author by means of an elementary theory (2). An attempt of explicitly introducing the neutron source effect into the usual one-energy group, space-independent kinetic equations was made in a subsequent work (3) and improved in a recent re-elaboration of such a work (4,5). It is the purpose of this paper to present a general picture of this approach and to show the applications to reactor experiments that it has originated.

THEORETICAL BACKGROUND

Under the assumption that the fundamental space mode of neutron flux within the multiplying system is preserved, one can describe the response of a low-power reactor to the step-insertion of an extraneous neutron source by means of the following one-energy group, space-independent, modified kinetic equations (3)

$$\frac{dn(t)}{dt} = \frac{(K-\Delta)(1-\gamma\beta)-1}{\ell}\, n(t) + \sum_{i=1}^{N} \gamma_i \lambda_i C_i(t) + S \qquad (1)$$

$$\frac{dC_i(t)}{dt} = \frac{K-\Delta}{\ell}\, \beta_i n(t) - \lambda_i C_i(t) \qquad (2)$$

where $\Delta>0$ (or $\Delta<0$), conventionally designated as "source effect" throughout this paper, indicates the decrease (or the increase) of the multiplication factor K caused by the step-insertion of the neutron source into the reactor. As initial conditions, the following equations, equivalent to assuming dynamic equilibrium, will be used

$$n(0) = n_o$$

$$C_i(0) = \frac{\beta_i}{\ell(1-\rho)(\omega_o + \lambda_i)}\, n_o \qquad (3)$$

where $\rho \equiv (K-1)/K$ is the initial reactivity and ω_o the corresponding stable inverse reactor period.

For constant K, S and Δ the solution to eqs. (1) and (2) can be written

$$n(t) = n_c + n_T(t) + n_F(t) \qquad (4)$$

(and similar equation for the precursor density) where the three terms on the right-

hand side denote constant, transient and fundamental (or asymptotic) components respectively.

For $\rho \neq \rho_L$, where $\rho_L \equiv \Delta/(1+\Delta)$ is the initial reactivity for which, after insertion of the neutron source, the reactor diverges linearly, the above components are given by

$$n_c = S\ell \Big/ \left[\Delta - \rho/(1-\rho)\right] \tag{5}$$

$$n_T(t) = \sum_{j=2}^{N+1} n_{j\circ} \exp(\omega_j t) \tag{6}$$

$$n_F(t) = n_{1\circ} \exp(\omega_1 t) \tag{7}$$

where ω_j are the N+1 roots of the inhour equation

$$\bar{\rho} = \frac{\omega\ell}{\omega\ell + 1}\left(\ell + \sum_{i=1}^{N} \frac{\gamma_i \beta_i}{\omega + \lambda_i}\right) \tag{8}$$

in which

$$\bar{\rho} \equiv (K-\Delta-1)/(K-\Delta) = \frac{1-(1+\Delta)(1-\rho)}{1-(1-\rho)\Delta} \tag{9}$$

is the reactivity of the "reactor plus neutron source" system. The amplitude of the exponentials is given by

$$n_{j\circ} = n_\circ A_j + S\, B_j \tag{10}$$

where the coefficients A_j, B_j defined by the following equations

$$A_j = \left[1 - \frac{1}{\ell(1-\rho)} \sum_{i=1}^{N} \frac{\gamma_i \beta_i \lambda_i}{(\omega_j+\lambda_i)(\omega_\circ+\lambda_i)}\right] \Big/ D_j \tag{11}$$

$$B_j = 1/(\omega_j D_j) \tag{12}$$

$$D_j = 1 - \frac{1-(1-\rho)\Delta}{\ell(1-\rho)} \sum_{i=1}^{N} \frac{\gamma_i \beta_i \lambda_i}{(\omega_j+\lambda_i)^2}\,, \tag{13}$$

are both independent of $n_\circ$ and S. In the present case the algebraically largest root ω_1 of the inhour equation (8) is different from zero and the remaining roots are negative. This means that the fundamental component is either a decreasing or an increasing exponential, depending on whether $\omega_1 \lessgtr 0$ i.e. on whether $\rho \lessgtr \rho_L$, while the transient component is equal to the sum of N vanishing exponentials. Furthermore, eq. (5) shows that, for $\rho < \rho_L$, the constant component is positive while it is negative for $\rho > \rho_L$. As for the coefficients it can be shown that they fulfill the conditions

$$\sum_{j=1}^{N+1} A_j = 1 \qquad \sum_{j=1}^{N+1} B_j = -\,n_c/S. \tag{14}$$

For $\rho = \rho_L$ one has $\omega_1 = 0$ and, due to eq. (12), $B_1 = \pm\infty$. By using l'Hospital's rule one obtains for the fundamental component*

$$n_{FL}(t) = Pt \tag{15}$$

where the slope is given by

$$P = S\ell/(\ell + \sum_{i=1}^{N} \gamma_i\, \beta_i/\lambda_i) \tag{16}$$

and, for the constant component*

$$n_{cL} = n_\circ A_1 - S \sum_{j=2}^{N+1} B_j. \tag{17}$$

In this case the fundamental component increases linearly; the transient component, still represented by eq. (6), consists of N vanishing exponentials, and the constant component is always positive. In addition, it must be noticed that the second eq. (14) is replaced by eq. (23) of Ref. 5.

Since the transient component vanishes in any case, one has from eq. (4)

$$\lim_{t\to\infty} \left[n(t) - n_c\right] = n_F(t) \tag{18}$$

which shows that the response of a low-power reactor to the insertion of a neutron source, referred to the constant component n_c, asymptotically gives the fundamental component.

Eq. (10) shows that $n_{j\circ} \gtrless 0$ for $n_\circ \gtrless n_{INV,j}$ where the quantity

$$n_{INV,j} \equiv -\,S\, B_j/A_j \tag{19}$$

can be defined, when positive and finite, as the inversion level of the j-th exponential. Furthermore, eq. (6) and the first eq. (14) show that $n_T(0) \gtrless 0$ for $n_\circ \gtrless n_{INV,T}$ where the quantity

$$n_{INV,T} \equiv -\,S \sum_{j=2}^{N+1} B_j/(1-A_1) \tag{20}$$

can be defined, when positive and finite, as zero initial transient level because insertion of the neutron source into the reactor at a power level $\gtrless n_{INV,T}$ makes the transient component have an initial value $\gtrless 0$. Thanks to eqs. (14) and (17) one has

$$n_{INV,T} = (n_c + S\, B_1)/(1-A_1) \quad \text{for} \quad \rho \neq \rho_L \tag{21}$$

and

---

* Subscript L indicates quantity related to linear divergence.

$$n_{INV,T} = n_{cL} \text{ for } \rho = \rho_L . \quad (22)$$

From eqs. (19) and (21) it can be seen that, for $\rho = 0$ and $\Delta > 0$, the inversion levels and the zero initial transient level are practically coincident with the constant component

$$n_{co} = S\ell/\Delta \quad (23)$$

toward which a critical reactor converges after insertion of a neutron source producing a decrease of K.

MEASUREMENTS OF NEUTRON SOURCE EFFECTS

The simplest and most accurate methods of measuring neutron source effects appear to be based on the utilization of data obtainable, for $\Delta > 0$, from an experiment of source insertion into a critical reactor (Figs. 5a and 7) and for $\Delta < 0$, from an experiment of linear divergence (Figs. 6b and 10). In the first case, if $\bar{\rho}_c < 0$ denotes the final reactivity $\bar{\rho}$ corresponding to $\rho = 0$, eq. (9) yields

$$\Delta = -\bar{\rho}_c/(1-\bar{\rho}_c) > 0 \quad (24)$$

while, in the second case, for which

$\rho = \rho_L < 0$ and $\bar{\rho} = 0$, it gives

$$\Delta = \rho_L/(1 - \rho_L) < 0 . \quad (25)$$

In this way the determination of Δ reduces to the measurements of the negative reactivities $\bar{\rho}_c$ and ρ_L respectively. The value of $\bar{\rho}_c$ can be determined by entering the inhour curve with the negative value of ω_1 obtained from the reading of $n(t) - n_{co}$, which, according to eq. (18), is proportional to $\exp(\omega_1 t)$. The value of ρ_L can be determined by measuring the negative period $1/\omega_o$, once the reactor has been established on the initial subcritical condition required by the linear divergence experiment.

Measurements were performed by the RITMO reactor, a water moderated, beryllium and water reflected flux trap type critical facility, fueled with fully enriched uranium (5,6). The reactor core consists of ten cylindrical fuel elements, located at a distance of about 15 cm from the center (Fig. 1). Source effects were measured with the DIR-1 Assembly (Fig. 2) which was designed to fit the central reactor cavity. Two types of central source holders were used depending on whether the SS-MgO tube had been inserted into the central supporting tube, as in Fig. 1, or not. For the experiments use was made of an aluminum encapsulated 5 Ci Am-Be neutron source NUMEC-AM-154, having an output of 1.7×10^7 neut/sec, a diameter of 2.15 cm and a height of 8.85 cm. The neutron source, held by a nylon string, could be inserted by gravity into any source holder in a drop time not exceeding 0.5 sec and positioned on the reactor core midplane with horizontal tolerances smaller than 0.2 mm. Current delivered by one of the control system compensated ionization chambers, located outside the beryllium reflector on the reactor core midplane, was utilized as signal proportional to reactor power.

In general, commonly used neutron sources produce positive effects. The magnitude of Δ may vary from some tens of 10^{-5} units to values negligibly small, depending on the position, either inside or around the reactor core, in which the neutron source is placed. But the sign of Δ usually comes out to be positive. A rather unusual condition,

TABLE I

Effects due to the insertion of a 5 Ci Am-Be neutron source into the RITMO reactor

Condition of SS-MgO Tube	Source Effect Δ (in 10^{-5} units)	
	Central Source Holder	Peripheral Source Holder
In position	-18.0±0.2	+50.8±1.5
Replaced by water	+10.7±0.2	+60.8±0.9

in which inversion of source effect occurs, was found at the center of the DIR-1 Assembly. Insertion of the neutron source into the central source holder produced negative source effects, such as those shown in Figs. 8 and 10, when the SS-MgO tube was in position, while it produced positive source effects, as those reported in Figs. 7 and 9, when the SS-MgO tube was replaced by water. Insertion of the neutron source into the peripheral source holder originated positive source effects, regardless of the SS-MgO tube being in position or not. The results of the measurements are reported in Tab. I.

INVERSION LEVELS

NUMERICAL ANALYSIS

The dependence of the coefficients A_j, B_j on the initial reactivity ρ and on the source effect Δ is shown in Fig. 3. The corresponding inversion levels $n_{INV,j}$, $n_{INV,T}$ and constant component n_c are reported in Fig. 4. It appears that the inversion level of the fundamental component ($j = 1$) exists only for $\rho < \rho_L$ while the inversion levels of the N transient terms ($j > 1$) exist only for $\Delta > 0$.

TABLE II

Significant cases of initial reactivity

Case No.	Source Effect	Reactivity	
		Initial	Final
1	$\Delta > 0$	$\rho < 0$	$\bar{\rho} < 0$
2	"	$\rho = 0$	"
3	"	$0 < \rho < \rho_L$	"
4	"	$\rho = \rho_L$	$\bar{\rho} = 0$
5	"	$\rho > \rho_L$	$\bar{\rho} > 0$
6	$\Delta < 0$	$\rho < \rho_L < 0$	$\bar{\rho} < 0$
7	"	$\rho = \rho_L$	$\bar{\rho} = 0$
8	"	$\rho_L < \rho < 0$	$\bar{\rho} > 0$
9	"	$\rho = 0$	"
10	"	$\rho > 0$	"

If the neutron source produced no reactivity effect ($\Delta = 0$), there would be only three significant cases of initial reactivity ($\rho \gtrless 0$). When this is not the case, i.e. when $\Delta \gtrless 0$, the significant cases become ten as shown in Tab. II, in which significant initial reactivities ρ are specified with corresponding final reactivities $\bar{\rho}$. For these ten cases reactor responses were calculated by means of eq. (4) for $\Delta \gtrless 0$ and for insertion levels n_o selected on the basis of the computed inversion levels. Due to their outstanding, practical interest only Cases 2, 9, 4 and 7 have been chosen for presentation and short comments.

The results reported in Fig. 5 for an initially critical reactor show that inversions of both the fundamental and the transient components occur for $\Delta > 0$ (Case 2) and that no inversions occur for $\Delta < 0$ (Case 9). The remaining two cases, shown in Fig. 6, refer to linear divergences in which the fundamental and the transient components can be easily separated. In both cases the fundamental component is a linear function of time. Inversion of the transient component occurs only for $\Delta > 0$ (Case 4). Details and further results can be found in Ref. 5.

EXPERIMENTAL VERIFICATION

Experiments were performed by dropping the neutron source into the reactor, for a given initial reactivity, at a given power level, and by recording the current signal delivered by the ionization chamber. Photographs of these recordings are shown in Figs. 7 to 10. Experimental verification of inversion levels for Cases 2, 9, 4 and 7 is reported in this paper; that for Cases 3 and 6 can be found in Ref. 5.

Fig. 7 shows the results obtained in Case 2 with two insertion levels, one lower (left curve) and the other higher (right curve) than the stabilization level n_{co}. Between A and B the reactor is critical. At B, the neutron source is dropped into the reactor. Between B and C the reactor power converges toward n_{co}. At this power level, step-removal and subsequent step-insertion of the neutron source caused no detectable variations of reactor power. The agreement with Fig. 5a is evident.

In Fig. 8 the results obtained for Case 9 are shown. The transient component, observable between B and E, is rising, as for the calculated curve of Fig. 5b. The fundamental component observable between E and L increases exponentially. At L, neutron source is removed and reactor power levels off. Notice that, between E and L, reactor power evolves according to a spurious exponential, because it includes a negative constant component, as appears in Fig. 5b and as will be seen in the next Section.

The results obtained in Case 4 are shown in Fig. 9. Between A and B, the reactor power increases exponentially, according to a previously adjusted initial reactivity $\rho_L > 0$. At B the neutron source is dropped into the reactor at an insertion level lower than all the inversion levels. The transient component observable between B and C is rising, in accordance with the lower curve of Fig. 6a. The fundamental component is rising linearly from C to D on the left part of Fig.

9 and between E and F on the right part of the same figure. At F the neutron source is removed from the reactor. Between G and I the reactor power increases exponentially, as between A and B. At I the neutron source is dropped into the reactor at a power level higher than all the inversion levels. The transient component observable between I and L is descending, in agreement with the upper curve of Fig. 6a. The fundamental component increases linearly from L to M, at which time the neutron source is removed. Finally, the brass dummy source (indicated by 6 in Fig. 2), dropped into the reactor at N, causes reactor power to decrease.

Fig. 10 shows the results obtained in Case 7. Between A and B, the reactor power decreases exponentially according to a previously adjusted initial reactivity $\rho_L < 0$. The transient component, observable between B and C, is clearly rising in agreement with the calculated curve of Fig. 6b. The fundamental component increases linearly from C to D. Transient components observed with different insertion levels always came out to be of the rising type.

As appears from the verifications of Cases 4 and 7, obtaining linear divergences with neutron sources producing positive or negative source effects requires adjustment of the reactor on the correct initial reactivity ρ_L. This may be achieved by a fine control means and by repeating divergence tests until a satisfactory linear behavior is obtained. There are no problems in the case of $\Delta < 0$ (Fig. 10) because removal of the neutron source after the divergence test causes reactor power to decrease. But for $\Delta > 0$ (Fig. 9), reactor power increases after removal of the neutron source, as at F and M of Fig. 9. To leave control means free for the fine adjustment of reactor supercriticality, it was found very convenient to replace, at the end of the linear test, the neutron source with a small absorber (brass dummy source), as shown in Fig. 9 at M and N. In addition, once the correct initial reactivity has been obtained, this procedure can be advantegeously used for investigating different insertion levels.

DETERMINATION OF NEGATIVE CONSTANT COMPONENTS

For $\rho < \rho_L$, the constant component n_c is positive and therefore directly observable as asymptotic stabilization level of reactor power. Also for $\rho = \rho_L$ the constant component n_{cL} is positive; in this case it can be determined simply by extrapolating the linear part of the reactor response back to the source insertion time.

For $\rho > \rho_L$ (Cases 5, 8, 9 and 10 of Tab. II), the constant component is negative. It can be determined by means of the equation

$$n_c = P\left(\ell + \sum_{i=1}^{N} \gamma_i \beta_i / \lambda_i\right) \Big/ \left[\Delta - \rho/(1-\rho)\right] \qquad (26)$$

which is obtained by eliminating the product $S\ell$ from eqs. (5) and (16). This procedure requires the measurement of the slope P, of the source effect Δ, of the reactivity ρ and knowledge of the delayed neutrons parameters (in general ℓ may be neglected). As an example, consider Case 9 of Fig. 8 for which $\rho = 0$ and $\Delta = -18.0\times10^{-5}$. From the straight lines of Fig. 10 the average value $P = 4.2\times10^{-11}$ A/sec can be obtained. Putting these values into eq. (26) and assuming $\sum \gamma_i \beta_i / \lambda_i \simeq 0.1$ sec gives $n_c \simeq -7.8\times3\times10^{-9}$ A, which is about forty times as large as the insertion level $n_o = 0.2\times3\times10^{-9}$ A, and therefore not very accurate. The most accurate determinations of negative constant components occur when n_o is of the same order of magnitude of, or greater than $|n_c|$. In such a case a semilog plot of $n(t)+|n_c|$ appears to be a straight line right after vanishing out of the transient component.

SOURCE-DROP TECHNIQUE

Elimination of the product $S\ell$ from eqs. (5) and (23) gives the relationship

$$\rho = \frac{(1 - n_{co}/n_c)\Delta}{1 + (1 - n_{co}/n_c)\Delta} \qquad (27)$$

which can be used for determining negative reactivities through the measurement of n_{co}, Δ and n_c. One starts with the reactor critical at a power level n_o higher (or lower) than the stabilization level n_{co} (Fig. 11a). When precursor equilibrium is achieved, the neutron source is dropped into the reactor. As a consequence, reactor power evolves toward n_{co}. Knowledge of this response enables one to determine ω_1 and hence Δ. Then reactivity is changed from zero to the negative value to be measured. Consequently, reactor power also changes and reaches a new stabilization level n_c lower than n_{co}. This procedure can be used when reactivity can be changed without endangering the reactor system. When this is not the case, it is necessary, once the stabilization level n_{co} has been reached, to shut the reactor down, to

carry out the variation of reactivity and, finally, to reposition control means (Fig. 11b).

An example of control rod calibration is shown in Fig. 12, in which source-drop measurements (performed without reactor shutdown) are compared with period measurements. Notice that only the first source-drop and the last period measurements (from 88 to 100% withdrawal)were performed practically in the same conditions. This fact may account for the ten percent difference between total rod worths obtained by the two methods. Results of other measurements, carried out by both source-drop procedures, can be found in Ref. 5. Also specified in that work are the precautions to be taken in using the source-drop technique.

The validity of eq. (27) implies the preservation of the fundamental space mode of neutron flux. Obviously, this condition is not fulfilled for large subcriticalities. Consequently, the observed stabilization level n_c contains the contributions of higher harmonics. For a correct use of the source-drop technique these contributions must be either avoided (by proper choice of source and detector position, based on comparison with measurements performed by a reliable technique, such as the pulsed-source method) or taken into account for possible corrections (e.g. by numerical analysis). Another factor that may invalidate eq. (27) is the dependence of $S\ell$ and Δ on the reactivity to be measured. Two-group diffusion calculations performed by the Exterminator code (7) have shown that, for K varying from 1.0 down to 0.85, relative variations of $S\ell$ and Δ as large as 50% are possible. Of course, spatial effects and reactivity-dependence must be considered together. Although present work on the source-drop technique is based on this line of investigation, it can not be excluded that a completely different approach may be necessary to correlate the observed stabilization levels n_{co} and n_c to the unknown reactivity.

CORRECTIONS DUE TO SOURCE EFFECT

Source-jerk technique. If n_c is the equilibrium level of the subcritical reactor with neutron source and n_1 is the "quasistatic" level after removal of the source, it can be shown by the procedure reported by Keepin (8) that the reactivity (of the reactor only) is given by the equation

$$\rho/\gamma\beta = \left[n_1 - n_c(1-\Delta)\right]/(n_1 - n_c\,\gamma\,\beta\,\Delta) \qquad (28)$$

the right-hand side of which reduces to the well known form $(n_1-n_c)/n_1$ for $\Delta = 0$.

Differential method. By eliminating the product $S\ell$ from eqs. (5) and (16) one obtains for a subcritical reactor

$$K - 1 = -P\left(\ell + \sum_{i=1}^{N} \gamma_i\,\beta_i/\lambda_i\right)/n_c + \Delta \quad . \qquad (29)$$

Apart from different notation, this equation differs from Hogan's formula (9) only for the presence of the source effect Δ, which appears as a correction term but that becomes important when the reactivity to be measured is comparable with the source effect.

Transfer function of an oscillating neutron source. For a neutron source oscillating within a low-power reactor characterized by the multiplication factor K, the time variations of Δ and S, in the small amplitude approximation for which the transfer function is defined, can be written

$$\begin{aligned} \Delta(t) &= \Delta + \Delta_p \exp(j\,\omega\,t) \\ S(t) &= S + S_p \exp(j\,\omega\,t) \end{aligned} \qquad (30)$$

where Δ_p and S_p are small perturbations of Δ and S. Consequently, one can write for the linear variation of neutron density

$$n(t) = n_c + n_p \exp(j\,\omega\,t) \qquad (31)$$

and a similar equation for precursor density. By standard methods one obtains

$$n_p/n_c = F\,W_s(j\omega) \qquad (32)$$

where

$$F \equiv \left[\,(\Delta + 1-K)S_p/S - \Delta_p\,\right]/\gamma\,\beta \qquad (33)$$

is a coefficient depending on the magnitude of the impressed variations of source parameters, and

$$W_s(j\omega) = \gamma\,\beta \Big/ \left\{ j\omega \left[\ell + (K-\Delta) \sum_{i=1}^{N} \frac{\gamma_i\,\beta_i}{j\omega+\lambda_i} \right] + \Delta - 1 - K \right\} \qquad (34)$$

is the reactor transfer function for the oscillating neutron source. Notice that, for $\Delta = \Delta_p = 0$, eq. (32) reduces to a form in agreement with the equations given by Langsdorf (10) for a pure neutron source. Furthermore, it may be interesting to point out that eq. (34) practically coincides, for

$\Delta = 0$, with the transfer function of a subcritical reactor with steady neutron source (see eq. (10-13) and Fig. 10-9 of Ref. 8).

Amplitudes and phase shifts of $W_s(j\omega)$ have been calculated for various degrees of subcriticality, with U-235 delayed neutron data taken from Tables 4-7 and 4-14 of Ref.8. As shown by the curves reported in Figs. 13 and 14 the influence of a typical source effect is rather small for large subcriticalities. The source effett causes both gain and phase lag to decrease significantly only when the reactor is slightly subcritical.

REFERENCES

1. D.J.Littler."A Method of Calibrating Neutron Sources Absolutely" Proc.Phys. Soc., 68A, 638 (1951).

2. E.Pedretti."Effect of an External Neutron Source on a Subcritical, Critical and Supercritical Reactor" Energia Nucleare, 9, 65 (1962).

3. E.Pedretti."Reactor Transient and Reactivity Effects due to an Extraneous Neutron Source" Energia Nucleare, 12, 254 (1965).

4. E.Pedretti."Neutron Source Inversion Levels and Source-Drop Technique for Negative Reactivity Measurements" Nucl.Sci. & Eng., 35, 149 (1969).

5. E.Pedretti. Study of Neutron Source Effects on the Low-Power RITMO Reactor and Development of a Source-Drop Technique for Reactivity Measurements, CNEN Report, RT/FI(69)11, Roma 1969.

6. E.Pedretti. First Criticality and Calibration Experiments of the RC-4 RITMO Reactor. CNEN Report, RT/FI(67)7, Roma 1967.

7. T.B.Fowler et al. Exterminator - A Multi-Group Code for Solving Neutron Diffusion Equations in One and Two Dimensions, ORNL-TM-842, Oak Ridge National Laboratory, Oak Ridge, Tennessee (1965).

8. G.R.Keepin. Physics of Nuclear Kinetics. p.251, Addison - Wesley Publ. Co., Inc., Reading, Massachussets (1965).

9. W.S.Hogan."Negative-Reactivity Measurements" Nucl.Sci. & Eng., 8, 518 (1960).

10. A.Langsdorf, Jr. The Thermal Neutron Reactor as an Instrument for Measuring Neutron Cross Sections. AECD - 3194, Argonne National Laboratory, Lemont, Illinois (1950).

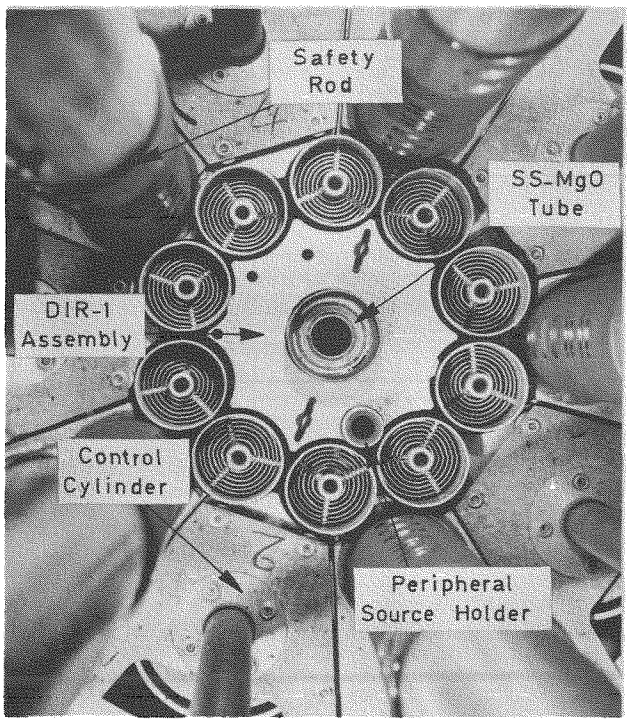

Fig. 1. Top view of the RITMO reactor core (without central source holder).

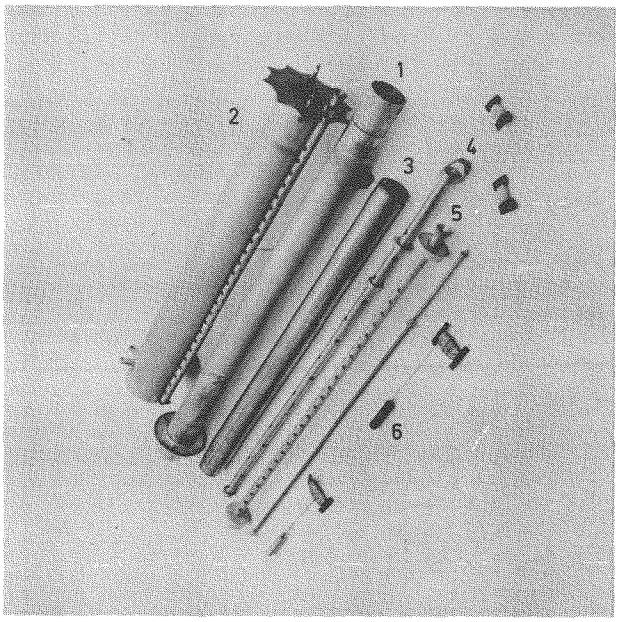

Fig. 2. Parts of the DIR-1 Assembly.
1. Al central supporting tube;
2. Al sleeve and peripheral source holder;
3. SS canned MgO tube;
4 and 5. Al central source holders;
6. Brass dummy source.

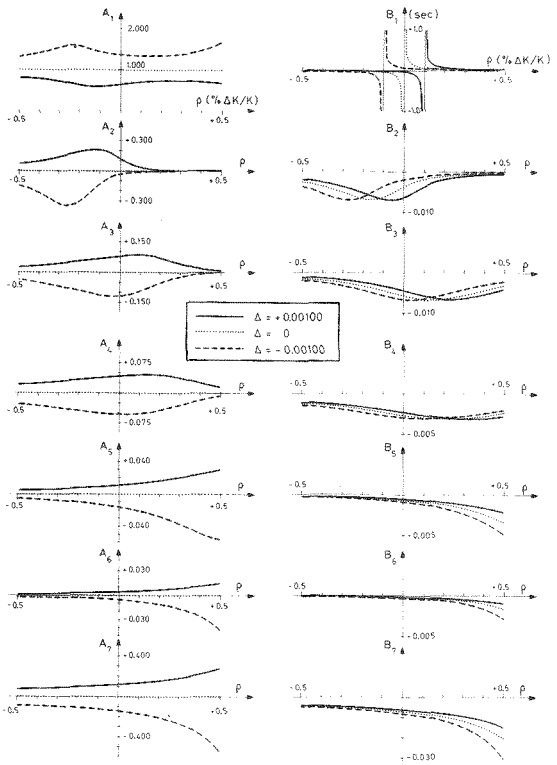

Fig. 3. Coefficients A_j and B_j.

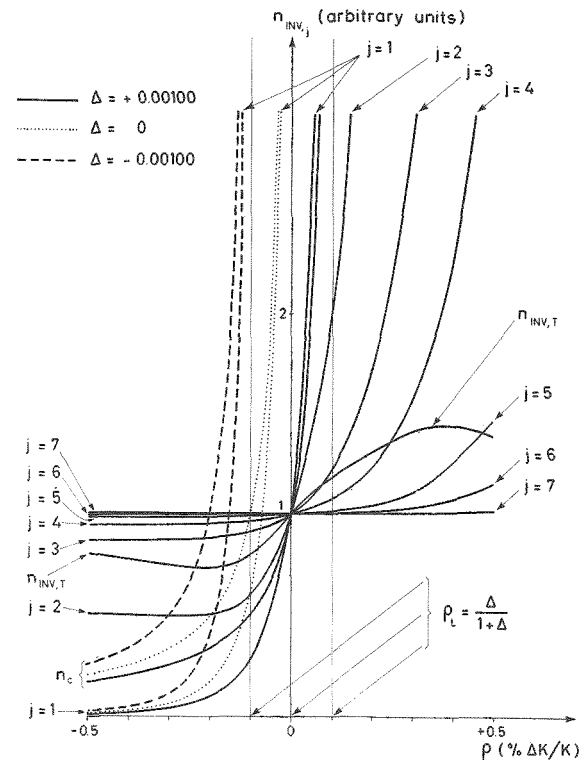

Fig. 4. Inversion levels and constant components (normalized to $S = |\Delta| / \ell$).

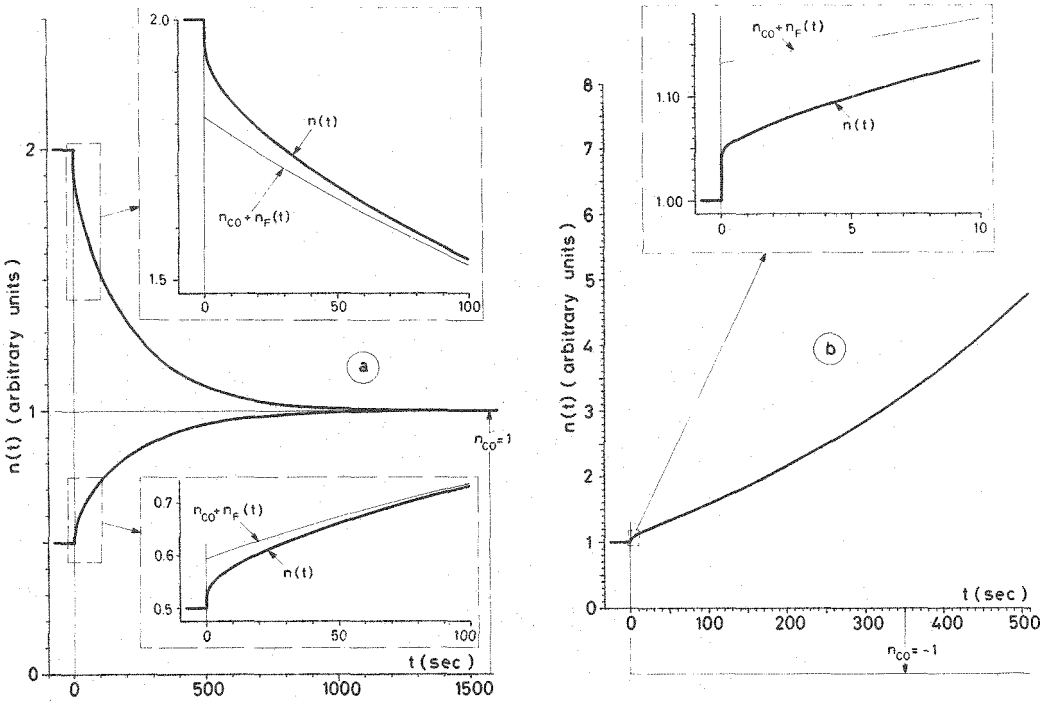

Fig. 5. Calculated responses of a critical reactor to the step-insertion of a neutron source with:
a. $\Delta > 0$ (Case 2); b. $\Delta < 0$ (Case 9).

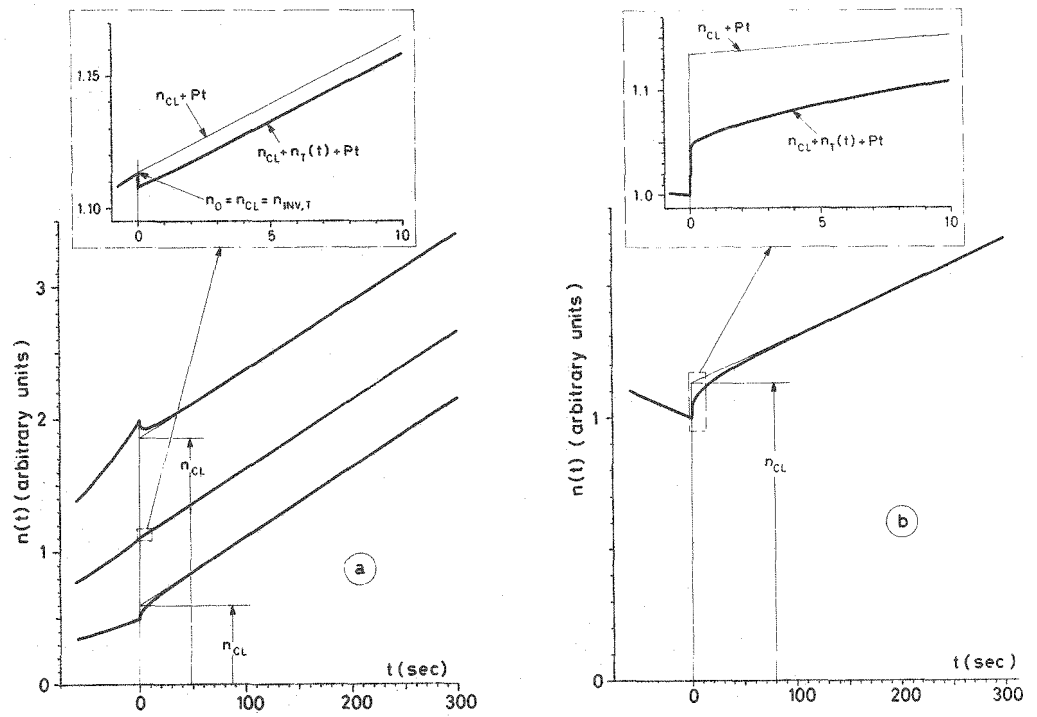

Fig. 6. Calculated responses of a reactor with $\rho = \rho_L$ to the step-insertion of a neutron source with:
a. $\Delta > 0$ (Case 4); b. $\Delta < 0$ (Case 7).

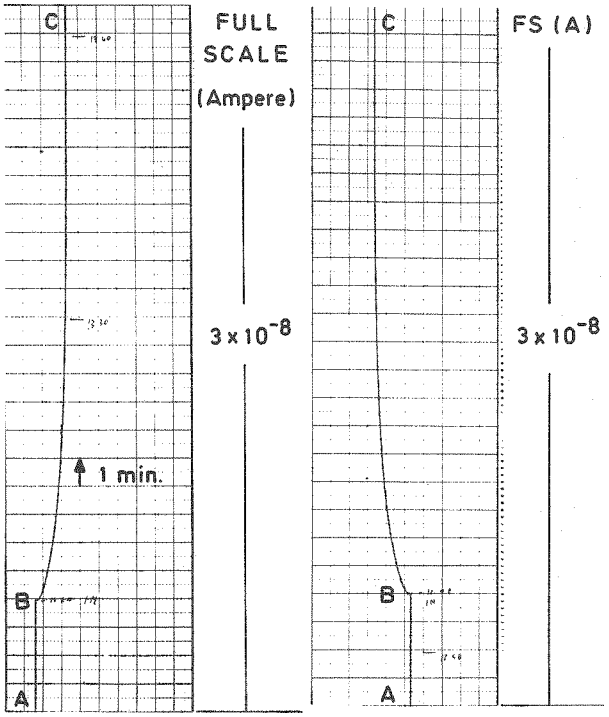

Fig. 7. Experimental response of a critical reactor to the step-insertion of a neutron source with $\Delta > 0$ (Case 2).

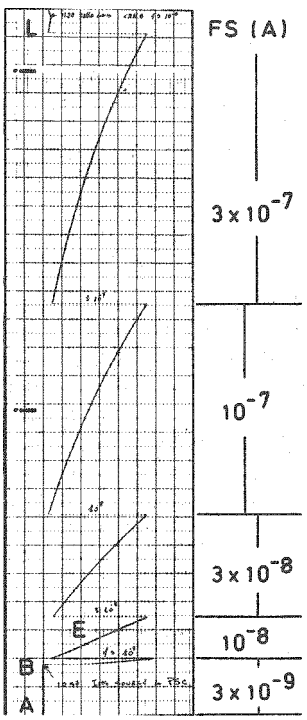

Fig. 8. Experimental response of a critical reactor to the step-insertion of a neutron source with $\Delta < 0$ (Case 9).

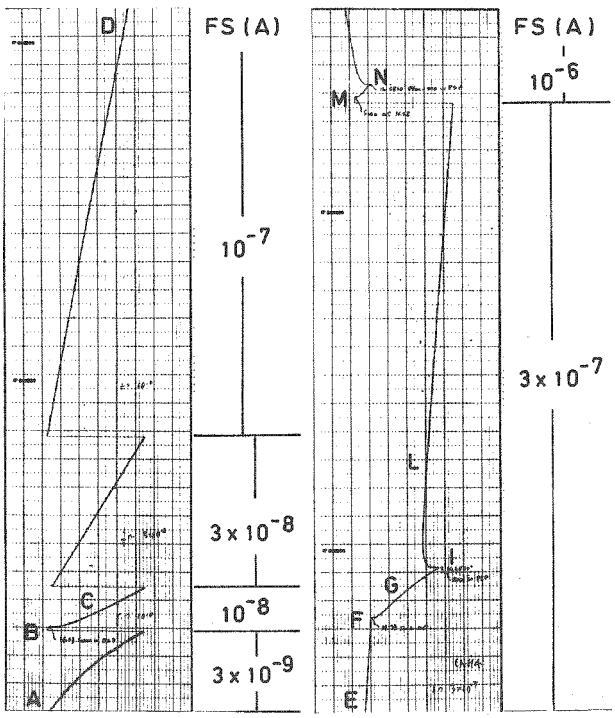

Fig. 9. Linear divergence obtained by a neutron source with $\Delta > 0$ (Case 4).

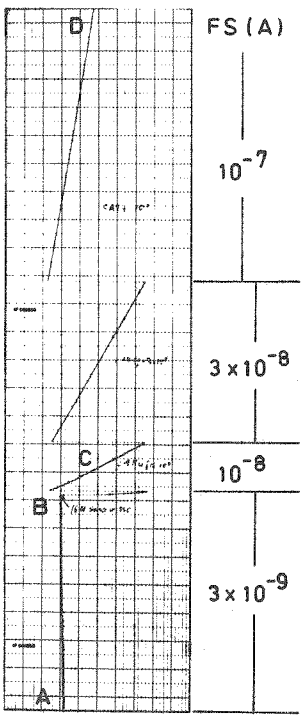

Fig. 10. Linear divergence obtained by a neutron source with $\Delta < 0$ (Case 7).

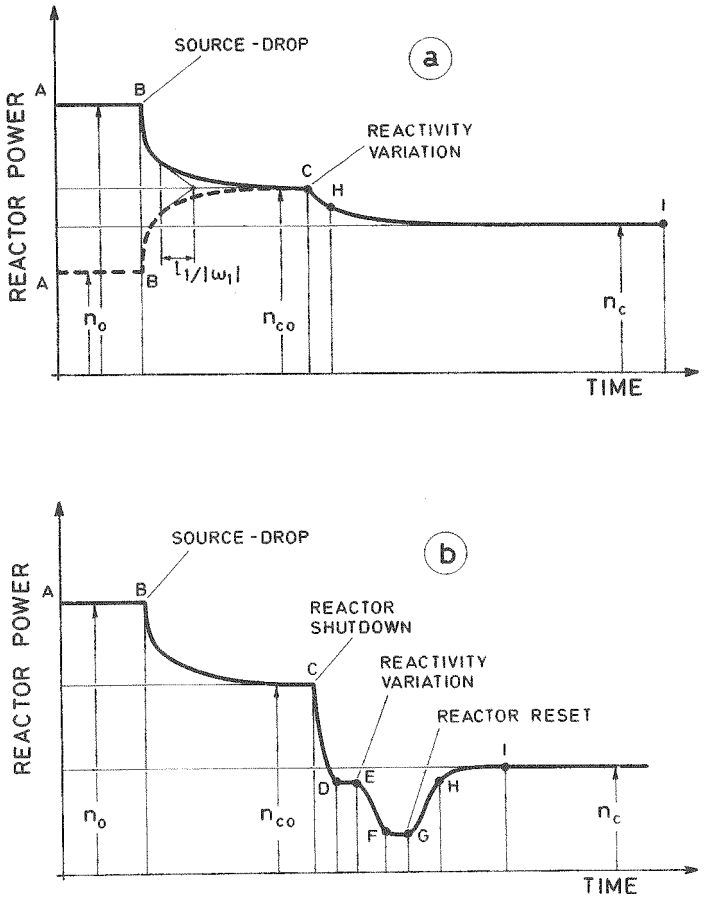

Fig. 11. Principle of source-drop technique
a. Without reactor shutdown
b. With reactor shutdown.

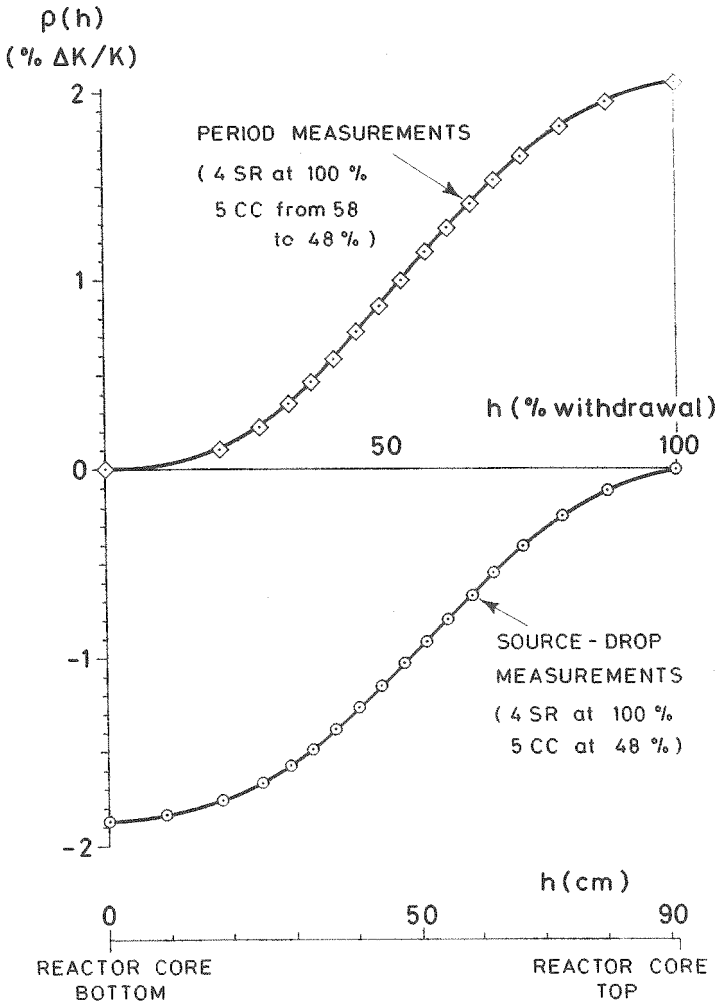

Fig. 12. Calibration of safety rod (DIR-1 without SS-MgO tube). SR = safety rod; CC = control cylinder.

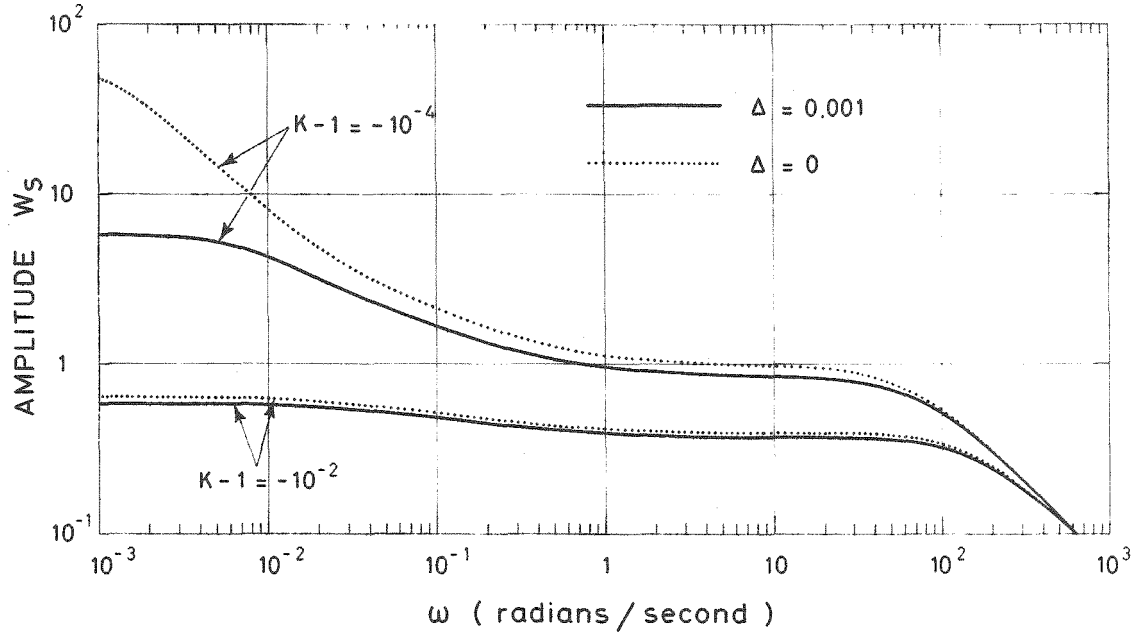

Fig. 13. Influence of a positive source effect on the amplitude of $W_s(j\omega)$ with $\ell = 10^{-4}$ sec.

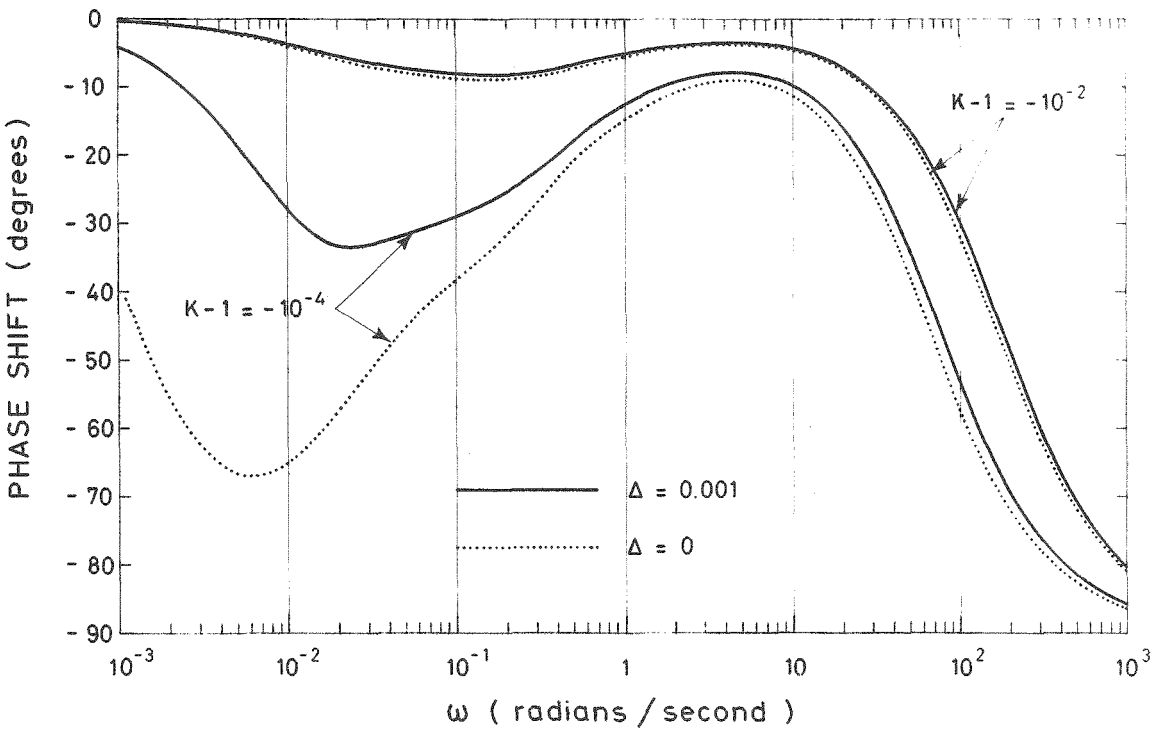

Fig. 14. Influence of a positive source effect on the phase shift of $W_s(j\omega)$ with $\ell = 10^{-4}$ sec.